Expression and Comparison of Tropomyosin Isoform Actin-binding Properties and Their Resolution within the Thin-filament Proteome

Khadar B. Dudekula

Expression and Comparison of Tropomyosin Isoform Actin-binding Properties and Their Resolution within the Thin-filament Proteome

Khadar B. Dudekula

PhD

2015

University of Bedfordhire

Expression and Comparison of Tropomyosin Isoform Actin-binding Properties and Their Resolution within the Thin-filament Proteome

By

Khadar B. Dudekula

A thesis submitted to the University of Bedfordshire in fulfilment of the requirements for the degree of Doctor of Philosophy

January 2015

University of Bedfordshire

Abstract

Tropomyosins(Tm) are a group of proteins that regulate the actin filaments in both muscle and non-muscle cells. In mammalian cells four Tm species are found: α-Tm (fast) encoded by *α-Tm* /*TPM1* gene, β-Tm, encoded by *β-Tm*/ *TPM2* gene, α-Tm (slow) encoded by *γTm* gene/ *TPM3* and δ-Tm encoded by *δTm* / *TPM4*gene. Mutations in Tm are linked to many cardiac and skeletal diseases like hypertrophic cardiac myopathy (*TPM1* and *TPM2*), familial cardiac myopathy (*TPM1*) and skeletal diseases like nemaline myopathy (*TPM2* and *TPM3*) along with other sarcomere proteins. The hypothesis on which this study is based is, the isoform composition in both muscle and non-muscle cells adapts in response to disease and physiological changes. A significant part of that adaptation is changes in the thin filament protein isoforms expressed and the post translational modifications of these proteins.

In this study Tpm3.12st isoform of *γTm* and other striated muscle tropomyosin isoforms (Tpm1 and Tpm2) and a non-muscle Tmp4 were characterised using a variety of techniques. The aim was to enhance our understanding of the role of tropomyosin interactions in regards to its efficiency of actin binding capacity as well as its effect on actin polymerisation.

Human tropomyosin 3 (Tpm3.12st) was expressed in *E. coli* to produce recombinant protein with three N-terminal sequence variants (Met, MM and (M)ASM). The proteins were characterised for their binding affinity with actin as this isoform has not been well characterised so far. Its properties are compared with other striated muscle tropomyosin Tpm1.1st and Tpm2.2st and non-muscle Tpm4.1cy. The proteins were purified through

ion exchange chromatography and the purity was checked by using SDS-PAGE and UV spectrometry. The molecular weights of the recombinant proteins produced were confirmed by mass spectrometry. Cosedimentation assays were performed for their actin binding affinity using ultracentrifugation. The variant of Tpm3.12st with AS N-terminal extension was found to have similar actin affinity to Tpm1.1st in the range of 0.1-0.8 μM (half saturation). However the variants with Met and MM N-termini bound to actin weakly with high half saturation concentration of ~ 6 μM and ~8 μM tropomyosin respectively. Measurement of actin polymerisation kinetics showed it is affected in presence of tropomyosin. From this study it is shown that tropomyosin accelerates the initiation step in actin polymerisation with varying differences within the isoforms in contrast to several previous studies. There have been very few studies of the effect of tropomyosin on actin polymerisation in the last two decades. This work shows that tropomyosin isoforms have a large and variable role in controlling actin polymerisation and understanding tropomyosin function will need further investigation in this area.

This study also developed an ELISA screening method using monoclonal antibodies for identification and quantification of Tpm3.12st which was tested against all the four tropomyosin isoforms. None of the twelve antibodies studied showed reactivity only with Tpm3.12st. From the data analysed it is deduced the amino acid residues in the region of 24-43 shows the prospect of designing a monoclonal antibody specific to Tpm3.12st isoform. Accurate quantification of tropomyosin isoforms is key to understanding their function and the effects of modulation of isoform composition in health and disease.

A reverse phase liquid chromatography method was developed which is compatible with the analysis of the thin filament proteome using top-down mass spectrometry. Reverse

phase liquid chromatography (RPLC) is one of the most popular methods used in mass spectrometry analysis where proteins are separated based on their hydrophobicity. The RPLC method developed in this study gives an efficient separation of major thin filament proteins along with small soluble proteins that is compatible to use for top down mass spectrometry for identification and quantification of proteins, PTMs and isoform composition. With a minimum amount of 2 mg of tissue using chicken and mouse heart and skeletal muscle samples a buffer system was optimized to extract thin filament proteins. With the optimized RPLC method actin, tropomyosin and troponin complex subunits (TnC, TnI and TnI) were successfully separated and the proteins were identified using SDS-page by comparison with the previous research results. This novel method of extraction and the optimised RPLC method will provide a "bird's eye view" of thin filament proteome providing information of PTMs of all the proteins together within one single extraction, reducing the time for analysis and the sample size. This has the potential to give insight into tissue, muscle and heart adaptations that could act as a prognostic indicator.

Declaration

I declare that this thesis is my own unaided work. It is being submitted for the degree of Doctor of Philosophy at the University of Bedfordshire.

It has not been submitted before for any degree or examination in any other University.

Name of candidate: Khadar Dudekula Signature: 

Date: 24th June 2015

Acknowledgments

I would like to thank my supervisor, Dr. Robin Maytum, for giving me the opportunity to work with this exciting project and for continuous guidance and support with his presence whenever needed and helping me to complete this thesis on time. I thank him and admire him for his patience and for being a great teacher, having enthusiastic discussions and for the knowledge he tried to transfer to me.

I would like to express my deep gratitude to Prof. Jan Domin for giving me the opportunity to join this department as research demonstrator and for awarding financial support to help in completing doctoral studies. I like to thank my second supervisor Dr. Adam Paige for his support and guidance throughout this period.

I want to thank all the members of Department of Life Sciences especially Dr. Maria Simon and Patrick Kelly for saving my experiments many times by letting me use reagents and equipment whenever needed. I want to thank Prof. Steve Marston for donating Tpm3 antibody.

I am thankful to Emma for donating mouse tissue samples and also our pudding days and providing me a shoulder when ever I need emotional through out the period of PhD research. I thank my friend Ghazala Khan for offering her ear and being a very supportive listener and letting me poke her in office just for fun. I would like to thank my friends Mary and Nithya for their unconditional immense support in all these years and midnight chats. I want to thank everyone who played a part in all these years of whom I missed to mention here.

My outmost gratitude and love goes to my elder brother, Khasim for being the most awesome person in my life and a strong pillar of support in every step until now, without

his support I would not have been able to reach the position I am at the moment. I thank my parents for their love and continuous support and my sister for helping me out with research articles and family talk. Finally I thank my son, Aman for his presence in my life with his great support and encouragement he has continuously provided with so much maturity for his age to whom I dedicate this thesis to.

Dedicated to my Son, Aman and my brothers, Khasim and Vali.

List of abbreviations

Ac	Actin
APS	Ammonium persulphate
BSA	Bovine serum albumin
cDNA	Complementary Deoxyribonucleic acid
DMSO	Dimethylsulphoxide
dNTPs	Deoxynucleotide phosphates
EDTA	Ethylene diamine tetra acetic acid
HRP	Horseradish peroxidase
Ip	Isoelectric point
kb	Kilo base pair
kDa	Kilo Dalton
LB	Luria Broth
PBS	Phosphate buffered saline
PCR	polymerase chain reaction
SDS-PAGE	Sodium dodecyl poly acrylamide gel electrophoresis
TAE	Tris-acetate EDTA buffer
TEMED	N, N, N',N'-tetraethylmethylenediamine
Tm	Tropomyosin
UV	Ultra violet
WT	Wild type

Tropomyosin isoform terminology used in this thesis

Isoform	Referred to in this thesis in some places
Tpm1.1st	Tpm1
Tpm2.2st	Tpm2
Tpm3.12st	Tpm3
Tpm4.1cy	Tpm4

Table of Contents

List of Figures

List of Tables

Chapter 1

1 Introduction

Striated muscle is highly organized versatile tissue with complex architecture of muscle fibers that contribute to a variety of functions in humans. Skeletal muscle is the basic example of striated muscle which has been extensively studied. The basic function of the muscles depends on individual properties of different muscle fibers and their proportion which results in functional diversity of muscles. The heterogeneity in their function depends on their differences in structural, molecular, contractile and metabolic properties that in turn characterize a muscle's function. These structural and functional differences in the muscle fibers are due to differential gene expression of the sarcomeric genes which results in numerous isoforms of the muscle fiber proteins such as myosin (myosin light chains –ELC and RLC, myosin heavy chains -α and β) (Schiaffino and Reggiani, 2011), actin (α-actin, β-actin) (Rubenstein, 1990), troponin (TnI, TnT, TnC) (Gomes et al., 2002) and tropomyosin (Tpm1, Tpm2, Tpm3 and Tpm4) (Gunning et al., 2005a), calcium regulatory proteins (Ca^{2+}-ATPase, α-subunit of dihydropyridine receptors) and many others. Muscles are not fixed entities, they are rather dynamic with remarkable adaptive capabilities. The adaptive capacity owes due to the presence of various isoforms of the proteins and post translational modifications that can adapt to functioning of the tissue. This adaptive nature of muscle structures is significant contributor to the survival of the organism (Canepari et al., 2010; Pette and Staron, 2000b).

The adaptive nature of the muscle fibers results in the physiological changes to the muscles in humans. These can change the mass and type of tissue present and their properties through post-translational modification of proteins present in them and modify the isoforms of the protein expressed (Canepari et al., 2010). These adaptations may lead to heart diseases and skeletal muscle diseases or diseases may cause the heart or muscles to adapt to new physiological demands (Tardiff, 2011a; Yuan and Solaro, 2008).

Studying the adaptations in the muscle isoforms gives an insight into the heart adaptations and the diseases caused by these transitions in the muscles. The present study is to develop a method to analyze the proteins present in the thin filament of the heart and skeletal muscles for studying post-translational modification and isoform switching to understand the adaptations occurring in both normal and diseased state. This study concentrates on tropomyosin and also characterization of tropomyosin 3.12st (Tpm3.12st), an actin binding protein in thin filament that helps regulate actin and plays a major role in muscle contraction.

This chapter gives an introduction to skeletal and cardiac muscle and gives a brief description of muscle structure and its physiological functions, muscle proteins and their isoforms and information about cardiac diseases and skeletal muscle diseases.

1.1 Muscle Tissue

Human body functions necessitates many driven movements both physically (walking, running, breathing), and physiologically (movement of contents in digestive tract, circulation of blood). Muscle tissue that is specialized in contraction is responsible for

these movements in the body. There are basically three types of muscle tissues found in the humans i) Skeletal muscles ii) Cardiac muscles and iii) smooth muscles.

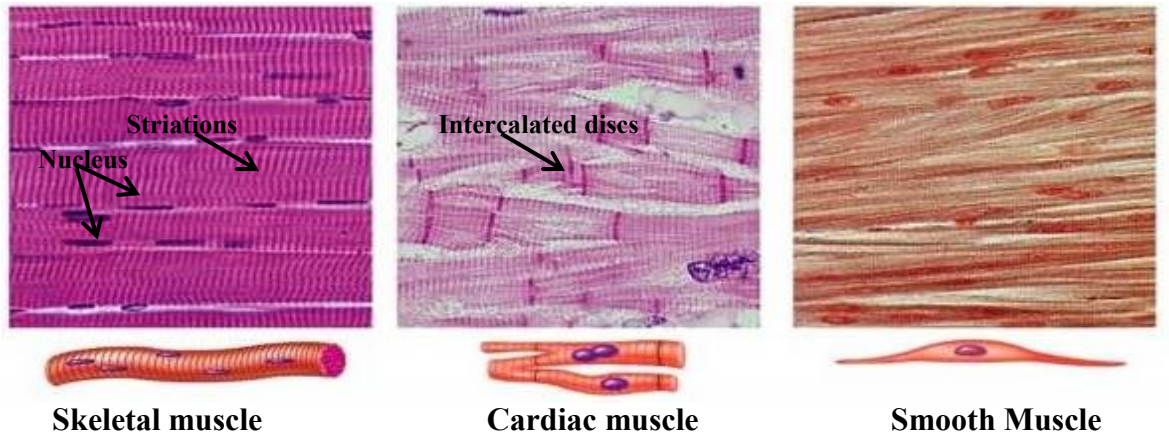

Figure 1.1: Skeletal muscle shows striations and is multinucleate. Cardiac muscles showing branching and intercalated discs. smooth muscles with no branches and striations and a single nucleus for each cell (Martini, 2001).

1.1.1 Skeletal muscle

Skeletal muscles are the large muscles found in the body they are responsible for the overall movements in the body and aid in locomotion along with maintaining body posture, generation of body heat and storing nutrients (Martini, 2001). Each skeletal muscle cell is called muscle fiber, arranged together in a highly organized fashion in repeated units in a bundle like manner. Due to their specific arrangement they look like long continuous striated structures with numerous nuclei in them (Figure 1.1). Skeletal muscles have specific cells called ‘myosatellite cella’, due to which they are capable of repairing themselves partially after an injury. Skeletal muscle fibers are bound together

by collagen and elastic fibers that collect together to form tendon which in turn is attached to bone. The tendon pulls the bones of the particular organ when contraction occurs in the muscles causing movement. The contraction process of the skeletal muscles is controlled by the nerve signals and they are not capable of functioning involuntarily. Hence they are called 'voluntary striated muscle fibers (Gordon et al., 2000; Martini et al., 2008).

1.1.2 Cardiac Muscle

Cardiac muscle (shown in Figure 1.1) is characteristic to only heart muscles, which is also striated but extensively branched tissue. Contraction of cardiac muscles assists in pumping and circulation of blood to the organs, and maintains blood hydrostatic pressure. Each cardiac muscle cell is called cardiocyte and is similar to skeletal cells in having striations however it has only one nucleus per each cell and is smaller than the skeletal muscle cell. Cardiac muscle cells are inter connected and consist of extensive branching, these connections form intercalated discs which consist of gap junctions where movement of ions takes places during contraction, desmosomes and proteoglycans link the cells together during contraction. Cardiac muscles have characteristic specialized cells called 'pacemaker cells' that regulate the muscle contraction in heart, rather than working on receiving the nerve signals. Hence cardiac muscles are called 'involuntary striated muscles'.

1.1.3 Smooth muscles

Smooth muscles (Figure 1.1) are present in the visceral organs of the body like digestive system, respiratory organs, blood vessels and others. They help in regulating the diameter of blood vessels, respiratory tract movement and respiration, food movement in the digestive tract etc. Smooth muscles are single cell units with their own nucleus. These cells are capable of dividing and thus are able to repair after an injury. The muscle fibers are arranged differently in smooth muscles than in the skeletal muscles and are not striated. Smooth muscle contraction is not controlled by the nervous system and hence they are called 'non-striated involuntary muscles'.

Even though there are structural differences in all these different muscle tissues, organization of muscle tissue, muscle regulation and contraction process is similar.

1.2 Organization of skeletal muscle

The cross section of muscle tissue (Figure 1.2) show bundle of muscle tissue is enclosed with in a thick tissue with collagen and elastin fibers called epimysium. The muscle tissue itself is formed of bundles of muscle fibers called muscle fascicle.

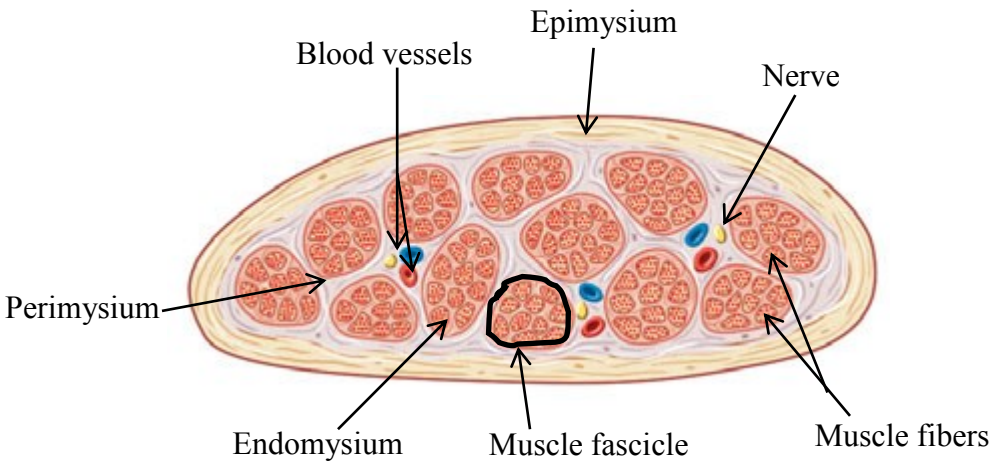

Figure 1.2: Cross-section of muscle tissue: Each muscle fiber is surrounded by soft connective tissue endomysium. Few muscle fibers form a bundle called muscle fascicle and numerous muscle fascicles are separated by perimysium and this whole muscle tissue is surrounded by epimysium. The overall muscle tissue is supplied with nerves for receiving signals for contraction and blood vessels supply oxygen and nutrition (MARTINI et al., 2008).

Perimysium separates muscle fascicle from each other and is also supplied with nerves and blood vessels that control muscle contraction and provide energy and nutrition respectively. These nerves and blood vessels branch out into endomysium controlling the function of the individual muscle fibers at micro level. Epimysium fills up the space between the individual muscle fibers, it contains myosatellites cells that are undivided stem cells, help in repairing the skeletal muscle when injured. Figure 1.2 is the cross section of muscle tissue showing the organization of the muscle fibers in individual skeletal muscle tissue.

Endomysium and perimysium elongate and join the epimysium to fuse to form tendon and join the bones, so whenever a contraction occurs the bone attached to that muscle also moves, resulting in the movement of the body.

1.3 Sarcomere

The muscle fibers contain myofibrils that are arranged in bundles of thin and thick filaments called myofilaments (Figure 1.3a). The myofilament is arranged in repeated contractile functional units called sarcomere.

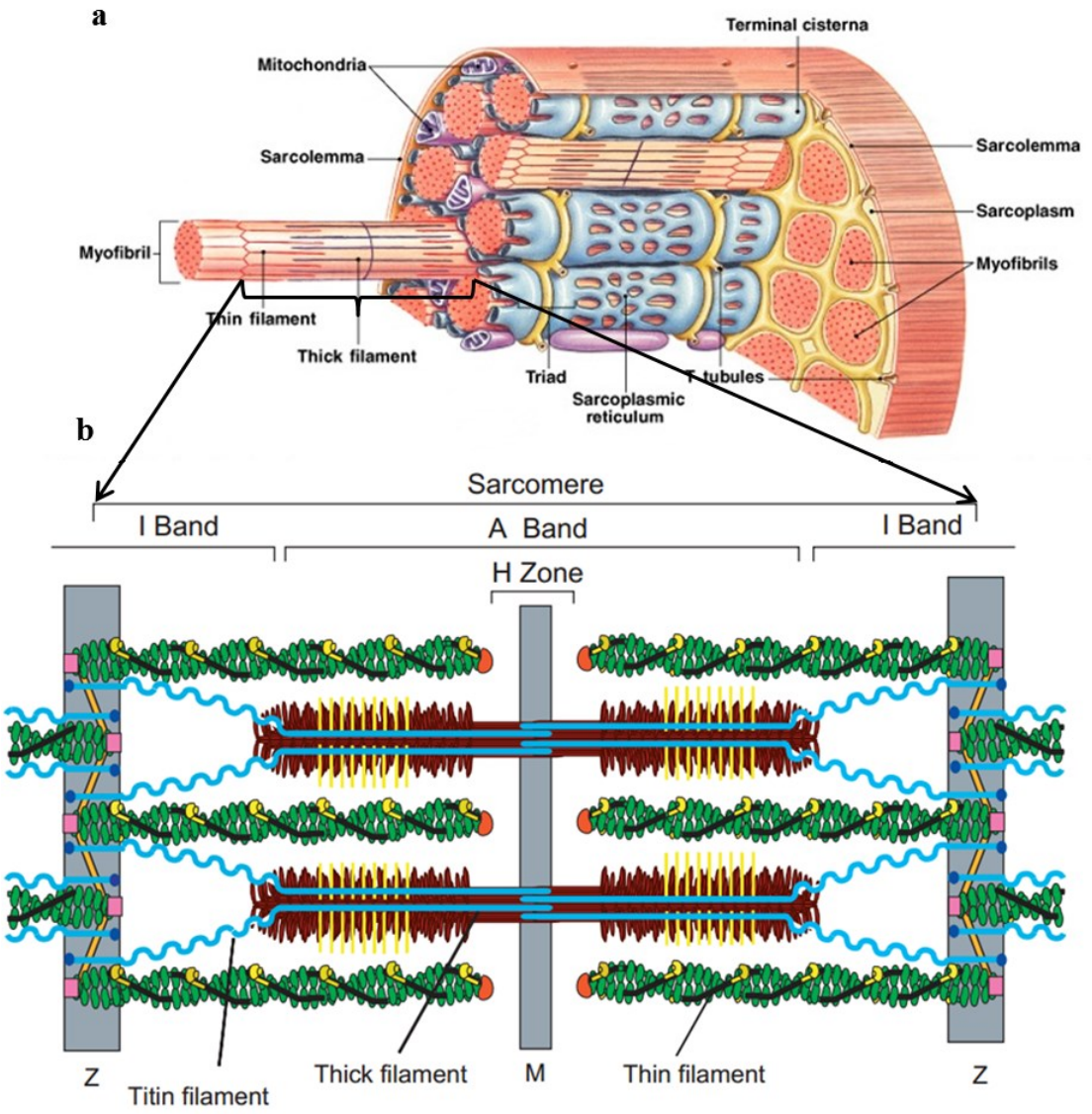

Figure 1.3: Major sarcomeric proteins: A. shows the arrangement of myofilaments. B. Single contractile functional unit-sarcomere showing I band, A band and M line and Z line, green -thin filament, brown – thick filament, Myosin binding protein C -yellow transverse line on thick filament, blue – titin, black line on the thin filament – tropomyosin, yellow structures on tropomyosin – troponin complex (Gregorio and Antin, 2000; Martini et al., 2008).

The sarcomere consist of thin and thick filament aligned parallel to each other (Figure 1.3b), and the interaction of both these filaments is assisted by stabilizing proteins of thin

and thick filament and the regulatory proteins thick and thin filaments. The differences in the arrangement, size and density of thin and thick filaments gives a banded appearance of sarcomere. The band A consists of thick filaments called myosin (brown) as in Figure 1.3b approximately 1.6 μm long at the center of the sarcomere connected by M line and runs lengthwise along whole A band. Myosin is The H-line or H- zone is a resting zone where only thick filaments are present. Thin filaments mainly consists of actin filaments (green) which are approximately 1.0 μm long and are associated with band I sliding over the thick filaments anchored by α-actinins (golden-on Z line) to Z-line where actin is capped by Cap Z (pink squares). The I band do not contain thick filaments. Thin filaments extend from A band of one sarcomere to A band of another sarcomere and the region from one Z line to another Z line makes one sarcomeric unit. The region where thin and thick filaments overlap is call the zone of overlap were these two proteins interact with each other to generate a force for muscle contraction which will be explained in muscle regulation section. Titins are the another type of filaments one of the largest proteins so far, helps to keep the thin and thick filaments aligned in proper fashion and also helps to the muscle to come to its original relaxing state after each contraction cycle. Titin (turquoise) is also believed to resist and prevent any disruption caused due to extreme stretch during contraction (Gregorio and Antin, 2000; Martini et al., 2008). One thick filament is surrounded by six thin filaments in the lattice structure of muscles.

1.3.1 Thick filament

Thick filament consists of a bipolar motor protein myosin II. It also contains a large protein titin and C, H, X and M proteins which are not discussed in detail in this thesis.

1.3.1.1 Myosin

The thick filament mainly consists of myosin that interacts with actin to produce force and the sarcomere shortening during contraction. The type of myosin present in muscles is myosin II and is one of the largest protein with a total molecular weight of ~500 kDa. It is made of six two polypeptide chains consisting of two heavy chains of ~220 kDa each and one pair of each essential light chains (ELC) and regulatory light chains (RLC) of ~20 kDa each (Martini, 2001).

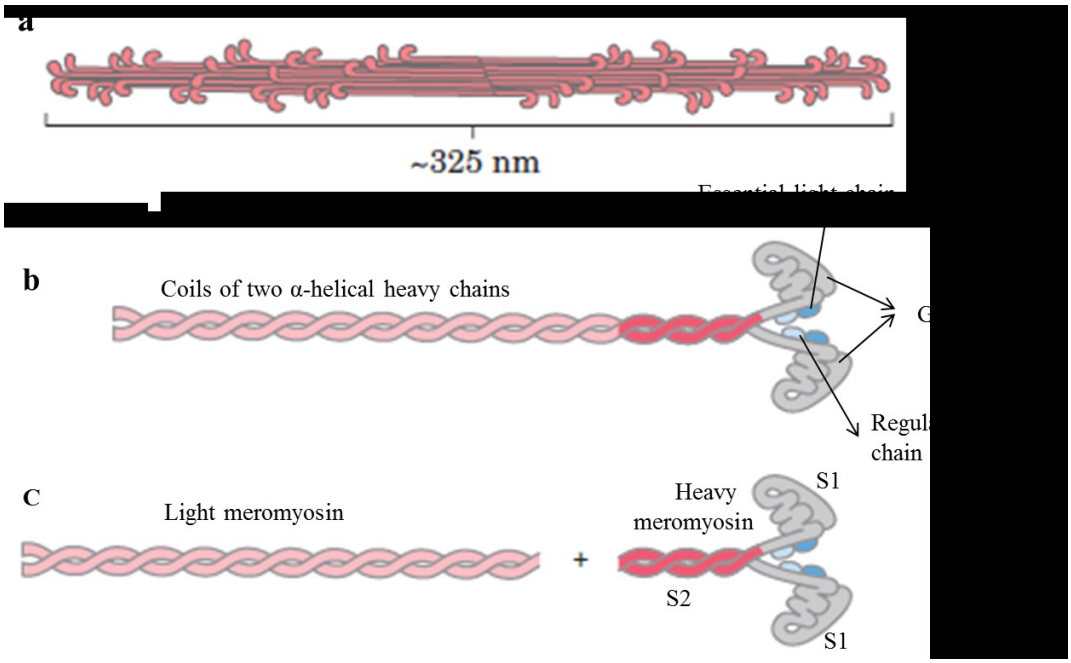

Figure 1.4: Myosin II structure. A. thick filament – myosin aggregates. **B**. Myosin II with two α-helical coiled coils of heavy chains (pink and red) at the C-terminal end and along all the length, globular heads at N-terminal end with two sets of ELC (blue) and RLC (pale blue). **C.** When Trypsin digestion cleaves myosin II heavy chain into light meromyosin (pink) and heavy meromyosin (red) and when heavy meromyosin is digested with papain, it is separated into two S1 molecules (globular heads) and S2 (Lehninger et al., 2008).

Myosin is a α-helical coiled coil, form a myosin heavy chain (MHC) coiled along its length at its C-terminal with a large globular head region at the N-terminal end which are termed as sub-fragment 1 (S1). The light chains ELC and RLC are associated myosin heads with each pair of ELC and RLC on S1 (Figure 1.4b). When the two myosin heavy chains (MHC) are digested with trypsin the cleavage separates them into light meromyosin and heavy meromyosin. Heavy meromyosin digestion with papain separates both S1 fragments from S2 fragment (Figure 1.4c) (Lehninger et al., 2008).

Myosin II forms aggregates in thick filament under physiological conditions (Figure 1.4a). The oppositely charged amino acids in the coiled coil tails called the myosin rods forms filaments with a regular interval repeats. This causes the S1 heads project outside the filament region and are arranged helically facing in the same direction creating a head-to-tail configuration giving myosin a biopolar structure.

The S1 heads are the site of ATP hydrolysis that provides energy to interact with actin filaments to generate force during contraction by filaments sliding over each other which will be explained in muscle regulation section 1.4

Myosin binding protein C (MyBP-C, yellow lines on myosin) in Figure 1.3b is a thick filament–associated protein found in the crossbridge containing C zones of striated muscle sarcomeres. The C-terminus of the MyBP-C interacts with light meromyosin section of the myosin rod and titin to maintain the thick filament structure. It also helps in regulating the muscle contraction by binding to subfragment-2 of myosin at its N-terminus by reducing the actomyosin ATPase activity. There are several models designed to explain the interaction of MyBP-C with myosin and how it contributes to contraction,

however these is no clear illustration model of its precise position and arrangement on the thick filament (Flashman, 2004). Genetic mutations of MyBP-C are one of the most common causes of hypertropic cardiacmyopathies. Three isoforms of MyBP-C are known to exist in adult muscle - human fast (*MYBPC2*) and slow skeletal (*MYBPC1*) isoforms and human cardiac MyBP-C (*MYBPC3*). The fast and slow skeletal isoforms are present either together in some muscle types or can even coexist (Pette and Staron, 2000).

The other proteins of thick filament, protein C bundles myosin rods together during development and proteins X and H are thought to have the same properties as C protein (Martini, 2001). The M protein in M line provides support to connect the thick filament to A band in the sarcomere. The large protein titin is an elastic molecule providing the elasticity property to the sarcomere and helps in the alignment of thick and thin filament in the sarcomere (Gordon et al., 2000; Gregorio and Antin, 2000).

1.3.1.2 Myosin isoforms

MHC in muscle fibers exists in two types, pure fiber with MHC having a single isoform and hybrid fibers with MHC having multiple isoforms. Myosin is one of the proteins that exhibits fiber specific isoforms and expression levels varies depending on the fiber type (Pette and Staron, 2000). Depending on the fibers, MHC exhibits four types of pure fiber types: one slow type I and three fast types. Slow type has isoforms MHC1β, and fast type has 2A (MHC2a), type 2D (MHC2d) and type 2B (MCH2b). When these fiber coexpress in different tissue fibers hybrid type isoforms are developed (Pette and Staron, 2000b; Schiaffino and Reggiani, 2011). Table 1.1 gives few examples of myosin heavy chain isoforms and their location in the fiber types.

Table 1.1: List of myosin heavy chain isoforms present in adult mammalian muscle fibers.

	Genes	Protein	Location
Skeletal	MYH1	MyHC-2X	Fast 2X fibers
	MYH2	MyHC-2A	Fast 2A fibers
	MYH3	MyHC-emb	Developing muscle fibers
	MYH4	MyHC-2B	Fast 2B fibers
	MYH8	MyHC-neo	Developing muscle fibers
	MYH13	MyHC-EO	Extraocular muscle fibers
Cardiac	MYH6	MyHC-α	Jaw muscle and heart
	MYH7	MyHC-β/slow	Slow muscle and heart
	MYH7b/MYH14	MyHC-slow/tonic	Extraocular muscle
	MYH15	MyHC-15	Extraocular and spindle fibers
	MYH16	MyHC-M	Jaw muscle

Adapted from Schiaffino and Reggiani (2011).

There are other several types of myosin proteins in muscle and non-muscle cell. Myosin I is one of the most extensively studied proteins that play a role in transporting membrane vesicles, movement of plasma membrane along with actin bundles, phagocytosis. Myosin I carries a head similar to myosin II but does not have a coiled long tail instead carries a single short tail (Cooper, 2000).

1.3.2 Thin filament proteins

Thin filament is the main site for the Ca^{2+} regulation of muscle contraction. The muscle contraction is turned "on or off" in presence or absence of Ca^{2+} (Tobacman, 1996). The main proteins that are associated in muscle contraction are actin, tropomyosin and

troponin complex associated with other actin binding and actin regulatory proteins in the thin filament (Figure 1.5).

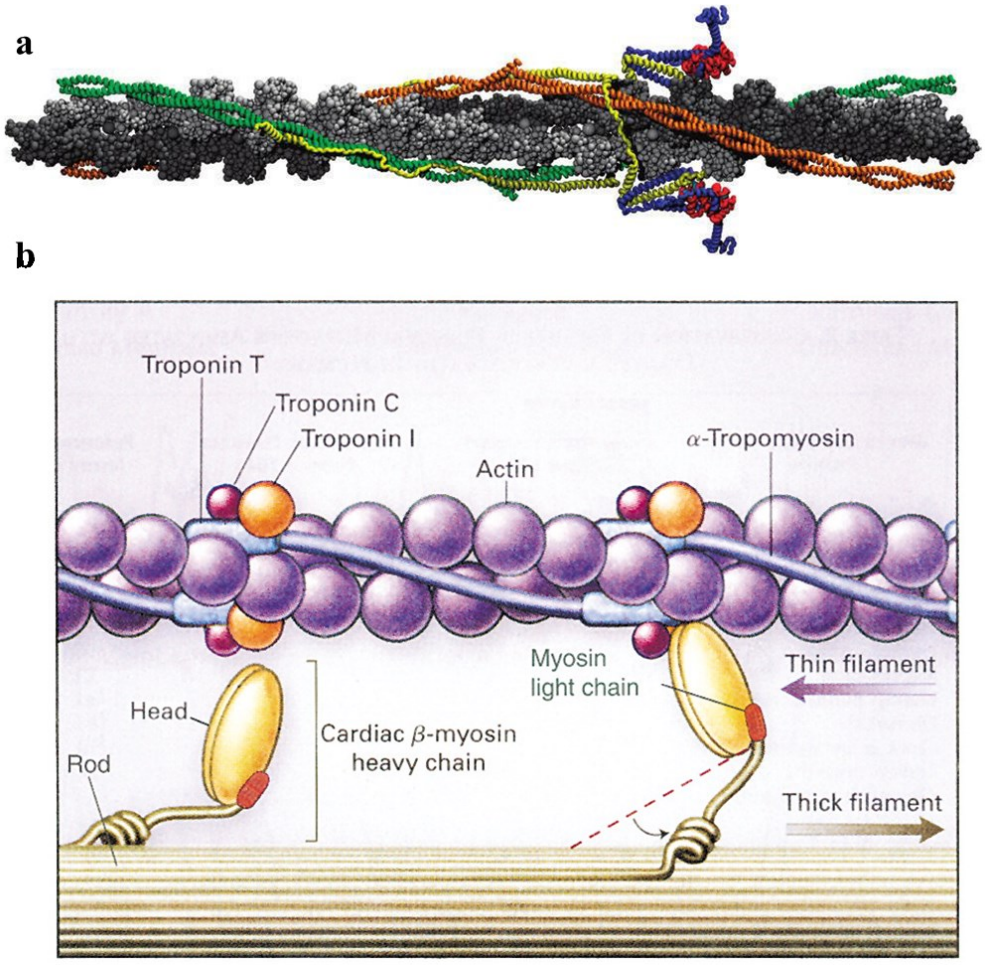

Figure 1.5: Thin filament: a. Human thin filament model: Actin filament – grey, tropomyosin –orange/green, troponin T – yellow, troponin I-blue, troponin C-red (Manning et al., 2011). **b.** Molecular arrangement of thick and thin filament proteins (Seidman and Seidman, 2001)**.**

1.3.2.1 Actin

Actin is a 42 kDa filamentous protein. Actin exists in two forms monomer (G) actin and filamentious (F) actin which is a polymer. Actin polymer (F-actin) is formed by spontaneous polymerisation of G actin and forms the backbone of the thin filament.

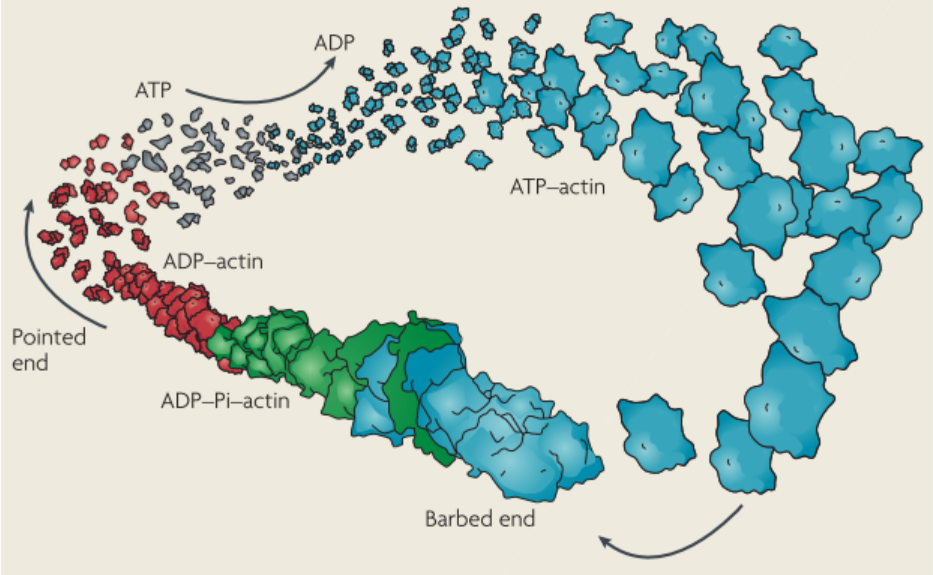

Figure 1.6: Actin polymerisation and treadmilling (Pak et al., 2008)**.**

Figure 1.6 shows the actin polymerisation dynamics and treadmilling. Actin polymerisation happens by hydrolysis of ATP and forms a filament. The actin filament is a polar molecule with pointed and barbed end. Monomer are added at both ends, however the polymerisation rate is faster at barbed end than the pointed end. The dynamics of actin polymerisation is explained in detail in chapter II (section 2.2.2). Actin forms actin-nucleotide complex in associated with ADP and the exchange of ADP-G actin with an ATP forms a ATP-G actin which initiates polymerisation (Pollard and Cooper, 2009).

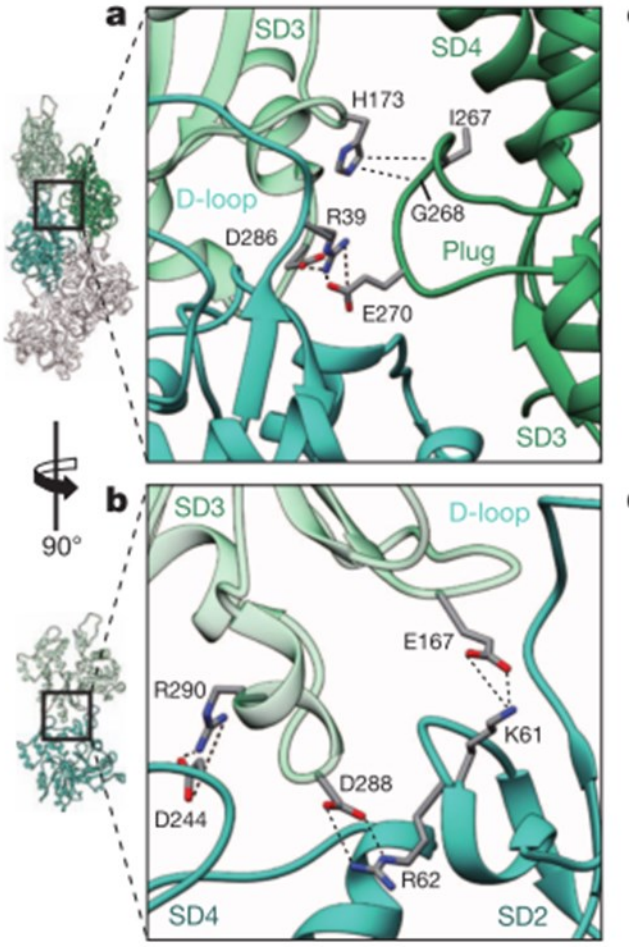

Figure 1.7: F-actin filament stability showing the interaction between two filaments. Both a and b show the actin subunits, the central F-actin subunit - cyan and adjacent subunits –shades of green. Dotted lines – salt bridges (Ecken et al., 2014).

The G actin is a bilobed structure with large and small domains. The transition of G-actin to F-actin takes place by flattening of the subdomains on binding to Mg^{2+} ions (Figure 1.8a and b). Myosin binding site located within the small domain (Kabsch et al., 1990) which is also the binding site for the metal ion like Mg^{2+} or Ca^{2+} (Ecken et al., 2014) (Figure 1.8c and d). F-actin is formed by two long-pitch helical strands. F-actin filament is stabilized by the interaction between the subunit domains between the two strands by

hydrophobic interactions and also by forming salt bridges (Figure 1.7). The filaments undergo interstand and intrastrand ineraction between the two filaments. Subdomians SD2 and SD4 of one actin and SD3 of the same actin of adjacent subunit forms the primary intrastrand interaction. D-loop and the SD3 betasheet form the significant interstrand contacts by enclosing tyrosine 169 with a lock and key fit with the other filament subunit. Introducing charges at the hydrophobic interfaces of this region disturbs polymerisation of F-actin as well as hampers its stability which can lead to different forms of skeletal muscle diseases (Ecken et al., 2014). SD1 and SD2 domains remain exposed to the solvent which consist of NH_2 and COOH termini and forms the binding site for myosin heads.

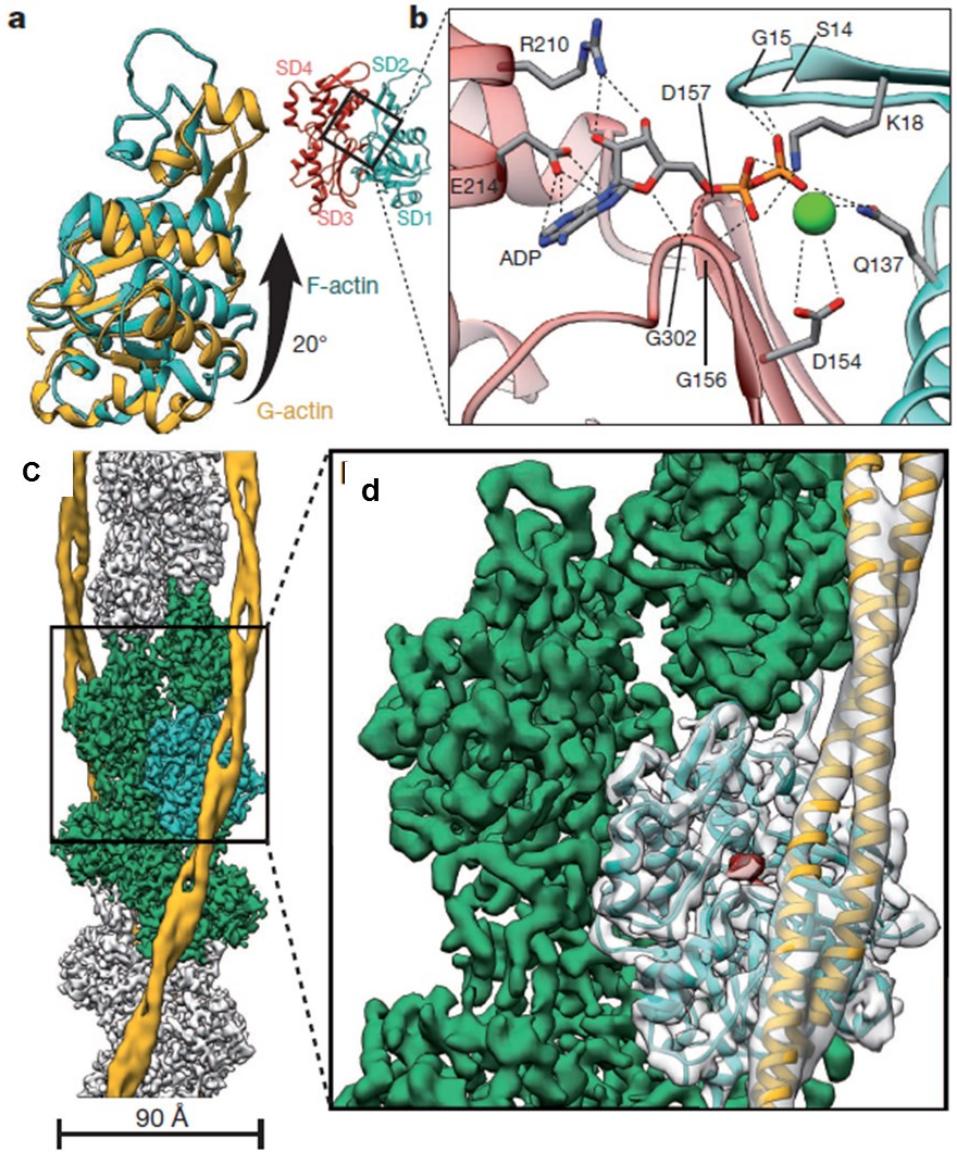

Figure 1.8: Transition of G-actin to F-actin. A. shows the conformational change occurring by rotation of SD1 and SD2 by flattening the molecule. **B.** The positon of nucleotide ADP and the binding of Mg^{2+} ion or Ca^{2+} ion (green). **C.** Cryo-EM structure of F-actin coiled (grey) with tropomyosin (yellow) **D.** the close up view of the subunit that is interacting with tropomyosin shown in green and cyan which is having the myosin binding site (red) (Ecken et al., 2014).

Actin like other muscle proteins exhibits tissue specific isoforms with in an organism. They are divided into two classes - skeletal muscle and smooth muscle isoactins with similar function and are labelled depending on their mobility on acrylamide gels. The major actin isoforms are α, β and γ, where β and γ non-muscle isoactins are predominant in cytoplasm of all eukaryotes and are distributed differentially depending on the cell type. Skeletal specific actin isforms are α-skeletal and α-cardiac similar to α-smooth muscle predominantly found in vascular tissue and γ-smooth muscle found in visceral tissues (Rubenstein, 1990a). The sequence difference of α-skeletal and γ-smooth muscle has only 6 amino acids of 375 residues, mainly found at the myosin binding site. The mechanical force generated by smooth muscle is higher than in skeletal muscle. Studies found that per unit of cross-sectional area of force generated smooth muscle produce same amount of force as skeletal muscle with only 20% of myosin as much myosin, showing that the number of crossbridges formed in smooth muscle seems greater than in skeletal muscle (Murphy et al., 1974), however Harris and Warshaw (1993) showed that there is no difference in the velocity of force generated by smooth muscle and skeletal muscle.

1.3.2.2 Tropomyosin

Tropomyosins(Tm) are the group of proteins that regulate the actin filaments in both muscle and non-muscle cells. Tm is ~42 nm long, present along the actin filament coiling around 4-7 actin molecules forming a sort of back bone to the actin filament and power the muscle contraction-relaxation process in striated muscle (skeletal and cardiac muscles) (Gordon et al., 2000). Tropomyosin is present in all eukaryotic cells ranging

from yeast to human beings. The details of structure and stability of tropomyosin molecule are discussed in Chapter II.

In mammalian striated muscle four Tm species are found: α-tropomyosin (fast)/*Tpm1* encoded by *α-Tm* gene, β-tropomyosin/ *TPM2*, encoded by *β-Tm* gene, α-tropomyosin (slow)/ *Tpm3* encoded by *γTm* gene and *Tpm4* encoded by *δTm* gene. Figure 3.1 to Figure 3.4 in Chapter III, shows the representation of Tm proteins encoded by their respective genes. Each striated muscle consists of at least two of the proteins either as homodimers Tpm1/Tpm3 (both α but fast and slow respectively) or heterodimers Tpm1/Tpm2 (Gimona et al., 1995). Tpm1.1st is predominant in cardiac muscle where as Tpm2.2st is found in skeletal muscle. Tpm3.12st is found in slow twitch skeletal muscle, but recent studies shows that along with predominant Tpm1.1st, Tpm3.12st is also present in cardiac muscles and may possibly have a role in cardiomyopathy causing mutations (Schevzov et al., 2011a). Studies from Creed et al., (2011) showed that Tpm3.iso12st isoform is involved in regulation of molecular composition of microfilaments and the composition of Tm available to actin filaments decides the functional properties of actin cytoskeleton. So far Tpm3.12st has not been characterized for its regulatory properties in human cardiac muscle and its significance in the human heart remains unclear.

Over 40 isoforms of Tm have been identified from the four genes. These are derived from alternative splicing of mRNA, alternative promoters and different 3' terminal modifications (Lees-Miller and Helfman, 1991; Leger et al., 1976). Each gene produces different protein isoforms and depending on the protein isoform the gene encodes, they have been given specific names. The function of different isoforms of Tm varies depending on the actin filament properties of the cell and the different isoforms of Tm

that are present in the particular cell. The stability of actin in different cells depends on the specific cell Tm isoform that regulates the actin filament properties. More details of tropomyosin gene and isoforms are discussed in Chapter III.

1.3.2.3 Troponin

In striated muscles contraction is regulated by Ca^{2+} concentration and association of actin with tropomyosin and troponin complex (Gordon et al., 2000). The force is generated by the hydrolysis of ATP during actomyosin cross bridge cycle. The proteins that are mainly involved in Ca^{2+} regulation include troponin (Tn) complex consisting of TnT, TnI and TnC. The troponin complex binds to actin co-operatively (Gordon et al., 2000) with tropomyosin and actin in 7:1:1 ratio, for every actin molecules 1 tropomyosin and 1 troponin complex. The troponin position its self on tropomyosin with an interval of ~ 37 nm along the length of F-actin-tropomyosin association. While TnT and TnI are specific to striated muscle proteins and have three pairs of fibre type specific isoforms where as TnC belongs to calmodulin gene family. Figure 1.9a-b shows the troponin complex and the binding sites of tropomyosin on TnT. The details of all these three proteins are discussed below.

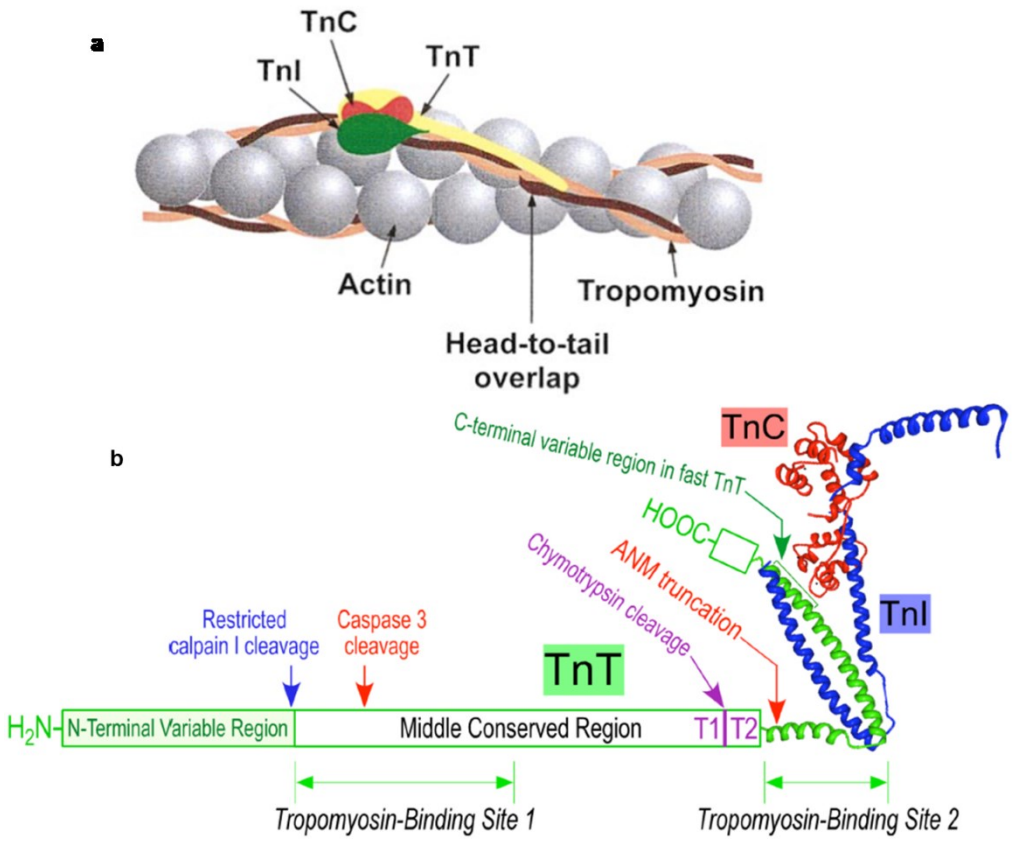

Figure 1.9: Troponin complex showing the binding sites of TnT to tropomyosin. A. molecular arrangement of troponin complex, tropomyosin and actin. TnT-yellow, TnI-Green and TnC-red, Tropomyosin dimer - brown shades, actin –Grey (Tobacman L.S, 1996). **B.** Structural interpretation of Tn complex showing the N-terminal region of TnT having the binding site for tropomyosin and the C-terminal region interacts with TnC and TnI as well as another binding site for tropomyosin (Wei and Jin, 2011).

1.3.2.4 Troponin T (TnT)

Troponin T acts as the glue to hold the troponin complex together binding to TnC and TnI along with being the main interacting site of tropomyosin and actin. It is also involved in co-operative activation of thin filament and responsible for regulation of thin filament during contraction. Figure 1.9a and b shows the sites occupied on the TnT that are responsible for the troponin complex binding to tropomyosin-actin . The TnT1 site

lies in the region of 1-158 residues and TnT2 site 159-259 residues at the C-terminal end of the sequence obtained by chymotrypsin cleavage. The globular TnT2 region at COOH terminal interacts the TnI and TnC along with Tm and the extended TnT1 region interacts with Tm along with the COOH terminal region including head to tails overlap region that is considered to be the highly flexible region of Tm (Schaertl et al., 1995).

The TnT is a 30-35 kDa protein varying with tissue type and the species of the organism with 223 – 305 amino acids again variable with in the vertebrate species. The large variable size of TnT is due to varying length at the N-terminal region with few N-terminal amino acids in fish or 70 residues long as in mammalian cardic TnT (Leszyk et al., 1987). The cleavage sites with enzymes calpain separates the N terminal region, and caspase cleaves the site of mutation that is related to nemaline myoptathy (Wei and Jin, 2011). Cardiac TnT is longer than skeletal TnT (~200 Å) approximately 20 Å longer than skeletal TnT (Flicker et al., 1982).

The binding of TnT to TnI-TnC-Tm and Actin is regulated both by presence and absence of Ca^{2+} ions. The interaction of Tn-Tm complex inhibits actomyosin ATPase in the absence of Ca^{2+} and in the presence of Ca^{2+} ions accelerates the same reaction (Farah et al., 1994). This interaction is essentially mediated by the COOH terminal TnT2, but the cooperative activation requires TnT1(Schaertl et al., 1995). This interaction activates the cooperativity of Tn complex along with Tm overlap regions and actin in addition to regulation of ATPase in presence or absence of Ca^{2+} ions (Pearlstone and Smillie, 1982). Hence TnT plays an important role in maintain the cooperative regulation of thin filament that is crucial to muscle contraction.

TnT exhibits various isoforms in humans and other mammals distributed as fast skeletal TnT, slow skeletal TnT and cardiac TnT. In humans cardiac TnT is encoded by *TNNT2* gene produces isoforms by multiple variants by alternative splicing. The most common isoforms are TnT1, TnT2, TnT3 and TnT4. All the isoforms are expressed at foetus stage with TnT1 and TnT3 being predominant isoforms whereas during development TnT1 is lost and TnT3 remains predominant until adult stage. TnT4 and TnT2 are present in least abundance in myocardium (Gomes et al., 2002).

1.3.2.5 Troponin I (TnI)

TnI inhibits the muscle contraction in the absence of Ca^{2+} where it binds tightly to myosin binding region on the actin and thus inhibits muscle contraction. There are three TnI isoforms expressed in humans namely slow skeletal TnI (sTnI), fast skeletal TnI (fTnI), and cardiac TnI (cTnI) encoded by TNNI, TNNI2 and TNNI3 genes respectively. The difference in N-terminal region (Figure 1.9b) of 31 amino acids in the cTnI differentiates the isoforms from skeletal isoforms. This region contains the important phosphorylation sites, where it is found to be phosphorylated by protein kinase A (PKA) with aderenaline stimulation at Ser23 and Ser24 which causes decrease in overall Ca^{2+} sensitivity (Yuan and Solaro, 2008). TnI binds to TnC and TnI at C-termial region, and has two actin binding regions with one containing the inhibitory peptide and the second region containing the actin binding region at the C terminus (Solaro and Van Eyk, 1996). The binding region of actin is highly conserved containing residues from 96-116 in rabbit skeletal muscle which is found to be able to reduce actomyosin ATPase activity on its own with a maximum inhibition of 1:1 ratio to actin. However in physiological conditions, in presence of tropomyosin the distribution is of TnI is regulated by

cooperative ratio of 7: 1:1 to actin and tropomyosin-troponin. This cooperative distribution is one of the main characteristic feature of thin filament regulation which plays an important role in muscle regulation (Kobayashi and Solaro, 2005).

1.3.2.6 Troponin C (TnC)

Troponin C belongs to calcium binding protein family expressed by TNNC1 gene and is representative of calmodulin super family. TnC is 18 kDa protein found in both skeletal and cardiac tissues. Figure 1.10 shows the Ca^{2+} binding site in the ribbon structure of TnC.

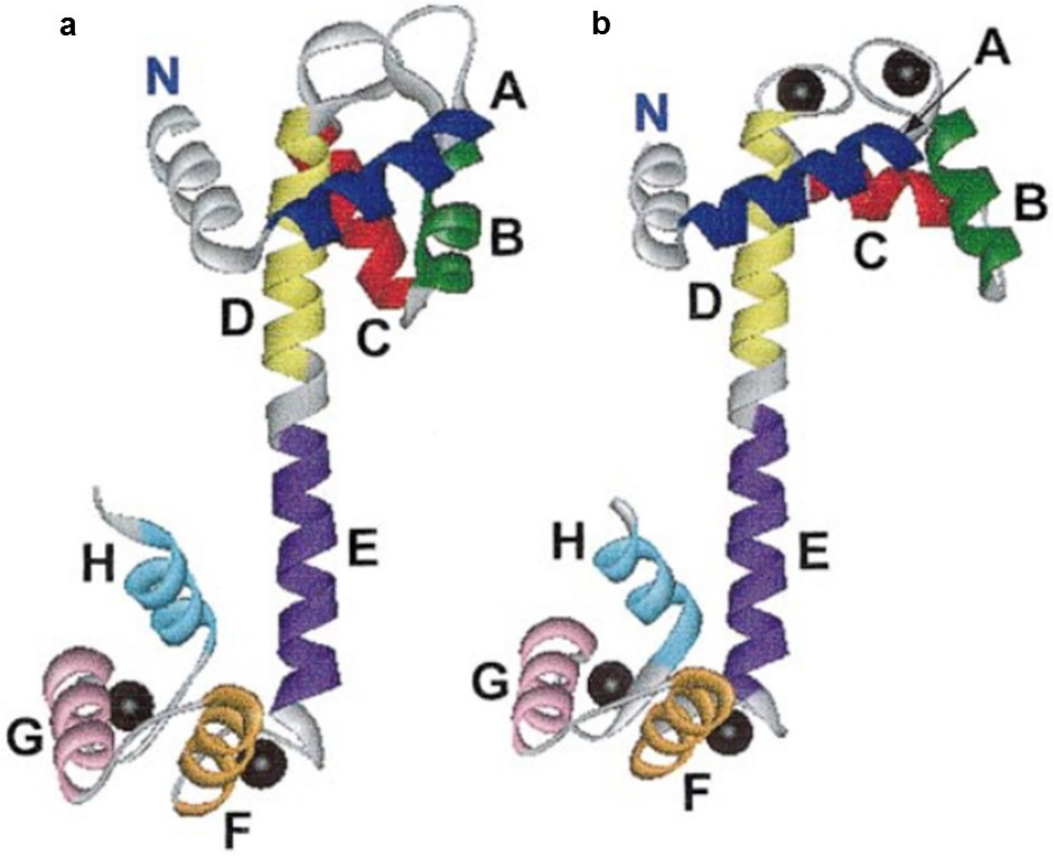

Figure 1.10: Ribbon structure of TnC. A. Turkey TnC with Ca^{2+} bound at C terminal (black solid circles) **B.** Rabbit skeletal TnC showing four Ca^{2+} bound at both N terminal and C terminal regions. Letters A –H are represented to show the orientation of the molecule. In B when the Ca^{2+} are bound at N terminal the orientation at C is more

perpendicular to E than in B whenre there is no Ca^{2+} bound at the position forming a E-F hand structure (Gordon et al., 2000; Houdusse et al., 1997).

TnC acts as a trigger for the initiation of muscle contraction in presence of when Ca^{2+} concentration reaches to a certain level accessible in the sarcomere. TnC is divided by two lobes, the C lobe that binds to a divalent metal ion usually Mg^{2+} in physiological conditions keeping the system in open state hence it is referred to as 'structural lobe' and the N lobe binds specifically to Ca^{2+} with higher selectivity than Mg^{2+} but has lower affinity to divalent ions than C lobe. It is referred to as regulatory lobe as it undergoes conformational changes when Ca^{2+} levels increases (Houdusse et al., 1997) forming an EF hand structure where the C region in Figure 1.10b is perpendicular to E. This kind of conformation change seems to be important for the interaction of TnC with the other Tn subunits. TnC isoforms are also distributed into skeletal TnC and cardiac TnC which is similar to slow skeletal TnC. cTnC differs from sTnC by having only single Ca^{2+} binding site at the N-terminal region (Gordon et al., 1997).

1.4 Muscle regulation-Cross bridge cycle

In striated muscle the binding of myosin heads to actin is mainly regulated by tropomyosin-troponin complex with Ca^{2+} activation of muscle contraction. Structural modelling of actin-tropomyosin interaction in presence/absence of myosin have given clear insight in explaining the positioning and conformations occurring in the Ac-Tm complex (Geeves et al., 2005).

When muscle contracts (shortens) the thick and thin filaments forms slide over each other to form actin-myosin cross bridges by the result of force generated by the cross bridge

linkage. Myosin ATPase activates the ATP molecule carried by myosin heads and when this is hydrolysed energy is used to power the muscle. The ATPase is activated by actin and inhibited by ADP and Pi (Lymn and Taylor, 1971). Myosin heads maintains two angles with the actin filament, 90^0 and 45^0 throughout the cycle. As shown in Figure 1.11, Starting from a- rigor state ATP binds to the myosin head and dissociate it form the actin filament, and the myosin moves away from the filament (b). The binding of ATP is followed by hydrolysis to ADP + Pi and the myosin head is weakly bound (c), strongly bound (d) and followed by rigor force generated by the movement of myosin and producing sliding movement of actin over myosin shortening the muscle filaments (contraction). The cycle completes when ADP (f) is released and the continued by addition of ATP (a) to continue the cycle of events (Geeves et al., 2005). Recently Desai et al., (2014) using single molecule imaging techniques propose that two myosin heads are required to activate thin filament which will enable the binding of consecutive binding of 11 myosin heads during initial stages of muscle contraction.

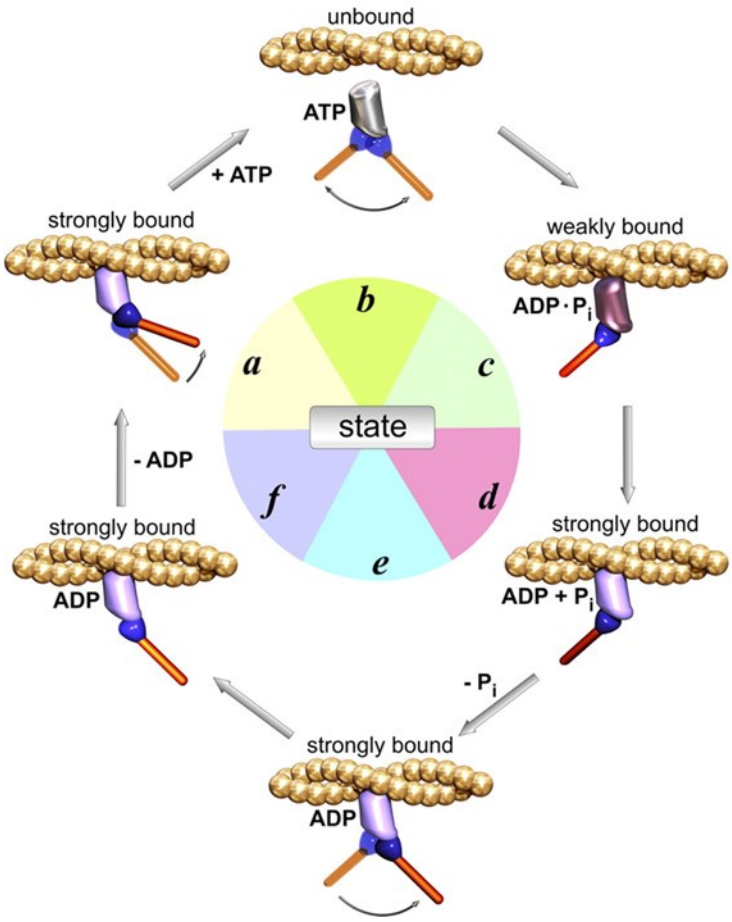

Figure 1.11: Cross bridge cycle. Starting from a- rigor state ATP binds to the myosin head and dissociate it form the actin filament, and the myosin moves away from the filament (b). The binding of ATP is followed by hydrolysis to ADP + Pi and the myosin head is weakly bound (c), strongly bound (d) and followed by rigor force generated by the movement of myosin and producing sliding movement of actin over myosin shortening the muscle filaments (contraction). The cycle completes when ADP (f) is released and the continued by addition of ATP (a) to continue the cycle of events (Geeves et al., 2005).

1.5 Three state model

The biochemical interactions occurring during muscle regulation are explained by three-state steric blocking model proposed by McKillop and Geeves (1993). According to this model, in the absence of Ca^{2+} tropomyosin physically blocks myosin from binding to actin. As shown in Figure 1.12a, the structural unit of the thin filament with 7 actin monomers (open circles) connected by tropomyosin represented as a blue straight line. The Ac-Tm-Tm unit always exists in dynamic equilibrium within the three states depending on the position of the Tm over the actin.

The equilibrium constant K_B exist between the blocked state (Figure 1.12a), where myosin (S1- represented a cone) binding does not occur in the absence of Ca^{2+} and the closed state. K_1 is the binding constant with S1 binding partially to the actin but there is no force generation at this state, and K_T exists between closed and open states, which depends on the number of S1 heads bound to actin sites. In presence of Ca^{2+} Tm moves, exposing the acting binding sites to allow S1 to bind to actin forming an A state with a rate constant of K_1 as seen in Figure 1.12a during open state (S1 binding at 90^0 to the actin unit).

K_2 (Figure 1.12a open state) determines the isomerisation of S1 to rigor-like state (R state) to form force generating cross-bridges with actin during contraction (S1 binding at 45^0). In the absence of Ca^{2+} the equilibrium returns back to blocked state. This model has been supported by others with different ionic strengths of actin and S1 units (Maytum et al., 1999, Geeves & Lehrer, 1994) and Moraczewska et al., (1999) showed that the length of Tm is important for the cooperative unit size of the actin and maintenance of equilibrium between open and closed states in contrast to McKillop and Geeves (1993).

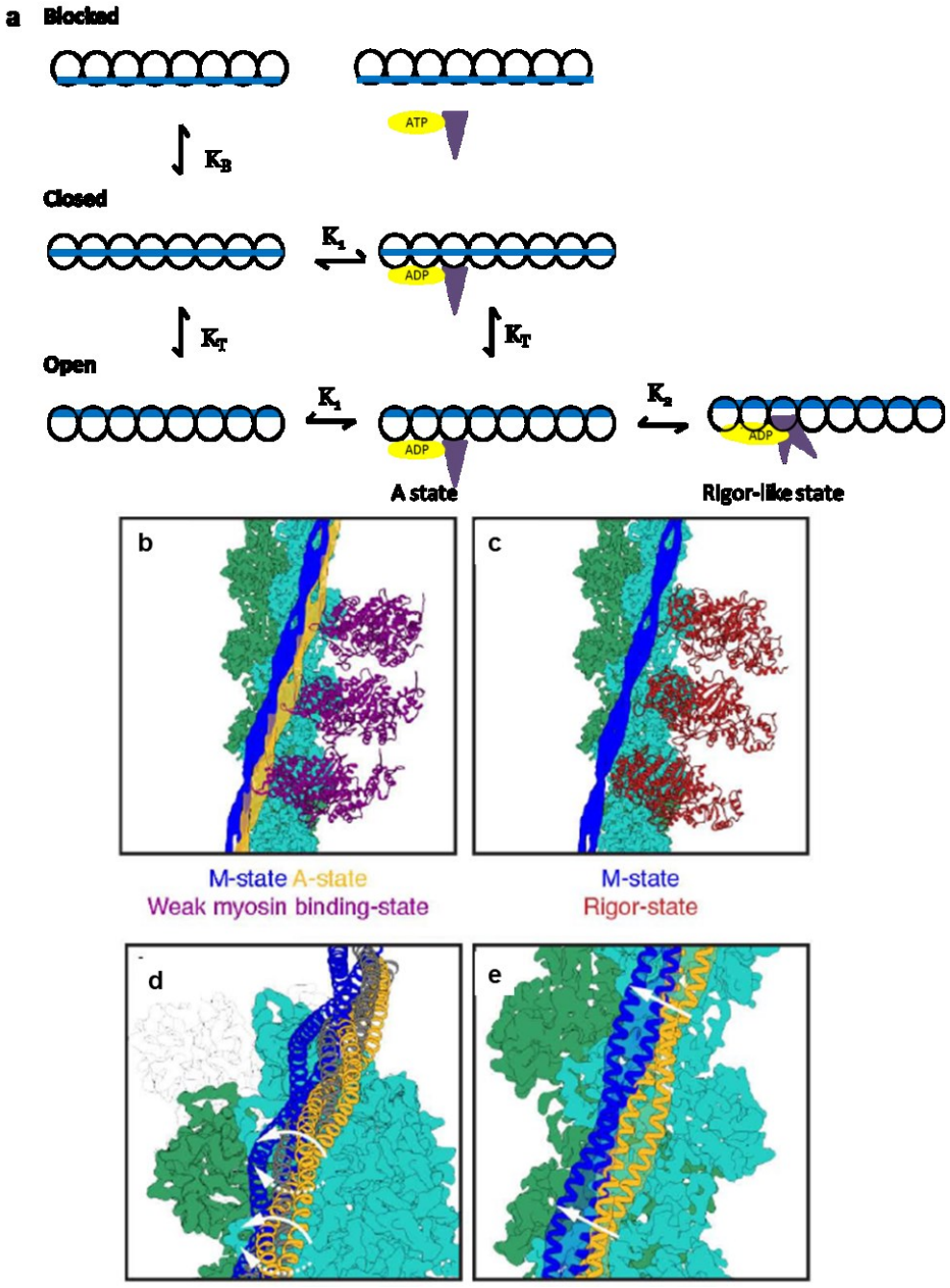

Figure 1.12: Three state model for muscle regulation. A. The three state steric blocking model adapted from McKillop and Geeves (1993) and Maytum et al., (1999). K_B – equilibrium constant between blocked/closed state, K_T – equilibrium constant between closed/open states K_1 – binding constant to the open/A state where myosin (S1) is partially bound to actin and K_2 the equilibrium between A/R states with S1 forming strongly bound crossbridges with actin to generate force. **B** and **C**. Cryo EM structure of A/M rigor -state from three state model, **D and E**. possible tropomyosin movement on actin filament during the M state, where in D the tropomyosin rolls or slides as in E (Ecken et al., 2014).

From the very recent studies it is now clear that tropomyosin does not bind to actin as a rigidly but rather but rather lay along actin in the groves in a semi rigid manner (Li et al., 2011). They overlap with each other in a head-to tail manner (Holmes and Lehman, 2008; Murakami et al., 2008). Recently Ecken et al., (2014) produced models of A state and M state of three state model using Cryo-electron microscopy. Figure 1.12b and c show the movement of tropomyosin in A state and M (R) state and suggest that tropomyosin may roll over the actin (Figure 1.12d) or slide (Figure 1.12e). Rotation would shift tropomyosin with an azimuthal rotation of ~16Å with a ~70Å left handed rotation of tropomyosin and sliding would have the azimuthal rotation of ~13Å in addition to a shift of half –tropomyosin repeat, only when tropomyosin is linked end to end with the N/C terminal overlap.

1.6 Diseases related to muscle dysfunction

Regular functioning of heart is essential for survival of organism due to changes in the work load or to adjust to the environmental conditions heart undergo adaptation process to meet the demands for the changes. In pathological conditions similar adaptations takes place continuously trying to maintain normality. This compensation effect for longer period of time results in cardiac diseases that may be fatal to the individual. The severity of the symptoms depends on whether the adaptation is a short term or a long term adaptation (Meerson and Breger, 1977).

Cardiomyopathies, group of heart disorders, are caused due to adaptation in the heart muscle. As shown in Figure 1.13 there are two basic types of cardiomyopathy, those that cause a thickening of the muscles – hypertrophic cardiomyopathies (HCM), and those where muscle is lost – dilated cardiomyopathies (DCM).

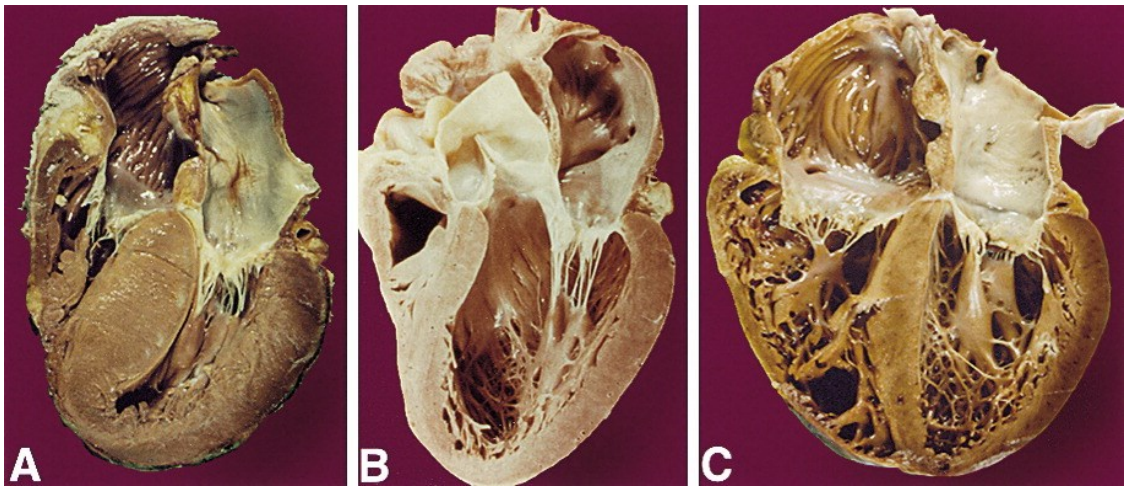

Figure 1.13: Normal (B), Hypertrophic (A) and Dilated (C) hearts. The hypertrophic heart shows thickening of the muscle, most significantly in the left ventricle wall and septum (dividing the two ventricles), decreasing the ventricular volume. In dilated cardiomyopathies, there is loss of muscle and the ventricular volume is increased (Seidman and Seidman, 2001).

1.7 Causes of cardiomyopathies

Most of the mutations causing cardiomyopathies are due to missense mutations mainly in MyBP-C, myosin heavy chain and myosin light chain mutations and mutations in geners encoding actin, troponin complex proteins and tropomyosin. A few are caused due to insertions or deletions or by alternate splicing. The mutant proteins are incorporated into the cardiac myofilament causing the genotypic and phenotypic variations in the heart (Seidman and Seidman, 2001). Hypertrophic cardiomyopathy can be caused by a variety of factors. HCM is characterized as enlargement of cardiac muscles with increase in size of the ventricular wall thickness (from >5mm to 30mm) (Gordon et al., 2000; Tardiff, 2011) to its original size (Figure 1.13). Simple hypertrophy of the heart may result as a response to exercise (athlete's heart) and this is not clinically significant. However

hypertrophy may also result due to the effects of disease. This can be a secondary effect, compensating for effects upon the circulatory system, but also as a genetically inherited disease (Familial Hypertrophic Cardiomyopathy, FHC) caused by mutations in the sarcomeric proteins (thin and thick filament) . Mutations in the genes encoding the cardiac contractile proteins are also responsible in dilated cardiomyopathies (Seidman and Seidman, 2011).

Heart adaptation results in physiological changes to the heart. These can change the mass and type of tissue present and can change tissue properties through post translational modification of proteins and genetic adaptations that change the isoforms of the protein expressed. Adaptations may lead to cardiac disease or vice versa. Adaptations occur to adjust to the physiological demands on the heart (Tardiff, 2011; Yuan and Solaro, 2008)

FHC can also describe mutations in sarcomeric proteins that lead to sudden cardiac death (SCD). However the degree of hypertrophy is not always linked to the incidence of SCD for all mutations, making diagnosis more difficult. Athletes and young children with high demands of physiological activity who have undiagnosed asymptomatic HCM are at high risk of SCD.

The diseases associated with the cardiomyopathies are related with mutations in both thick and thin filament proteins of the sarcomere.

1.8 Thin filament diseases

Thin filament mainly consists of actin, troponin (TnI, TnC, TnT), tropomyosin. A variety of mutations occurring in thin filament have been reported that causes different types of cardiomyopathies. There is a lot of literature available in case of Troponins and especially TnI (Peng et al., 2013; Seidman and Seidman, 2011; Tardiff, 2011). Alpha Tm is found to cause FHC due to altered contractile function with Asp175Asn mutation and is reported to lead to severe dilated cardiomyopathy (DCM) (Prabhakar et al., 2001; Regitz-Zagrosek et al., 2000; Thierfelder et al., 1994). There are few mutations relating to actin alone that cause cardiomyopathies. Mutations in actin are linked to DCM in some cases identified by two mutations in actin Glu361Gly and Arg312His and the incident of HCM with actin mutation alone is found to be very rare (Seidman and Seidman, 2001; Tardiff, 2011).

Mutations in beta-Tm (βTm) and gamma Tm (γTm) cause nemaline myopathy (NM) along with mutations occurring in actin, nebulin and troponin. NM is accompanied with electron-dense rods in skeletal muscle. The main cause of the mutation is found in the γTm / *TPM3* gene present in slow-twitch skeletal muscle (Durling et al., 2002, Clarkson et al., 2004). Mutations in *TPM3* gene are also been associated with neuromuscular transmission defect in congenital myopathy, chronic leukaemia and over expression of *TPM3* have been linked with heptatocellular carcinoma in humans. Congenital myopathy with fibre type disproportion (CFTD) associated with mutations in *TPM3* gene along with selenoprodin N, skeletal muscle α-actin and skeletal muscle rynanodine receptor (Li et al., 2011a; Nance et al., 2012).

1.9 Disease causing protein modifications

The post-translational modifications (PTMs) of sarcomere proteins affect the structure and function of proteins resulting in shifts in isoform populations, forming degradation products, addition or deletion of protein availability, altered protein expression, availability of Ca^{2+} ions and ATPase activity (Tardiff, 2011b; Zhang and Ge, 2011b). Cardiac proteomics presents the next level in understanding cardiac disease and adaptation, where the physiological changes and genetic mutations taking place in the heart responsible for cardiac adaptations can be explained in terms of the changes occurring in sarcomere at the protein level. These changes are being identified using advanced techniques of mass spectrometry for protein isoform identification, PTMs and protein interactions (Arab et al., 2006a; Arrell et al., 2001a; Peng et al., 2010; Peng et al., 2014a; White and Eyk, 2007). Some progress in this area has already been made with Ge et al., (2009a) used top-down high resolution mass spectrometry analysis to characterize cardiac myosin binding protein-c phosphorylation sites. The phosphorylation sites of rat cardiac troponin have been reported by Solis et al., (2008) by top-down MS using electron capture dissociation ionisation.

1.10 Aim of this study

The general aim of this study is to quantify tropomyosin isoforms with various techniques in different scenarios. First attempt is to express Tpm3.12st isoform in *E. coli* and characterise its actin binding properties using co-sedimentation assays. Three variants of Tpm3.12st are produced with additional small amino acid residues to mimic the N-terminal acetylation of the protein. This will enable to investigate this isoform

affinity to actin in comparison with other muscle isoforms (Tpm1.1st, Tpm2.2st and Tpm4.1cy).

Second aim is to use tropomyosin recombinant proteins to study the effect of each tropomyosin isoform on actin polymerisation dynamics in order to understand the actin polymer association as tropomyosin exhibit different properties in various tissues (Gunning et al., 2008a).

Third objective was an attempt to design a monoclonal antibody specific to human Tpm3.12st sequence to use for identification of this isoform in tissues and cells. The present antibody used for Tpm3 is CG3 (Lin et al., 1985) which identifies all Tpm3 isoforms, both high molecular and low molecular weight isoforms.

And finally, a novel method was developed to extract thin filament proteins from muscle tissue (skeletal and cardiac) and other soluble proteins for separation and identification of these proteins using reverse phase liquid chromatography (RP-HPLC). This method when integrated with mass spectrometry would be potentially used to quantify thin filament protein isoforms and their post translational modifications which will provide information on the protein composition and ratio of isoform composition.

Chapter II

Expression and Characterisation of Human Tropomyosin 3 (Tpm3) isoform 12.st in *Escherichia coli*

&

Effect of Tropomyosin Isofroms on Actin Polyerisation

2 Introduction

Tropomyosin is a significant component of thin filament and has multiple roles in regulating actin filaments in tissues and cells. Tropomyosin is α-helical dimer protein, polymerizes head-tail to form a continuous filament along the grooves of actin filament (Gunning et al., 2008a). The head to tail association along the length of protein is important for actin binding (Hitchcock-degregori, 1993). As mentioned in chapter I tropomyosin with troponin complex form a Ca^{2+} sensitive switch that regulates muscle contraction. Crick (1952) suggests that helical coils are present in the form of heptad repeats with hydrophobic amino acids every first and fourth residues forming the hydrophobic core. The hydrophobic interactions of amino acids in proteins play major role in the stability and three dimensional structure of proteins. Alteration in the positioning of hydrophobic core amino acids affects the stability of the proteins. Tropomyosin structure is extensively studied as it is the first α-helical coiled coil protein where its amino acid sequence was determined (Kwok and Hodges, 2004; Parry et al., 2008).

Tropomyosin is a two-stranded α-helical coiled coil protein characterised by a heptad repeat, the positions denoted as "abcdefg" with hydrophobic amino acids positioned at **a** and **d**. These non-polar amino acids initiates the formation of a left handed α-helical coiled structure from two right handed helical coils to form a dimer tropomyosin α-helical coiled coil structure Figure 2.1B. The term 'coiled coil' is referred to the structures that are wound together into super helical coils as exhibited by tropomyosin molecule shown in Figure 2.1A. The positions **e** and **g** are occupied by oppositely charged acidic and basic amino acids which interact with the other filament of the dimer to form salt bridges supporting the α-helix stability. The outer amino acids **b**, **c** and **f** are occupied either with ionic or polar amino acids forming the external hydrophilic surface (Perry, 2001; Zhu et al., 1993). In two stranded tropomyosin helical coil, the hydrophobic **a** and **d** positions of the opposite coil lie perpendicular interacting with each other (**a**-**d** and **a'**-**d'**) as shown is Figure 2.1B. Due to the variation in the distance of the carbon bonds between **a** and **d**, position **a** usually have isoleucine, valine and threonine and the position **d** usually have leucine and alanine at its hydrophobic core. The interactions of hydrophobic core **a** and **d** residues are critical for stability of the coiled coil (Zhou et al., 1992)**.** The relationship between the increase in the hydrophobicity of the residues at **a** and **d** is directly proportional to the increase in the stability of the hydrophobic core of the coil (Kovacs et al., 2006). However, sometimes destabilizing clusters are also present at the hydrophobic core such as alanine, lysine, aspartate, cystein, proline, arginine and few others (Kwok and Hodges, 2004). Tropomyosin is considered to have both stabilizing and destabilizing regions where few hydrophobic positions at **a** and **d** are occupied with polar or ionic amino acids. These regions of

stability associated with destabilizing position at hydrophobic core gives tropomyosin structure its unique stability (Kirwan and Hodges, 2010).

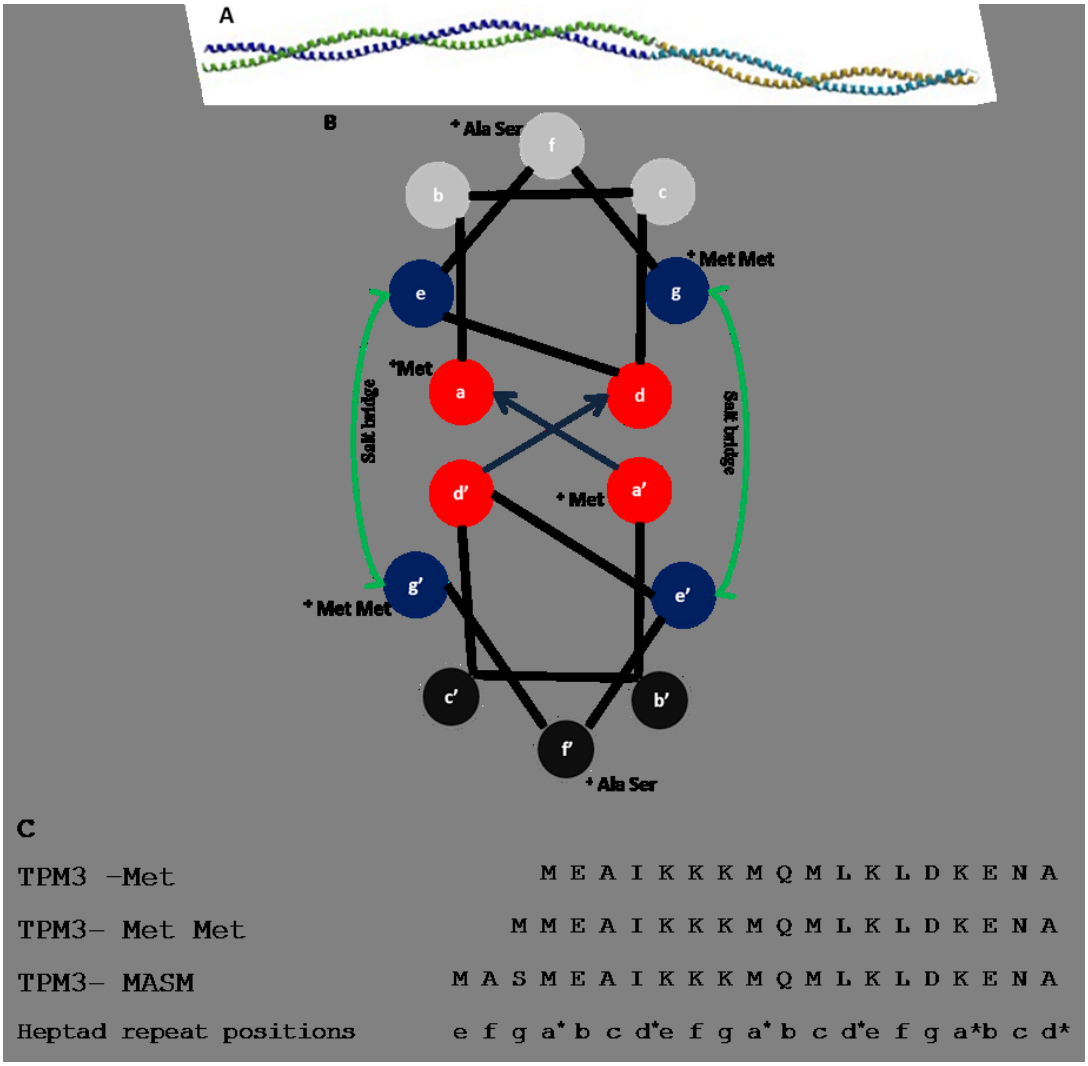

Figure 2.1: Heptad repeat arrangement of tropomyosin αhelical coil: A. α-helical coiled coil tropomyosin (RSBC-PDB). B. Cross-section view of alpha helical chain showing seven residues (a-g). a and d are hydrophobic which keeps coiled coil stable with the help of salt bridges between e and g and also showing the position of charge transferred when additional amino acids are added to the N-terminal of a recombinant proteins that are used to produce for this study. The figure shows the position of additional amino acids added at the N-terminal of the recombinant proteins used in this study C. Shows the initial N-terminal amino acids of the protein sequence and their position in the alpha-helical model. *shows the position of hydrophobic core residues.

2.1 Tropomyosin expressed in *E. coli* and N-terminal methionine acetylation

N-terminal acetylation of a protein is the addition of acetyl group to the α-amines of the N-terminal amino acid in the sequence or the amines of the lysine side chains. The acetylation alters the reactive amine group to unreactive amide carrying no charge at the end. This change in the N-terminal sequence changes the steric arrangement and stability of the protein structure and 80% of proteins undergo this modification (Phillips, 1963).

The process of N-terminal methionine or acetylation is an enzymatic activity catalyzed by methionine aminopeptidase (MetAps) and N^{α} acetlytransferase (NAT) and is found to be a co-translational process. The removal of the N-terminal-Met is determined by the adjacent amino group to the methionine. The smaller amino residues Alanine (Ala), Valine (Val), Serine (Ser), Threonine (Thr), Cysteine (Cys), Glycine (Gly) and Proline (Pro) are targeted by the MetAps for acetylation and if there is any larger groups present the N-terminal-Met is retained and not acetylated (Bradshaw et al., 1998) which is due to the steric hindrance deduced from crystal structure of MetAps (Lowther and Matthews, 2000). On the other hand, NAT catalysis is carried out by the NAT complex and is classified into 3 groups, Nat A, B and C. NAT show the same principle of N-terminal-Met with only limited residues of specificity with glycine, alanine, serine and threonine (GAST substrates) at the downstream of the amino acid chain. Although there is a requirement of smaller amino residue adjacent to N-terminal-Met, there is difference in the tolerance of the different classes of these MetAps and NAT complexes *E. coli* lacks these Nat complex (Xiao et al., 2010).

Tropomyosin synthesized in eukaryotes is acetylated at its N-terminal methionine as a posttranslational modification to perform its function in binding to actin and regulate

muscle contraction along with troponin complex. Tropomyosin amino acids at the N-terminal and C-terminal ends play crucial role in head-tail association of the protein and for binding to actin filament. The first and last 9-11 amino acids at the N-terminal and C-terminal form an overlap region and disruption of this region lowers the affinity to actin filament (Cho et al., 1990; Urbancikova and Hitchcock-DeGregori, 1994). Urbancikova and Hitchcock-DeGregori (1994) postulated that in order for co-operative binding of tropomyosin to actin, the N-terminal methionine should be modified to an amide or the N-terminal amino acid in fusion protein should be in a peptide bond.

Skeletal tropomyosin expressed in *E. coli* is found to have 30-fold weaker binding to actin than the native protein isolated from striated muscle. The difference is that the methionine at the N-terminus of the sequence is not acetylated in the protein produced in *E. coli* (Heald and Hitchcock-DeGregori, 1988; Maytum et al., 2001; Monteiro et al., 1994; Moraczewska et al., 1999; Palm et al., 2003). It is known so far that the acetylation of methionine helps in maintaining the stability of Tm helical strands and its high affinity for actin in presence of troponin. However, it is thought to protect the proteins from degradation by N-terminal proteases. In contrast, according to Hwang et al., (2010) and Kim et al., (2013) N-terminal polyubiquitylates creates degradation signals called N-degrons that cause degradation of destabilizing N-terminal residue of the protein in *Saccharomyces cerevisiae*.

Escherichia coli is widely used to produce the recombinant tropomyosin to study the properties and characterization of the proteins. *E. coli* is one of the extensively used prokaryotic organisms in research and commercial use for genetic manipulation and recombinant protein expression and production. Because of its advantages in inexpensive

carbon source, easy scale-up and its rapid collection of biomass, *E. coli* has become one of the most commonly used expression systems. However, proteins produced in prokaryotes do not undergo post-translational modifications such as phosphorylation, acetylation and methylation (Baneyx and Mujacic, 2004).

To make functional recombinant proteins in *E. coli,* addition of small amino acids at the N-terminus mimics the N-terminal acetylated function of native tropomyosin. Heald and Hitchcock-DeGregori (1987) produced fusion recombinant α-tropomyosin with additional 80 amino acids at its N-terminal which did bind to actin but was incapable of polymerizing and regulating the actomyosin ATPase. Monteiro et al., (1994) showed that by adding two or three aminoacids at the N-terminus of chicken skeletal tropomyosin produces native like protein. The recombinant proteins retained function of actin binding capacity, polymerises in a cooperative manner and also regulates ATPase activity during muscle contraction. Maytum et al., (2000) verified the work of Monteiro's work in yeast tropomyosin produced in *E. coli* and also demonstrated that small changes in N-terminal sequence maintains the actin binding property, however it affects the actomyosin regulation by changing the apparent equilibrium constant between open and closed states. This in turn affects the conformation of Tm on actin and the availability of actin binding sites to myosin during muscle regulation. Coulton et al., (2006) showed that unacetylated αTm of smooth muscle does bind to actin, however the recombinant αTm expressed in *E. coli* where Ala Ser peptides were added to mimic the acetylation have ~100 fold increase in affinity to actin. Maytum and Konrad (2006) developed a system with yeast NatB acetylation complex co-expressed with α-tropomyosin in *E. coli* and recently Johnson et al., (2010) validated the expression system by successfully co-expressing

yeast NatB acetylation complex with mammalian α-tropomyosin *E. coli* but with varying levels of acetylation.

2.2 Effect of Tropomyosin isoforms on actin polymerization

Actin is a filamentous protein that provides cells mechanical support and is responsible for cell movement. Actin in cellular processes is also involved in sensing surrounding environment and cell division and intercellular movements (Pollard and Cooper, 2009). Approximately 400 genes encode actin in all the biological organisms and the eukaryotic cytoskeleton has been evolved from prokaryotes showing highly conserved amino acids between the species even though they have divergent sequences (Erickson, 2007). Actin is one of the most abundant proteins on earth as it is found at a high cellular concentration in all organisms. Actin was discovered in muscles in 1940s which plays major role in muscle contraction along with other motor protein myosin (Richards and Cavalier-Smith, 2005). All eukaryotes have genes for actin and genes for the actin binding myosin protein which produces force to actin filament generating movement through hydrolysis of ATP (Erickson, 2007).

In vivo and *in vitro* studies showed that actin forms spontaneous filaments from actin monomers by hydrolysis of ATP and many other proteins are involved in the polymerisation and regulation of actin as shown in Figure 2.2 (Pollard and Borisy, 2003; Pollard and Cooper, 2009). The conserved sites present in all the actin molecules both in eukaryotes and homologs in prokaryotes were found to be the amino acids involved in binding of ATP and the once involved in filament formation were not conserved (Richards and Cavalier-Smith, 2005; van den Ent et al., 2001).

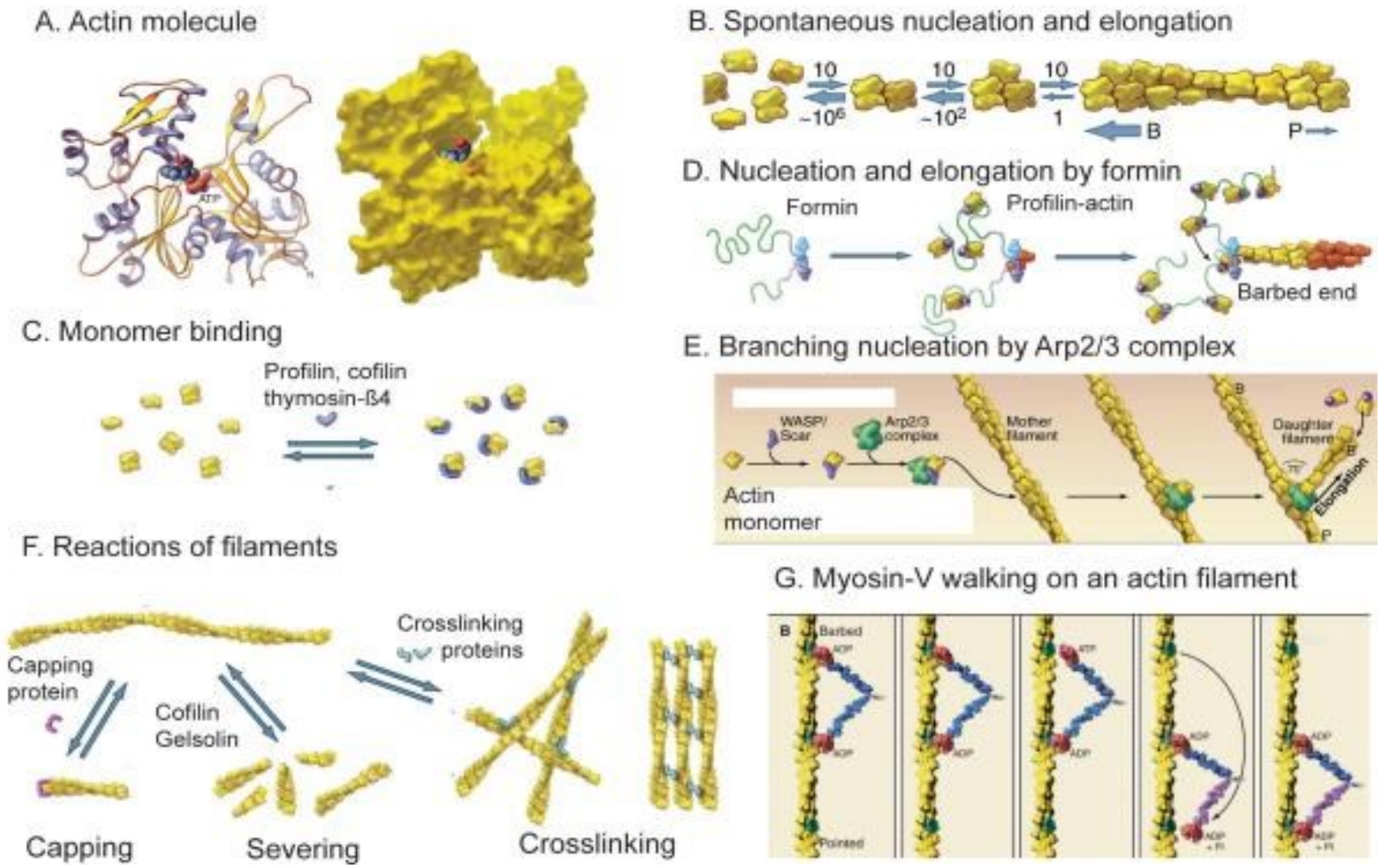

Figure 2.2: Structure of actin, filament formation and regulation processes. A. Ribbon model and space filling model of actin molecule. B. Filament formation of actin showning nucleation and elongation process. C. Monomer actin binding proteins – Prolifin, cofilin and thymosin-ß4. D. Nucleation and elongation by formin. E. Regulation of actin by Arp2/3 complex, F. Filament reactions occurring in actin , G. Myosin-V walking on the actin filament (Pollard and Cooper, 2009)**.**

2.2.1 Actin binding proteins and filament formation

Actin filament formation is one of the essential processes for the contractile structures in many organisms. The polymerisation of actin is initiated spontaneously to form a nucleus (Figure 2.2 a and b) which is a very slow process, but once the filament is formed the elongation process is quite rapid as long as the monomer concentration is constant until it reaches a steady state where polymerisation completes at which point no net actin polymerises (example polymerisation curve shown in Figure 2.5) (Pollard and Cooper, 2009). Monomers are added to both sides of the filament, however polymerisation is faster on barbed end than the pointed end. The actin polymer is a helical polar structure as all the monomers in the filament are pointed in the same direction. The association of monomeric actin is associated with hydrolysis of ATP to ADP which is incorporated with the filament actin (Straub and Feuer, 1950). Filament actin bound to ADP continue polymerisation process but the rate at which the polymerisation occurs is five times slower than ATP bound actin (Cooke, 1975). It is also stated by Cooke (1975) that ATP hydrolysis of actin nucleotide complex is not the only factor that initiates polymerisation of actin.

Many accessory proteins are involved in maintaining the availability of monomers, initiation, polymerisation, regulate the length of actin filament and the turnover of actin filaments depending on the requirement of the system, for example more than hundred accessory proteins are involved in actin regulation process in eukaryotes (Richards and Cavalier-Smith, 2005). Examples of the accessory proteins that are involved in actin polymerisation are shown in Figure 2.2. Thymosin ß4 which blocks the assembly of actin

monomers by binding to ATP, profilin inhibits nucleation and pointed-end elongation of filament, but not barbed end elongation (Figure 2.2b). Nucleation promoting factors (NPF) such as WASp (Wiskott-Aldrich Syndrome protein) bind to actin monomer along with actin related protein -Arp 2/3 complex and formins (Figure 2.2e) (Pollard, 2007) to bind to already existing filament competing with profiling which prevents monomer to bind to filament at barbed end. Arp 2/3 complex promotes elongation until capping protein stops the growth of the filament. Formins found in the actin bundles of cytokinetic contractile structures and filopodia, remains associated with the filament ends at the barbed end preventing the capping proteins to stop elongation (Wallar and Alberts, 2003). Cofilin is another protein that binds to NPF proteins and initiated nucleation. Other proteins called capping protein such as tropomodulin binds to tropomyosin bound actin and caps the filament at the pointed end to stop filament elongation (Weber and Pennise, 1994). Cofilin along with gelsolin break the actin filaments into fragments which are formed into crosslinks by crosslinking proteins (Figure 2.2f) (Pollard and Cooper, 2009; Richards and Cavalier-Smith, 2005).

2.2.2 Actin polymerisation kinetics

Actin polymerisation has been studied from many years. The first studies focusing on actin polymerisation kinetics were developed by Oosawa and Asakura (1975). Later on Wegner and Engel (1975) described the process focusing on the importance of the kinetics involved in nucleation and elongation during polymerisation measured using light scattering and microscopy. According to the theory, actin polymerisation is initiated by the result of nucleation and elongates with continuous binding of actin monomers to

the ends of filaments. Nucleation consist of aggregation of few monomer units forming a dimer, trimer or a tetramer forming a small filament and elongation occurs by sequential addition of monomers on either side of the actin filament. The rate constants of the steps involved in association and dissociation of monomers were found to be similar in contrast to the nucleation step which was very low, and shows that this step is really slow to start.

According to Wegner and Engel (1975) the preliminary aggregate of size n-1 forms rapidly and is capable of dissociation at the same rate, hence is always in equilibrium with the monomer instead of initiating a polymer formation. The filament growth is initiated when the aggregate formed is stable enough to add more monomers and form a filament when the concentration of monomer reaches a steady state (critical concentration of unpolymerised actin). In simple terms the polymerisation reaction can be shown in the equation below

$$[Ac_G] + [Ac_G] \underset{k_d}{\overset{k_a}{\rightleftharpoons}} [A_{F+1}] \qquad (1)$$

Where Ac_G is G-actin and Ac_f is F-actin, k_a and k_d are association and dissociation constants. When k_a is greater than k_d polymerisation occurs, when k_a is equal to k_d the system is stable and when k_d is greater than k_a depolymerisation occurs.

In biological systems polymerisation happens at both ends of the filament (Oosawa and Asakura, 1975). The equilibrium constant for binding of monomer to a polymer at both the ends is similar as it leads to the formation of same polymer (Wegner, 1976). Even though the association and dissociation constants at both ends may not be similar,

however the ratio of the rate constants for both these reactions should be same as shown in equation 2.

$$K = \frac{k_a}{k_d} = \frac{k_{a'}}{k_{d'}} \qquad (2)$$

Where k_a and $k_{a'}$ are the association constants of barbed end and pointed end respectively and k_d and $k_{d'}$ are the respective dissociation constants.

The critical concentration (c) in this case can be calculated using equation 3 (Tobacman and Korn, 1983).

$$c = \frac{k_+}{k_-} \qquad (3)$$

Where k_+ is the sum of the rate constants of association and k_- is the sum of the dissociation constants at both ends of the filaments.

The rate of polymerisation (dA_p/dt) can be given by the equation (4).

$$\frac{dA_p}{dt} = \frac{dA_m}{dt} = k_+ F A_m - k_- F = k_+ F(A_m - A_m^{\infty}) \qquad (4)$$

Where A_m^{∞} = k_+ / k_-, which is the concentration of monomeric actin at steady state (critical concentration) and A_m is the concentration of monomeric (G) actin, k_+ is the sum of rate constants of monomer addition and k_- is the sum of dissociation of monomer actin at both the ends of the filament, F is the concentration of polymer, F actin (Tobacman and Korn, 1983; Wegner, 1976).

The rate of nucleation can be expressed as in Equation 5, which is the rate of change in number of filaments per unit volume (Wegner, 1976).

$$\frac{dF}{dt} = K_{n-1}\, k_{+}(A_m)^{n-1}(A_m - A_m^{\infty}) \qquad (5)$$

Where, K_{n-1} is the association constant in relation to the concentration of monomer with the aggregate of size n-1.

Equation 4 and 5 together are inter-related which can be used to predict the rate of actin nucleation and polymerisation. Integrating the numerical values in these equations would generate polymerisation curves that depend on the size of the nucleus, monomer actin concentration and critical concentration of monomeric actin.

Apart from forming filaments, end-to-end association of actin filaments and spontaneous fragmentation also happen in natural physiological conditions creating more nucleation sites for polymerisation to proceed which changes the kinetics of the polymerisation reaction (Wegner, 1982a).

2.2.3 Actin nucleation kinetics

Nucleation is the process of formation of aggregate that forms the basis for the filament to elongate (Wegner and Engel, 1975). Formation of nucleus is the very first step in actin polymerisation which leads to elongation. Nucleus formation is considered unfavorable followed by favorable rapid elongation process. There are lots of studies pursued to interpret the correct actin polymerisation dynamics. Sept and McCammon (2001) studied kinetics of actin filament nucleation using thermodynamic Brownian dynamics (BD) uses

advance simulation technique to predict protein association rates. According to them the formation of nucleus is entropically unfavorable agreeing with physiological studies previously (Frieden, 1983a; Frieden and Goddette, 1983b; Tobacman and Korn, 1983; Wegner, 1976; Wegner and Engel, 1975). Cardilli and collaborators (2009) proposed composition algebra models to show geometric representation of actin polymerisation dynamics. Frieden (1983b) and Cooper et al., (1983a) showed a scheme of association and dissociation constants for each step of polymerisation – nucleation , elongation and steady state dynamics as shown in equations i - viii. Step and McCammon (2001) predicted the favorable pathway for polymerisation from initiation of nucleus to the elongation process as shown in the Figure 2.3 in agreement with Frieden and Goddette (1983a) and Cooper et al., (1983a) that the nucleus undergoes a conformational change in order to bind additional monomer to form a filament, like binding to a salt ion like Mg^{2+}. From all the above mentioned studies the formation of a trimer is the critical nucleus that is favorable to proceed to elongation. However Tobacman and Korn (1983) proposed that the critical stable nucleus to proceed to polymer is a tetramer.

i. $A + A \rightleftharpoons A_2$

ii. $A_2 + A \rightleftharpoons A_3$

iii. $A_3 + A \rightleftharpoons A_4$

iv. $A_4 + A \rightleftharpoons A_5$

v. $A_5 + A \rightleftharpoons A_6$

vi. $A_6 + A \rightleftharpoons A_n$

vii. $A_n + A \rightleftharpoons A_{n+1}$

viii. $A_n \rightarrow 2A_n$

In the above equations, i is the initiation of nucleus forming a dimer and vii is the elongation step and viii is the fragmentation step. The rate constants of each step are given in the Figure 2.3 adapted from Tobacman and Korn (1983) and Sept and McCammon (2001).

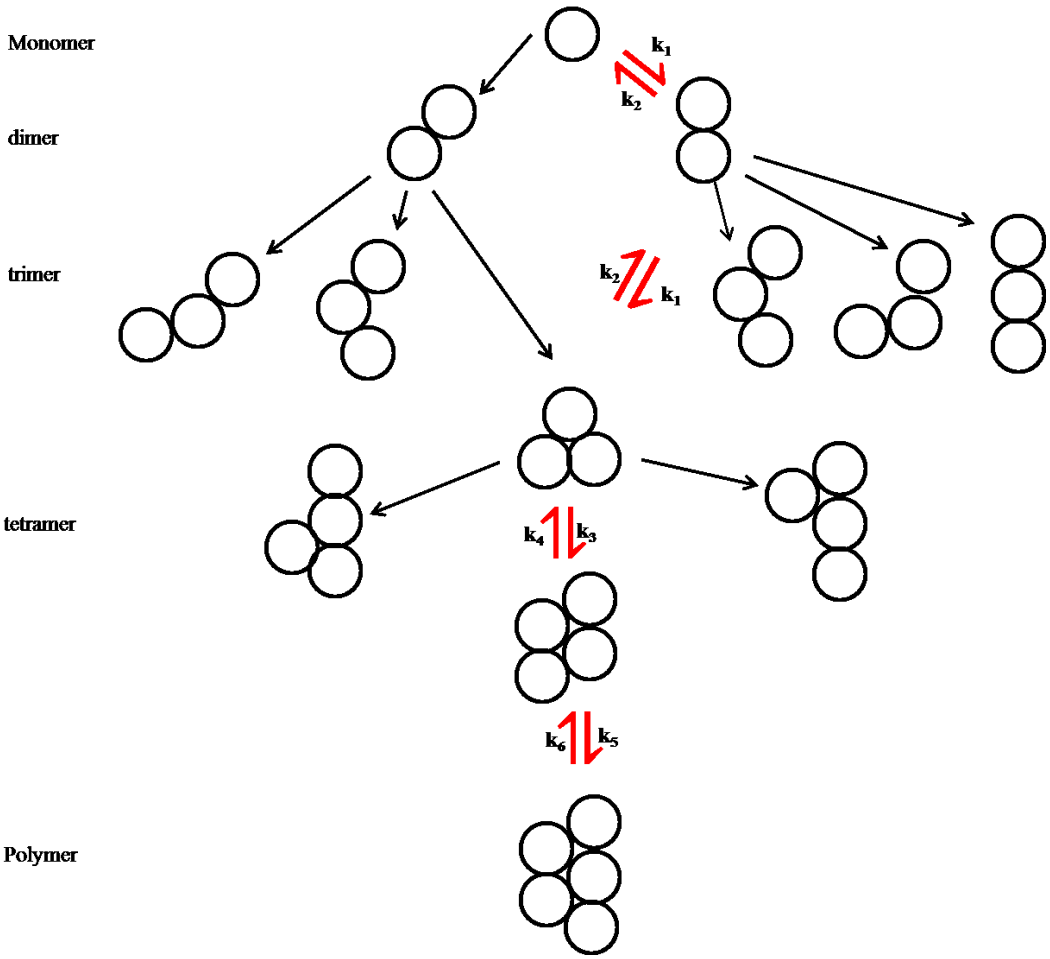

Figure 2.3: Actin nucleation – polymerisation pathways. Pathways of polymer formation from a monomer actin shows the different conformations possible to from a dimer and the predicted possible conformation favored to form a trimer and tetramer and continuation to a polymer. The favored pathway is shown in red and reversible reaction rate constants are given (Cooper et al., 1983a; Sept and McCammon, 2001; Tobacman and Korn, 1983).

2.2.4 Effect of Tropomyosin on actin polymerisation and kinetics

Tropomyosin regulates and stabilizes actin filaments in physiological conditions. In striated muscle tropomyosin regulates the availability of myosin binding sites on actin during contraction in presence of Ca^{2+} ions (Gunning et al., 2008a). Spudich and Watt (1971) established the fact that tropomyosin along with troponin inhibits ATPase by binding to actin and not myosin during muscle contraction. In non-muscle cells tropomyosin primary role is believed to regulate actin filament proteins and protect the actin filaments from severing proteins (Lin et al., 1988; Pittenger et al., 1994b). Studies from *Caenorhabditis elegans* found that tropomyosin stabilises actin filaments and it has an opposite effect when ADF/cofilin are present. ADF/cofilin depolymerizes filament actin and in presence of tropomyosin this effect is inhibited (Ono and Ono, 2002). The presence of tropomyosin on actin filaments was also found to inhibit the Arp2/3 complex, which is bound to actin filament initiation to form a branch on the filament.

Wegner and collaborators initiated studies on the kinetic analysis of actin in presence of tropomyosin. Wegner (1980) studied the difference in interaction of tropomyosin homodimer (α/α) and heterodimer (α/β) on actin polymerisation these tropomyosin isofroms differ with 39 amino acid residues between α chain and β chain. The 23 of these residues are situated at the surface of the tropomyosin chain. When tropomyosin is bound to actin filament, 9 residues present at the C-terminal end of the tropomyosin interact to form a polar end-to-end contact with the adjacent tropomyosin molecule at the N-terminal end. Tropomyosin binds to actin in a flexible manner that is loosely attached to F-actin as it is shown that specific regions of tropomyosin are not even bound to actin filament making it flexible to achieve conformational changes during contraction process (Lamkin et al., 1983).

Figure 2.4: Tropomyosin binding possibilities on actin filament. 1. Individual isolated binding along the actin filament, 2. Single contiguous binding and 3. Double contiguous binding (redrawn from Wegner, 1980).

As discussed in section 2.1, the interaction of actin-tropomyosin is of co-operative nature. Figure 2.4 shows the different types of tropomyosin binding to actin, position 1 shows the binding of isolated tropomyosin molecule (a dimer) bound to actin. Isolated binding of tropomyosin occurs when magnesium ion concentration is very low (0.5 mM) and position 2 single contiguous binding occurs when tropomyosin molecule is interacting with other tropomyosin molecule on one side of the helix and position 3 double contiguous interaction where head-to tail interaction on both sides of the tropomyosin molecule occurs. The single and double contiguous binding happens when magnesium concentration is higher (1.0 – 2 mM) (Wegner, 1979). These contiguous end-to-end interactions of tropomyosin on actin molecules determine the flexibility of the actin filament as well as maintain its own flexible interaction with actin in turn maintaining the co-operative binding with each other (Lehman et al., 2013).

2.2.5 Hill equation simulation

The data obtained from the fluorescent labelled actin polymerisation and the polymerisation in presence of tropomyosin were fit to least squares to a sigmoidal curve using Hill equation to time course of polymerisation of actin to study the effect of tropomyosin on actin polymerisation using Origin 6.0 software.

The basic Hill model has three parameters, x the independent variable which is the time (in seconds) taken to reach the polymerisation saturation in this reaction and y is the dependent variable, the fluorescent intensity in arbitrary units.

The equation below was used by the software for fitting the data.

$$Y = V_{max} [x^n] / [k^n] + [x^n] \qquad (6)$$

Where, V_{max} is maximum saturation, x is time in seconds, k is the dissociation constant and n is the Hill coefficient which determines the degree of polymerisation and is the measure of sigmoidicity. Figure 2.5 shows the computer generated Hill model simulations showing sigmoidal curves. The slope of the curve remains same as long as one parameter remains constant either the half time (k) or the Hill coefficient (n). As the n changes the sigmoidicity changes but the slope of the curves remains same.

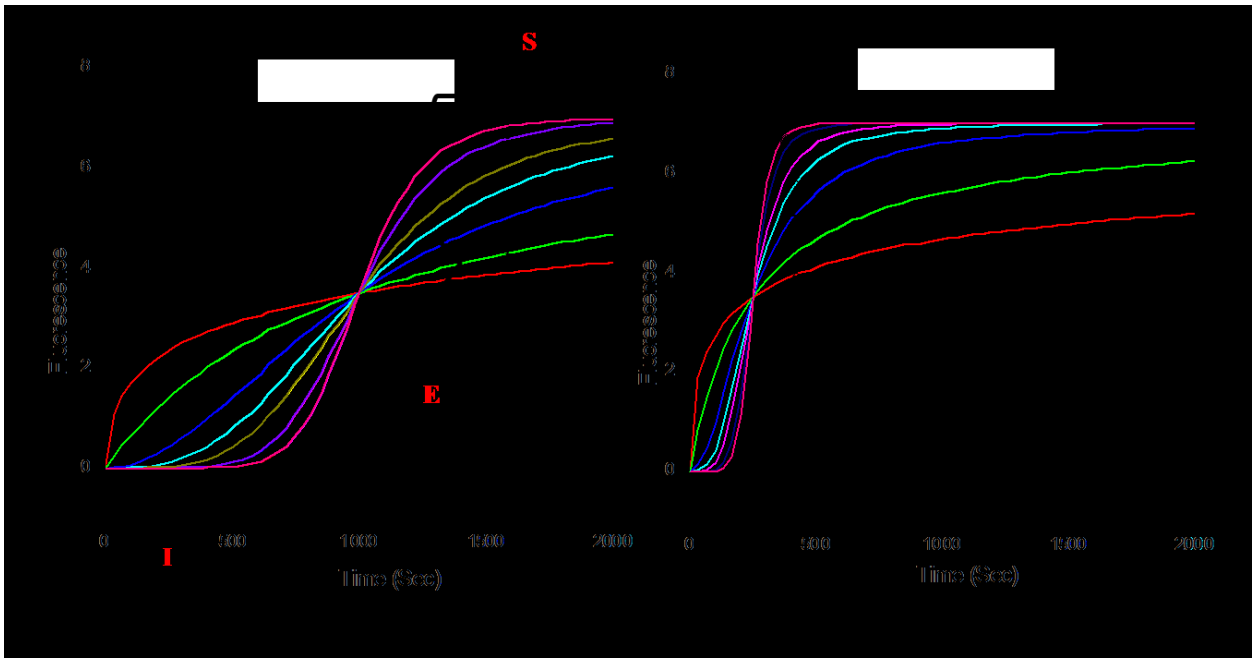

Figure 2.5: Hill simulations for actin polymerisation. A is simulated with rate constant k = 1000 sec which gives the half saturation value with varied n values to show the change in sigmoidicity. B have a value of k = 250 sec with variable n value. Changes in both k and n changes the slope which in this case is the rate of elongation. I – initiation, E – elongation and S- steady state –completion of polymerisation.

In non-muscle cells at low ionic concentrations of monomeric actin, the curves show higher sigmoidicity with a long lag phase which indicates that the elongation is due to self-reproduction or filaments forming by spontaneous fragmentation. Studies show that at lower ionic concentrations due to the lower available actin monomers, nucleation process is slower which causes the longer lag-phase with higher sigmoidicity (Cooper et al., 1983b; Lal and Korn, 1986; Wegner, 1976; Wegner and Engel, 1975).

In the present study, a series of actin polymerisation curves were generated by experiments conducted using pyrene labelled G-actin in presence and absence of tropomyosin. Pyrene G actin when polymerises shows an increase in fluorescence when excited at 365 nm without affecting polymerisation kinetics and any binding sites of

actin-tropomyosin interaction (Kouyama and Mihashi, 1981). The first phase of experiments actin polymerisation concentration was optimised using 2 μM and 6 μM PyG-Ac to see the difference in actin polymerisation kinetics in comparison with previous studies. To proceed to actin polymerisation in presence of tropomyosin two concentration of Tpm1 as initial tropomyosin (0.5 μM and 5 μM) was chosen to check the effect of actin polymerisation at low concentration and to see the difference at low concentration and by saturation concentration of tropomyosin. 6 μM tropomyosin was chosen to proceed with other assays using various tropomyosin isoforms as this should give saturation of actin.

Actin polymerisation in presence and absence of tropomyosin follow a sigmoidal pathway, however the half time of the steady state polymerisation taken from the time course curve cannot be used to calculate the nucleus number (Cooper et al., 1983a; Frieden and Goddette, 1983a). Hence in this study the time course polymerisation curves generated using Hill equation are compared qualitatively to show the polymerisation pattern of actin-tropomyosin, and the data is not sufficient to calculate the nucleation-elongation kinetics.

2.2.6 Aims and Objectives

The aim of this chapter is to express recombinant human tropomyosin 3 isoform 12.st (Tpm3 iso12st) from striated muscle, (will refer in the whole thesis as Tpm3) in *E. coli* in three different versions with variation at the N-terminus. Using co-sedimentation assays the protein is characterized for its actin binding affinity compared along with other tropomyosin isoform Tpm1.1st, Tpm2.2st and Tpm4.1cy as this isoform is not yet been

characterized for its actin binding affinity and little is known about its role in thin filament. For this study I produced Tpm3 which is considered to be 285 amino acids (aa) length. In this study, three versions of Tpm3 were produced with 284 aa with on singl "Met" at the N-terminal end of the sequence, 285 aa with "Met-Met" which is the original sequence (Figure 2.6) and 286 aa (Met)-Ala-Ser" at the N-terminal end of the sequence. The positions of the positive charge transfer when these aminoacids are added to the N-terminal end of the sequence are shown in Figure 2.1B.

The importance of studying the effect of tropomyosin on actin polymerisation is it gives the ability to quantitatively measure the incorporation of monomer to polymer and how presence of tropomyosin molecule affects this polymer association. Given to its role in mammalian cellular processes it is important to understand tropomyosins effect on actin polymerisation as it is known that isoforms of tropomyosins are in different concentrations in the cell (Schevzov et al., 2005).

2.3 Materials

Chemicals used for the experiments were obtained from Sigma-Aldrich, Thermo-Fisher and BDH. 30% Protogel (Acrylamide-bisacrylamide) obtained from National diagnostics. Enzymes and buffers were obtained from New England Biolabs and Thermo-Fisher. DNA plasmid extraction kit is from Eppendorf and homemade kit. Gel purification kit used from Eppendorf. Table 6.1 in appendix gives the list of all the chemicals and their suppliers used for the experiments. Recipes of all the buffers are found in buffers section (Section 6.2) in the appendix.

2.4 Experimental Methods

2.4.1 Construction of different tropomyosin isoform expression vectors

Fully sequenced cDNA clones of human tropomyosin 3 isoform 12st (Tpm3.12st) (NCBI sequence accession number NP_689476.2 shown in Figure 2.6 in *E. coli* culture were obtained from Thermo scientific. Tpm4 isoform 1 (284aa*)* cDNA clones was obtained from Thermo Scientific, where the sequence was codon optimised for expression in *E. coli.* The nucleotide sequence alignment comparing the human Tpm4 sequence (accession no: NM_001145160.1) and the synthesised codon optimised gene is shown in Figure 2.7.

The oligonucleotide primers were obtained from Sigma- Aldrich. Tpm3 primers were designed according to Maytum et al., (2000) with a native sequence of 285 Met Met(MM) amino acids(aa), a 284 aa with single Met (M), and 286 aa Met, Ala, Ser (MAS) at the amino terminal to substitute the N-terminal acetylation in *E. coli* with 5'-*Nde I* and 3'- *Xho I* restriction sites. *Xho I* is used for TPM3 it has multiple *BamHI* cleavage sites in the sequence itself. For Tpm4 DNA was synthesized with 5'-*Nde I* and 3'-*Bam HI* restriction sites. Table 2.1 shows the forward 5' and reverse 3' primers designed with the cleavage sites in bold.

```
            ....|....| ....|....| ....|....| ....|....| ....|....| ....|....| ....|....|
                     10         20         30         40         50         60         70
Tpm3.12st   MMEAIKKKMQ MLKLDKENAL DRAEQAEAEQ KQAEERSKQL EDELAAMQKK LKGTEDELDK YSEALKDAQE

            ....|....| ....|....| ....|....| ....|....| ....|....| ....|....| ....|....|
                     80         90        100        110        120        130        140
Tpm3.12st   KLELAEKKAA DAEAEVASLN RRIQLVEEEL DRAQERLATA LQKLEEAEKA ADESERGMKV IENRALKDEE

            ....|....| ....|....| ....|....| ....|....| ....|....| ....|....| ....|....|
                    150        160        170        180        190        200        210
Tpm3.12st   KMELQEIQLK EAKHIAEEAD RKYEEVARKL VIIEGDLERT EERAELAESK CSELEEELKN VTNNLKSLEA

            ....|....| ....|....| ....|....| ....|....| ....|....| ....|....| ....|....|
                    220        230        240        250        260        270        280
Tpm3.12st   QAEKYSQKED KYEEEIKILT DKLKEAETRA EFAERSVAKL EKTIDDLEDE LYAQKLKYKA ISEELDHALN

            ....|

Tpm3.12st   DMTSI
```

Figure 2.6: Tpm3.12st protein sequence used for designing primers (NCBI sequence accession number NP_689476.2).

Table 2.1: Primer sequence designed for human tropomyosins to express in *E. coli*.

Gene	5'(sense)primer (5'-3')	3'(antisense)primer (5'-3')
Tpm3-Met (284aa)	gcgca▼tATGGAGGCCATCAAGAAAAAGATGC	gcgc▼tcgagTTATATAGAGGTCATGTCATTGAGGGCG
Tpm3-MM (285aa)	gcgca▼tatgATGGAGGCCATCAAGAAAAAGATGC	gcgc▼tcgagTTATATAGAGGTCATGTCATTGAGGGCG
Tpm3-ASM (286aa)	gcgca▼tatggcgagcATGGAGGCCATCAAGAAAAAGATGC	gcgc▼tcgagTTATATAGAGGTCATGTCATTGAGGGCG
Tpm4 * (284aa)	gcgca▼tATGGAAGCCATCAAGAAGAAAATG	TATGCTAGTTATTGCTCAG (T7 reverse)

Note: The upper case and lower case amino acids represent the original human TPM3 sequence and the additional fusion aa at the N-terminal respectively. TPM1, TPM2 and TPM4 were designed with BamHI and NdeI restriction sites and TPM3 with NdeI and XhoI retriction sites. * TPM4 was synthetically synthesised. "▼" Restriction sites.

The sequence for Tpm3 oligonucleotides were designed with NdeI and XhoI restriction sites and for Tpm4 with BamHI and NdeI restriction sites. (BamHI-G▼GATCC, NdeI-CA▼TATG, XhoI-C▼TCGAG). Clones of Tpm1 and Tpm2 and clones of Tpm1 HCM mutation A63V and K70T were given by Dr. Robin Maytum.

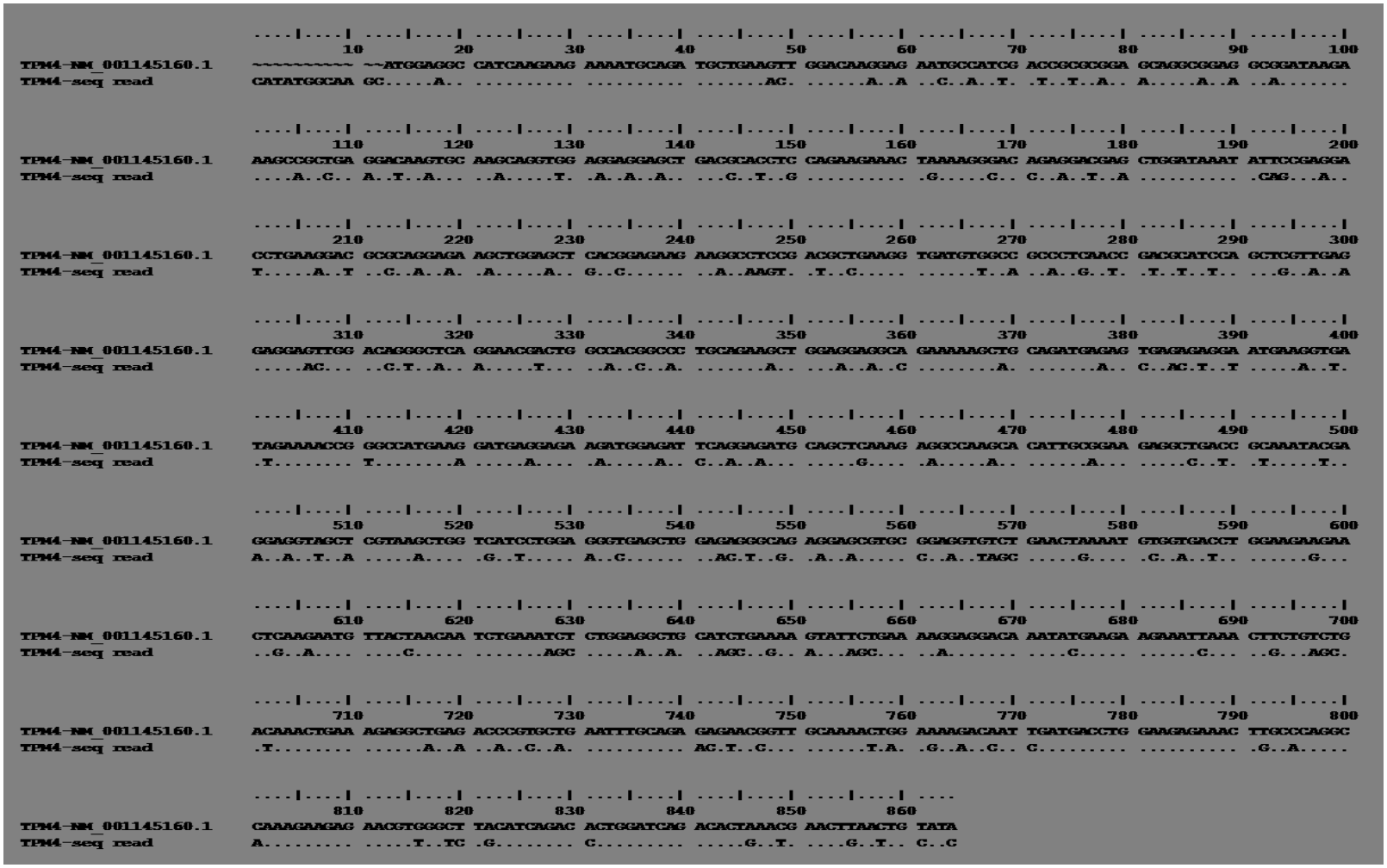

Figure 2.7: Tpm4- Nucleotide sequence alignment: The top sequence is from the human Tpm4 sequence with accession number. The bottom one Tpm4-Seq read, is the codon optimized synthesized gene used for expression of protein in this study.

2.4.1.1 Amplification of Tropomyosin cDNA isoforms

The Tpm3 cDNA clones obtained were in glycerol stock with 25 ug/ml of chloramphenicol resistance clone. 50 ml LB media with 25 ug/ml chloramphenicol was inoculated with cDNA culture (100 ml of LB: 1g bacteriological peptone, 5 g yeast extract and 5 g NaCl. pH 7.5) and grown 8 hours at 37^0C and plasmid DNA was extracted using mini plasmid extraction kit from Eppendorf. Three variant of Tpm3 iso12st were synthesised with the primer designed as shown in Table 2.1. Tpm4 gene was synthetic DNA and hence the DNA was used directly for amplification.

2.4.1.2 Polymerase chain reaction

PCR was used to amplify the gene of interest and also to insert additional peptides at the N-terminus of the sequence to synthesize three fusion variants of Tpm3. The variants in this work will be referred as Tpm3-Met, Tpm3-MM and Tpm3-MASM. Tpm4 gene was used directly for amplification with additional 3 peptides to mimic the N-terminal acetylation of the sequence. 50 µl of PCR mixture was prepared containing 10µl of 10X NEB Thermo pol PCR buffer, 200 µM dNTPs, approximately 20 ng template DNA, 33 nM primers with 2 units of *Taq* polymerase. A thermal cycler was set as shown in Table 2.2

Table 2.2: PCR cycle used for DNA amplification

Cycle	Temperature	Time
Heating the reaction mix	94^0C	2min
Denaturation	94^0C	20sec
Annealing	50^0C	20sec
Extension	72^0C	50sec
Elongation	72^0C	4min

30 cycles of denaturation, annealing and extension were run for DNA amplification.

The PCR reaction products were separated by using 1.5% agarose gel electrophoresis with GeneRuler 1 kb DNA ladder. The band matching the size of the insert (853 bp) was cut from the gel and purified using eppendorf gel clean up kit following manufacturer's instructions. The DNA extracted was stored at -20^0C for further use.

2.4.1.3 Expression of tropomyosin in E. coli with pJC20 plasmid vector

2.4.1.4 pJC20 Vector

The pJC20 plasmid vector (Figure 2.8) is widely used for efficient and specific over expression of cloned genes in *E. coli.* pJC20 is a high-copy number expression vector with T7 RNA polymerase promoter, and its expression is controlled by lac promoter

induced with IPTG. The pJC20 vector has multiple cloning sites with *NdeI, BamHI* and *XhoI* restriction sites. It has high copy region of replication, with ampicillin resistant gene and T phi terminator. The small size of the vector allows sub cloning of large inserts and high plasmid copy numbers obtained results in high yields of the expression genes. It is found to be stable in both XL1blue and BL21DE3 strains of *E. coli* (Clos and Brandau, 1994).

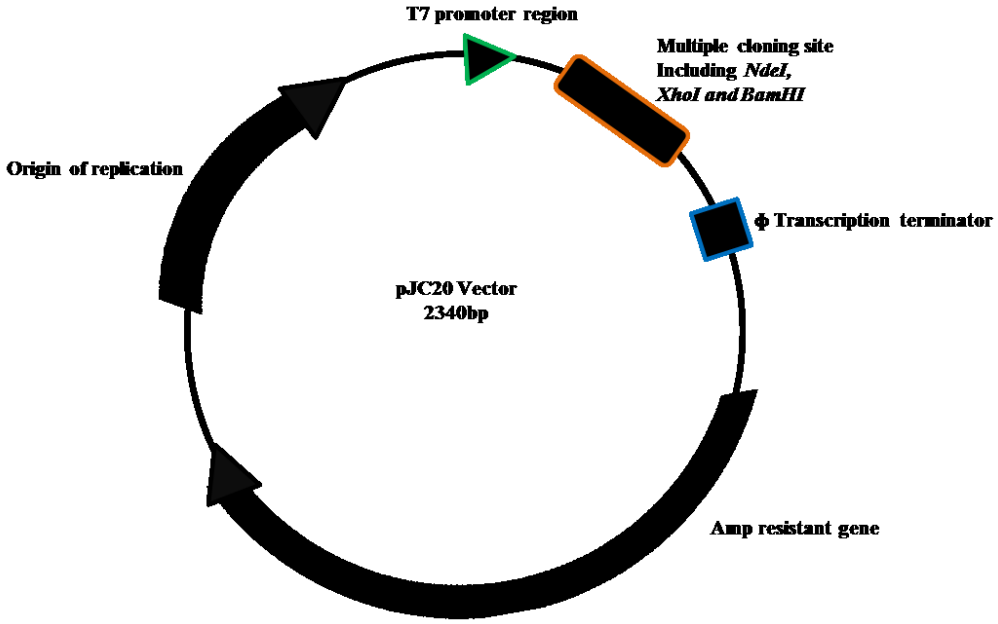

Figure 2.8: pJC20 vector used for cloning: pJC20 is a 2340 bp circular plasmid expression vector with T7 RNA polymerase promoter region and multiple cloning sites with *NdeI, Bam HI* and *XhoI* restriction sites. It has high copy region of replication with ampicillin resistant gene and T phi terminator.

2.4.1.5 Restriction digestion of PCR product

Purified DNA from the PCR product and pJC20 vector were double digested using Thermo scientific FastDigest *NdeI* and *XhoI* for TPM3 variants and for TPM4 *NdeI* and *BamHI* restriction enzymes were used. Approximately 300 ng of DNA (40 µl) was mixed with 1µl of each buffer with 5 µl of 10X FastDigest Green buffer and made upto 50 µl with ultrapure water. The mixture was incubated for 30 min at 37^0C. The pJC20 vector was also digested with same enzymes at the same time. The digest product was separated on 1.5% agarose gels. The band of interest and the vector band were cut from the gel and purified by Eppendorf gel clean up kit using manufacturer's instructions.

2.4.1.6 Ligation

To insert the Tpm3-DNA into plasmid DNA, T4 ligase was used for ligation. Before performing ligation, the ends of the plasmid DNA were dephosphorylated using NEB Calf intestinal Alkyl phosphatase (CIP), it catalyses the dephosphorylation of 5' ends of DNA. Dephosphorylation of plasmid DNA prevents re-ligation of the linear plasmid reducing the background of ligated colonies. An amout of 2 µl of CIP is added to the purified plasmid DNA with 3 µl of NEB buffer 3 and incubated for 1 hour at 25 ^{0}C. The plasmid is again purified through the same column used for gel clean up kit to remove the buffer before ligation.

For ligating the insert with plasmid DNA, Thermo Scientific T4 DNA ligase is used. T4 ligase catalyzes the formation of a phosphodiester bond between 5'-phosphate and 3'-hydroxyl termini in double stranded DNA. Insert DNA was added to pJC20 DNA in 3:1 ratio, with 1 µl (1 Weiss unit) T4 DNA ligase and 2 µl of 10X T4 ligase buffer and made

upto 20 µl of total volume by ultrapure water. The mixture was incubated at 20 ^{0}C for 30 min.

2.4.1.7 Preparation of E. coli competent cells

Competent *E. coli* cells were prepared according to Nishimura et a.,(1990). LB agar place was streaked with bacterial starter culture. A single colony was inoculated into 50 ml of LB medium supplemented with 10 mM $MgSO_4$ and 0.2% glucose (medium A), Mg^{2+} ions and glucose stimulates transformation efficiency. The culture is grown to mid logarithmic phase at 37 ^{0}C, reached when the OD^{600} is between 0.6-1.0. The cells were chilled on ice for 30 min and pelleted by spinning at 1500 g for 10 min at 4 ^{0}C. The pellet was resuspended gently on ice in 0.5 ml medium A and 2.5 ml of storage buffer (sterile medium B: LB medium supplemented with 36% glucose, 12% PEG, 12 mM $MgSO_4$, pH 7.0) was added to the cells and mixed well. The competent cells were stored at -80 ^{0}C in l00 µl aliquots.

2.4.1.8 Transformation

Plasmid with Tpm3 gene was transformed into XL blue competent cells to screen for the colonies with the insert. Transformation was performed by adding 10 µl of ligation mixture containing the Tpm3 plasmids to 100 µl XL blue competent cells defrosted on ice. The cells were mixed gently and incubated on ice for 15 min and given a heat shock at 42 ^{0}C for 2 min and immediately transferred on ice. After 2 min of incubation on ice, 900 µl of LB was added to a final volume of 1 ml and the mixture was incubated at 37 ^{0}C for 1 hour. 100 µl of culture were plated on LB-agar plate with ampicillin (LB-Amp plates) which is used as a screening agent for selecting the colonies with plasmid.

2.4.1.9 DNA purification and Sequencing

The colonies were screened using PCR and the colonies with positive result were selected were inoculated in 1 ml each of LB with 100 µg/ml ampicillin culture media and grown over night at 37 ^{0}C in a shaker. DNA was purified using FastPlasmid DNA mini-prep kit according to manufacturer's instructions. 4 µl of DNA was used to run on 1.5% agarose gel to determine concentration using the Generuler 1 kb DNA ladder.

The insert was later verified by restriction digest screening. The presence of 852 bp band confirms the presence of insert. The DNA coding region of the plasmid is verified by using Eurofin MWG operon sequencing read and by sequence alignment with the database sequence using BioEdit sequence alignment editor.

2.4.2 Protein Expression

The purified plasmid DNA was transformed to BL21DE3 that has T7 RNA polymerase. Three single colonies were picked for checking expression and were grown in 1 ml culture containing 0.1 mM ampicillin at 37 ^{0}C. Cells were grown until the OD at 600 nm reached around 0.8 considered to be reaching late exponential phase. Isopropyl-β-D-thiogalactopyranoside (IPTG) is added at a concentration of 0.4 mM and the cells were induced for 3 hr for expression.

To check the expression of protein 150 µl of cells were pelleted at 8K rpm for 1 min and the pellet was resuspended in 20 µl dH_2O and 20 µl SDS Laemmli buffer was added. The

proteins were resolved on 13.5% SDS-PAGE gel to check expression levels. There were few colonies expressing protein and one colony was selected used for scaling up the protein for growing in 1L LB media with 100 mg/L ampicillin and followed the same procedure for expression (Maytum et al., 2000).

2.4.2.1 Purification of Tropomyosin from E. coli BL-21 strain

Tropomyosin was extracted according to Maytum et al., (2000), where cells from 1 L culture were harvested by centrifugation at 8K rpm for 10 min and the pellet was resuspended and homogenised in 40 ml of lysis buffer (20 mM Tris pH 7.5, 150 mM NaCl, 5 mM EDTA). The homogenate was sonicated for 1 min x 4 cycles keeping on ice for 1 min after each cycle. The lysate was boiled for 10 min in boiling water bath, cooled on ice and centrifuged at 13K rpm for 15 min to pellet cell debris. The supernatant with dissolved proteins was adjusted to pH 4.6 with 1M HCl and 0.1 HCl at the end for isoelectric precipitation of tropomyosin as the pI of tropomyosin is at pH 4.6. The precipitate was collected by spinning the supernatant 13K rpm for 10min and the pellet was resuspended in 15-20 ml of 5 mM sodium phosphate buffer pH 7.0. The pH is adjusted to pH 7.0 after resuspension. Protein was further purified using Q-sepharose anion exchange column using a high salt phosphate buffer 5mM sodium phosphate buffer pH 7.0 with 1M NaCl and low salt 5 mM sodium phosphate buffer pH 7.0 with 100 mM NaCl. Protein was eluted at 40% (0.46 M) salt concentration and was precipitated isoelectrically at pH 4.6. The purity of protein is checked at 280/260 nm absorbance and concentration was calculated using sequence mass and by its extinction co-efficient $E^{1\%}$ of 0.6 cm^{-1} obtained from ExPASY ProtParam. Impurities like DNA and RNA show

absorbance at 260 nm by checking the UV spectrum at this wavelength gives the amount of impurities present in the protein sample. Figure 2.9 shows the UV spectrum of pure protein and the protein with nucleic acid impurities. The purity of protein was visualised on SDS-PAGE polyacrylamide gels by collecting fractions at each stage of purification. Figure 2.10 shows the flow-chart of the overall procedure of expression and purification of tropomyosin isoforms.

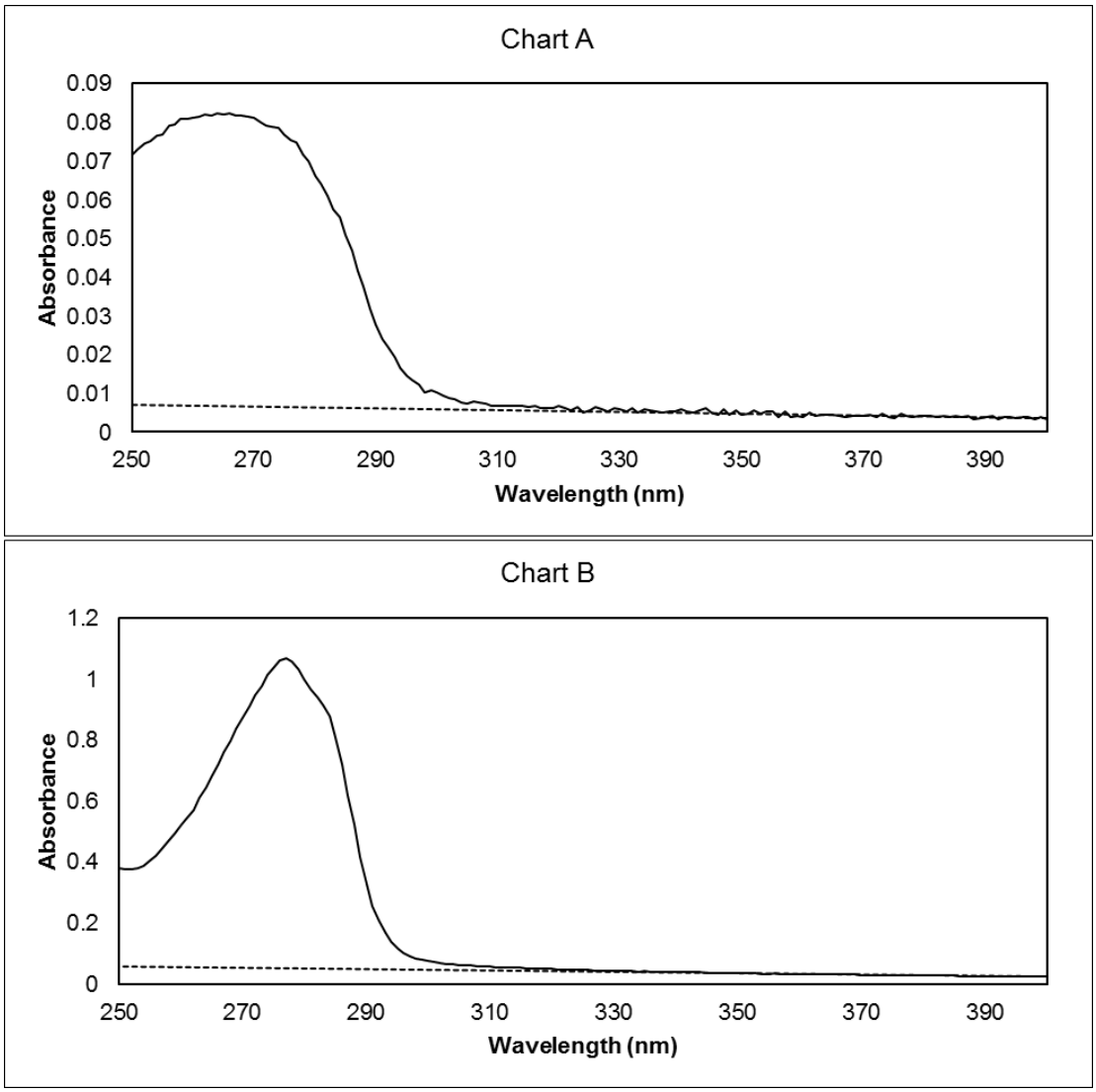

Figure 2.9: UV spectrum of impure and pure protein. Chart A shows the impurities like nucleic acids absorbed at 260nm present in the protein. Chart B shows the final pure protein with lower traces of contaminants.

2.4.2.2 Optimization of protein purification

Three different methods were tested for obtaining pure protein. Once the boiled lysate was obtained equal amounts of lysates were separated for optimising the method for

purification. Isoelectric precipitation (pI), where tropomyosin is precipitated out from the solution at the pI of the protein, for tropomyosin its pI is at pH 4.6 (Bailey, 1948). For ethanol precipitation method, 3 times the volume of chilled ethanol was added to the lysate and incubated on ice for 30 min and the spin down at 13K rpm for 10 min. Ammonium sulphate precipitation, 65% of ammonium sulphate was added and incubated on ice for 30 min and centrifuged at 13K rpm for 10 min (Bailey, 1948; Cummins and Perry, 1973). The pellet obtained from all the three methods were re-suspended in 5 mM sodium phosphate buffer pH 7.0 and further purified using Q-sepharose anion exchange column.

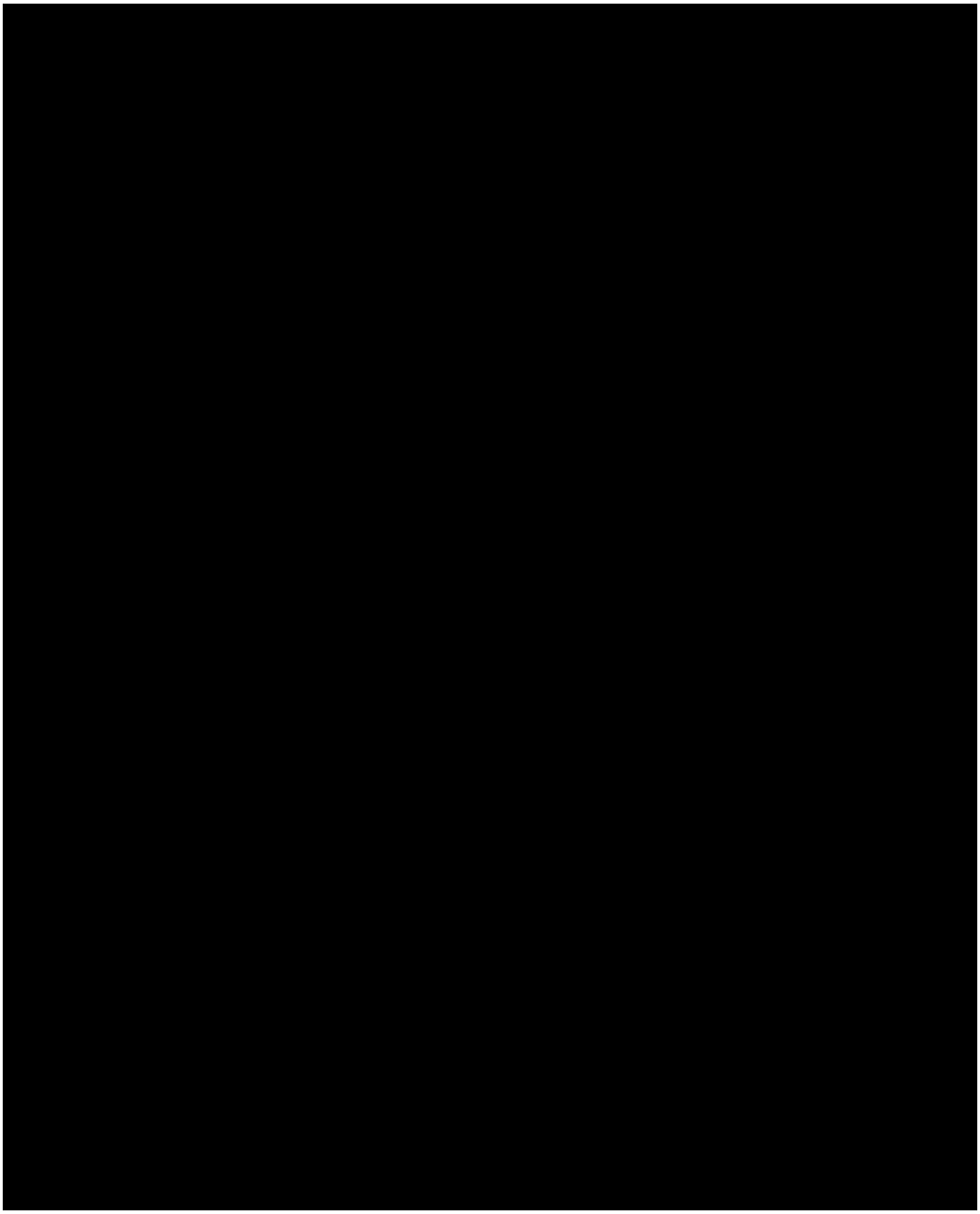

Figure 2.10: Work flow of the methodology of protein expression of TPM3 in *E. coli.*

2.4.2.3 Determination of molecular mass by electrospray mass spectrometry (MS)

The protein molecular weight was determined using electron spray mass spectrometry. Prior to analysis with MS, 100 µl of purified tropomyosin was dialysed overnight with 1 mM Ammonium bicarbonate for desalting as ammonium bicarbonate is volatile in mass spectrometer and does not stick to protein preventing any mass shift in the peaks. The dialysed sample was spin down at 13K for removing any precipitate and aggregates formed. 20 µl of sample was acidified with 0.1% formic acid and 40% methanol was added for determining for its mass using Finnigan Mat LCQ ion-trap MS. The mass is calculated by multiplying the series of the mass/ charge ratio obtained from the spectra with number of charges minus the number of charges.

2.4.3 Preparation of muscle acetone powder

Acetone powder was prepared essentially according to Spudich and Watt (1971). Approximately 1000 g of fresh chicken breast meat was used for extraction actin. The meat was rinsed with cold distilled water and chilled on ice for one hour. The meat was rinsed with pre-chilled 1 mM EDTA, pH 7.5 and minced in pre-chilled mincer rinsed with cold 1 mM EDTA. The extraction process involves subsequent mixing of mince muscle in different buffers step wise. The first step of extraction was by stirring the mince muscle on ice in two liters of prechilled ice-cold phosphate buffer containing (0.15M potassium dihydrogen phosphate (KH_2PO_4), 0.15M dipotassium phosphate (K_2HPO_4), 0.1M KCl, pH 6.5) for 10 min. This was filtered through sterilized gauze and the muscle is transferred to buffer containing 2 liters of ice-cold 0.05 M sodium

bicarbonate buffer for 10 min while stirring on ice. After filtering, 2 liters ice-cold 0.1 M EDTA, pH 7.5 was added and stirred for 10 minutes on ice and filtered. The mince was washed twice with 2 liters of ice-cold distilled water for 5 min and the filtrate was discarded at each stage of the process. Later the muscle power was extracted by washing the residue with 1 liter of acetone at room temperature repeating washing and filtering steps with 1 L of acetone 5 times. During the whole extraction process the temperature of all the buffers and the muscle was maintained at 4 ^{0}C on ice until acetone wash. The powder obtained was dried overnight on paper towels under the hood. The dried powder was sieved with a fine metal sieve separating the fine and coarse dried muscle powder. The final yield of both fine and coarse muscle powder was transferred into 50 ml falcon tubes and weighted for the estimation of total yield.

2.4.3.1 Extraction of actin from acetone powder

Actin was extracted form chicken skeletal muscle acetone powder as described by Cooper et al., (1983b) and Jeffries Criddle et al. (1985b) with few minor modifications. 1. 5 g of acetone power was added to 150 ml of pre-chilled buffer to 0 ^{0}C containing 10 mM Tris, 0.5 mM ATP, 0.2mM $CaCl_2$ and 1 mM DTT, pH 8.0. The mixture was stirred on ice for 1hr slowly and filtered through cheese cloth using a Buchner funnel containing filter paper under pressure. The filtrate is first spun at 8K rpm for 10 min to remove any solid residues after filtration. G-actin (G-Ac) is polymerised by adding final concentrations of 100 mM KCl, 2 mM $MgCl_2$ and stirred at room temperature for 2 hrs. The polymerised actin is precipitated by spinning at 55K rpm for 1 hr (Beckman Coulter model Optima Max-XP with MLA55 rotor). The pellet is resuspended in

depolymerisation buffer (depol buffer) containing 5 mM Tris, 0.2 mM $CaCl_2$, 1 μM ATP, 0.5 mM DTT, 1 mM NaN_3 adjusted to pH 7.5 and dialysed against it overnight changing it for couple of times. On day 2, the dialysis residue is spun at 55K rpm for 1 hr to remove any left polymerised actin. The volume of the supernatant is measured and the G-actin concentration is determined UV absorption at 280 (scanned between 260-500 nm to correct for light scattering) absorbance and concentration was calculated using sequence mass and by its extinction co-efficient $E^{1\%}$ of 1.108 cm^{-1} at 280 nm. The purity of protein was visualised on SDS-PAGE polyacrylamide gels by collecting fractions at each stage of purification. The G-actin is diluted to 1mg/ml concentration using depolymerisation buffer. G-actin is polymerised by adding ATP to a final concentration of 5 μM, 100 mM KCl and 2 mM $MgCl_2$. Stirred slowly at room temperature for 1 hr and spun at 55K rpm for 1 hr. The pellet is resuspended in MOPS buffer containing 100 mM KCl, 20 mM MOPS, 5 mM $MgCl_2$ and 1 mM NaN_3, pH 7.0 and dialysed against it overnight at 4 ^{0}C. The concentration of polymerised F-actin (F-Ac) is determined by UV scanning and its extinction coefficient of 1.108 cm^{-1}. Required amount of F-Ac was distributed for co-sedimentation assays and for pyrene labelling

2.4.3.2 Pyrene labelled G-actin

The required amount of F-actin needed for actin polymerisaiton assays was used for fluorescent labelling with pyrene which was performed according to Cooper et al., (1983b). N-(1-pyrenyl) iodoacetamide (Pyrene) was used for labelling, prepared by dissolving in dimethylformamide to a concentration of 6 mg/ml (16 μM). It was stored at

-20 ^{0}C. 7.5 mol of pyrene were added per mole of actin. The amount of pyrene to add for specific volume of F-actin was calculated by using the formula:

Concentration of F-Ac **X** Total volume of F-Ac x 1.5 / Concentration of pyrene

Pyrene was added slowly to the F-Ac while stirring and the mixture was kept in dark for 20 hours at room temperature while stirring slowly all the time. After 20 hours the mixture was spun at 8000 rpm to remove precipitated pyrene. The labelled F-Ac is sediment by spinning at 55 K rpm for 1 hour. The pellet was homogenised in depol buffer and dialysed against depol buffer in dark for 24 hours at 4 ^{0}C. The pyrene labelled G-Ac (Py-G-Ac) was stored on ice in 4 ^{0}C refrigerator, this way it was found to store better than just storing in 4 ^{0}C in refrigerator.

The concentration of Py-G-Ac was measured using the extinction co-efficient of $E^{1\%}$ 22000 M^{-1} cm^{-1} at 344 nm (Kouyama and Mihashi, 1981).

2.4.4 Co-sedimentation assays

Actin in polymerised form (F-actin) can be precipitated by centrifugation at greater than 30K rpm. Therefore any protein (like tropomyosin, Tn and myosin) bound to actin will also be pelleted when added to it and the unbound protein would be left in the supernatant. The same principle is used to determine the affinities of various tropomyosin isoforms with actin.

For co-sedimentation assays varying concentrations of tropomyosin (eg. 0.0 to 10 μM) were added to 10 μM actin in standard MOPS assay buffer containing 20 mM MOPS, 200 mM NaCl, 5 mM $MgCl_2$, making to a total volume of 100 μl. The reaction mixture

was incubated at room temperature for 15 min and spun for 30 min at 55K rpm (Beckman Coulter model Optima Max-XP with MLA130 rotor). Supernatant was transferred to fresh Eppendorf centrifugation tubes and the pellet is resuspended 70 µl MOPS buffer and 30 µl 4X Laemmli buffer making the total volume to 100 µl, and to 30 µl of supernatant 30 µl of 4X SDS buffer was added. 15 µl of the sample was loaded on 13.5 % SDS-PAGE ((Laemmli, 1970) to separate the protein bands. Gels were stained with Coomassie Brilliant Blue G250 and destained with 20% methanol containing 5% acetic acid.

2.4.4.1 Densitometry

Densitometry analysis of the co-sedimentation assay SDS-gels was used to calculate the binding constants of tropomyosin and actin. Proteins bands from the cosedimentation assay gels were quantified by scanning them with Biorad GS800 calibrated densitometer along with a Stouffer 21 step density tablet used for calibration. The densities of the protein bands were obtained after calibration of the image with ImageJ software. Quantification analysis was performed using Image J software (Schneider et al., 2012)

A standard curve was generated by plotting the total tropomyosin (density of Tm in pellet and supernatant) against known concentrations which was used to calculate the free Tm concentration in the supernatant as shown in Figure 2.21. The dissociation constant (k) at half saturation and the Hill coefficient were determined by plotting the staining ratio (ratio of Tm and actin densities from the pellet) as a function of free Tm concentrations. The data was fitted to Hill equation using Origin 6.0 software.

Hill equation used by the software

$$Y = V_{max} [x^n] / [k^n] + [x^n]$$

Where, V_{max} is maximum saturation, x is concentration of the ligand (Tm) , k is the dissociation constant and n is the Hill coefficient which determines the degree of the interaction between the binding sites which is used as the measure of degree of cooperativity.

2.4.5 Fluorescence Spectrometer

Actin polymerisation with presence and absence of tropomyosin was monitored by fluorimetry. Fluorescence intensity was measured using Amico-Bowman Seires 2-Luminescent spectrometer with wavelengths 365 nm and 389 nm for excitation and emission respectively according to Lal and Korn (1986). The emission measured was set manually to 10% and all assays were measured with detector voltage of 690 volts set manually. The band width was set to 0.5 nm for excitation and 8 nm for emission to reduce photo bleaching. Measurements were made at room temperature in a 0.5 cm glass cuvette with 300 µl assay total assay volume.

2.4.5.1 Actin polymerisation assays conditions

Recombinant tropomyosin isoforms prepared as described in section 2.4.22.4.1.3, were used for Ac-Tm polymerisation assays according to Lal and Korn (1986). Total assay volume was maintained at 300 µl with 6 µM Py-G-Ac alone and 5 uM tropomyosin and made up to the volume with depol buffer. Py-G-Ac was incubated with 1 mM EGTA

before polymerisation was initiated by adding 100 μM KCl, 2 mM $MgCl_2$ and 0.1 mM ATP. Binding measurements were made by sedimentation of fully polymerised actin at 20 ^{0}C. The samples were spun down at 55 K rpm in Beckman Coulter Optima Max-XP with MLA130 rotor of the assays for 1 hour. The pellet and supernatant were analysed using 13.5 % SDS-PAGE gels.

2.5 Results

2.5.1 Sequence Confirmation

The sequence of all the clones constructed were confirmed by aligning the sequences obtained from Eurofin MWG operon sequencing read and by sequence alignment with the database sequence using BioEdit sequence alignment editor. The nucleotide sequence was translated to amino acid sequence using BioEdit and the sequence of Tpm3-Met, MM and MASM and Tpm4 and the Protparam sequence parameters are given in Appendix section 6.3.

2.5.2 Expression and Purification of γTm (Tpm3)

A

Tpm3-Met	MEAIKKKMQMLKLDKENAL
Tpm3-MM	MMEAIKKKMQMLKLDKENAL
Tpm3-MASM	(M)ASMEAIKKKMQMLKLDKENAL
Human Tpm3	MMEAIKKKMQMLKLDKENAL

B

TPM4-MASM	(M)ASMDAIPKKMQMLKLDKENAL
Human TPM4	MEAIKKKMQMLKLDKENAL

Figure 2.11: N-terminal constructs of TPM3 and TPM4: Amino acid sequence alignment results of the clones used for expression are shown above. Panel A, For Tpm3-Met the single Methionine at the N terminal of all the constructs was expected to remove by post-translational process and is shown in brackets. All the clones had sequences synthesized similar to the human TPM3. Panel B shows the clone sequence read of TPM4 and the sequence used for expression (human TPM4) and has higher similarity to rat and human skeletal TPM1.

Tropomyosin was expressed at high levels in *E. coli*, and is soluble in lysis buffer. Figure 2.11 shows the expressed constructs with N-terminal sequence. The first Methionine is brackets indicating the removal of Methionine by posttranslational process which was confirmed by Mass spectrometry analysis of intact protein (Figure 2.17). Table 2.3 shows the masses of all the protein isoforms synthesised and the difference in calculated mass and the predicted mass. Methionine for TPM3-Met is not removed in the recombinant protein which is confirmed with a mass of 32823.6 Da with an acceptable error of ~4.9 Da and Tpm3-MM 32950.8 with an error of ~0.9 Da also have an intact methionine at the N-terminal. However for Tpm3-MASM with a mass of 32980.46 Da

and mass difference of ~127.64 it seems N-terminal methionine is removed by post translational process. There was difficulty calculating the m/z value as the spectrum had lot of background.

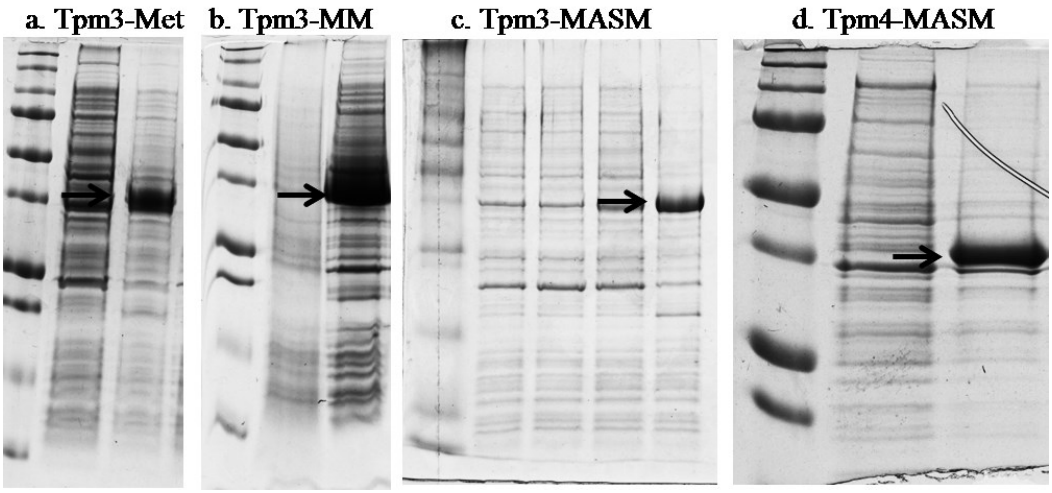

Figure 2.12 : Commassie Blue –stained SDS gels showing protein expression of Tpm3 and Tpm4 in *E. coli.* Gels a, b, c and d show the protein expression of Tpm3-MET, Tpm3-MM, Tpm3-MASM and Tpm4-MASM respectively. Uninduced (first lane from marker) and induced culture with IPTG (shown with an arrow). 120 µl of culture is spun down at 9K rpm and the pelette is resuspended in 20 µl dH_2O and 10 µl 4X SDS sample buffer. The sample is boiled at 95 ^{0}C and 15 µl is loaded on the gel. Arrows shows the expressed protein band.

Figure 2.12 shows the Coomassie Blue-stained SDS-PAGE gels of three variants of Tpm3 – Met, MM and MASM. Total bacterial extracts of uninduced and induced (by IPTG) extracts (lane a and b respectively) are shown. The uninduced culture did express any protein and the induced extracts shows high level of expression with successful total yields of approximately 60 mg per one litre of culture.

2.5.3 Purification

Recombinant protein tropomyosin was purified by eluting it with increasing the salt concentration using anion exchange Q Sepharose column (GE Helath care HiPrep Q XL 16/10) Tropomyosin was eluted at 40% salt (0.46 M NaCl). The purification profile is shown in Figure 2.13. Figure 2.14 shows the Coomassie Blue-stained SDS-PAGE gel at various stages of protein purification and also different approach for purification. The Lane 1 from the marker is bacterial extract induced by IPTG followed by soluble total protein in lysis buffer after boiling and removal of solid residue lane 2; lane 3 shows the protein precipitated by isoelectric precipitation by adjusting the pH between 4.5-4.6. Lane 4 shows the next stage of purification where protein is purified by ion-exchange chromatography and the eluent collected at 40% salt (Figure 2.13) is adjusted to pH 4.6 to precipitate out tropomyosin. Two different approaches were tried to purify tropomyosin to optimise the amount of extraction and the purity of the sample. After ion-exchange chromatography, first method was performed as explain before by isoelectric precipitation, and the second method (Lane 5) by precipitation the total protein from the 40% eluent by adding 6times volume of ethanol.

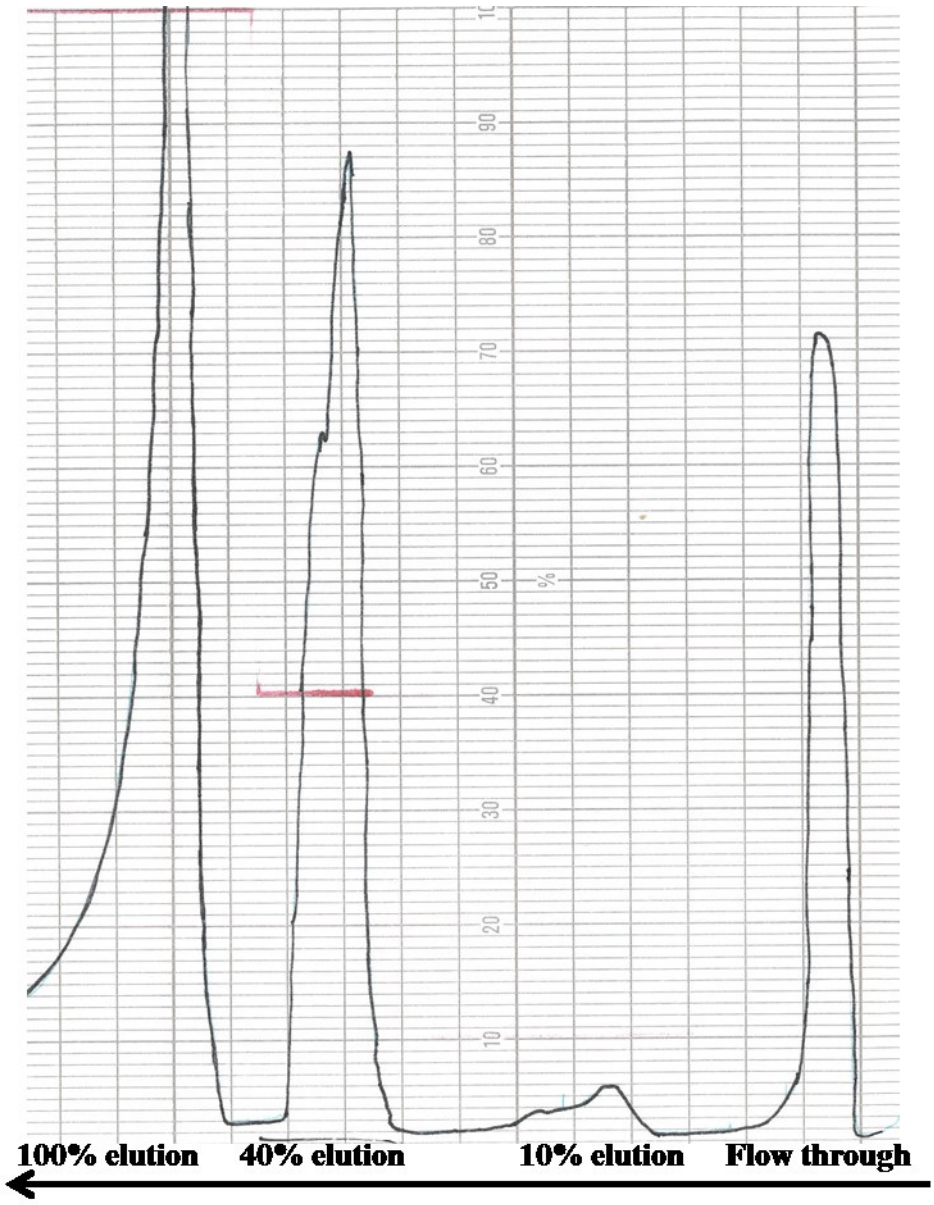

Figure 2.13: FPLC elution profile for purification of tropomyosin. Tropomyosin was bound to column by 5 mM phosphate buffer with 100 mM NaCl (buffer A) and protein was eluted by increasing the salt concentration from 5 mM phosphate buffer with 1 M NaCl (buffer B). Tropomyosin is collected at 40% elution and was purified further by isoelectric precipitation.

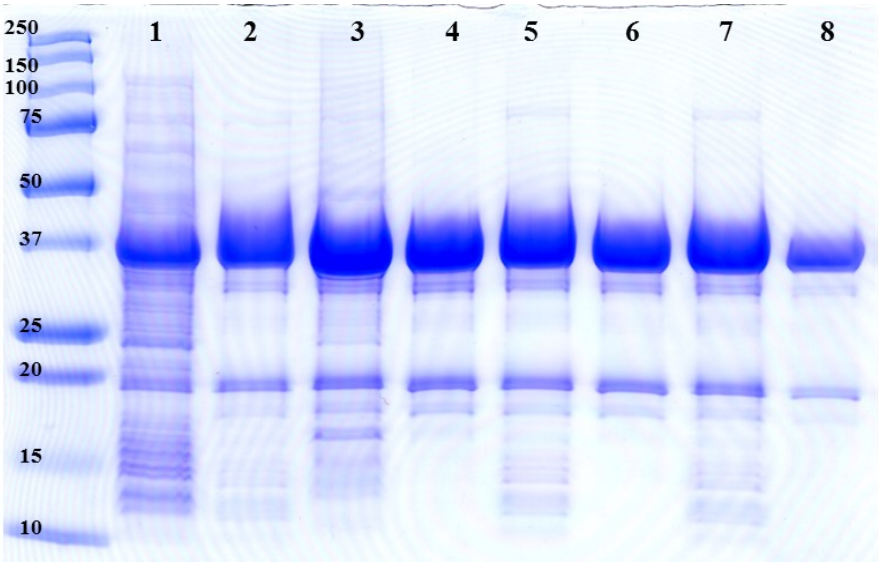

Figure 2.14: Stages of purification of Tropomyosin (MASM): Lanes: 1. TPM3 expressed in culture induced by IPTG, 2, protein extract in lysis buffer after boiling, 3. Protein by iso-electronic precipitation at pH 4.5-4.6, 4. pH precipitated protein purified by anion exchange chromatography(IEC), 5. Ethanol precipitation, 6. EtOH precipitated protein purified by IEC, 7. Ammonium sulphate precipitate, 8. Ammonium sulphate precipitate protein purified by IEC.

The pellet was collected by spinning the sample at 8K rpm and was resuspended in 5mM phosphate buffer, and further purified by isoelectric precipitation (lane 6). The third method was by salting out by adding 60% ammonium sulphate (lane 7). The precipitate was further purified by followed isoelectric precipitation after resuspending it in 5mM phosphate buffer (Lane 8). Figure 2.15 shows the UV spectrum of the protein purified by three methods. The ethanol precipitation method yield was higher compared to other two methods for the same volume of soluble protein taken. However the protein purified by isoelectric precipitate of 40% eluent was found to be more pure and free from other nucleic acids as shown from the spectrum. Protein purified using ammonium sulphate precipitation method did give pure protein and also the yield was very low. Figure 2.16

shows all the tropomyosin isoforms synthesised for this research work along with two HCM mutations A63V and K70T and at the same time reflects the difference in the molecular weight of all the protein isoforms.

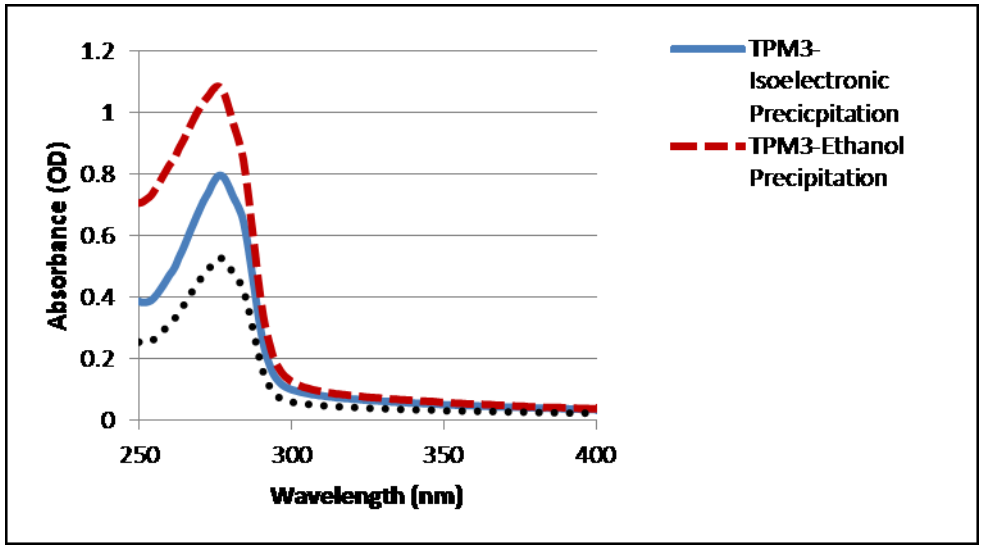

Figure 2.15: Absorption spectra of different methods for protein purification: Ethanol (EtOH) precipitation (red) has given more yields but the purity of the protein is less than the isoelectric precipitation (blue) while ammonium sulphate precipitation (black) has less yield as well as purity than the other two methods. Hence isoelectric precipitation is chosen for future purification processes.

Figure 2.16 shows all the tropomyosin isoforms synthesised for this research work along with two HCM mutations A63V and K70T and at the same time reflects the difference in the molecular weight of all the protein isoforms. It is observed that the tropomyosin isoforms run differently on the SDS gels even though the molecular weight of the tropomyosin isoforms does not vary much. This may be due to the fact that tropomyosin is usually a heat resistant protein and after it is denatured at higher temperature by boiling it refolds to its natural state, hence the protein may still be in its native state on the gel.

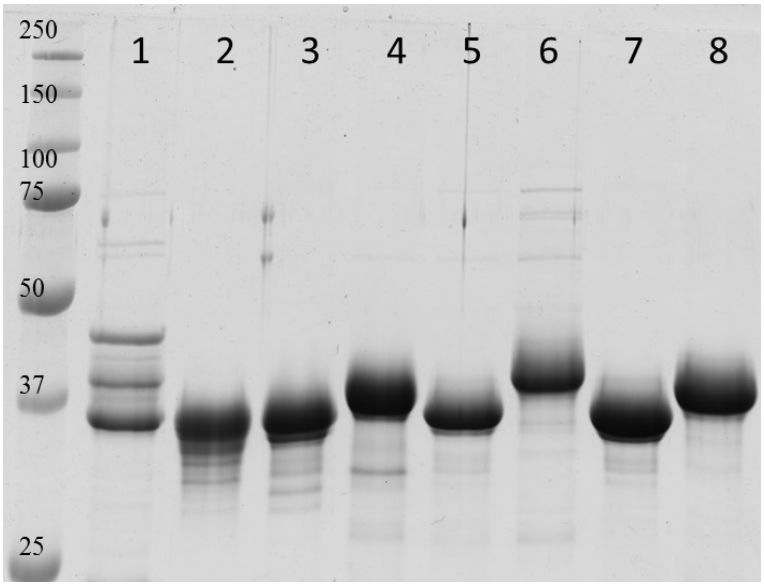

Figure 2.16: Gel showing all the isoforms of recombinant tropomyosins. Lane1 - Tropomyosin extracted from mouse heart (left ventricle), lane 2 – γTpm-Met, lane 3 – γTpm-MM, lane 4 - γTpm-MASM, lane 5- αTpm-MASM, lane 6 – βTpm-truncated, lane 7 – αTPM1- A63V (HCM mutation), lane 8 – αTPM1 – K70T (HCM mutation).

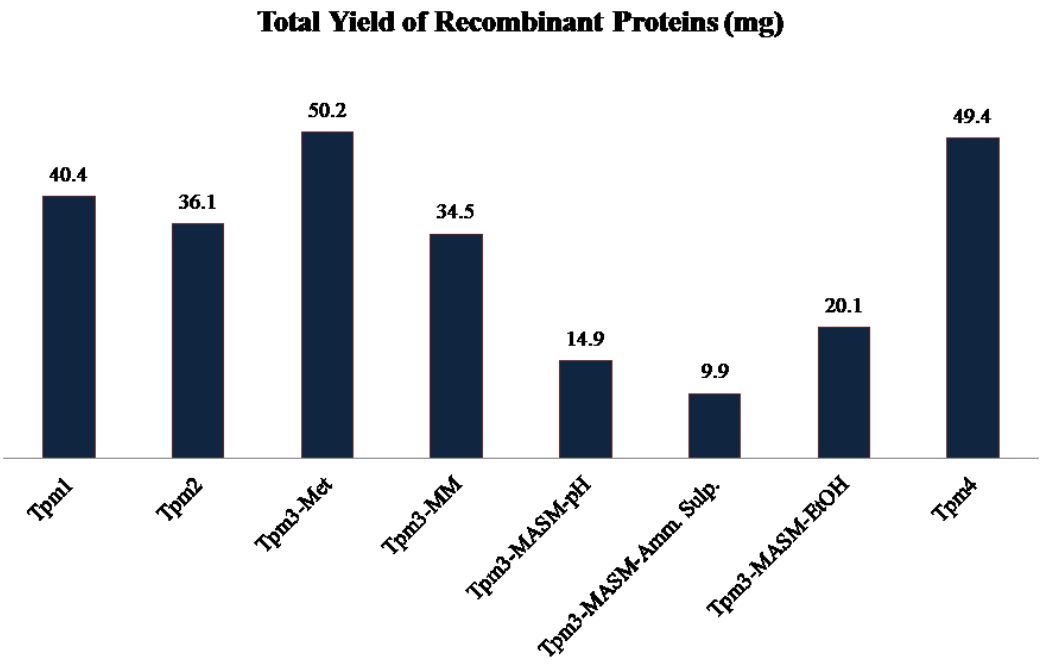

Figure 2.17: Total yield of recombinant proteins per litre of culture. pH- protein purified by isoelectric precipitation, Amm.Sulp – Ammonium sulphate, EtOH – Ethanol. For Tpm3- MASM the yield is shown form all the three methods employed for optimizing the purification method.

2.5.4 Mass spectrum of intact pure protein

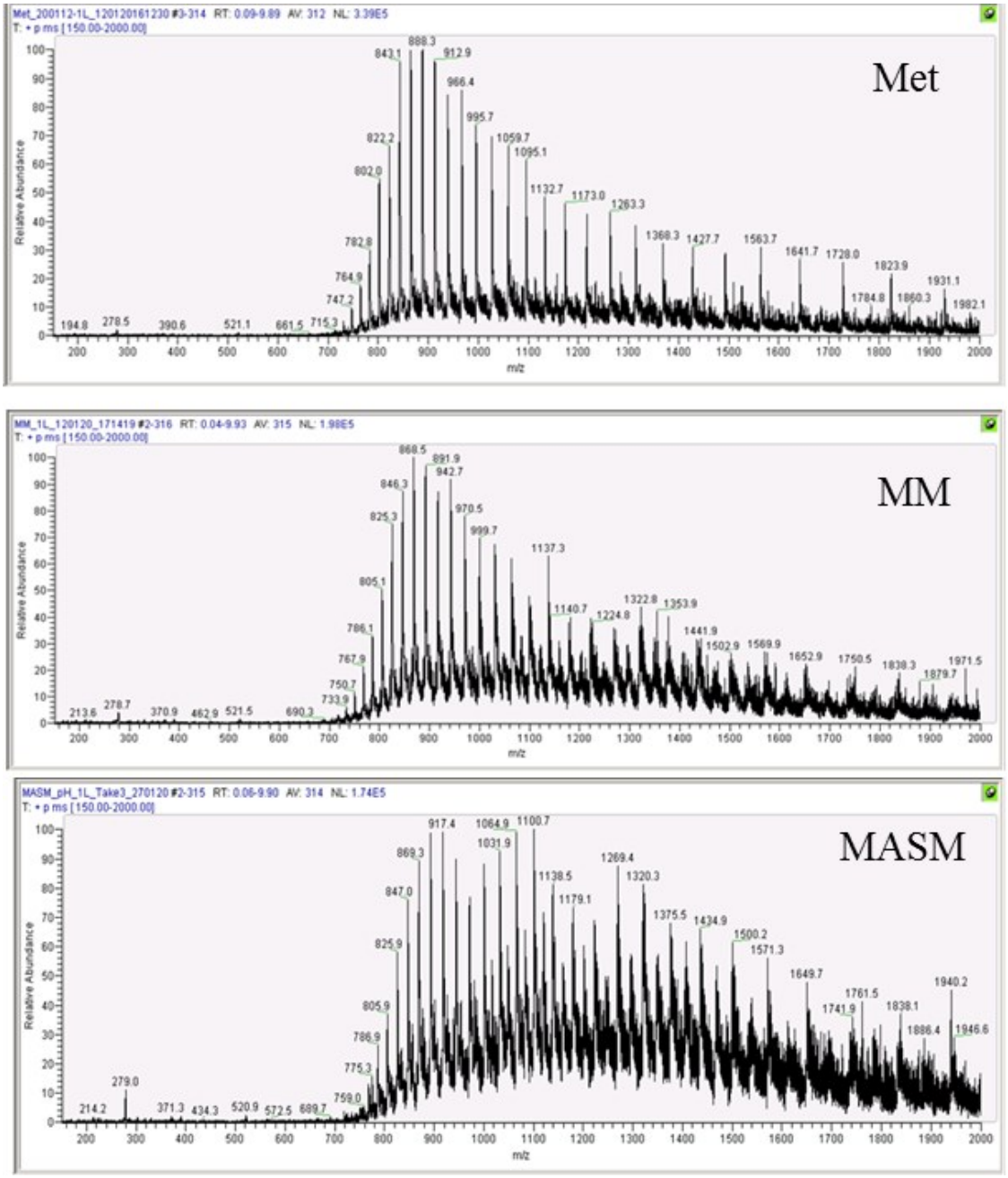

Figure 2.18: MS spectra of the electrospray ionization: The mass is calculated by mass/charge ratio (m/z) obtained from the spectra and determining the number of charge states of the peaks obtained. Approximately 10µg of protein is injected with 40% methanol and 0.1% formic acid for confirming the protein mass.

Table 2.3: Mass of the tropomyosins calculated from the m/z ratio of mass spectrum: The difference in the sequence mass and the calculated mass of all the recombinant tropomyosin isoforms expressed in *E. coli.* Mass calculated from the m/z ratio of the mass spectrometry analysis.

Protein	Sequence MW (Da)	Calculated-MW	Difference (Da)
Tpm1	32856.15	-	-
Tpm2	32850.7	32854.74	4.04
Tpm3-Met	32818.7	32823.6	4.9
Tpm3-MM	32949.9	32950.8	0.9
Tpm3-MASM	33108.1	32980.46	127.64
Tpm3-Met-K249Q	32818.7	32824.1	5.4
Tpm4	32722.6	32773.98	51.37

The above table 3 shows the mass calculated from form the mass/charge peaks obtained from mass spectrometry analysis. Tpm2, Tpm3-Met, MM and another version of Tpm3 was accidently produced with a mutation at 249 residue with a lysine to glutamine substitution (Tpm3-Met-K249Q), all were found to have intact methionine at the N-terminal end of the sequence.Tpm3-MASM with a mass difference of 127.64 shows that the initial methionine is cleaved during post-translational modification with an error of 4 Da. On the other hand Tpm4 had a calculated mass difference of 51.37 Da which may be due to loss of isoleucine at the C-terminal end or the protein may have not expressed correctly, which needs to be confirmed and needs characterising separately. Hence the results of Tpm4 are not taken into consideration further in the whole thesis.

2.5.5 Actin Preparation

Actin was prepared form chicken breast meat. For 1000 grams of mincemeat a total of 74.04 g of fine acetone powder and 37.35 g of coarse powder were obtained. Figure 1.14 shows the stages of actin extraction from muscle powder.

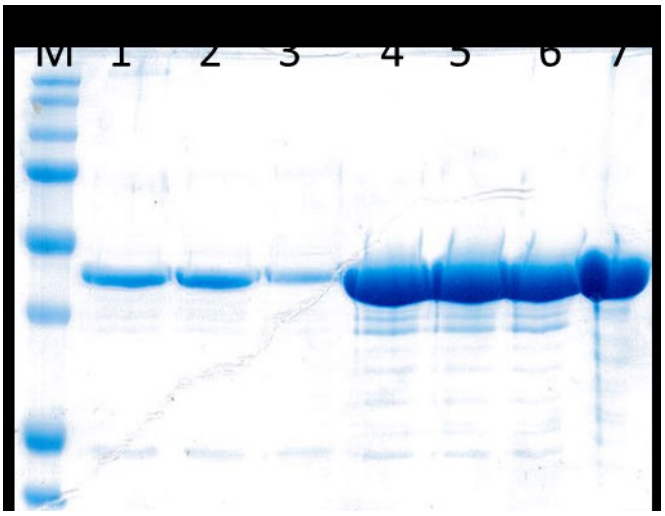

Figure 2.19: Actin purification stages. 1. G actin extracted form muscle powder after filtration, 2. Polymerised F-actin. 3. Supernatant left after pelleting out F-actin. 4. F actin pellet resuspended in depolymerisation buffer. 5- F-actin used for labelling, 6. Pyrene labelled F actin, 7. Depolymerized pyrene labelled G-actin.

2.5.6 Pyrene G-actin quantification

Purified Py-G actin as described in methodology was pure as seen in the SDS-Gel in Figure 2.19. The purity was also confirmed by the UV absorption spectrum at 280 nm and the labelling ratio obtained was 1.09 from this method (Figure 2.20).

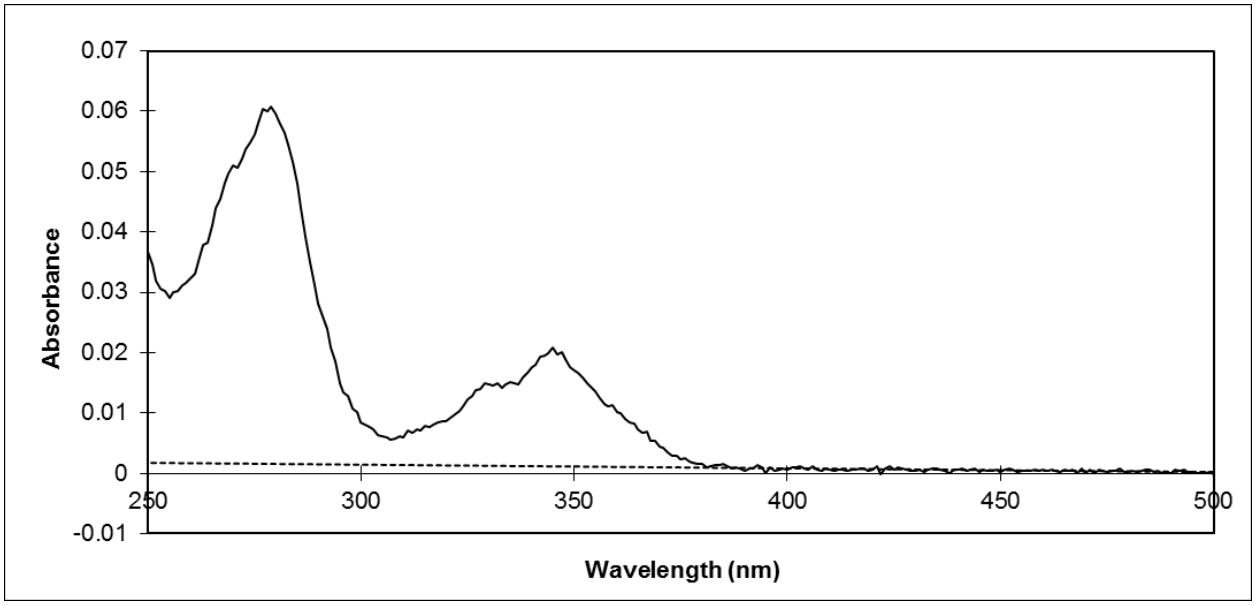

Figure 2.20: UV spectrum of purified pyrene labelled G-Actin. The peak at 280 nm shows the pure G actin and pyrene has an absorption spectrum at 344 nm. Using the excitation coefficient of 22000 M^{-1} pyrene concentration was calculated.

2.5.7 Affinity of Tropomyosin with actin filaments

The affinity of tropomyosin isoforms with actin filament was determined by co-sedimentation assays and the standard curve generated is shown in Figure 2.21. The results of the binding affinity of tropomyosin to actin for all the isoforms produced in this study are shown in figures from Figure 2.22 to Figure2.29. The curves are fitted to Hill equation and the values obtained for both $K_{50\%}$ (the concentration of free Tm at which half actin is saturated) is referred to as binding constant and 'n'the Hill coefficient that determines the sigmoidicity of the curve measures the degree of co-operativity. The maximum saturation (Vmax) of actin by tropomyosin which was set constant at 4.0 staining ratio calculated from the tropomyosin/actin (Tm/Ac) in the pellet. The value 4.0 is used because the actin and tropomyosin stain differently on a gel. The staining ratio

cannot be taken as equivalent for both the proteins as they differ in their molecular weight.

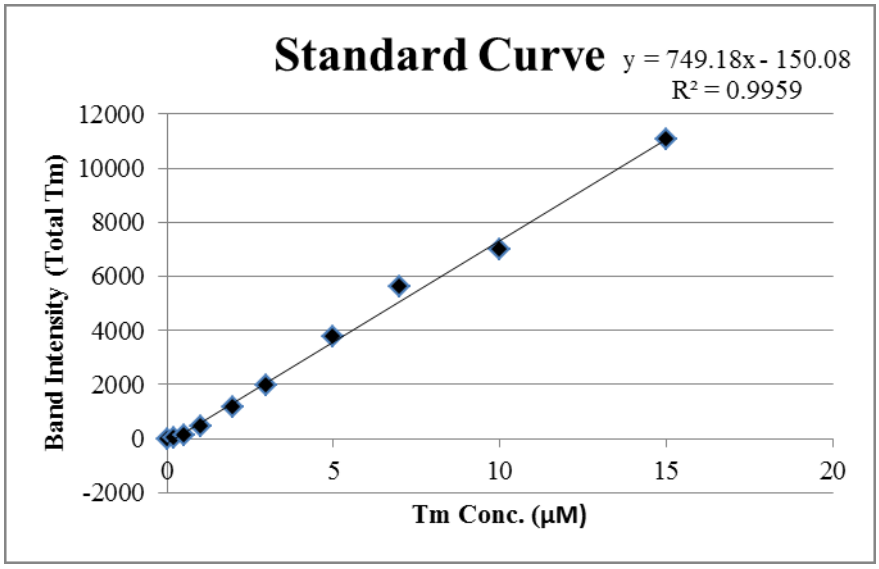

Figure 2.21: A standard curve used to calculate free tropomyosin concentration in the supernatant. Standard curve is generated by plotting band intensity against the concentration of Tm used for the assay.

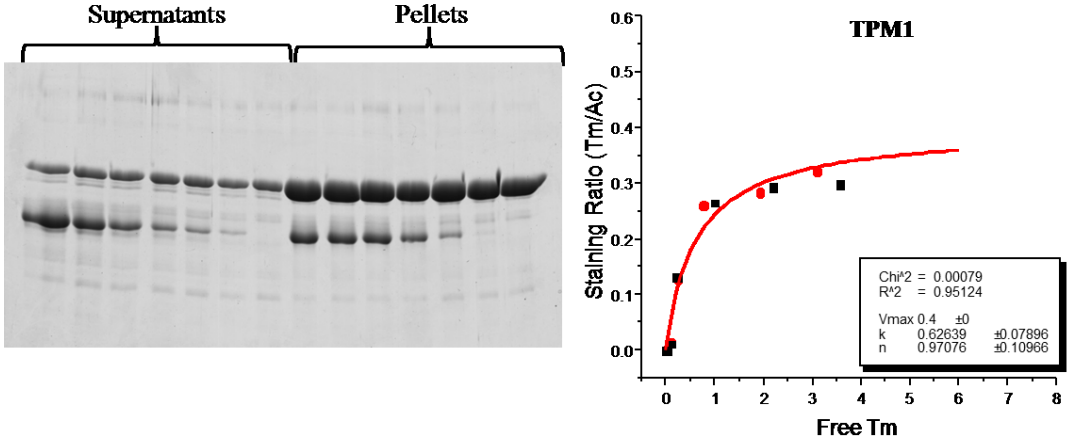

Figure 2.22: Actin binding co-sedimentation assay result of Tpm1. The experimental details are described in the methodology section. The sequence of bands from left to right are 10 µM actin mixed with 0.1, 0.2, 0.5, 1.0, 3.0 and 5.0 µM Tm. Left picture shows the gel and the right panel shows the fitted binding curve of Tpm1. The curves are fitted to a version of Hill equation and the values obtained for both $K_{50\%}$ (the concentration of free Tm at which half actin is saturated) and 'n'the Hill coefficient that determines the sigmoidicity of the curve measures the degree of co-operativity. The results show Tpm1 shows higher affinity with actin with $K_{50\%}$ at 0.6µM of free Tm. The values of $K_{50\%}$ and n are given in table 2.4. Circles, squares are the data sets obtained from 2 replicates of the experiment.

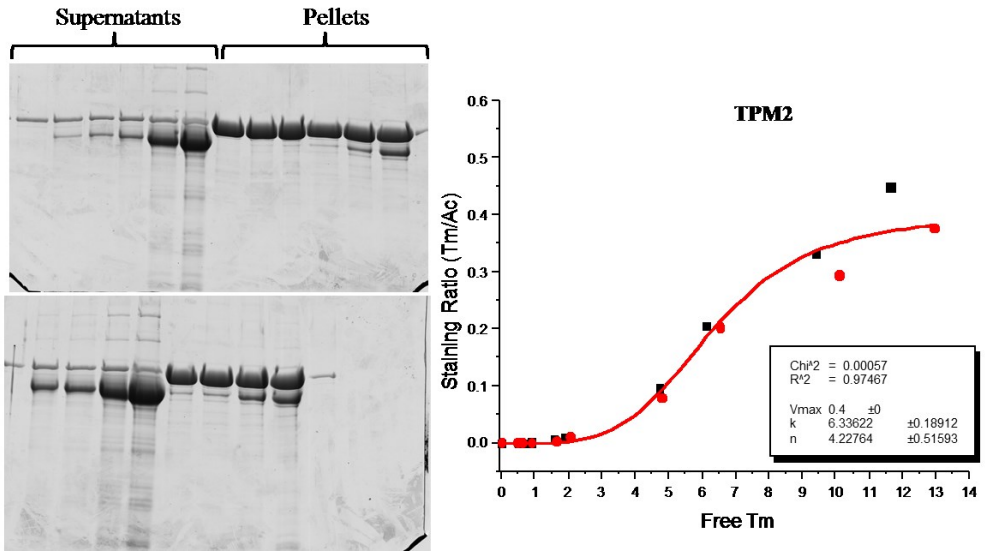

Figure 2.23: Actin binding cosedimentation assay results of Tpm2. The experimental details are described in the methodology section. Left picture shows the gel and the right panel shows the fitted binding curve. The curves are fitted to a version of Hill equation and the values obtained for both $K_{50\%}$ (the concentration of free Tm at which half actin is saturated) and 'n'the Hill coefficient that determines the sigmoidicity of the curve measures the degree of co-operativity. The values of $K_{50\%}$ and n are given in The experimental details are described in the methodology section 2.4.4.

Table 2.4. Top gel on the left side has concentrations of 0, 0.1, 0.2, 0.5, 1.0, 5.0 and 10.0 μM and the bottom gel has 2.0, 3.0, 7.0, 15.0μM Tm. Higher concentrations are used to show the saturation of actin with Tm. Tpm2 shows lower affinity to actin agreeing with previous research results. Circles, squares are the data sets obtained from 2 replicates of the experiment.

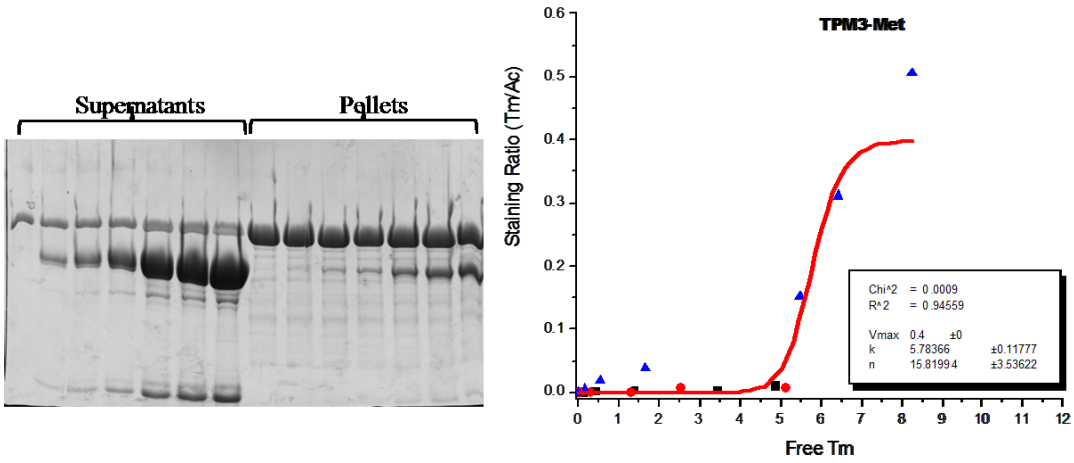

Figure 2.24: Actin binding cosedimentation assay results of Tpm3-Met. The experimental details are described in the methodology section. Left picture shows the gel and the right panel shows the fitted binding curve. The curves are fitted to a version of Hill equation and the values obtained for both $K_{50\%}$ (the concentration of free Tm at which half actin is saturated) and 'n'the Hill coefficient that determines the sigmoidicity of the curve measures the degree of co-operativity. The values of $K_{50\%}$ and n are given in The experimental details are described in the methodology section 2.4.4.

Table 2.4. Top gel on the left side has concentrations of 0, 0.1, 0.2, 0.5, 1.0, 5.0 and 10.0 µM. Circles, squares and triangles are the data obtained from 3 replicates of the experiment. For third replicate (triangles) assays was performed up to 10 µM and the previous once (circles and squares) upto a maximum of 5 µM Tm.

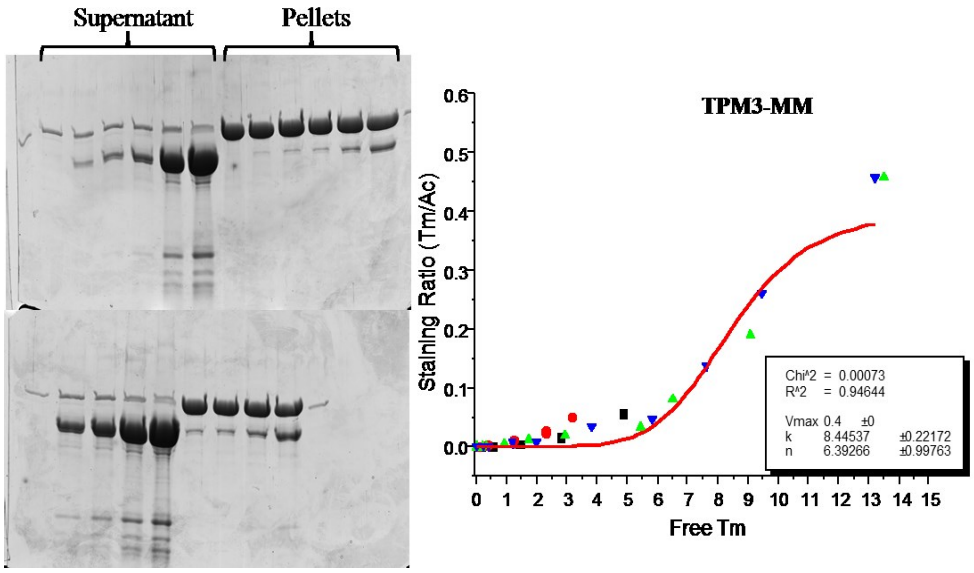

Figure 2.25: Actin binding cosedimentation assay results of Tpm3-MM. The experimental details are described in the methodology section. Left picture shows the gel and the right panel shows the fitted binding curve. The curves are fitted to a version of Hill equation and the values obtained for both $K_{50\%}$ (the concentration of free Tm at which half actin is saturated) and 'n'the Hill coefficient that determines the sigmoidicity of the curve measures the degree of co-operativity. The values of $K_{50\%}$ and n are given in The experimental details are described in the methodology section 2.4.4.

Table 2.4. The concentration of Tm, top gel on the left are 0, 0.1, 0.2, 0.5, 1.0, 5.0 from left to tight and 10.0 µM and the bottom gel has 2.0, 3.0, 7.0, 15.0 µM Tm.

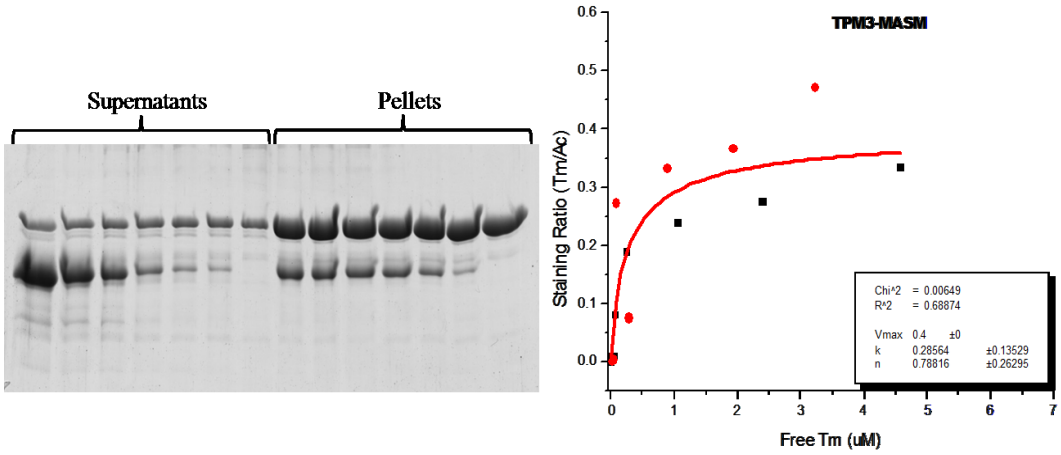

Figure 2.26: Actin binding cosedimentation assay results of Tpm3-MASM. The experimental details are described in the methodology section. Left picture shows the gel and the right panel shows the fitted binding curve. The curves are fitted to a version of Hill equation and the values obtained for both $K_{50\%}$ (the concentration of free Tm at which half actin is saturated) and 'n'the Hill coefficient that determines the sigmoidicity of the curve measures the degree of co-operativity. The values of $K_{50\%}$ and n are given in The experimental details are described in the methodology section 2.4.4.

Table 2.4. The sequence of bands from left to right are10µM actin mixed with 0.1, 0.2, 0.5, 1.0, 3.0 and 5.0 µM Tm. Circles, squares are the data sets obtained from 2 replicates of the experiment.Tpm3-ASM shows higher affinity with actin with $K_{50\%}$ 0.2µM free Tm.

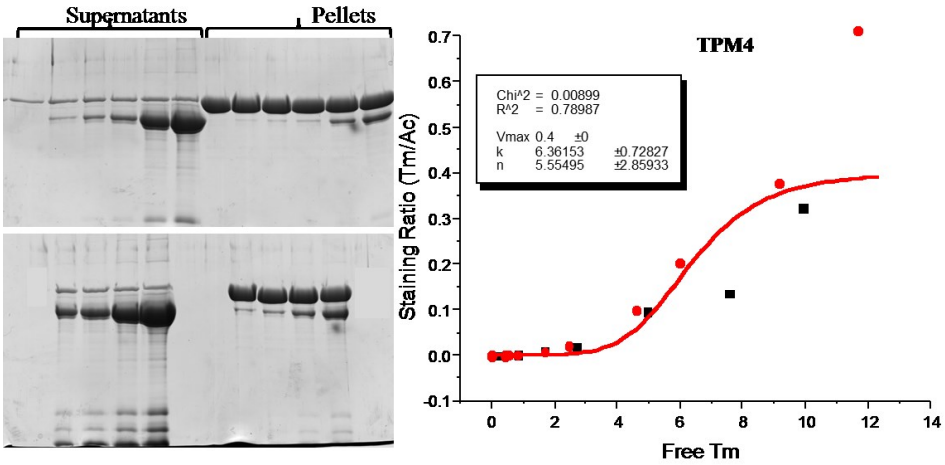

Figure 2.27: Actin binding cosedimentation assay results of Tpm4-ASM. The experimental details are described in the methodology section. Left picture shows the gel and the right panel shows the fitted binding curve. The curves are fitted to a version of Hill equation and the values obtained for both $K_{50\%}$ (the concentration of free Tm at which half actin is saturated) and 'n'the Hill coefficient that determines the sigmoidicity of the curve measures the degree of co-operativity. The values of $K_{50\%}$ and n are given in The experimental details are described in the methodology section 2.4.4.

Table 2.4. Top gel on the left side has concentrations of 0, 0.1, 0.2, 0.5, 1.0, 5.0 from left to tight and 10.0 µM and the bottom gel has 2.0, 3.0, 7.0, 15.0 µM Tm.

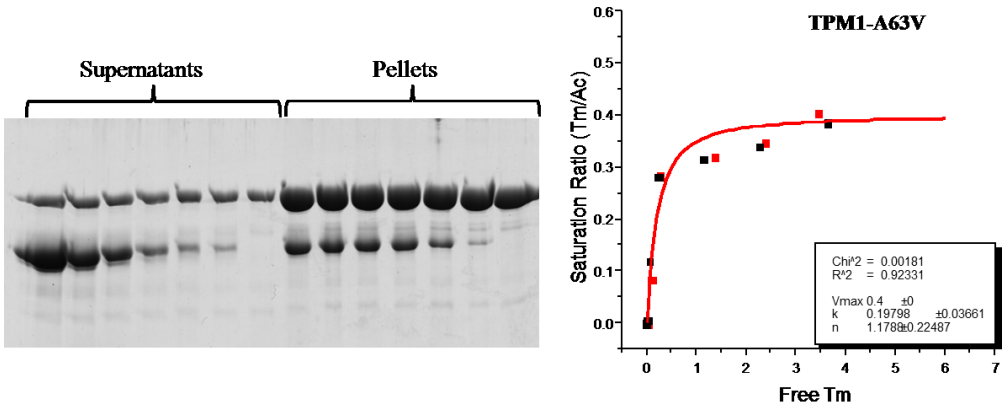

Figure 2.28: Actin binding cosedimentation assay results of Tpm1-A63V (HCM mutation). The experimental details are described in the methodology section. Left picture shows the gel and the right panel shows the fitted binding curve. The curves are fitted to a version of Hill equation and the values obtained for both $K_{50\%}$ (the concentration of free Tm at which half actin is saturated) and 'n'the Hill coefficient that determines the sigmoidicity of the curve measures the degree of co-operativity. The values of $K_{50\%}$ and n are given in The experimental details are described in the methodology section 2.4.4.

Table 2.4. The sequence of bands from left to right are10μM actin mixed with 0.1, 0.2, 0.5, 1.0, 3.0 and 5.0 μM Tm. Circles, squares are the data sets obtained from 2 replicates of the experiment.

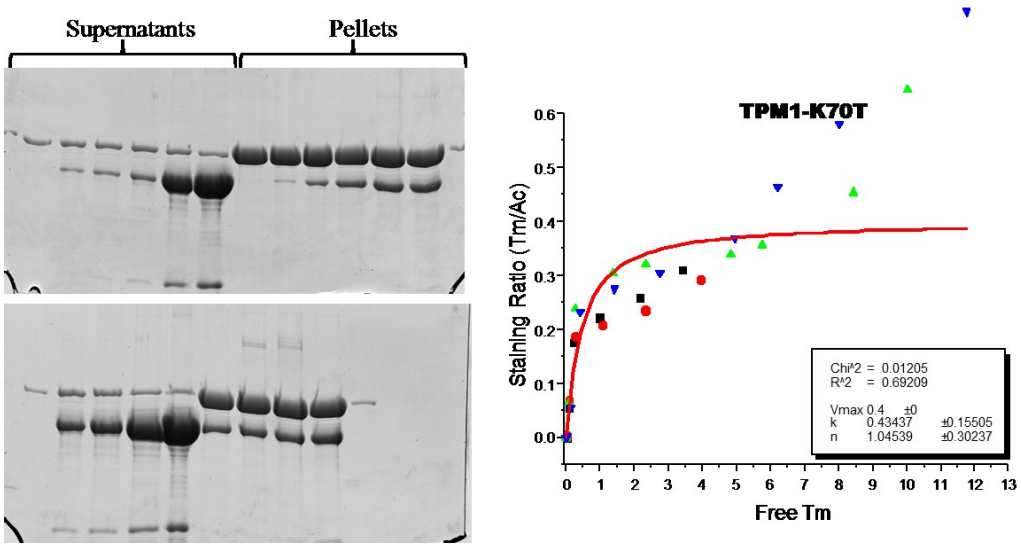

Figure2.29: Actin binding cosedimentation assay results of Tpm1-K70V (HCM mutation). The experimental details are described in the methodology section. Left picture shows the gel and the right panel shows the fitted binding curve. The curves are fitted to a version of Hill equation and the values obtained for both $K_{50\%}$ (the concentration of free Tm at which half actin is saturated) and 'n'the Hill coefficient that determines the sigmoidicity of the curve measures the degree of co-operativity. The values of $K_{50\%}$ and n are given in The experimental details are described in the methodology section 2.4.4.

Table 2.4. Top gel on the left side has concentrations of 0, 0.1, 0.2, 0.5, 1.0, 5.0 and 10.0 μM. Circles, squares and triangles are the data sets obtained from 4 replicates of the experiment. For third and fourth replicate (triangles) assays was performed upto 15 μM and the previous once (circles and squares) upto a maximum of 5 μM Tm.

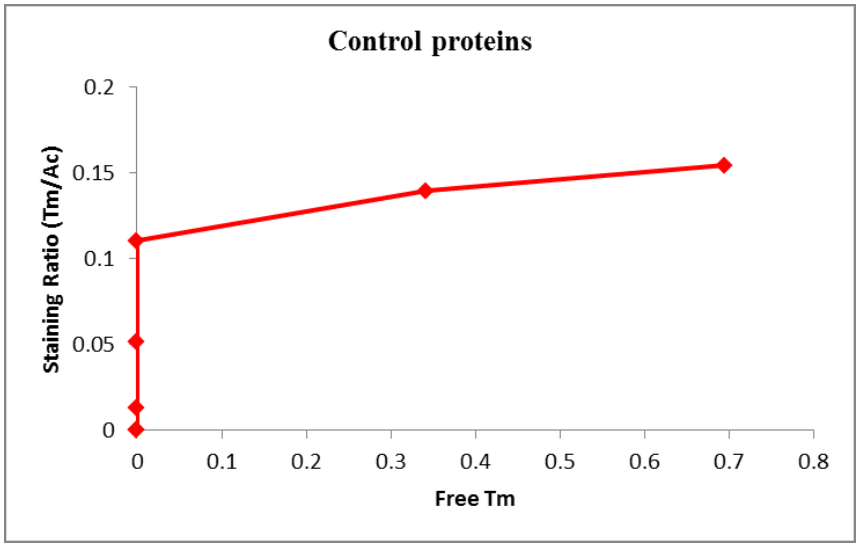

Figure 2.30: Co-sedimentation curve of control proteins: The experimental details are described in the methodology section 2.4.4.

Table 2.4: Table showing parameter for curve fits for actin binding co-sedimentation assays. Vmax is the complete saturation of tropomyosin with actin, $K_{50\%}$ is concentration of free tropomyosin at which half of actin is saturated and n is the Hill coefficient that determines the sigmoidicity of the curve measures.

Tm isoform	Vmax	$K_{50\%}$	N
TPM1 (ASM)	0.4	0.62 ± 0.07	0.97 ± 0.10
TPM2 (truncated)	0.4	6.33 ± 0.18	4. 22 ± 0.51
TPM3-Met	0.4	5.78 ± 0.11	15.81 ± 3.53
TPM3-MM	0.4	8.44 ±0.21	6.39 ± 0.99
TPM3-ASM	0.4	0.28 ± 0.13	0.78 ± 0.26
TPM4 (ASM)	0.4	6.36 ±0.72	5.55 ± 2.85
TPM1-A63V	0.4	0.19 ± 0.03	1.17 ± 0.22
TPM1-K70T	0.4	0.43 ±0.15	1.04 ± 0.30

It can be seen that Tpm1-ASM, Tpm3-ASM, Tpm1-A63V and Tpm1-K70T affinities shown fall in the range of 0.1 to 0.6 µM free tropomyosin agreeing with previous results of tropomyosin binding to actin (Heald and Hitchcock-DeGregori, 1988; Maytum et al., 2001; Monteiro et al., 1994). All these protein isoforms have cleaved N-terminal Met by post translational process and the additional ASM remains at N-terminal of the sequence

where it replaces the acetlyation of the protein. The HCM mutation A63V found to bind very tightly and the other Tpm3 isoform variants with Met and MM does not seem to have same affinity as the 3 amino acid fusion (MASM) as their $K_{50\%}$ values show greater saturation values of ~ 6 μM for Met and ~8 μM for MM supported from the mass spectrometry data given in Table 2.3. Isoform Tpm2 was a truncated WT version where the N-terminal sequence was not modified and is seen that the affinity to actin is very low and does not bind co-operatively (curve loses its sigmoidicity) that corresponds to the previous results On the other hand Tpm4 even thought has been modified at the N-terminus did not show strong affinity to actin.

2.5.8 Actin-tropomyosin polymerisation assays.

It was not possible to calculate the curves data to fit to a single kinetic model, however the curves fitted with Hill equation were in good agreement with previous time course polymerisation curves. Particularly at low total ionic concentrations the measured curves were having significantly longer initiation and elongation times showing more sigmoidicity in contrast to higher ionic concentration of G actin. For this reason the results of actin polymerisation studies with tropomyosin presented are not analysed quantitatively as it needs to establish a kinetic model for this kind of reaction. There are other simulated kinetic models available for actin-tropomyosin described previously, however it needs more data on nucleation and elongation measurements to fit to the right model. This set of experiments were analysed qualitatively in comparison with the results obtained from previous research results which were primarily done by using Tpm1

(Frieden, 1983a; Hitchcock-DeGregori and Heald, 1987; Lal and Korn, 1986; Wegner, 1980; Wegner and Ruhnau, 1988; Weigt et al., 1991).

The fluorescent intensity of Pyrene labelled actin increased to 7 fold (Figure 2.31) from monomer to filamentous polymerised actin similar to previous studies (Cooper et al., 1983b; Kouyama and Mihashi, 1981). The critical concentration of actin in physiological conditions was measured to be 0.1 μM which remains constant independent of concentration of F-Ac. Critical concentration is the total amount of monomer actin left unpolymerised. Critical concentration was not measured in this study.

Figure 2.31 shows the time course polymerisation curves of actin in two different concentrations of 2 μM and 6 μM of Pyrene G-actin. Figure 2.31A shows the time course polymerisation of 2 μM actin. The polymerisation is initiated by adding 2 mM $MgSO_4$, 0.1 M KCl, 0.1 mM ATP to pre-incubated Py-Ac with 0.1 mM EGTA. The dots shows the data points and the line shows the simulated curved using the data. Figure 2.31B shows polymerisation curve of 6 μM actin assays under same condition as mentioned for 2 μM. The red line is the freshly prepared Py-Ac and black line is actin which was 10 days old for 6 μM and 12 days old for 2 μM, which I used to show the difference in the polymerisation time course. The polymerisation of 6 μM actin is faster than 2 μM actin and the final steady state is reached faster with 6 μM with a half time taken for polymerisation taken is 230 seconds which is less than for 2 μM (721 seconds) to reach half polymerisation rate. The half times (k) is given in Table 2.5. It is observed that for 2 μM there is not much difference between fresh and 12 days old actin, but the amount of polymer formed seems higher and the rate of polymerisation seems to be slow with k

value increasing to double to 1490 sec which was not the same for 6 μM. Due to these minor differences all the data is compared with both of these curves.

Figure 2.31C shows the difference between the curves of 2 μM and 6 μM actin. 2 μM actin show longer initiation phase and the elongation time is longer due to slow formation of nucleus which in turn is due to lower concentration of actin (Wegner and Engel, 1975). Due to the slower elongation rate it took longer time to reach steady state for 2 μM (polymerisation still continues after 120 min) than 6 μM actin (reached steady state in 35 min).

The data obtained from all the assays were compared with actin polymerisation with 6 μM actin both fresh and old polymerisation curves in order to eliminate any difference occurring due to storage. All the assays were performed after spinning the sample at 55 k rpm to remove any precipitated G actin.

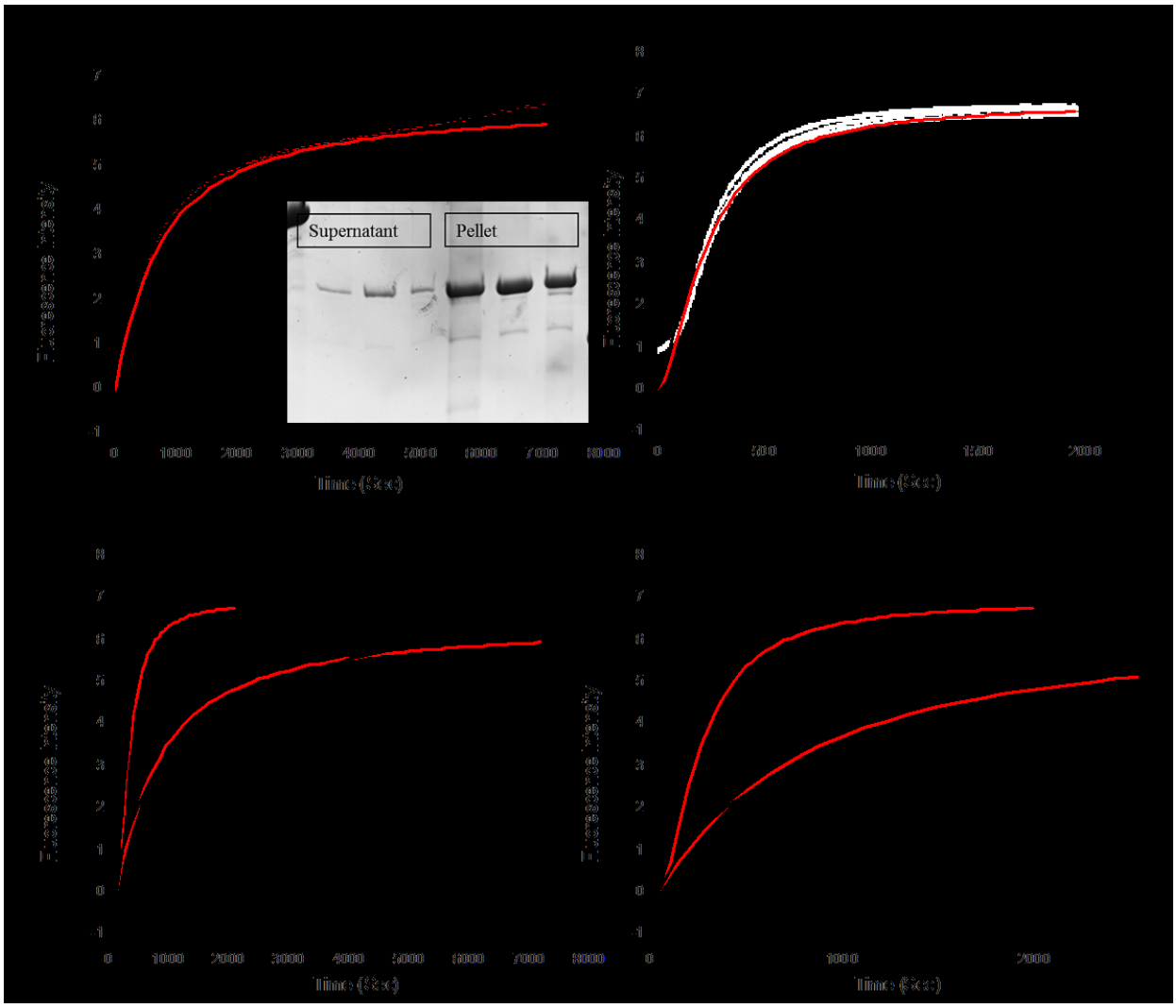

Figure 2.31: 2 µM and 6 µM Actin polymerisation. The data is fit to sigmoidal Hill equation, the data points are not shown as there are too many data points to interpret with the fitted curve. Red line is freshly made Pyrene G Actin and black line is 10 days old for 6 µM and 12 days old for 2 µM Py-G actin used for polymerisation. A. 2 µM actin only, B. 6 µM actin only, C. comparative curves of A and B, D. Comparitive curves of A and B showing the lower time scale for clear emphasis of the initiation stage.

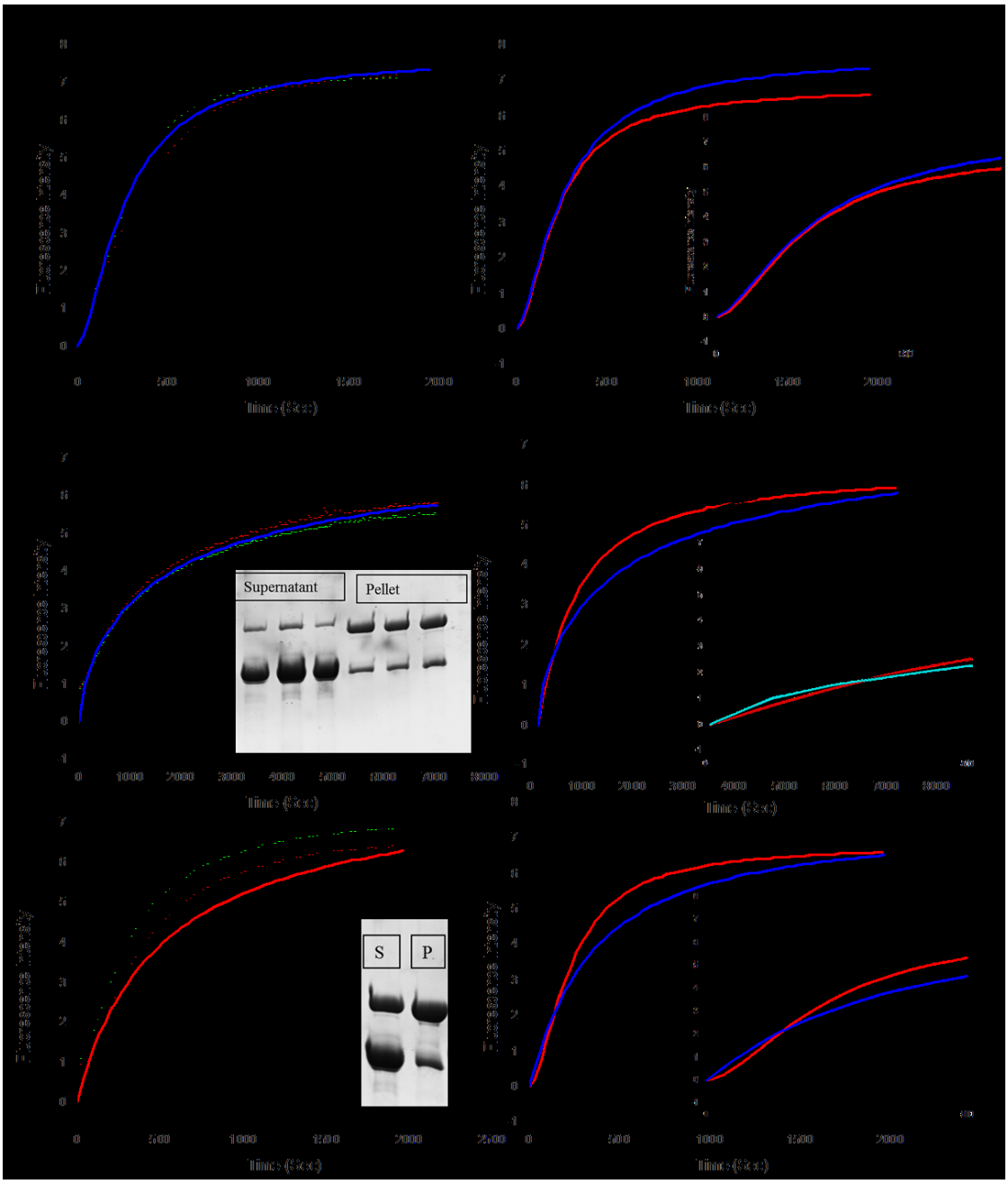

Figure 2.32: Actin polymerisation with different concentrations of Tpm1. A. 6 µM PyG-actin polymerised with 0.5 µM Tpm1, **B**. A integrated with 6 µM actin curves showing the polymerisation rate difference in presence and absence of Tpm1 with both fresh actin (red line) and 10 day old actin (black line) **C**. 2 µM Py-G-actin with 5 µM Tpm1 and D integrated with 2 µM actin alone, E and F are with 6 µM actin with 5 µM Tpm1. The inset in the graphs on the left hand side (A, C and E) shows the coomassie stained SDS-gels of the assays on the righ hand side (B, D and F) the inset shows the same curves with a different time scale to show the nucleation phase clearly. After completion of the polymerisation, the samples were spun down and the supernatant and

pellet were separated. The pellet was resuspended in equal amount of buffer along with SDS sample buffer and run on 13.5 % SDS gels. S- supernatant, P-Pellet. The dots on the graphs are the data used for generating the curves.

2 μM and 6 μM actin were polymerised with different concentrations of Tpm1. Curve A and B from Figure 2.32 shows in presence of 6 μM actin in presence of 0.5 μM Tpm1 show higher polymerisation rate than actin alone and has very slight higher rate of initiation (Table 2.5) but the end fluorescence intensity was higher than the actin alone indicating there is more polymerisation at very low Tpm1 concentration. This curve is compared with the fresh actin as both polymerisaiton assays were perfomed on the same day. The curves from 6 μM in presence of 5 μM Tpm1 (Figure 2.32E and F) show a different scenario as it is seen that presence of Tpm1 in this case has higher initiation rate than actin alone but the elongation rate (half time 337 sec) the final polymerisaiton product has lowered. With 2 μM actin in presence of 5 μM Tpm1 (Figure 2.32C and D) the increase in fluorescence is slower than 6 μM actin however the initiaiton is slightly higher than actin alone and the elongation rate is lowered with half maximal polymerisation time of 1757 sec, however the final fluorescence intensity was same as in the absence of Tpm1 (V_{max} of 8 for actin alone and 7.9 in presence of Tpm1). The initiation and elongation of polymerisaiton seems to affect differently with different concentrations of actin and tropomyosin. With the observations and time restriction, 6 μM actin and 5 μM tropomyosin concentration were chosen to continue with other assays for comparison of other isoforms of tropomyosins.

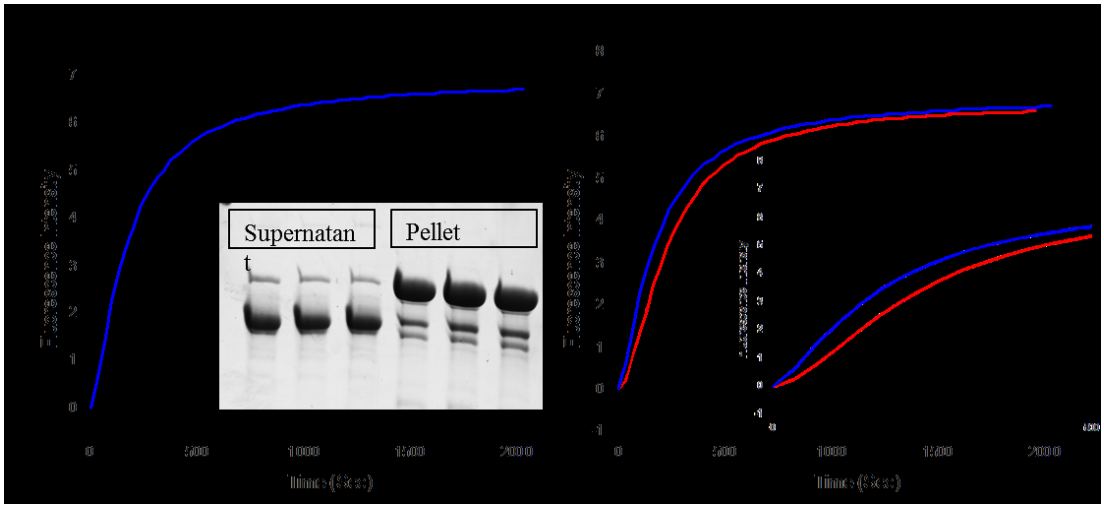

Figure 2.33: Time course polymerisation curves of actin with Tpm2. A. 6 µM actin in presence of 5 µM Tpm2. The inset shows the sedimented pellet and supernatent run on SDS page gel to check the binding efficiency. B. Curve A integrated into 6 µM actin actin curves for comparison. Blue line represent the Tpm2 curve. The inset shows the same curves with different time scale to show the initiation more closer. Fluorescence intensity is in arbitrary units.

Polymerisation curves of 6 µM in presence of Tpm2 (Figure 2.33 A and B) show an overall increase in polymerisation rate with higher initiation and elongation fluorescence intensity (k =170 sec) with final polymerisation fluorescence intensity being slightly higher than actin alone with a maximal polymerisation intensity of 6.9 (actin alone 6.7). Assay performed on day 3 of actin preparation (Refer to Table 2.5).

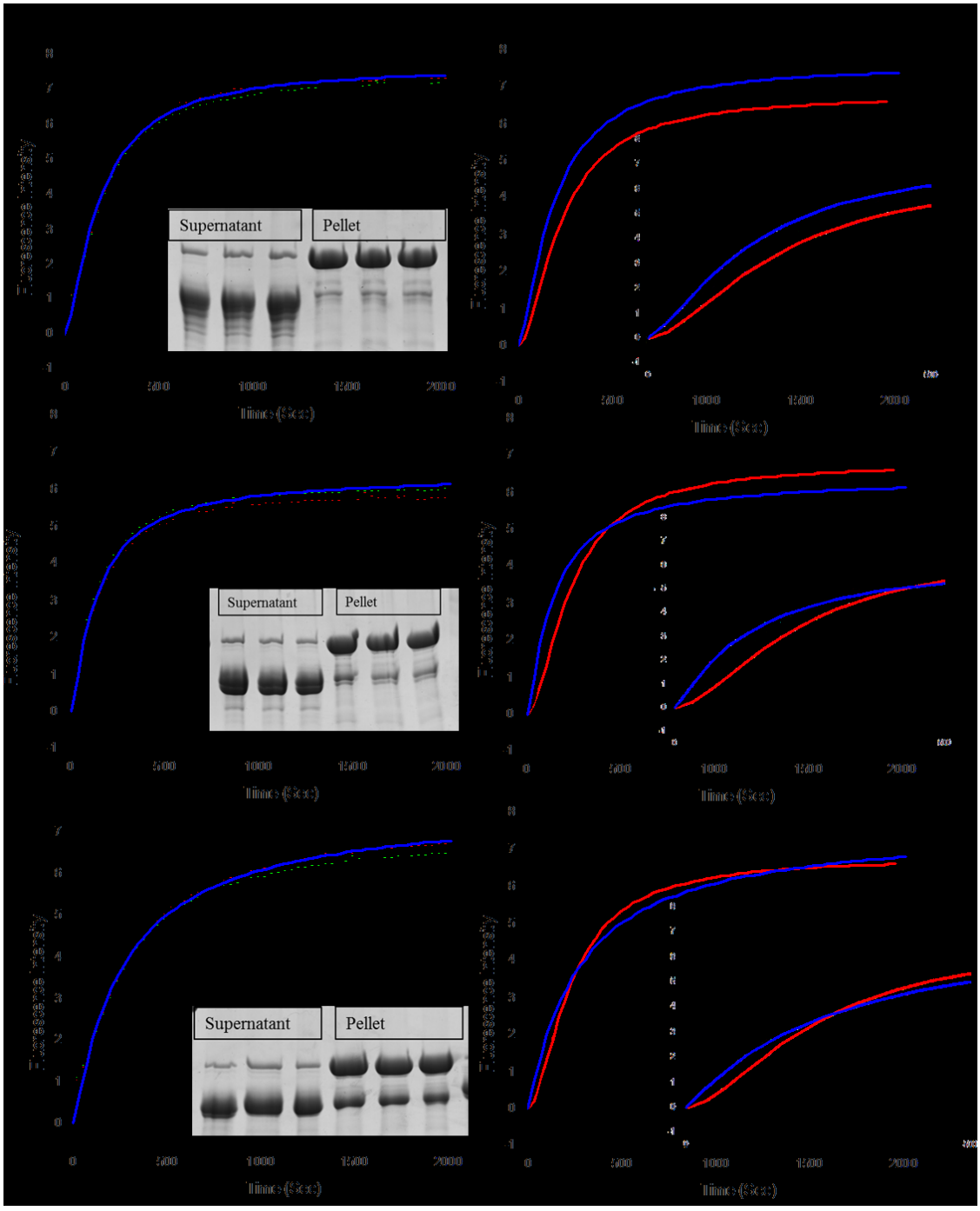

Figure 2.34: Time course polymerisation curves of actin with Tpm3. The expeimental conditions are as desciebed in methodology. A. 6 µM actin in presence of 5 µM Tpm3 Met. The inset shows the sedimented pellet and supernatent run on SDS page gel to check the binding efficiency. B. Curve A integrated into 6 µM actin curves for comparison. Blue line represent the Tpm3 curve. The inset shows the same curves with different time scale to show the initiation more closer. Curves C and D are 6 µM actin in presence of

Tpm3-MM and Curves E and F are in presence of Tpm3-MASM. Fluorescence intensity is in arbitrary units.

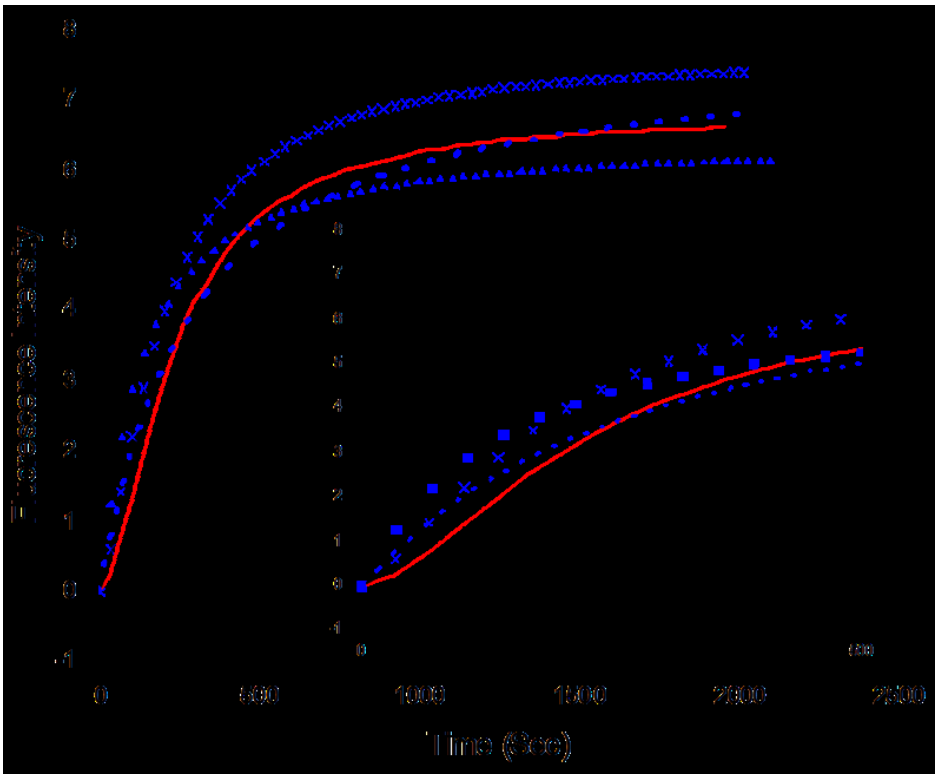

Figure 2.35: Comparison of time course polymerisation curves of Tpm3-Met, MM and MASM. Crosses – Met, squares – MM and dots- MASM. Red line-fresh actin, black line – 10day old actin.

The time course polymerisation curves of Tpm3 variants are shown in Figure 2.34 and Figure 2.35. Tpm3-Met (Figure 2.34 A and B) seems to have an increase in polymerisation rate similar to Tpm2 with an half maximal polymerisation value of 183 sec and the maximum fluorescent intensity with 7.6 (Tpm1 6.7). In presence of Tpm3-MM (Figure 2.34 C and D) the initiation was much faster with k = 138 sec as well as elongation rate but the maximum intensity upon completion was 6.38 units which was lower than actin alone, which shows the number of actin filaments formed are lower in presence of Tpm3-MM. In case of Tpm3-MASM (Figure 2.34 E and F) the initiation rate

is higher but the elongation rate is lower than actin alone with k value of 266 sec, however the maximum intensity (7.9 units) after the completion of polymerisation was higher in presence of Tpm3-MASM. Figure 2.35 shows the difference in effect of polymerisation on actin with three different N-terminal variants of Tpm3. There is lot of variation how they affect the initiation and elongation even though the experiments were performed on the same day with all these variants on day four of actin preparation.

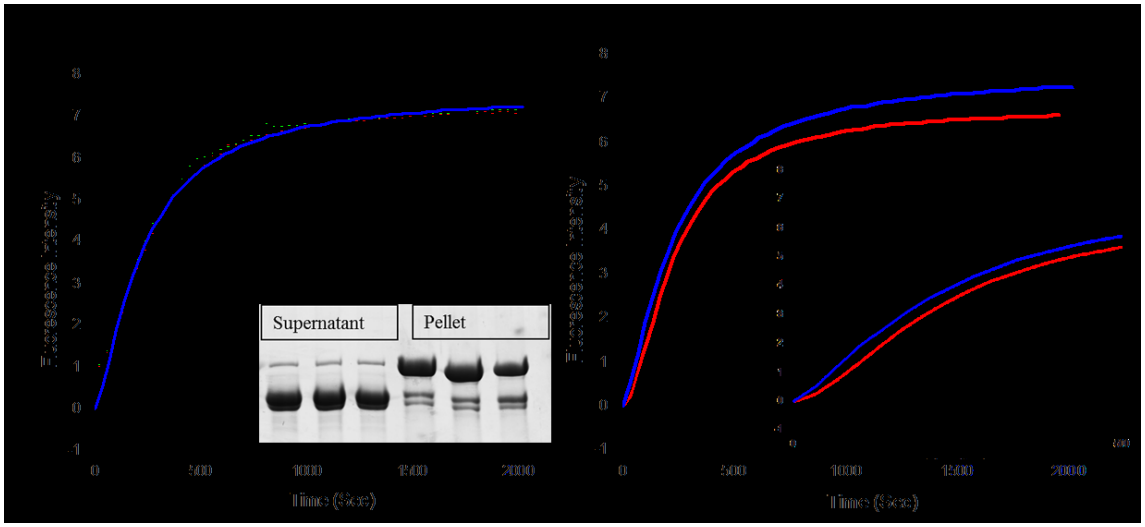

Figure 2.36: Time course polymerisation curve of actin with Tpm4. A. 6 µM actin in presence of 5 µM Tpm4. The inset shows the sedimented pellet and supernatent run on SDS page gel to check the binding efficiency. B. Curve A integrated into 6 µM actin actin curves for comparison. Blue line represent the Tpm4 curve. The inset shows the same curves with different time scale to show the initiation more closer. Fluorescence intensity is in arbitrary units. Assay was performed on day 5 of actin preparation.

The actin polymerisation assay performed were on day 5 of actin preparation. Tpm4 is more closer to 10 day old actin with slight decrease in elongation rate and the final fluorescence intensity (Figure 2.36 A and B).

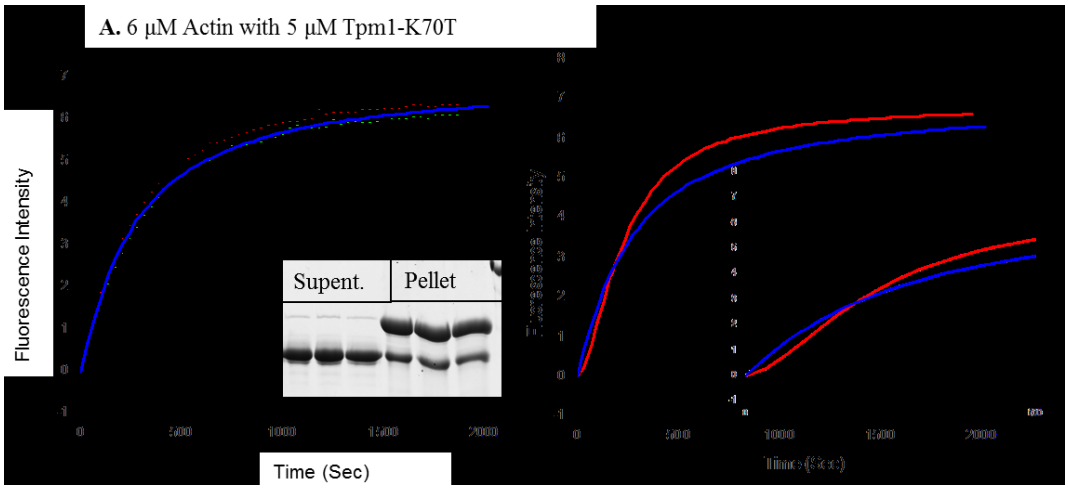

Figure 2.37: Time course polymerisation curve of actin with Tpm1-K70T. A. 6 µM actin in presence of 5 µM Tpm1-K70T. The inset shows the sedimented pellet and supernatent run on SDS page gel to check the binding efficiency. B. Curve A integrated into 6 µM actin actin curves for comparison. Blue line represent the Tpm1-K70T curve. The inset shows the same curves with different time scale to show the initiation more closer. Fluorescence intensity is in arbitrary units. Assay was performed on day 5 of actin preparation.

Tpm1-K70T is a N-domain α-straited muscle tropomyosin mutation associated with familial hypertrophic cardiamyopathy. The effect of actin polymerisation in presence of this mutated α-tropomyosin is similar to Tpm1, how ever the rate of initiation is higher and elongation is inhibited (k = 261 sec) with the final fluorescence intensity (6.9 units) lower than Tpm1.

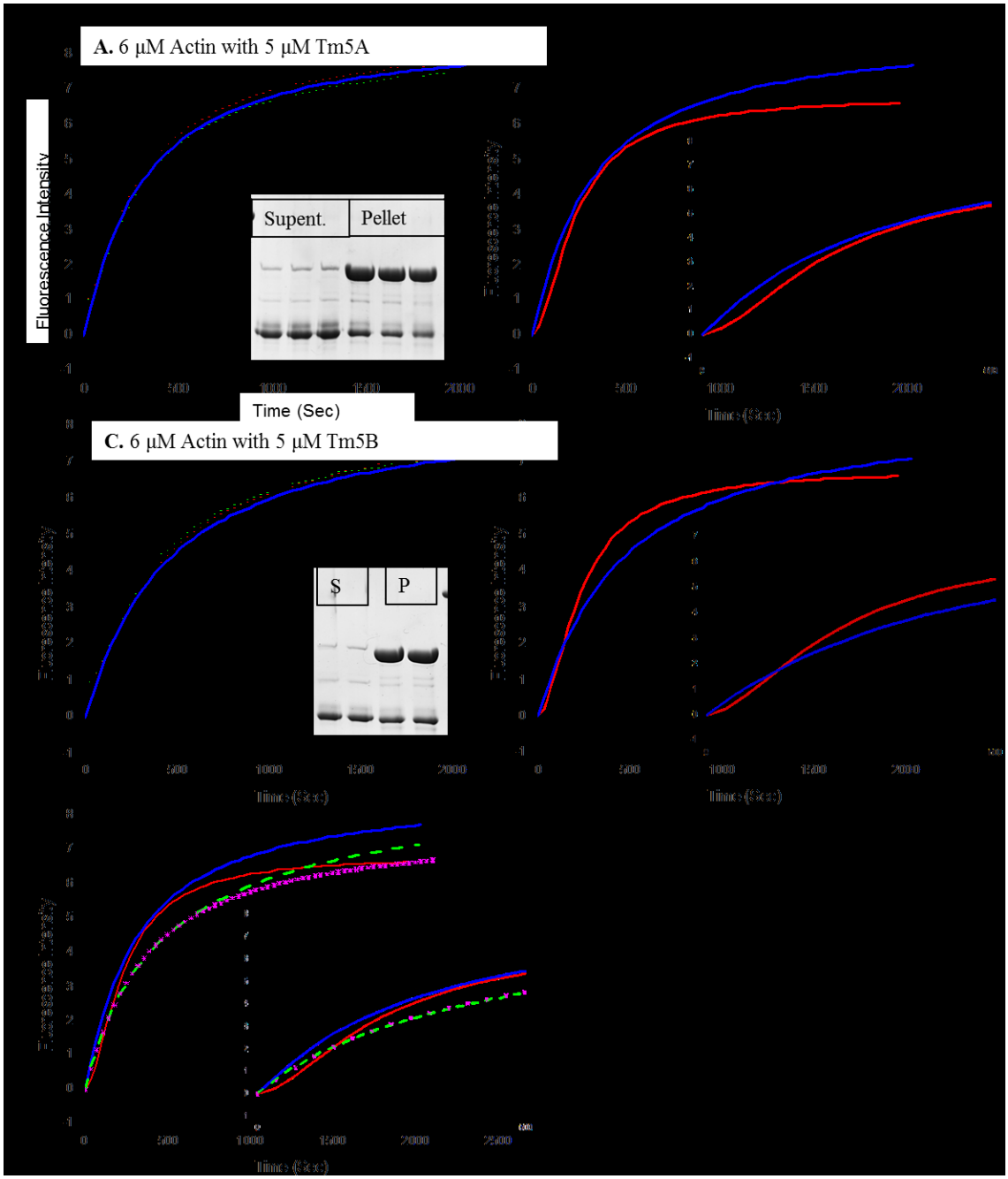

Figure 2.38: Time course polymerisation curve of actin with smooth muscle fibroblast Tm5A and Tm5B. A. 6 µM actin in presence of 5 µM Tm5A B. Tm5B. The inset shows the sedimented pellet and supernatent run on SDS page gel to check the binding efficiency. C and D are Curve A and B integrated into 6 µM actin actin curves for comparison. Blue line represent the Tm5A and Tm5B in respective graphs. E. comparison of Tm5A – blue, Tm5B- green and Tpm1 – pink. The inset shows the same curves with different time scale to show the initiation more closer. Fluorescence intensity is in arbitrary units. Assay was performed on day 6 of actin preparation.

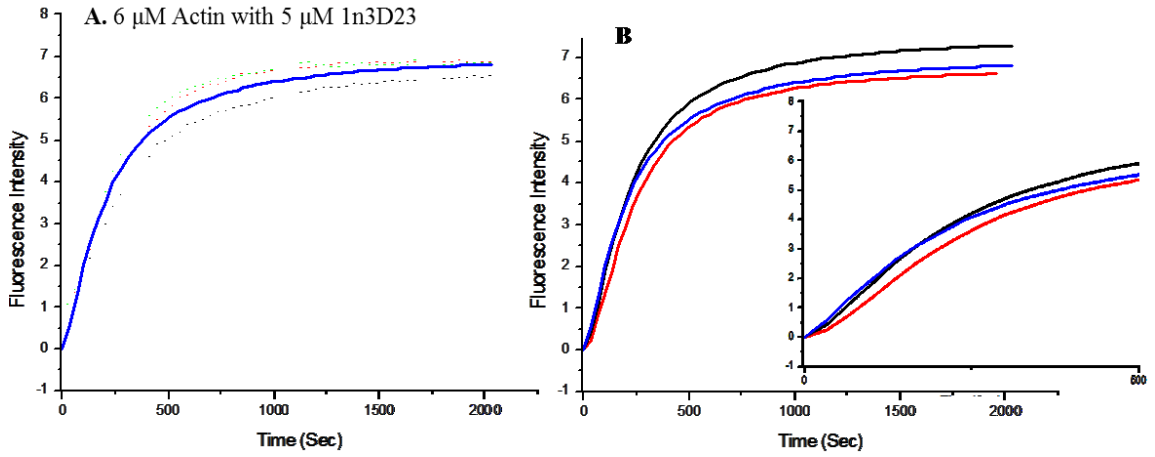

Figure 2.39: Time course polymerisation curve of actin with ultra short non-muscle tropomyosin Tm n3D23. A. 6 µM actin in presence of 5 µM Tm n3D23. The inset shows the sedimented pellet and supernatent run on SDS page gel to check the binding efficiency. B. Curve A integrated into 6 µM actin actin curves for comparison. Blue line represent the Tm n3D23. The inset shows the same curves with different time scale to show the initiation more closer. Fluorescence intensity is in arbitrary units. Assay was performed on day 6 of actin preparation.

Tm5A and Tm5B are non-muscle tropomyosin from fibroblasts and Tm-n3D23 is a ultra-short non-muscle tropomyosin. Tm5A and Tm5B have similar regulatory properties of actin and myosin but were found to have a lot of variation with their affinity to actin (Maytum et al., 2000). As shown in the Figure 2.38A in presence of Tm5A, in comparison with 10day old actin, the initiation is higher than actin alone and elongation seems to be slower (k = 302.99 sec) but the final filament fluorescent intensity was much higher than actin on its own (V_{max} = 8.7 units) and although Tm5B (Figure 2.38B) show higher initiation similar to all other tropomyosins its elongation is much slower than Tm5A (k = 441.4 sec). Similar to other tropomyosin isoforms ultrashort non-muscle tropomyosin Tm n3D23 (Figure 2.39) had similar affect of higher initiation rate and much lower elongation rate in comparison to actin alone with k value of 201 sec.

Table 2.5: The Hill simulation time course polymerisaiton curves of actin polymerisation. V_{max} – complete saturation time, k – half time of saturation. N –gives the sigmoidicity of the curves (Hill coeffecient).

Assay	Vmax	k	n
2 µM Ac (day 1)	6.41341 \(177)0.02411	721.40188 \(177)6.69911	1.12103 \(177)0.01318
2 µM (day 12)	8.17183 \(177)0.12906	1490.51515 \(177)67.71559	0.77825 \(177)0.01726
6 µM Ac	6.79897 \(177)0.02371	230.26024 \(177)2.01503	1.67922 \(177)0.02671
6 µM Ac (day 10)	7.54053 \(177)0.01786	213.35069 \(177)1.31172	1.50153 \(177)0.01544
2 µM Ac + 5 µM Tpm1	7.93094 \(177)0.04955	1757.51627 \(177)33.42959	0.7226 \(177)0.00552
6 µM Ac + 0.5 µM Tpm1	7.71071 \(177)0.03207	262.56128 \(177)2.40288	1.51509 \(177)0.02282
6 µM Ac + 5 µM Tpm1	7.52435 \(177)0.10722	337.36483 \(177)10.86806	1.07594 \(177)0.0317
6 µM Ac + 5 µM Tpm2	6.92937 \(177)0.01388	170.15193 \(177)1.02045	1.41178 \(177)0.01346
6 µM Ac + 5 µM Tpm3-Met	7.64579 \(177)0.01625	184.45092 \(177)1.10895	1.42833 \(177)0.01382
6 µM Ac + 5 µM Tpm3-MM	6.39838 \(177)0.02743	138.96029 \(177)1.85502	1.1848 \(177)0.02234
6 µM Ac + 5 µM Tpm3-MASM	7.60812 \(177)0.03559	266.04345 \(177)2.94049	1.05738 \(177)0.0121
6 µM Ac + 5 µM Tpm4	7.5958 \(177)0.01926	223.60541 \(177)1.37502	1.40113 \(177)0.01355
6 µM Ac + 5 µM Tpm1-K70T	6.9657 \(177)0.03736	261.8039 \(177)3.2538	1.11002 \(177)0.01557
6 µM Ac + 5 µM Tm5A	8.70107 \(177)0.03655	302.99147 \(177)2.93621	1.06805 \(177)0.01017
6 µM Ac + 5 µM Tm5B	8.53348 \(177)0.08301	441.42902 \(177)9.69262	1.04655 \(177)0.01721
6 µM Ac + 5 µM Tm-n3D23	7.12115 \(177)0.03489	201.25058 \(177)2.55238	1.35653 \(177)0.02663

The curves were fit to the Hill equation taking all the triplicate data available. The error bars are not calculated as the curves were generated using the formula giving the best fit using all the data together.

2.6 Discussion

The recombinant tropomyosin synthesized from E. coli has unacetylated N-terminal methionine, and in few cases the N-terminal methionine is cleaved depending on the residue present next to N-terminal residue as explained earlier. In contrast tropomyosin extracted from muscle has intact N-terminal methionine but acetylated. Höög et al., (1987) showed expression of human alcohol dehydrogenase in E. coli and confirmed that proteins expressed in *E. coli* do have eliminated N-terminal methionine but lack N-terminal acetylation of serine after removal of the first methionine, but still express active unfused protein with correct folding. In *E. coli* only few ribosomal proteins are acetylated, and some proteins do not need acetylation to perform their function. The 'local' structure of tm amino terminal is essential for head-to-tail polymerisation and for actin binding (Urbancikova and Hitchcock-DeGregori, 1994). When the N terminal methionine is acetylated, the nitrogen is having an amide bond similar to peptide bond, which is uncharged. On the other hand, the unacetylated nitrogen group carries a positive charge in free amino state as shown in Figure 2.1b (Brown et al., 2001; Heald and Hitchcock-DeGregori, 1988; Monteiro et al., 1994).

In mammalian Tpm-3 the initial methionine occupies the hydrophobic core **a** position (Figure 2.1a and b). As tropomyosin helical coiled coil follows heptad rule, the native Nt-Met amino group is acetylated with a hydrophobic side chain. In recombinant tropomyosin produced in *E. coli*, the Nt-Met is not acetylated and carries a positive charge at the hydrophobic core position. The net positive charge of the two coils may cause electrostatic repulsion which destabilizes the helix (Monteiro et al., 1994) and the results shows weak binding to actin. Addition of 2 or 3 amino acids shifts the positive

charge to positions **e** and **f** respectively thereby reducing the electrostatic repulsion and stabilizing the coil keeping the native folding of the protein. The addition of peptides at the Nt of tropomyosin alters the stability and structure of tropomyosin molecule and affects the equilibrium constant from open to closed transition which determines the available actin binding sites to myosin during muscle regulation. The regulation properties of recombinant tropomyosin varies on the length of the peptide added to the Nt end (Maytum et al., 2000; Monteiro et al., 1994).

In this study, Tpm3-Met and Tpm3-MM variants, Nt-Met is not removed because of the larger size of the amino acids present next to the Nt-Met which cause steric hindrance (Lowther and Matthews, 2000) and also due to the sequence specificity of the Nt ends (Bradshaw et al., 1998). In the Tpm3 sequence the amino acid next to Methionine is Glu (E) and Met (M) which are large for the MetAps to catalyze (Xiao et al., 2010) hence it retains the Met and is not acetylated in contrast to (M)ASM variant where the second and third residue are smaller and Nt-Met is cleaved which is confirmed by masses obtained by mass spectrometry analysis. The present study confirms the previous research in the cleavage of Nt-Met in proteins produced in *E. coli.*

Expression of Tpm4 protein in *E. coli*, the yield was very high in comparison to any other tropomyosin isoform produced in this study. The gene used was an ORF cDNA clone synthesized synthetically using the codons of *E. coli.* According to Goodman et al., (2013), using Nt rare codons that are enriched at the Nt of the genes than the common ones increases the expression efficiency by >14 fold. Rare codons are frequently rich in A/T third position and codons ending in A/T were correlated with increased protein expression as compared with decrease in expression with G/C codons (Kudla et al.,

2009). The proteins expressed in *E.coli* with change in the codons exhibit the same secondary structure with no change in total free energy of folding through the Nt region (Goodman et al., 2013). As seen from Figure 2.7 the synthesized sequence has G and C replaced with A and T from the native sequence. This may be the reason that there was higher protein expression with Tpm4.

Purification of Tropomyosin

The method used for purification of proteins with isoelectric precipitation produced higher yields (Maytum et al., 2000). All the three methods used for precipitating protein before purifying through anion exchange column, gave pure protein with less nucleic acid impurities. Ethanol precipitation gave higher yield of protein compared to pI and ammonium sulphate precipitation, however Ip precipitation had less impurities compared to the other two methods as confirmed by the UV spectroscopy results. The disadvantage of tropomyosin purification by pI precipitation at pH 4.6, is that DNA also get precipitated at the same pH as well as in ethanol, by careful adjustment of pH and anion exchange chromatography, nucleic acids can be removed from protein samples.

Affinity of Tm for Actin

From the studies of Drabikowski and Nowak (1968) the ratio of bound F-actin – tropomyosin is 1:2 assuming Tm is in dimer state, where four strands of tropomyosin is bound to 2 strands of actin filament. Actin filament is completely saturated with tm alone at 1:2 ratio. At lower proportion of tropomyosin below the saturation ration, not all tm is bound to actin but rather exist in an equilibrium state of bound and free tropomyosin. This has been extended later by biophysical and structural studies that tropomyosin binds to actin in 1:7 ratio with one tropomyosin molecule, assuming to be in dimer state binds

around seven monomer actin molecules (Heald and Hitchcock-DeGregori, 1988; Hitchcock-DeGregori and Heald, 1987; Maytum et al., 2000; Maytum et al., 2001; Urbancikova and Hitchcock-DeGregori, 1994).

In this study the results show that by adding 2 additional amino acids (Ala, Ser) to Tpm3-Met sequence restores all the fundamental functional aspects of tropomyosin affinity to actin such as expected actin affinity and cooperativity as compared to Tpm1. Deletion of one amino acid (Met) from Tpm3-MM, from the sequence lowers its affinity and loses its cooperativity. Tpm3-MM keeping the original sequence (MM) of 285 aa at the N-terminal synthesised in *E. coli* also had lower affinity to actin may be due the unacetylated methionine remained at the end which does not seem to favour higher affinity to actin binding due to a positive charge carried at the hydrophobic core position (a) and the tropomyosin coil becomes unstable (Hitchcock-DeGregori and Heald, 1987; Monteiro et al., 1994) as compared to the truncated Tpm2 which does not have any fusion amino acids at the N-terminal sequence have lower affinity and loses its cooperativity. Further studies are required to confirm the original sequence of Tpm3 in humans to confirm the number of methionie at the N-terminal end of the sequence.

Tpm4 binds to actin filaments and is present in both muscle and non-muscle. Its expression is lower in heart and muscles and is highly expressed in smooth muscles such as in lung tissue, liver, stomach and spleen for stabilising the cytoskeleton actin filaments (Gunning et al., 2005b; Helfman et al., 1999b). Helfman (1999b) studied LMW Tpm4 by expressing with fusion Green fluorescent protein to show that LMW Tpm4 need other LMW isoforms of Tm like TM5, TM5a and TM5b to incorporate into actin filaments in neonatal rat cardiomyocytes. Zhao et al., (2008) suggests that HMW form of TPM4-

variant1 with 284aa is a heart-specific variant and plays an important role in heart contractility. They studied zebra fish embryonic heart by Tol2 transposon-mediated mutagenesis and showed that removal of functional Tpm4 stops the heartbeat of the embryonic heart and the death of the embryos. There is not enough data available for assigning the main function of Tpm4 in heart so far. From the co-sedimentation assays of Tpm4 with poor affinity to actin on its own, suggests that Tpm4 need other Tm isoforms coexpressed to perform actin regulation. Further characterisation studies are required to confirm the results for Tpm4 binding affinity to actin.

In conclusion, expression of tropomyosin with two amino acid residues (Ala, Ser) extension at the N-terminal was reported to restore the native like function of Tm as revealed by a number of assays (Monteiro *et ai,* 1994). This study investigated this claim by applying actin-binding assays to compare Tpm3.12st isoform with already characterised Tpm1.1 and Tpm2.2 and found the substitution with two amino acids have similar actin binding affinity as native tropomyosin and similar to Tpm1.1 and Tpm2.2, resulting with binding efficiency in the range of 0.6 μM. free tropomyosin. Therefore, the Ala-Ser extension expressed at the N-terminus of Tm is a good mimic of the acetyl group for Tpm3.12st as well. From this study it is also suggested that the initial N-terminal end of the sequence for Tpm3.12st may be a single Met instead of Met-Met as Met Met on its own did not bind to actin as it is expected to behave normal without any modification. Further confirmation of this study is required to confirm the N-terminal end of the Tpm3-12st sequence.

Effect of tropomyosin isoforms on actin polymerisation

The fluorescent reagent N-(1-Pyrenly)Iodoacetamide used for labelling F-actin conjugates at the sulfhydryl group at Cys374 of F-actin (Kouyama and Mihashi, 1981; Tobacman and Korn, 1983). The increase in intensity of fluorescence of PyG-actin is enhanced to about 10 times by polymerisation to F-actin agreeing with the previous results (Cooper et al., 1983b). The advantages of using pyrene actin to study polymerisation kinetics is that at the initiation step of polymerisation, the fluorescence increase is at 100% rise and is not influenced by any dust particles or shearing or any other light scattering solid residues left in the assay solution which may result in change the polymerisation kinetics (Frieden and Goddette, 1983a; Wegner, 1982a). This will also has advantage of lower signal-noise ratio as opposed to light scattering experiments which was confirmed by Cooper et. al., (1983b) by studying the polymerisation with both stirred and unstirred solution. Stirring the sample breaks the polymers formed, the fluorescence assays does not affect the fluorescent signal form an unstirred solution as it does with light scattering experiments. Fluorescence studies is independent of the percentage of pyrene actin used as the critical concentration is not changed using 5% pyrene actin with the rest being unlabeled actin (Criddle et al., 1985a; Kouyama and Mihashi, 1981; Lal and Korn, 1986). Hence a trace amount of pyrene actin can be used with a bulk amount of unlabeled actin for polymerisation studies without compensating results. The concentration of monomeric actin does not change the critical concentration of actin after polymerisation however the concentration of polymeric actin varies once the reaction reaches a steady state (Tobacman and Korn, 1983; Wegner and Engel, 1975). However in this study the actin used is all pyrene labelled G-actin.

The polymerisation curves of actin in two different concentrations (2 μM and 6 μM) are shown in Figure 2.31. The curves agree with previous studies (Cooper et al., 1983b; Frieden and Goddette, 1983a; Lal and Korn, 1986; Wegner, 1982a; Wegner, 1982b) in that by increase in the concentration of actin the polymerisation rate also increases, however the sigmoidicity of the curves is lost as the concentration is increased. Wegner (1982a) showed that at very low concentrations of actin, there is increase in sigmoidicity of the curves which may be due to spontaneous fragmentation and is found to be independent of Mg^{2+} and K^{+} concentrations. This is primarily a concentration effect on initiation as the rate of polymerisation depends on the rate of nucleation during initiation phase.

According to Tobacman and Korn (1983) the nucleation rate is directly proportional to the fourth power of monomeric actin indicating that the first nucleus formed to proceed to form a polymer is a tetramer. The data obtained in this study is not sufficient to study the nucleus size and the size of the polymer after the polymerisation reaction reached a steady state as it is previously stated that the halftime (given in Table 2.5) of the polymerisation reaction does not give the nucleus size (Frieden and Goddette, 1983a; Hitchcock-DeGregori et al., 1988). The critical concentration was also not calculated as the concentration of F-actin was not measured after spinning the assay solution which was used to run on the gel to check the efficiency of the binding. The present study gives a qualitative comparison of the effect of various tropomyosin isoforms on actin polymerisation and further studies are required to quantify the size of nucleus, nucleation –elongation rate constants and the reaction pathway by which tropomyosin is effecting the initiation phase of actin polymerisation.

According to Lal and Korn (1985) the fluorescent intensity during polymerisation was not reduced in presence of Tropomyosin due to hydrolysis of ATP on F-actin. The critical concentration of monomeric actin remained same 0.1 μM even though the association constant of actin polymerisation was reduced to 40% in presence of tropomyosin (Wegner, 1980).

The main characteristic function of tropomyosin in both muscle and non-muscle cells is the prevention of spontaneous fragmentation of actin filaments by severing protein and tropomyosin has negligible or no effect on actin polymerisation.

The effect of tropomyosin on actin polymerisation is found to vary depending on the concentration of actin and tropomyosin (Hitchcock-DeGregori et al., 1988; Wegner and Ruhnau, 1988). Tpm1 with two different concentrations of actin and tropomyosin show different polymerisation curves. With low concentration of Tpm1 (0.5 μM) the overall polymerisation was higher with initiation and elongation and the maximum fluorescent intensity was higher as well. As the concentration of Tpm1 increased to 5 μM, initiation was higher but the elongation and maximum fluorescent intensity after completion of polymerisation was lower than actin in absence of Tpm1. With lower concentration of actin (2 μM) and 5 μM showed the similar curve as using 6 μM actin (Figure 2.32). Hence it's the concentration of tropomyosin that effects how actin kinetics are modulated, as long as the actin monomers are available the tropomyosin has same affect at a particular concentration. All the isoforms of tropomyosin have accelerated the initiation step and inhibited the elongation. The final filament intensity was higher in presence of tropomyosin indicating that there are more number of F-actin filaments and therefore it can be proposed that tropomyosin affects the critical concentration of actin.

Tpm2, Tpm3- MET and Tpm4 are shown to have an overall increase in polymerisation for an unknown reason. When compared to the affinity with actin these three isoforms have very low binding affinity to actin with lower cooperativity.

The results in this study partially contradict previous research results which state that tropomyosin inhibits both initiation and elongation rate constants of actin mostly because they bound to the actin filaments and not to monomer actin (Hitchcock-DeGregori et al., 1988; Lal and Korn, 1986; Wegner, 1979; Wegner, 1980; Wegner, 1982b; Wegner and Ruhnau, 1988). However Pragay and Gergely (1968) reported that muscle tropomyosin accelerates the polymerisation of ATP-actin but is more pronounced with ADP-F-Actin studied by viscosity measurements at 0 ^{0}C and the acceleration is more pronounced at 25^{0}C. Wegner and Ruhnau (1988) and Hitchcock De-Gregory (1988) both studied the effect of tropomyosin by nucleated polymerisation and spontaneous polymerisation reported that tropomyosin inhibits actin polymerisation. The inhibition did not overcome even after addition of F-actin nuclei, suggesting that tropomyosin along with inhibition of polymerisation may also inhibit elongation as well as fragmentation of filaments.

Non-muscle tropomyosin were tested with muscle actin as it has been shown that both muscle and non-muscle actin does not show any variation in polymerisation kinetics (Buzan and Frieden, 1996; Nefsky and Bretscher, 1992). Tm5A and Tm5B have different effect on elongation, but both show acceleration of initiation.

Tropomyosin has found to bind to actin at a rate of 2.5 x 10^6 to 4 x 10^6 $M^{-1}s^{-1}$ (Wegner and Ruhnau, 1988). Actin polymerisation is not only affected by presence of tropomyosin in presence of ATP, due to conformational change of filaments and ATP hydrolysis when

the polymerisation is near to steady state (Keiser and Wegner, 1985). Tropomyosin stabilizes actin filaments and prevent from spontaneous fragmentation (Wegner and Savko, 1982), changes in the concentrations of tropomyosin has also been reported due to high cooperativity of actin-tropomyosin binding, changes in conformation of actin is found when tropomyosin is head to tail association and in complete absence of tropomyosin (Wegner, 1976).

When a salt binds to divalent metal ion (Mg^{2+} or Ca^{2+}) monomer actin, the monomer undergoes a conformational change which is considered to be a significant step in polymerisation. This stage is called monomer activation step, which is the intermediate conformation of G-actin – F-actin (Fig. 3.2). Which can be shown as :

$$G \rightleftharpoons GF \rightleftharpoons F$$

Where, GF is called F-monomer that undergoes conformational change before forming a nucleus (Cooper et al., 1983a). Cooper et al., reported that this monomer activation step studying actin polymerisation in presence of Ca^{2+} and Mg^{2+} ion individually. In presence of Ca^{2+} ions the initiation of nucleation was slower and in presence of Mg^{2+} the initiation of polymerisation is faster, leading to state the principle that when Mg^{2+} binds to G-Ac a intermediate monomer conformation is formed (GF) which is a faster reaction and initiates the polymerisation faster. However the elongation rates have shown to be same with time in both the cases. The effect of tropomyosin on actin polymerisation show a different rates of polymerisation in presence of troponin and myosin (Cho et al., 1990; Hitchcock-DeGregori and Heald, 1987; Maytum et al., 2003; Smith et al., 2003).

In conclusion, in contrary to previous research results, tropomyosin isoforms show acceleration of the initiation step of actin polymerisation. As tropomyosin binds to only F-actin, how it has effect on initial polymerisation step is unknown. The stage of actin at which tropomyosin starts binding to actin, how big the actin filament should be for tropomyosin to affect polymerisation, does tropomyosin forms a surface for the monomer to form nucleus faster than in the absence of tropomyosin molecules? These are the question that arise from this study to clarify further. In physiological conditions there are many other major factors affecting nucleation and polymerisation of actin such as NPF proteins WASp and Arp 2/3 complex, profilin, cofilin, and other actin binding proteins that affect the whole polymerisation process. Establishing kinetic dynamics in all these conditions is not easy. Techniques like single molecule imaging developed by Kad and his collaborators (Desai et al., 2014; Kad and Van Houten, 2014) studied cooperativity of thin filament activation by direct imaging of single molecule of myosin binding to actin and DNA repair. Using the single molecule imaging technique, an experiment can be set up by taking a single tropomyosin molecule in the pool of actin monomers to observe the mechanism of actin polymerisation in presence of tropomyosin. This may give deeper understanding of role of tropomyosin in actin polymerisation. Li et al (Li et al., 2010) used fluorescent electron microscopy and molecular dynamic simulation to study conformation changes of tropomyosin on actin showed that tropomyosin when bound to actin is semirigid and is essential for assembly of actin filaments. This method has potential in understand the dynamics of actin -tropomyosin binding. Schmidt et al., (Schmidt et al., 2014) showed weak monomer binding of tropomyosin to actin leads to nucleation sites which enhanced the interaction of actin to tropomyosin mostly dependent

on end-end interactions of tropomyosin molecule using TIRF microscopy with Alexa 532 labelled tropomyosin. Techniques mentioned about may help to built polymerisation and building kinetics models for tropomyosin -actin polymerisation that would enable to fully understand the dynamics of tropomyosin on actin polymerisation.

Chapter III: Identification of Tropomyosin 3.12.st (TPM3.12st) using monoclonal antibodies

3 Introduction

Tropomyosins are highly conserved components of actin filaments both in vertebrates and non-vertebrates. Over 40 isoforms of Tm have been identified from four genes in mammals. The four genes encoded by tropomyosin (Tm) are αTm (*TPM1)*, βTm (*TPM2)*, γTm (*TPM3)* and δTm (*TPM4)*. These genes undergo extensive alternative splicing of mRNA or have alternative promoters and different N-terminal modifications to give rise to >40 isoforms. The isoforms are differentiated broadly into two types depending on their molecular weight, high molecular weight (HMW) and low molecular weight (LMW) Tms (Lees-Miller and Helfman, 1991; Leger et al., 1976).

Tm isoforms regulate actin filaments and have different affinities with actin by either interacting or inhibiting or competing with various actin binding proteins (Bryce and Schevzov, 2003; Pittenger et al., 1995). Both in-vitro and in-vivo studies show that different Tm isoforms localize specifically at subcellular level in numerous cell types by directly affecting the actin filament concentration (Schevzov et al., 2008). Coulton (2010) and Stark (2010) showed in fission yeast that the localization of Tm isoforms is demonstration of evolutionary mechanism in regulating actin filament composition.

3.1 Tropomyosin gene

There are four genes that express tropomyosin, *Tpm1* (*α-Tm*) located on chromosome 15q22, *Tpm2* (*β-Tm)* located on 9p13, *Tpm3* (γ-*Tm)* located on 1q21.2 and *Tpm4* (δ-*Tm*) located on 19p13.1 and these genes encodes >40 isoforms (Figure 3.1 to Figure 3.4) by alternative splicing, 3' differential processing and presence of alternative promoters. Recently the nomenclature of the primary mammalian tropomyosins form humans, rat and mouse has been amended by Geeves et.al., (2014). These are shown in Figure 3.1 to Figure 3.4 shows the genes of Tpm1, Tpm2, Tpm3 and Tpm4 and their isoforms respectively with NCBI accession number of human isoforms (Rat and mouse accession numbers are not given in the tables).

Replication of ancestral gene is thought to given rise to the tropomyosin gene family in vertebrates (Lees-Miller and Helfman, 1991). As shown in the nomenclature, formal protein names are assigned according to the gene, isoform number and most importantly the tissue they are expressed, for example the Tpm1 encodes proteins Tpm1.1st- Tpm1 gene isoform 1 striated muscle that is encoded in both skeletal and cardiac, Tpm1.3sm, which is isoform 3 encoded in smooth muscle and Tpm1.10br, Tpm1.11br and Tpm1.12br proteins encoded in brain and Tpm1.9cy encoded in cytoplasm (Geeves et al., 2014; Lees-Miller and Helfman, 1991; Perry, 2001). Each gene produces both high molecular and low molecular weight proteins by alternative splicing of the exons and transcriptional initiation. Form the different Tms, exon 1a in with either 2a or 2b encoded N- terminal end encodes HMW isoforms with 284 aa that are mostly predominant in striated muscles and exon 1b (excluding exon 2) encodes LMW isoforms with 248aa that

are mostly expressed in smooth muscle tissue. All these variants have either 6a or 6b and variation of exon 9 (9a, 9b, 9c or 9d) at the C-terminal end. Exons 3, 4, 5, 7 and 8 are common to all the Tm isoforms regardless of the tissue they express.

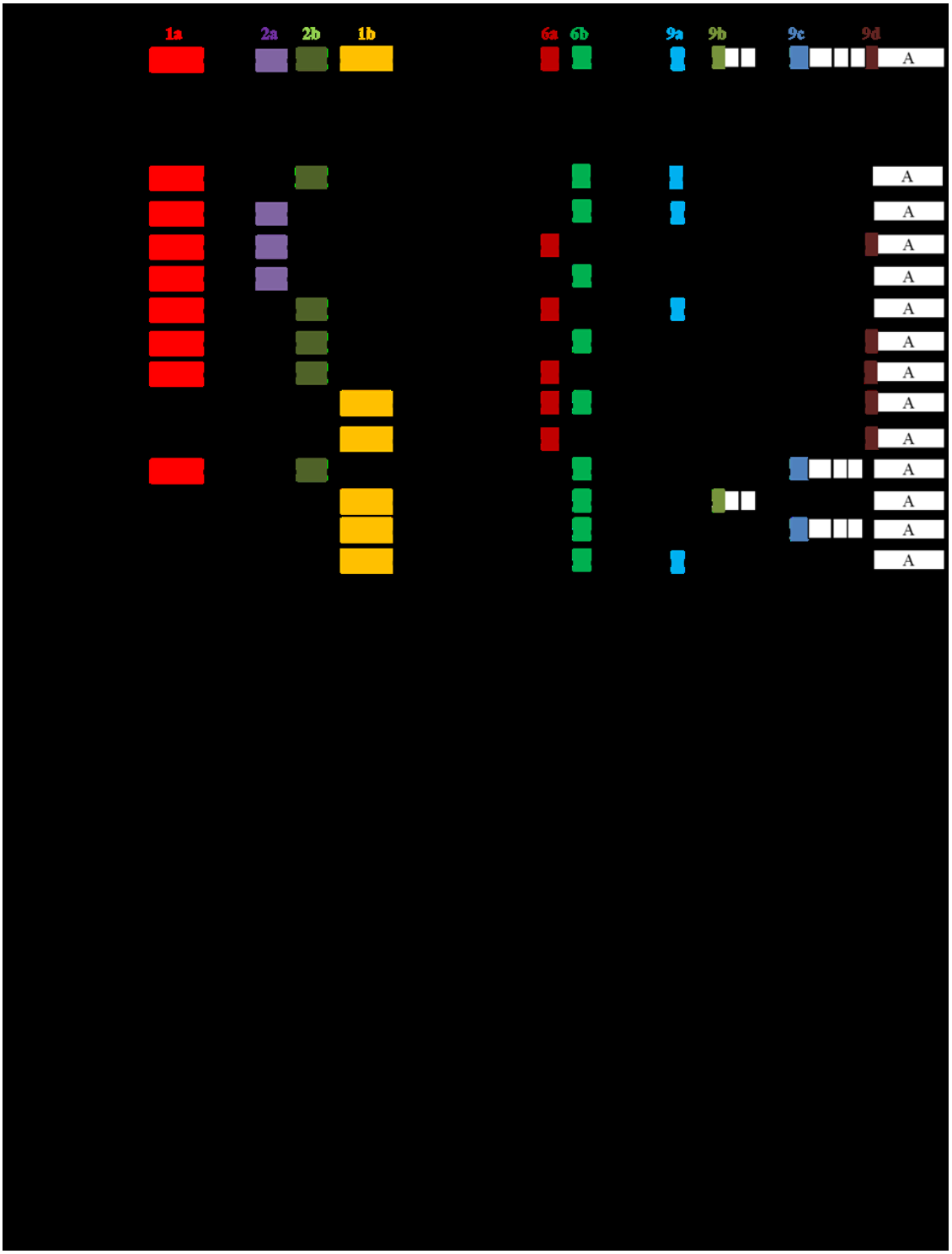

Figure 3.1: Tropomyosin isoform sorting of *TPM1/ αTm* Gene: a. *TPM1* gene (human gene ID: 7168) and the isoforms formed by alternative splicing of exons gives rise to a variety of isoforms. Muscle isoforms have 1a and either 2a or 2b and also either 6a or 6b. They also exhibit variations at the carboxyl terminal at exon 9 terminating with a polyA tail. Low molecular weight isoform have 1b as the N-terminal exon. The black boxes

represent the exons common to all isoforms, open boxes represent untranslated regions and lines represent introns and A represents poly A tail. b. Table showing the isoforms expressed by Tpm1 gene, protein name and the human protein accession number. St-straited (cardiac/skeletal tissue), sm-smooth, Br –brain, cy, cytoplasm (Geeves et al., 2014; Lees-Miller and Helfman, 1991).

a

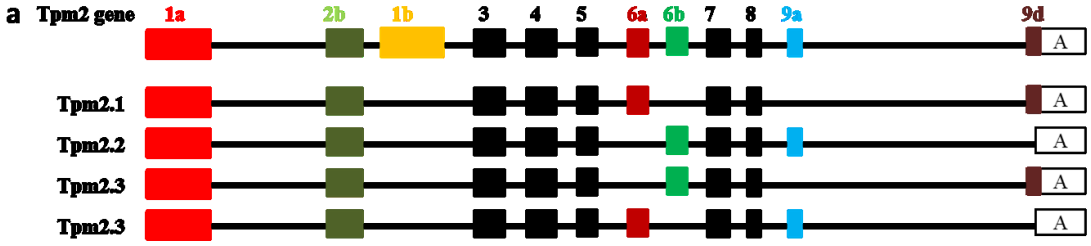

b

Isofrom Names	Common names	Alternative names in use	Formal protein name	Accession number (Human)
Tpm2.1	Tm smβ	βTm Tm1, Tm1β, smooth Tm, smooth α-Tm	Tpm2.1 sm/cy	NP_998839.1
Tpm2.2	Tm skβ	B skeletal Tm, β cardiac Tm	Tpm2.2 st	NP_003280.2
Tpm2.3	-	-	Tpm2.3	NP_001288155.1
Tpm2.4	-	-	Tpm2.4	NP_001288156.1

Figure 3.2: Tropomyosin isoform sorting of *TPM2/ βTm* Gene: a. *TPM2* gene (human gene ID: 7169) and the isoforms formed by alternative splicing of exons gives rise to a variety of isoforms. Muscle isoforms from β gene have 1a and 2b and either 6a or 6b. They exhibit variations at the carboxyl terminal at exon 9 with 9a or 9d terminating with a polyA tail. The black boxes represent the exons common to all isoforms, open boxes represent untranslated regions and lines represent introns and A represents poly A tail. b. Table showing the names given to the isoforms, protein name and the human protein accession number. St-straited (cardiac/skeletal tissue), sm-smooth, cy, cytoplasm (Geeves et al., 2014; Lees-Miller and Helfman, 1991).

a

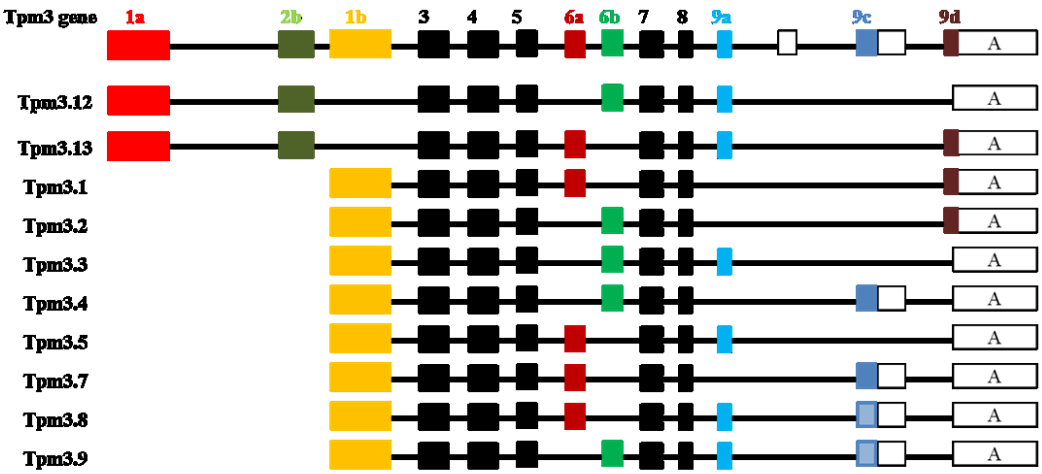

b

Isofrom Names	Common names	Alternative names in use	Formal protein name	Accession number (Human)
Tpm3.12	Tm skα-slow	γTm αsTm1, slow skTm	Tpm3.12st	NP_689476.2
Tpm3.13	-	-	Tpm3.13cy	None
Tpm3.1	Tm5NM1	-	Tpm3.1cy	NP_705935.1
Tpm3.2	Tm5NM2	-	Tpm3.2cy	NP_001036816.1
Tpm3.3	Tm5NM3	-	Tpm3.3cy	NP_EAW53237.1
Tpm3.4	Tm5NM4	-	Tpm3.4cy	NP_001036818.1
Tpm3.5	Tm5NM5	-	Tpm3.5cy	NP_001265118.1
Tpm3.7	Tm5NM7	-	Tpm3.7cy	NP-001036817.1
Tpm3.8	Tm5NM8	-	Tpm3.8cy	None
Tpm3.9	Tm5NM9	-	Tpm3.9cy	None

Figure 3.3: Tropomyosin isoform sorting of *TPM3/ γTm* Gene: a. *TPM3* gene (human gene ID: 7170) and the isoforms formed by alternative splicing of exons gives rise to a variety of isoforms. Muscle isoforms from γ gene have 1a and 2b and either 6a or 6b. They exhibit variations at the carboxyl terminal at exon 9 with 9a or 9c or 9d terminating with a polyA tail. Tpm3.8 and Tpm3.9 have 9c exon shaded light as it can be substituted with 9a in some cases. Low molecular weight isoforms have 1b as the N-terminal exon. The black boxes represent the exons common to all isforms, open boxes represent untranslated regions and lines represent introns and A represents poly A tail. b. Table showing the names given to the isoforms, protein name and the human protein accession number. St-straited (cardiac/skeletal tissue), cy, cytoplasm (Geeves et al., 2014; Lees-Miller and Helfman, 1991).

a

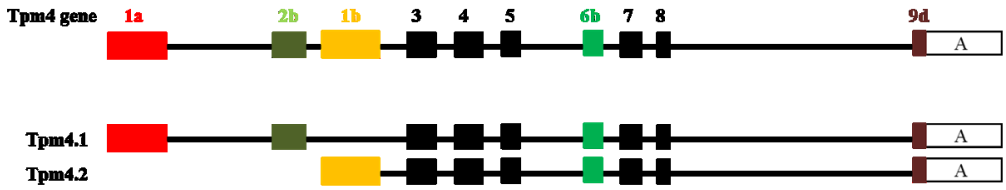

b

Isofrom Names	Common names	Alternative names in use	Formal protein name	Accession number (Human)
Tpm4.1	Tm4HMW	δTm	Tpm4.1cy	NP_001138632.1
Tpm4.2	Tm4	-	Tpm4.2cy	NP_003281.1

Figure 3.4: Tropomyosin isoform sorting of *TPM4/δTm* Gene: a. *TPM4* gene (human gene ID: 7171) and the isoforms formed by alternative splicing of exons gives rise to a variety of isoforms. Muscle isoforms from δ gene have 1a and 2b and 6b exons. The *Tpm4* gene has only 9d at the carboxyl terminal terminating with a polyA tail. Low molecular weight isoform have 1b as the N-terminal exon. The black boxes represent the exons common to all isforms, open boxes represent untranslated regions and lines represent introns and A represents poly A tail. b. Table showing the names given to the isoforms, protein name and the human protein accession number. cy, cytoplasm (Geeves et al., 2014; Lees-Miller and Helfman, 1991).

3.2 Distribution of Isoform Expression

Each isoform express distinct patterns depending on specific tissues and also exhibit variation during development of an organism from embryonic to adult stage The proteins expressed by these genes are differentially distributed depending on the differential functional distribution. There are more number of Tm isoforms are expressed in non-muscle cells like in fibroblasts of rat, mouse, human and chicken fibroblasts (5-7 isoforms) and smooth muscles, such as brain cells have 3 specific isoforms which are unique to neurons itself. On the other hand primary muscle related isoforms in striated muscle (both cardiac and skeletal) have 2 to 4 isoforms found so far (Helfman et al., 1999a; Lees-Miller, 1990).

Isoforms from *Tpm1* gene predominates in most of the organs, in striated muscle (both cardiac and skeletal muscle) Tpm1.1st predominates followed by lower amounts of Tpm1.2st (κTm) Tpm2.2st. Tpm1.1st is predominant in fast cardiac muscles and Tpm2.2st in both fast skeletal and slow skeletal muscles in different proportions.

In the heart, cardiac muscle filaments is differentiated form fast skeletal and slow skeletal muscle due to specific adaptation demands of the organ for continuous function. Tpm1.1st is found to be predominant in small mammalian hearts like mouse, rat, rabbit and dog however Tpm2.2 is also found in larger mammals like sheep, cow, pig hearts in 1:4 ratio (Leger et al., 1976). Rajan et al., (2010) found κTm in human heart muscle and Peng et al., (2013) suggested that there is variation in distribution of expression of these isoforms in different regions of the heart by top down mass spectrometric analysis from tropomyosin purified form human heart tissue. The novel κTm is found to be highest in left atria followed by right atria and right ventricle but not detected in left ventricle and phosphorylation of α-Tm was higher in atria rather than in ventricles. The presence of γTm in heart is not confirmed by both studies conducted by Marston et al., (2013)and Peng et al., (2013) using different techniques.

It is a well-known fact that in skeletal and cardiac muscle Tm plays a major role in muscle contraction in association with troponin (Tn) complex. When calcium ions are released in the muscle cell, troponin C binds to the calcium ions causing a conformational change initiated by troponin-tropomyosin complex, which in turn is initiated by the ATPase activity causing contraction. However, troponin is not present in smooth muscle and non-muscle cells and hence the contraction is solely controlled by the calcium-sensitive regulatory mechanism. The role of Tm in these smooth and non-muscle cells is

found to regulate the actin filaments, intracellular transport, motility and cytoskeleton structure (Pittenger et al., 1994). Muthuchamy et al., (1993) by tropomyosin-mRNA studies in mouse heart showed that the ratio of β-Tm to α-Tm exists in 1:4.5 ratio at embryonic state and the amount of βTm declines to a ratio of 1:60.5 in adult heart showing that it is important in cardiogenesis in mouse heart and shift in the isoform composition. On the contrary, it is known that the amount of mRNA directly proportional to the protein expressed, Rethinasamy and Muthuchamy (1998) found that the composition variation of protein isoforms occurs at translation state in mice.

The variation in the exon composition found in different isoforms leads to different functions of tropomyosin proteins affecting actin binding affinity, head-to-tail polymerisation and the interaction of Tm with other binding proteins (Lees-Miller and Helfman, 1991; Pittenger et al., 1994b). Recently Hook et al., (2004) showed that the low molecular weight products of *TPM3* (γTm) gene are necessary for the cell survival of embryonic stem cells and embryonic development as these are not found in the adult stage of mouse. Again in 2011, Hook et al., studied the embryonic viability of knock out mice by knocking off either 1a or 1b and 6a or 6b exons and 9a or 9b/c/d and found that non-viable mice were produced by deletion of 1b exon and partial viability with deletion of 9d exon but no effect on viability with deletion of 9c exon. All these cells had full expression of α and β Tms (Hook et al., 2011). But in humans normal and failing heart muscles have typically 95% α-Tm with a smaller amount of β and γ Tms are found and 4% of κ isoform (product of *TPM1* gene) are found (Marston et al., 2013; Maytum et al., 2011; Purcell et al., 1999; Rajan et al., 2010).

The main objective of this chapter was to produce monoclonal antibodies specific to HMW Tpm3 to identifying Tpm3-iso12st protein in muscle tissue which could be used with tissue extracts, cell extracts or by histocytochemistry in healthy and diseased tissues instead of using CG3 antibody (Lin et al., 1985) which identifies both HMW and LMW proteins that are expressed by *TPM3* gene.

Twelve antibodies against HMW Tpm3.12st sequence were prepared. Recombinant Tm proteins characterised in Chapter II were used for antibody reactions. Dot blot technique was used to identify the reactivity of the antibodies with Tpm1.1st, Tpm2.2st and Tpm3.12st isoforms in native and denatured state. As the results were not consistent, western blotting was employed for characterisation with antibodies with denatured protein of all the four Tpm1.1st, Tpm2.2st, Tpm3.12st and Tpm4.1cy isoforms. From the results obtained with western blotting, an ELISA method was developed to compare the sensitivity of Tpm3.12st with only Tpm1.1st using different dilutions of antibodies with various concentrations of proteins.

3.3 Materials

All the list of materials used for the experiments are given in Table 6.1 in Appendix (page 252). Others that are not stated in the list are given in the text.

3.4 Experimental Methods

3.4.1 Monoclonal antibodies production

Specific monoclonal bodies for Tpm3 were bought from Abmart Inc. China. The company produced the monoclonal antibodies based on their key technology algorithm called SEAL –Protein **S**urface **E**pitopes Targeted by Monoclonal **A**ntibody **L**ibrary where antibodies for the target protein are made only by protein sequence (Figure 3.5). The immunogen design algorithm will predict potential epitopes for a target protein and each epitope peptide contains 10 amino acids strictly. Those potential epitopes are then integrated into Abmart expression vector to produce recombinant antigens for further immunization (Abmart Inc). Based on the Tpm3.12st protein sequence 12 potential epitopes were selected, with each epitope contains 10 amino acid residues. All the selected peptides were integrated consequently into expression vectors to generate antigens for further immunization in mice.

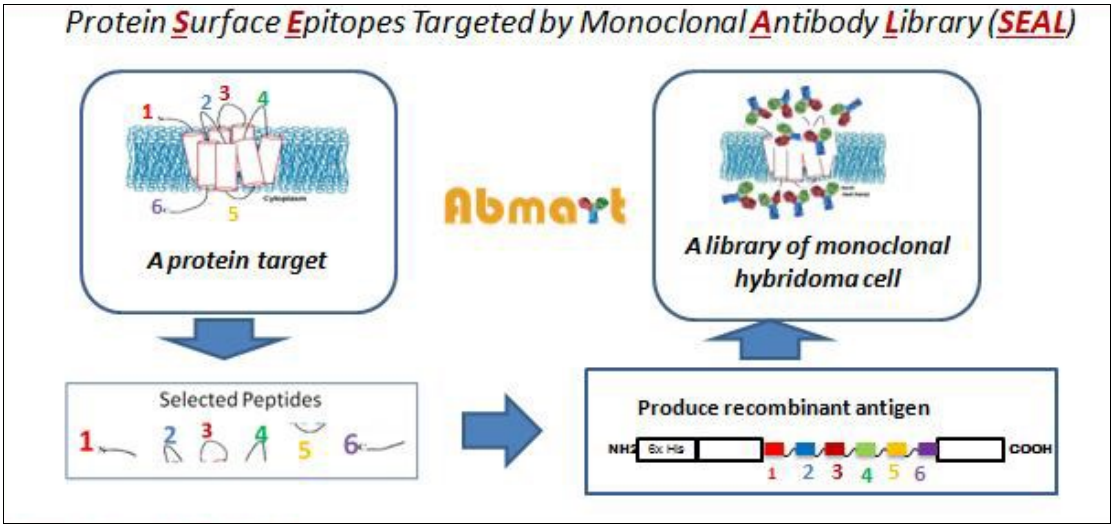

Figure 3.5: SEAL technology for antibody production (Abmart Inc.)

Protein immunogen was over expressed in *E. coli* and purified by Ni-affinity chromatography. After purification the antigen was used in animal immunization. Three 8-12 week old female mice were immunized with an immunogen and the mouse with best immune response was chosen to produce hybridomas cells from spleen. The spleen cells were fused with SP2/0 myeloma cells to generate the hybridomas in HAT medium. Stable clones that secrete antibodies with the ability to bind to antigen were selected and injected in the peritoneal cavity of mice. After 10-14 days tumors containing an antibody rich fluid called ascites fluid is produced. The ascites fluid is collected and tested for the reactivity of the antigen. Methodology work flow is shown in the Figure 3.6. The screening confirmed 12 antibodies, that recognize 5 peptides from the sequence and are listed in Table 3.1 and the exon position of the epitopes aligned with Tpm3.12st sequence of the antibodies are given in the Figure 3.7.

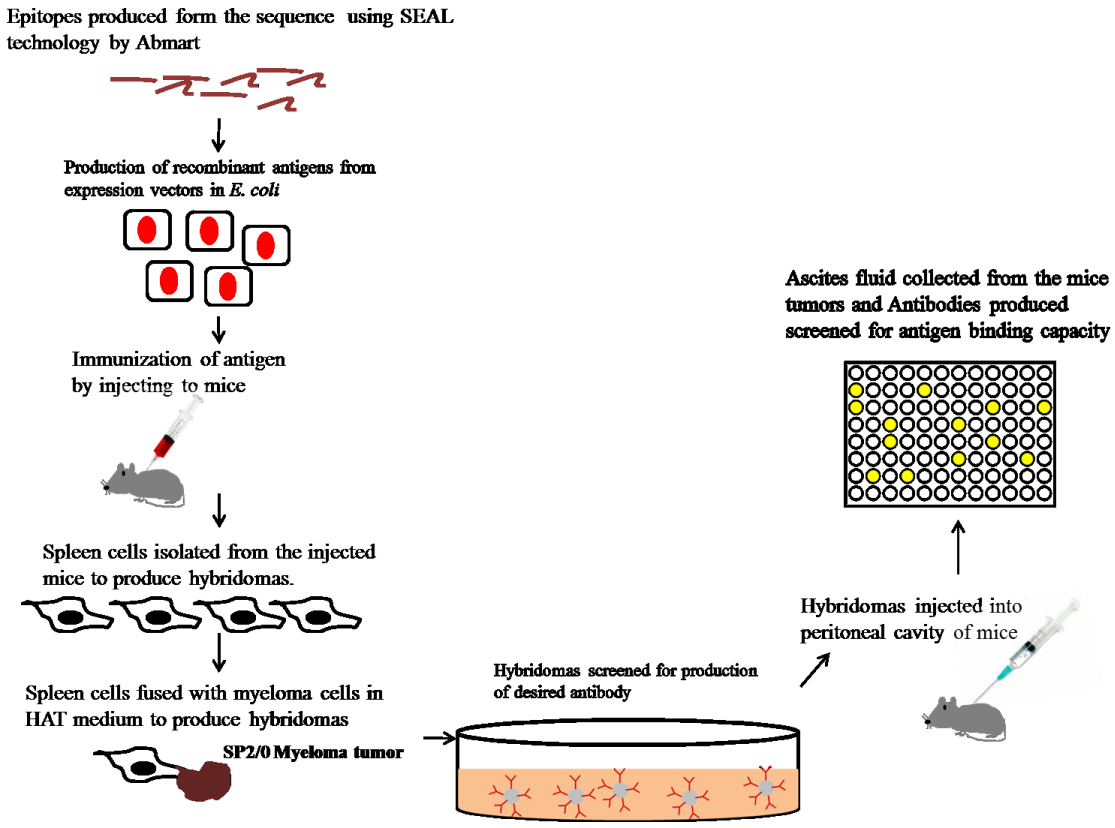

Figure 3.6 : work flow for the production of monoclonal antibodies.

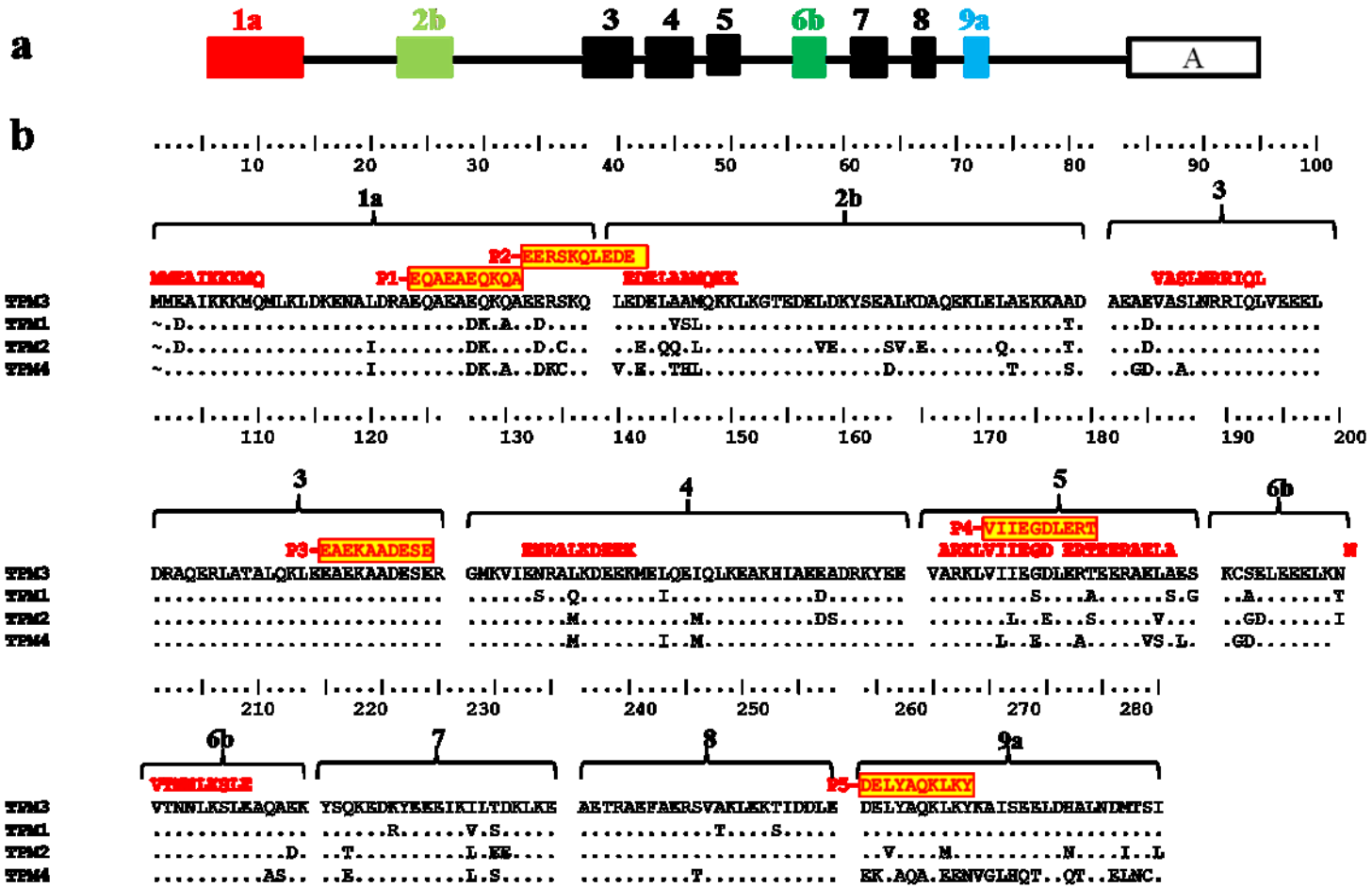

Figure 3.7: Sequence alignment of Tpm3 with Tpm1, Tpm2. a. Shows the *TPM3* gene and Fig. b shows the sequence resemblance alignment of high molecular weight (284 aa) human Tpm1, Tpm2, Tpm3 and Tpm4 protein sequence with exons. The sequence alignment also shows the sequence resemblance of the epitopes of monoclonal antibodies produced for this study with the peptide number given. The highlighted epitopes are the antibodies used and the non-highlighted once are the once that are the initial epitopes produced by the company to check the specificity. P- peptide number, dots represent the amino acid residue identity.

Table 3.1: List of antibodies and the corresponding peptide sequence, epitope similarity of all the four isoforms and the predicted binding assumption. Non-identical residues are highlighted in red. The antibody rows with similar colour have same peptide recognition.

Antibody number	Residue position	Peptide Sequence	Theoretical binding assumption	Epitope similarity for all four isoforms
1 (2,6,9)	259-268	DELYAQKLKY P5	Tpm3,Tpm1	DELYAQKLKY-Tpm1 DEVYAQKMKY-Tpm2 DELYAQKLKY-Tpm3 EKLAQAKEEN-Tpm4
2	259-268	DELYAQKLKY P5	Tpm3,Tpm1	DELYAQKLKY DEVYAQKMKY DELYAQKLKY EKLAQAKEEN
3	171-180	VIIEGDLERT P4	Tpm3	VIIESDLERA VILEGELERS VIIEGDLERT VILEGELERA
4	116-125	EAEKAADESE P3	Tpm1,Tpm2, Tpm3,Tpm4	EAEKAADESE EAEKAADESE EAEKAADESE EAEKAADESE
5	24-33	EQAEAEQKQA P1	Tpm3	EQAEADKKAA EQAEADKKQA EQAEAEQKQA EQAEADKKAA
6	259-268	DELYAQKLKY P5	Tpm3,Tpm1	DELYAQKLKY DEVYAQKMKY DELYAQKLKY EKLAQAKEEN
7 (8,10,11,12)	34-43	EERSKQLEDE P2	Tpm3	EDRSKQLEDE EDRCKQLEEE EERSKQLEDE EDKCKQVEEE
8	34-43	EERSKQLEDE P2	Tpm3	EDRSKQLEDE EDRCKQLEEE EERSKQLEDE EDKCKQVEEE
9	259-268	DELYAQKLKY P5	Tpm3,Tpm1	DELYAQKLKY DEVYAQKMKY DELYAQKLKY EKLAQAKEEN
10	34-43	EERSKQLEDE P2	Tpm3	EDRSKQLEDE EDRCKQLEEE EERSKQLEDE EDKCKQVEEE
11	34-43	EERSKQLEDE P2	Tpm3	EDRSKQLEDE EDRCKQLEEE EERSKQLEDE EDKCKQVEEE
12	34-43	EERSKQLEDE P2	Tpm3	EDRSKQLEDE EDRCKQLEEE EERSKQLEDE EDKCKQVEEE

3.4.2 Dot Blot

Dot blot technique is similar to western blotting except that the proteins are not separated by gel electrophoresis. Hence native protein can be used for identification and analysis of proteins by using antibody probe. The advantage this method gives is by saving the amount of protein used and the time and reagents consumed are less when compare to western blotting.

In this method proteins are spotted on a nitrocellulose membrane and are then hybridized with specific antibody probe. Nitrocellulose membrane (GE healthcare Hybond ECL nitrocellulose membrane) was cut into strips and each strip is used for the 12 antibodies using for identification of Tpm3. Using a pencil the strips are labelled and dots were spotted with 1cm apart to indicate the region where protein is being spotted as shown in results Figure 3.10. First all the recombinant proteins produced in Chapter II (Tpm1, Tpm2, Tpm3 –all there version, Tpm1 A63V, Tpm1-K70T) were used to establish the Ab sensitivity (Figure 3.10A) In the second experiment (Figure 3.10B) different concentrations of Tpm1 and Tpm2 were at constant dilution of Abs, 1 in 8K dilution was used to check sensitivity of protein concentration to Ab and third time constant protein concentration with constant Ab dilution was used but with protein in its native and denatured state with Tpm1, Tpm2 and Tpm3 as shown in Figure 3.10C. The denatured protein is prepared by incubating the protein with 0.1% SDS at 95^0C for 5min, cooled and then used for blotting. 2 µl of 10 µM protein was spotted slowly on the membrane. The membrane was allowed to dry for 1 hour and was blocked with 5% no fat milk (Marvel semi-dried milk powder) in 1X phosphate buffer saline with 0.05% Tween 20

(1X PBS-T) for 1 hour at room temperature. Membrane strips were incubated for 1 hour with assigned primary monoclonal antibody in individual 50 ml falcon tubes. The list of monoclonal antibodies is given in Table 3.1.

After washing three times for 10 min in 1X-PBS-T, the strips were incubated with horseradish peroxide (HRP) -rabbit anti-mouse IgG antibody (1:50K v/v) for 1 hour. The membrane strips were washed thoroughly again for 3X10 min with 1X-PBS-T and treated with 1% Dextran sulfate in 10 mM citrate-EDTA buffer pH 5.0 for 10 min before treating with 3,3',5,5'-tetramethlybenzidine (TMB) to develop the membranes. Blue colour bands appear where ever there is antibody binding.

3.4.3 Western Blotting

3.4.3.1 SDS-PAGE

Proteins were analysed by sodium dodecyl sulphate polyacrylamide gel electrophoresis (SDS-PAGE) using 13.5% acrylamide (Laemmli, 1970). Total protein is denatured and reduced in 4X SDS sample buffer containing 500 mM Tris, 40% Glycerol, 10% SDS, 10% β-mercaptoethanol, 0.05% bromophenol blue. Approximately 3 µg of protein was loaded onto the gel and was run at 200 volts for 45 min to 1 hour. Fungal tropomyosin from *Neurospora crassa,* which is of 14494 kDa (161 residues) protein is used as a negative control for the antibody binding and is processed similar to the other human tropomyosin isoforms. All the gels were run in duplicates for assessment of individual monoclonal antibodies efficiency to Tpm3.12st.

3.4.3.2 Blotting

Gels were soaked for 5 min in transfer buffer containing 48 mM Tris-HCl, 40 mM Glycine, 2% SDS, 20 % methanol to equilibrate the gel. Nitrocellulose membrane was also soaked in transfer buffer for 5 min and protein bands were transferred onto the membrane using Bio-Rad Trans-Blot semi-dry electrophoretic transfer cell following the manufacturer's protocol for 35 min at 10-15V as shown in Figure 3.8. Bio-Rad precision plus prestained standard marker was used for the SDS-PAGE to visualize the transferred bands. The membrane was blocked with 5% milk in phosphate buffer saline with 0.05% Tween-20 (PBS-T) for 1 hour to prevent non-specific binding. Membranes were rinsed with PBS-T and incubated in 1/2000 dilution monoclonal primary antibody for 1 hour at 37 ^{0}C. The epitopes of the protein for the antibodies are given in the Figure 3.7. The list of monoclonal primary antibodies and their theoretical binding expression are given in Table 3.1. All antibodies and CH1 (Lin et al., 1985)were made in 1 in 2000 dilution except Ab11 and CG3 (Lin et al., 1985) antibody which were used at 1 in 500 dilution. The monoclonal CG3 antibody is mapped to aa 29-44 by exon 1b of Tm5 gene (LMW isoform of Tpm3). The CG1 and CG3 antibodies were donated by Prof. Marston from National Heart and Lung Institute, Imperial College, London. The membranes were washed 3 times 10 min in 1X PBS-T and were incubated in 1 in 50K dilution of horseradish peroxidase (HRP) anti mouse conjugate form Sigma Aldrich as secondary antibody for 1 hour at 37 ^{0}C and washed 3 time 10 min in PBS-T. Both primary and secondary antibodies were diluted in 1X PBS buffer. Membranes were washed with 1% dextran sulfate in citrate-EDTA buffer pH 5.0 for 10 min and rinsed with PBS before developing the membranes with 3,3',5,5'- Tetramethylbenzidine (TMB) liquid substrate

solution for membranes from Sigma Aldrich. Pictures of the membranes were taken using a 8 megapixel camera and pictures were processed using Image J software (Schneider et al., 2012).

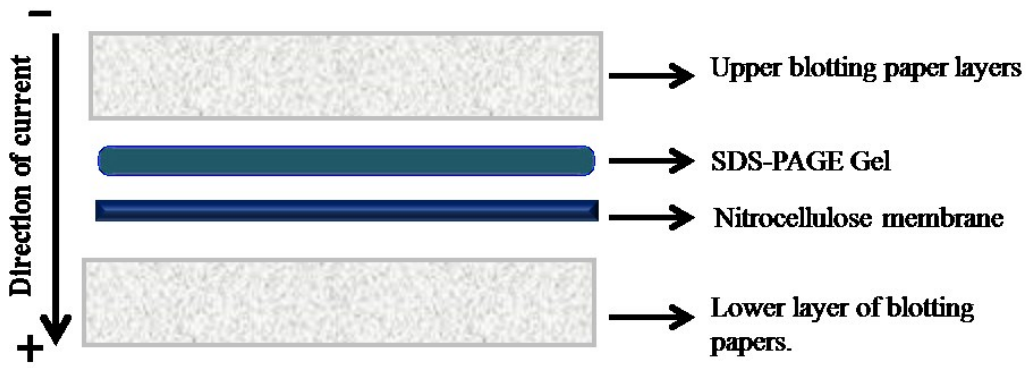

Figure 3.8: Arrangement of membrane and SDS-PAGE for transfer of proteins in Bio-Rad Trans-Blot semi-dry electrophoretic transfer cell.

3.4.4 ELISA

The enzyme linked immunosorbent assay (ELISA) is an effective method for detecting and quantifying a specific protein using an antigen/antibody either in a complex mixture or confirmation of pure protein (Engvall and Perlmann, 1971). An indirect ELISA is used to quantify the Tpm3.12st in comparison to Tpm1.1st.

The assay was optimized by using checkerboard titration method to establish the Abs reaction with tropomyosin. Different dilutions of Abs were prepared by serial dilutions starting from 1/ 4 and following to 1/8, 1/16, 1/32, 1/64, 1/128, 1/256, 1/512 and different concentration of Tpm1 and Tpm3 were prepared. (10 µM, 1.0 µM, 0.1 µM, 0.01 µM and

0.001 µM). Standards (b1-Ab was coated on the wells and b2-blank wells treated as Tm) were also coated by adding varying dilution of Abs to each well and treated as Tm when processing the assay. Costar 96 well, flat bottom medium binding plates were used. The checker board plating of the Abs and proteins is shown in Table 3.2 where each concentration of Tm was probed with all dilutions of Ab.

Table 3.2: Preliminary optimization of ELISA plate set-up for method development of Ab reaction. b1 are the well coated with Ab of variable dilutions and b2 empty wells coated with only buffer, both b1 and b2 were treated same as Tm to generate standard curve to check background intensity of Abs.

Tm Conc. → / Ab dilution ↓	10 µM	1.0 µM	0.1 µM	0.01 µM	0.001 µM	10 µM	1.0 µM	0.1 µM	0.01 µM	0.001 µM	Ab coated	No Ab
1/512	tpm3	tpm3	tpm3	tpm3	tpm3	tpm1	tpm1	tpm1	tpm1	tpm1	b1	b2
1/256	tpm3	tpm3	tpm3	tpm3	tpm3	tpm1	tpm1	tpm1	tpm1	tpm1	b1	b2
1/128	tpm3	tpm3	tpm3	tpm3	tpm3	tpm1	tpm1	tpm1	tpm1	tpm1	b1	b2
1/64	tpm3	tpm3	tpm3	tpm3	tpm3	tpm1	tpm1	tpm1	tpm1	tpm1	b1	b2
1/32	tpm3	tpm3	tpm3	tpm3	tpm3	tpm1	tpm1	tpm1	tpm1	tpm1	b1	b2
1/16	tpm3	tpm3	tpm3	tpm3	tpm3	tpm1	tpm1	tpm1	tpm1	tpm1	b1	b2
1/8	tpm3	tpm3	tpm3	tpm3	tpm3	tpm1	tpm1	tpm1	tpm1	tpm1	b1	b2
1/4	tpm3	tpm3	tpm3	tpm3	tpm3	tpm1	tpm1	tpm1	tpm1	tpm1	b1	b2

An assay was developed by coating 50 µl of tropomyosin in each well following the Table 3.2 arrangement diluted with sodium phosphate buffer, pH 7.5 and plates were incubated for 2 hours at 37 ^{0}C. Plates were rinsed 2 times with 250 µl 1X PBS, pH 7.0 and dried on paper towels to remove excess protein. 300 µl of blocking buffer (5% milk in 1X PBS-T) was added to each well and incubated at room temperature (RT) for 30 min and the plates were washed with wash buffer, 1X PBS-T, pH 7.0, three times for 10 minutes on a shaker. 100µl of primary antibody Tpm3.12st specific monoclonal antibodies was added to each well and incubated for 30 min at 37 ^{0}C. The plates were washed three times for 10 min at RT to remove excess unbound primary antibodies and

100 µl of horseradish peroxidase (HRP) anti mouse conjugate as secondary antibody was added in 1/50K dilution to each well and incubated for 30 min at 37 ^{0}C. Secondary antibody acts as a probe for quantifying the signal by reacting with the substrate producing a colorimetric reaction. The plates were washed three times for 10 min at RT and dried on paper towels. TMB (3, 3′,5 ,5′-Tetramethylbenzidine) liquid substrate, supersensitive, for ELISA from Sigma Aldrich (T4444-100ML**)** was used which produces a pale blue colour at RT. The reaction is stopped by adding 0.2 M H_2SO_4 which gives a pale yellow colour that was measured at 450 nm by UV microplate reader. Standard curves were generated by plotting the OD on Y-axis and the dilutions of Ab on X-axis. The protein reactivity curves were plotted against OD on y-axis and the concentration of Tm on X-axis. Figure 3.9 shows the work flow of the ELISA methodology followed.

The assay was repeated three times on different days and hence the mean values cannot be taken as this will result in in-accurate data. The results from about method were not reproducible for protein reactions, however it was helpful to establish the dilution at which there was least background (non-specific binding) of Ab. This was calculated by taking the ratio of b1 and b2 and the value with lower ratio Ab was taken for further quantification experiment.

Repeating the experiment with different concentration of tropomyosin with constant Ab dilution, the set of concentration used below were found to give a linear reaction intensities. For quantification of protein, 1/16000 dilution of Ab was used as this dilution had very low non-specific binding, and different concentrations of tropomyosin was used. An assay was developed by coating 50 µl of tropomyosin in triplicates at a concentration

between 0.1 nM to 50 nM in 0.1 M sodium carbonate buffer, pH 9.6 and incubated at 4 ^{0}C overnight. A typical assays plate design used for this experiment is shown in Table 3.3. Nunc-Immuno Maxisorp flat bottom 96well microwell plates were used for this method. The protocol was similar with changes in coating the plates overnight at 4 ^{0}C rather than 2 hours at 37 ^{0}C and the incubation times were increased from 30 min to 1 hour at each stage and the rest of the method was followed similar as mentioned above.

Table 3.3: Elisa plate assay design: The setup of the plate used for quantifying Tpm1 and Tpm3 using two antibodies for each plate.

Ab → conc Conc ↓ nM	Ab1 - 1/16K	Ab1 - 1/16K	Ab1 - 1/16K	Ab1 - 1/16K	Ab1 - 1/16K	Ab1 - 1/16K	Ab2- 1/16K	Ab2- 1/16K	Ab2- 1/16K	Ab2- 1/16K	Ab2- 1/16K	Ab2- 1/16K
0.1	tpm1	tpm1'	tpm1"	tpm3	tpm3'	tpm3"	tpm1	tpm1'	tpm1"	tpm3	tpm3'	tpm3"
0.5	tpm1	tpm1'	tpm1"	tpm3	tpm3'	tpm3"	tpm1	tpm1'	tpm1"	tpm3	tpm3'	tpm3"
1	tpm1	tpm1'	tpm1"	tpm3	tpm3'	tpm3"	tpm1	tpm1'	tpm1"	tpm3	tpm3'	tpm3"
2	tpm1	tpm1'	tpm1"	tpm3	tpm3'	tpm3"	tpm1	tpm1'	tpm1"	tpm3	tpm3'	tpm3"
5	tpm1	tpm1'	tpm1"	tpm3	tpm3'	tpm3"	tpm1	tpm1'	tpm1"	tpm3	tpm3'	tpm3"
10	tpm1	tpm1'	tpm1"	tpm3	tpm3'	tpm3"	tpm1	tpm1'	tpm1"	tpm3	tpm3'	tpm3"
50	tpm1	tpm1'	tpm1"	tpm3	tpm3'	tpm3"	tpm1	tpm1'	tpm1"	tpm3	tpm3'	tpm3"
	b	b'	b1	b1'	c	c'	b	b'	b1	b1'	c	c'

Note: b-blank with only secondary antibody, b1 empty wells treated with primary and secondary antibody and c is wells coated with primary antibody and treated as protein. (' - duplicate, " - triplicate).

3.4.5 Reaction of HRP with TMB

ELISA assays are mostly performed by using horseradish peroxidase (HRP) as a marker enzyme. HRP is a metalloenzyme found in the root of horseradish plant. The most commonly used is the HRP-C which is most abundant and has been successful in

production of recombinant enzyme (Veitch, 2004). HRP have heme group at its center and uses hydrogen peroxide to oxidize both organic and inorganic compounds. The detection limit of HRP on its own in colorimetric assays is very low. This was overcome by using 3,3',5,5'-Tetramethylbenzidine (TMB) which forms a blue colour soluble substrate linked with HRP gives higher detection limits which can be read at 650 nm (Porstmann and Kiessig, 1992).

In immunoassays the protein is linked with HRP as a secondary antigen that can be oxidized with TMB to detect the protein levels. TMB acts as electron donor for the reduction of hydrogen peroxide in presence of HRP. 3,3',5,5'-Tetramethylbenzidine is oxidized to blue colour 3,3',5,5'-Tetramethylbenzidine diimine which can be stabilized by adding acid (H_2SO_4) by lowering its pH to forming a yellow colour substrate which can be read at 450 nm (Josephygg et al., 1982) and also stops the reaction. Stopping the reaction is important as the intensity of the colour keeps increasing along with increase in time resulting in excess intensity which may not give accurate results.

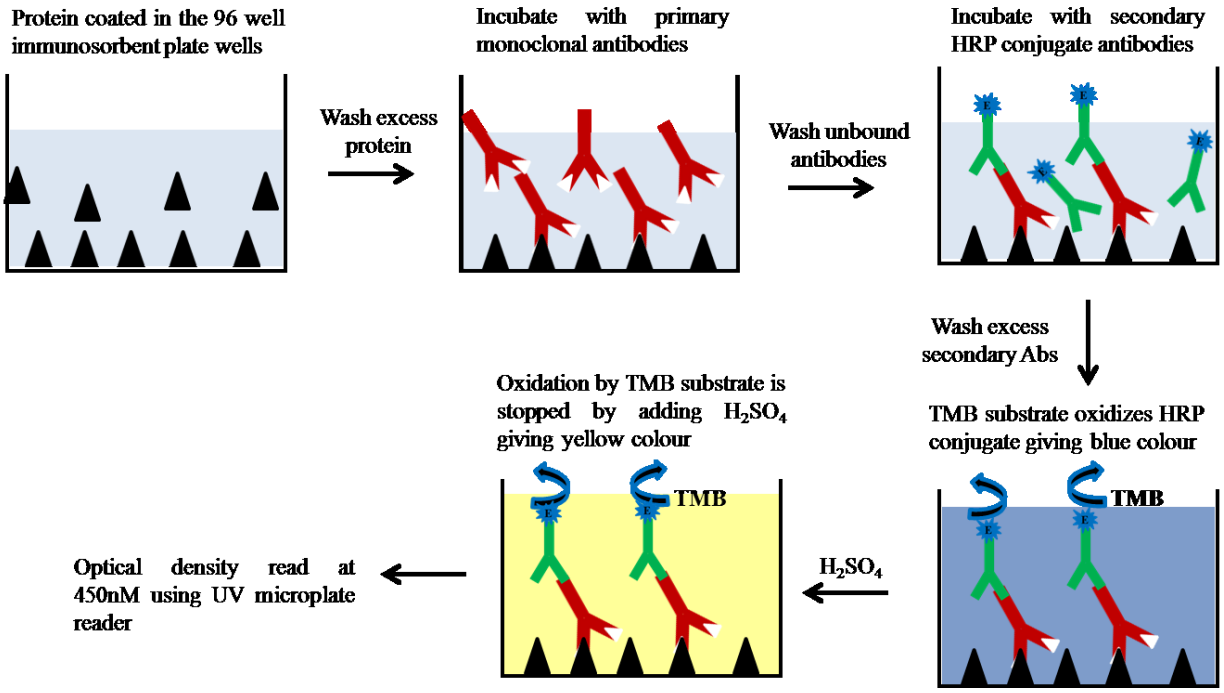

Figure 3.9: Work flow of indirect ELISA methodology.

3.4.6 Interpretation of Elisa data used for quantifying Tpm1 and Tpm3.

The data obtained from the experiment as explained in the section 3.4.4 (according to Table 3.3), was fitted according to 4 parameter logistic nonlinear regression model which gives a sigmoidal curve in relation to concentration. This is a generalized model used for ligand binding assays such as ELISA (Findlay and Dillard, 2007). The 4-parameter logistic (4-PL) model is generally used as a reference model for calibration curves that gives a sigmoidal relationship. This provides an accurate representation of the measured sensitivity response and the concentration of the analyte. Origin 6 software was used for interpretation of the calibration curves of the data obtained from the assays. The 4-PL model formula used by the software to interpret the data is as follows:

$$y = \frac{A_1 - A_2}{1 + (x/x_0)^p} + A_2$$

Where , y is the response, A_1 is the initial value at zero analyte concentration, A_2 is the final value, x_0 is the slope (the inflection point on the calibration curve) and p is the slope factor. The response is monotonic, increase with concentration as the $A_1 < A_2$ and decrease in concentration as $A_1 > A_2$ and the calibration curve is symmetric at x_0 with response at a specific concentration and the slope factor p defines the steepness of the curve. As the curve is sigmoidal the slope (x_0) changes through out depending on the concentration.

3.5 Results

3.5.1 Dotblot

Dot blot results (Figure 3.10) show three repeated experiments of Dot-blot reactions of all the 12 antibodies produced against five epitopes of Tpm3 sequence. In blot Figure 3.10A and Figure 3.10C protein used was at 10 μM and in Figure 3.10B, various concentrations of proteins (10, 1.0, 0.1, 0.01, 0.001) was used as mentioned in methodology. It can be observed from Figure 3.10A that Tpm3-MASM has higher sensitivity to the Abs than Tpm3-Met and Tpm3-MM. From all three blots Ab4, Ab5 and Ab7 have lower reactivity on their own when used as a positive control. Blots from Figure 3.10A and C, Ab1, Ab2, Ab3, Ab4 and Ab9 show reactivity with Tpm2 in both native and denatured state. In Figure 3.10A, B Tpm1 and Tpm2 have sensitivity to Ab11 and Ab12 with both Tpm1 and Tpm3 in native state in contrast to Figure 3.10C where they have reactivity to Tpm1 only in denatured state. In blots Figure 3.10B similar to other blots (A and C) show sensitivity to all antibodies, however at low concentration of 0.1 and 0.01 Ab 11 and Ab12 show reactivity to only Tpm3. With the above results the difference in reaction of the antibodies, western blotting was performed where the protein is in the denatured state and ELISA with native protein.

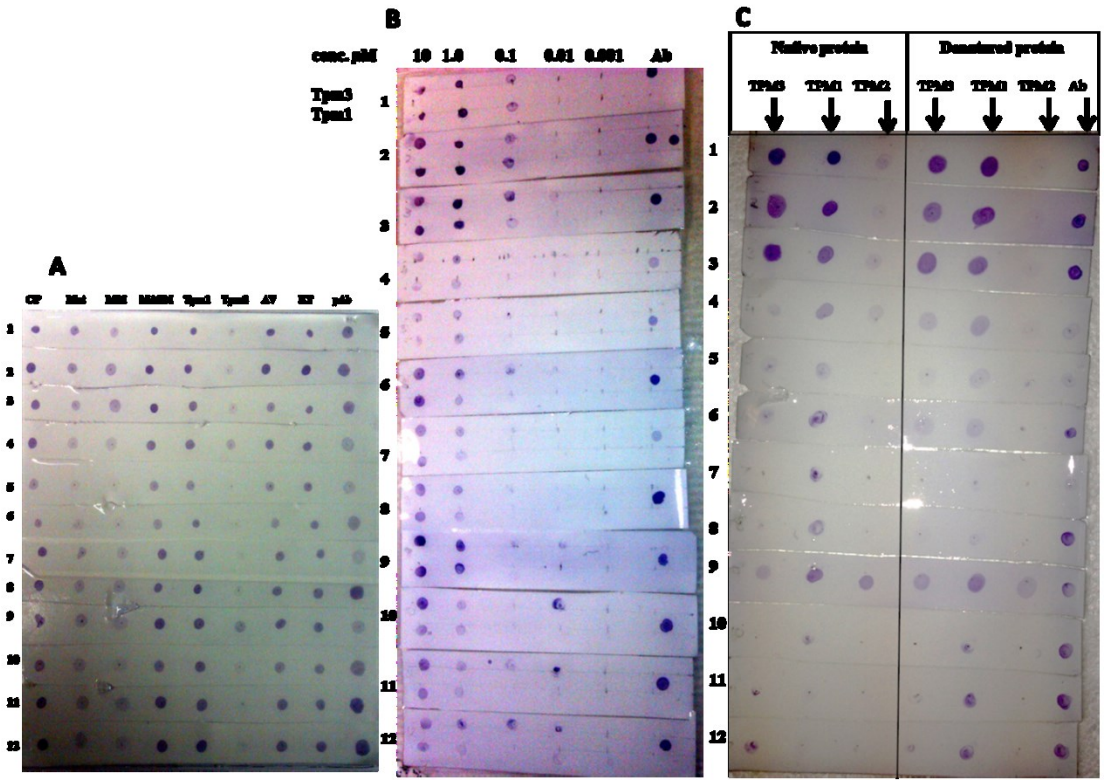

Figure 3.10: Dot blot strips showing the antibody reaction. Three experiments of Dot-Blot of all the 12 antibodies produced against the 5 epitopes**. A.** Each blot in A have all the recombinant proteins produced in native state for this study (No Tpm4). Cp-control proteins mainly containing tropomyosin and troponin, AV is a cardiomyopathy mutation A63V and K70T. **B.** Tpm3 and Tpm1 in different concentration of native protein, top layer-Tpm3 and bottom layer -Tpm1. **C.** Each blot contains both native and denatures versions of the proteins as labelled. left to right: Tpm3, Tpm1, Tpm2. The vertical numbers show the antibody numbers.

3.5.2 Western Blotting

Western blotting was performed by loading 3 µg of protein onto 13.5% acrylamide gels and the proteins were transferred through semi-dry membrane transfer as described in the methodology. Affinity of the monoclonal antibodies obtained from western blotting show a different profile compared to dot blot results. Figure 3.11 shows the Coomassie Blue stained gel of all the isoforms used for the western blotting. Tropomyosin of fungi

Neurospora crassa, which is of 14494 kDa protein with 161 aa was used as a negative control for the antibody binding. From the gel it is clearly seen the isoforms run differently on the gel even though they do not vary much in their calculated molecular weight. Tpm4 run same as Tpm2 even though Tpm4 is has more sequence similarity to Tpm1.

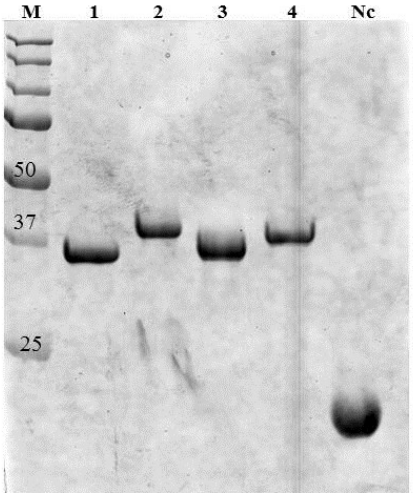

Figure 3.11: Coomassie Blue stained SDS-PAGE gel used for western blotting. M-Marker, 1-Tpm1, 2-Tpm2, 3-Tpm3, 4-Tpm4 and Nc- *Neurospora crassa* tropomyosin. Details of protein loaded on the gel are given in methodology section.

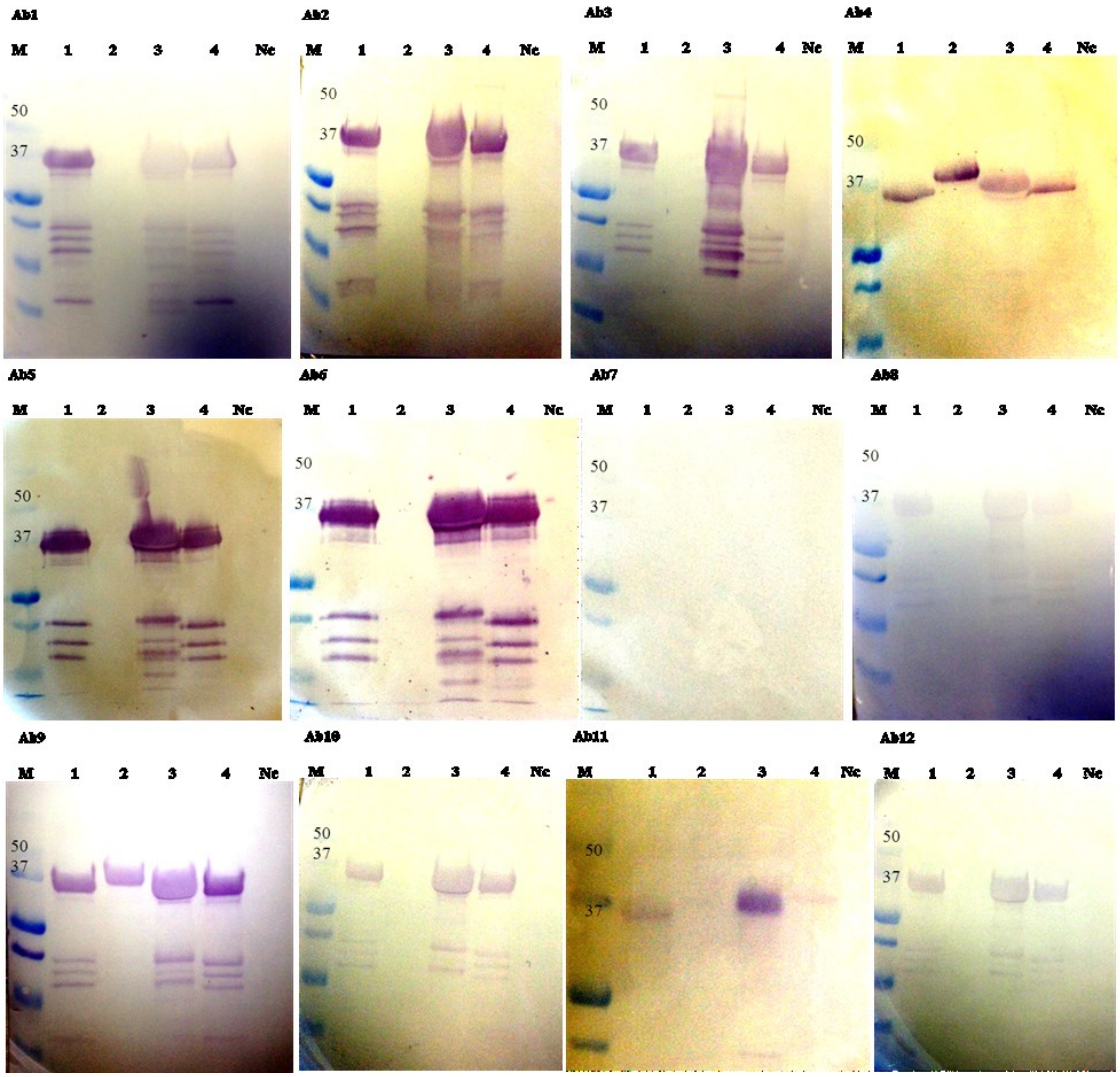

Figure 3.12: Western blots probed with 12 monoclonal antibodies individually. Details of the method are given in the methodology section. Ab-Antibody with number, M- Marker, 1-Tpm1, 2-Tpm2, 3-Tpm3, 4-Tpm4, and Nc – *Neurospora crassa* tropomyosin. The membrane was reacted with primary monoclonal antibody linked with HRP and developed with TMB substrate that gives blue colour to the protein bound to the membrane. The pictures of the developed membranes were taken by 8 megapixel camera and processed with Image J software.

All the antibodies have affinity to Tpm1, Tpm3 and Tpm4 with different sensitivity other than Ab7 (EERSKQLEDE) which did not show reactivity to any of the isoform (Figure 3.12). Ab4 and Ab9 are the once that identified Tpm2 unlike the rest of the Abs and have same level of sensitivity to all the isoforms. In contrast to dot blot where Ab1, 2, 3 showed reactivity with Tpm2, western blot did not show the same result even after repeated attempts. Another factor that was also observed is that the Coomassie stained gel (Figure 3.11) does not show any stained lower molecular proteolytic protein bands at the given amount of protein loaded on the gel, but the membranes probed with antibodies shows different proteolytic protein fragment profiles with individual monoclonal antibodies.

The reaction of all the isoforms probed with CG1 (Figure 3.13) gave the expected outcome (Marston et al., 2013; Schevzov et al., 2011) , but the CG3 (Figure 3.13) seems to have slight affinity to Tpm4 as well, as opposed to the previous studies which was supposed to bind only to Tpm3 (Marston et al., 2013; Schevzov et al., 2011).

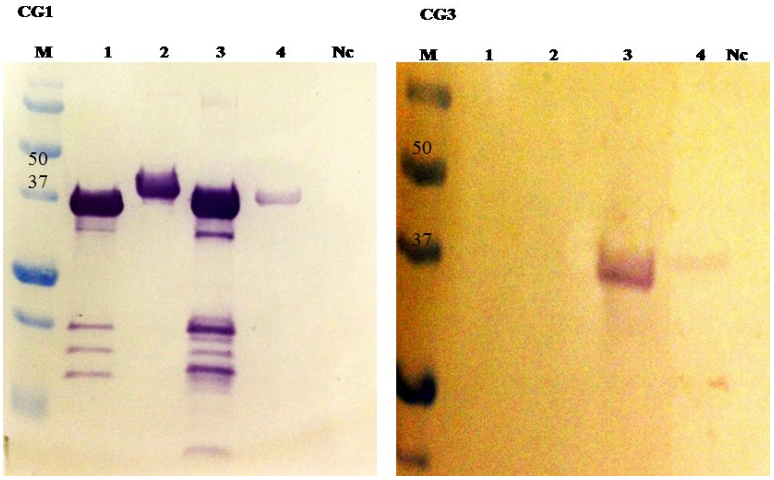

Figure 3.13: Western blots of tropomyosin isoforms probed with CG1 and CG3. The membranes after protein transfer were treated same as the Tpm3 monoclonal antibodies as detailed in methodology.

3.5.3 ELISA

ELISA immunoassay was used to determine to quantify the sensitivity of monoclonal antibodies of Tpm3 in comparison to TPM1.

3.5.3.1 Standard Curves

Figure 3.14, Figure 3.15Figure 3.16, show the preliminary optimization reaction standard curves generated by the intensities obtained from wells coated with Abs and empty wells treated similar to tropomyosin at varying dilutions to check the non-specific binding and establish an Ab dilution with lowest background reaction. The assay was repeated three times and the results of standard curves of all the three reactions are given in the Figures mentioned above. Form the curves, ratio between b and b2 were calculated to check the dilution with minimum back ground and 1/16K dilution of Abs was chosen for using in further protein quantification assays, the lowest back ground can also been seen clearly from the curves in the figures. Only Tpm1 is chosen as it is the most dominant isoform with high sequence similarity with all the other isoforms.

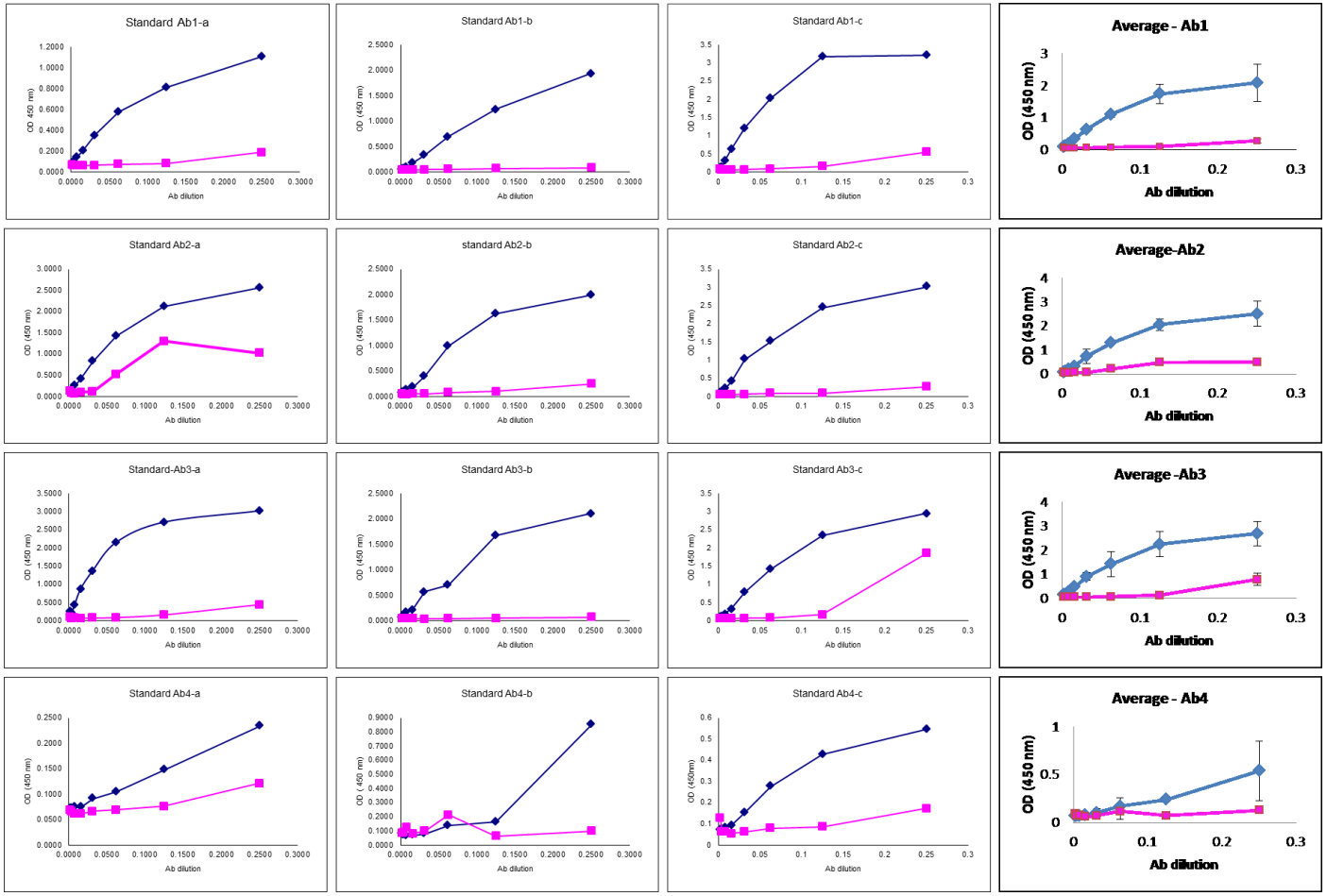

Figure 3.14: Standard curves of Ab1, Ab2, Ab3 and Ab4. Triplicate standard curves of Ab1, Ab2 and Ab3 and Ab4 and the average with error bars are shown above. Curves were generated by taking the OD on Y-axis and Ab dilutions on the X-axis to check the background of the antibody binding. Blue line is Ab coated in the well and treated similar to Tm (b1) and Pink line is empty wells treated similar to Tm (b2). a, b and c corresponds to triplicate reactions of the Abs.

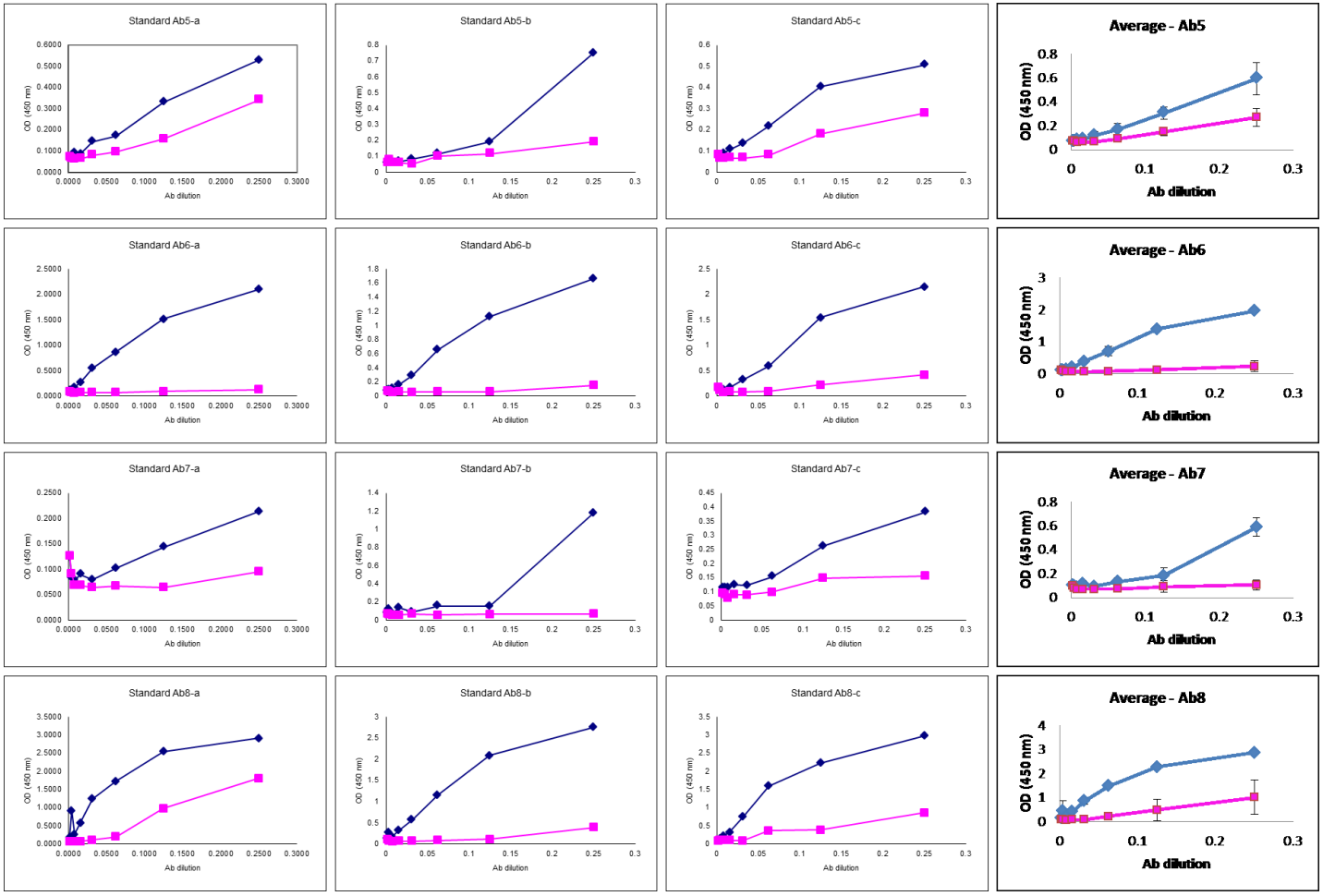

Figure 3.15: Standard curves of Ab5, Ab6, Ab7 and Ab8. Triplicate standard curves of Ab4, Ab5 and Ab6 are shown above. Curves were generated by taking the OD on Y-axis and Ab dilutions on the X-axis to check the background of the antibody binding. Blue line is Ab coated in the well and treated similar to Tm (b1) and Pink line is empty wells treated similar to Tm (b2). a, b and c corresponds to triplicate reactions of the Abs.

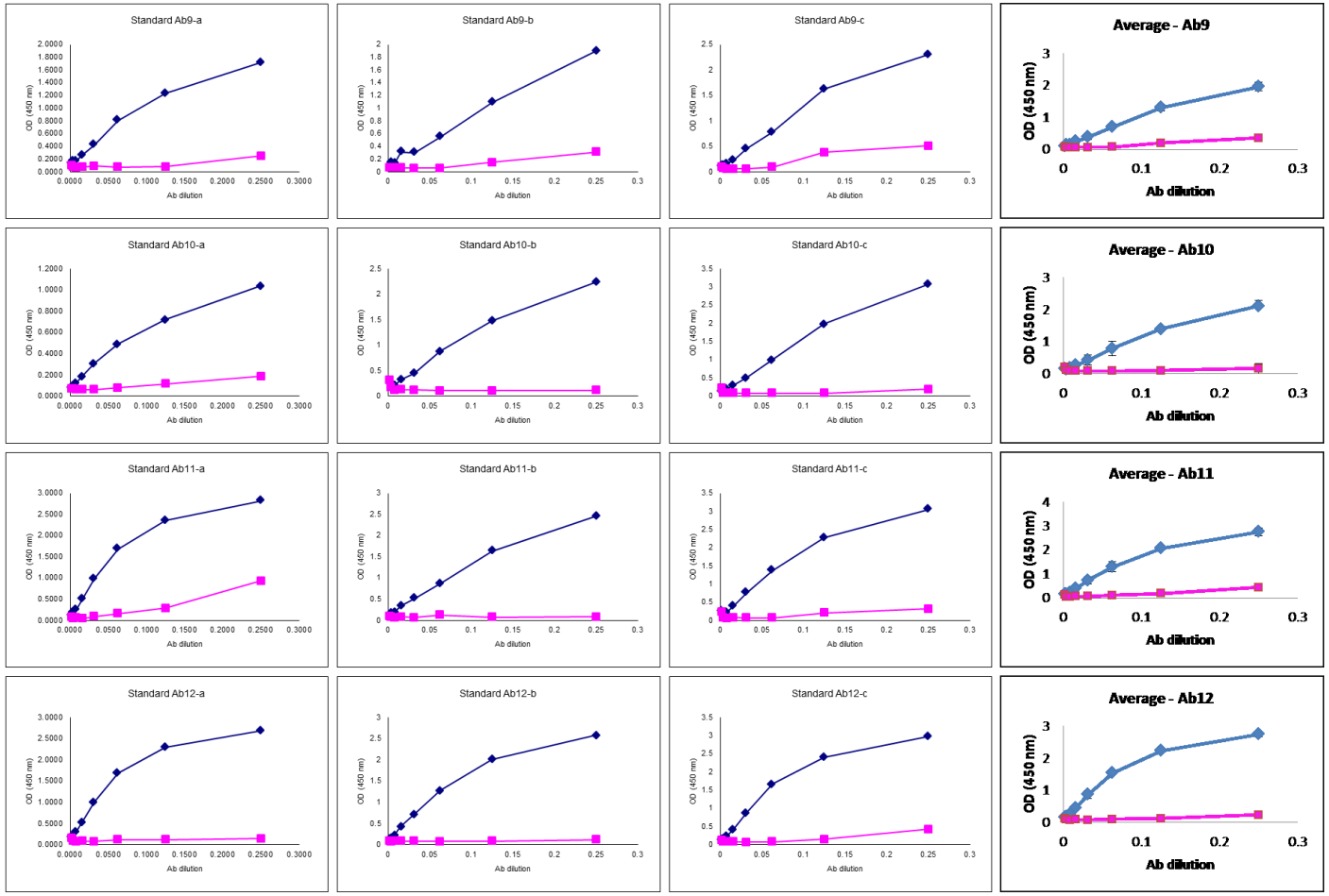

Figure 3.16: Standard curves of Ab9, Ab10, Ab11 and Ab12 reaction. Triplicate standard curves of Ab10, Ab11 and Ab12 are shown above. Curves were generated by taking the OD on Y-axis and Ab dilutions on the X-axis to check the background of the antibody binding. Blue line is Ab coated in the well and treated similar to Tm (b1) and Pink line is empty wells treated similar to Tm (b2). a, b and c corresponds to triplicate reactions of the Abs.

3.5.3.2 ELISA Preliminary optimization of checker board Assay

The results from Figure 3.17, Figure 3.18 andFigure 3.19 show the optimization of ELISA method for monoclonal Abs affinity to Tpm3.12st. Ab1, Ab2 and Ab3 show increase in binding according to the increase in concentration.

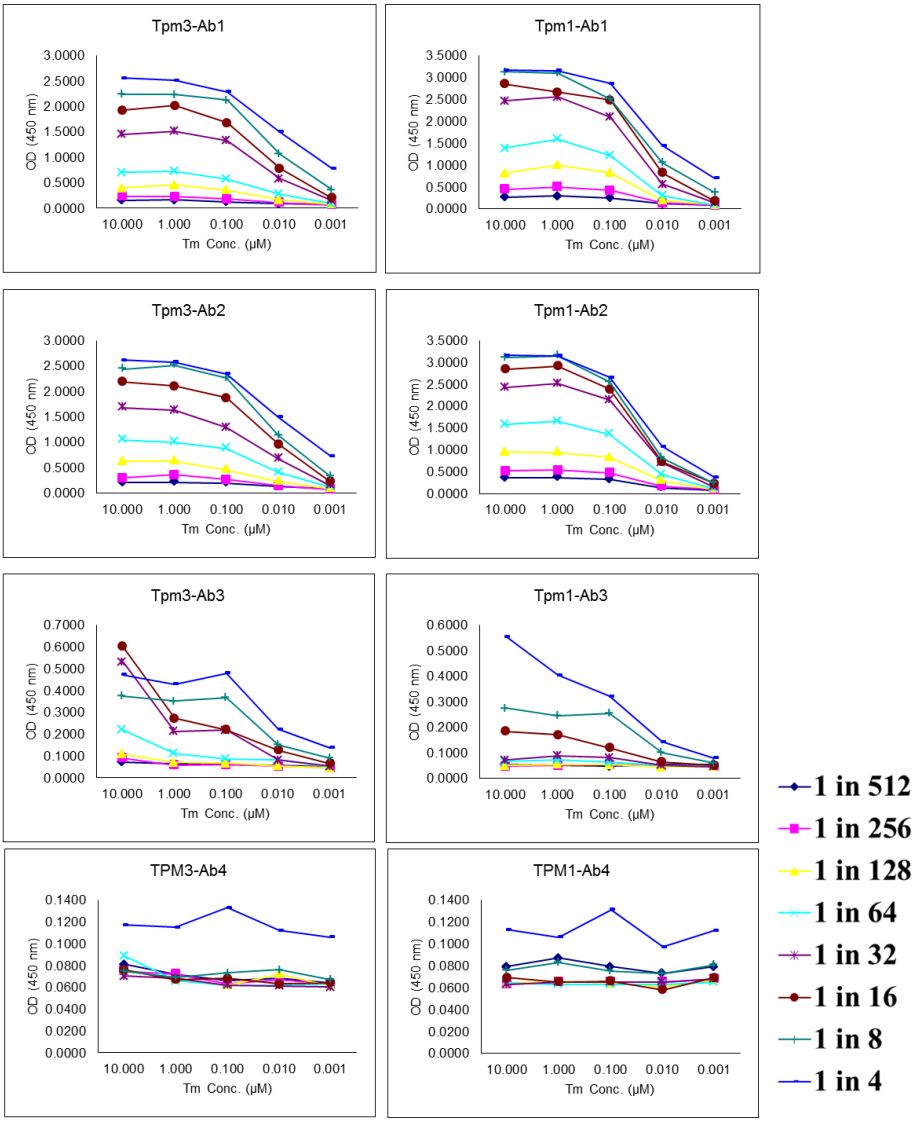

Figure 3.17: Preliminary ELISA assay with varying dilutions of Ab1, Ab2, Ab3 and Ab4 with different concentrations of Tpm3 and Tpm1. Varying dilutions of Abs were reacted to different concentrations of protein as explained in methodology. OD was

measured at 450 nm and plots were generated by taking OD on Y-axis and the concentrations of Tm on X-axis. Series of the curves are shown on the side.

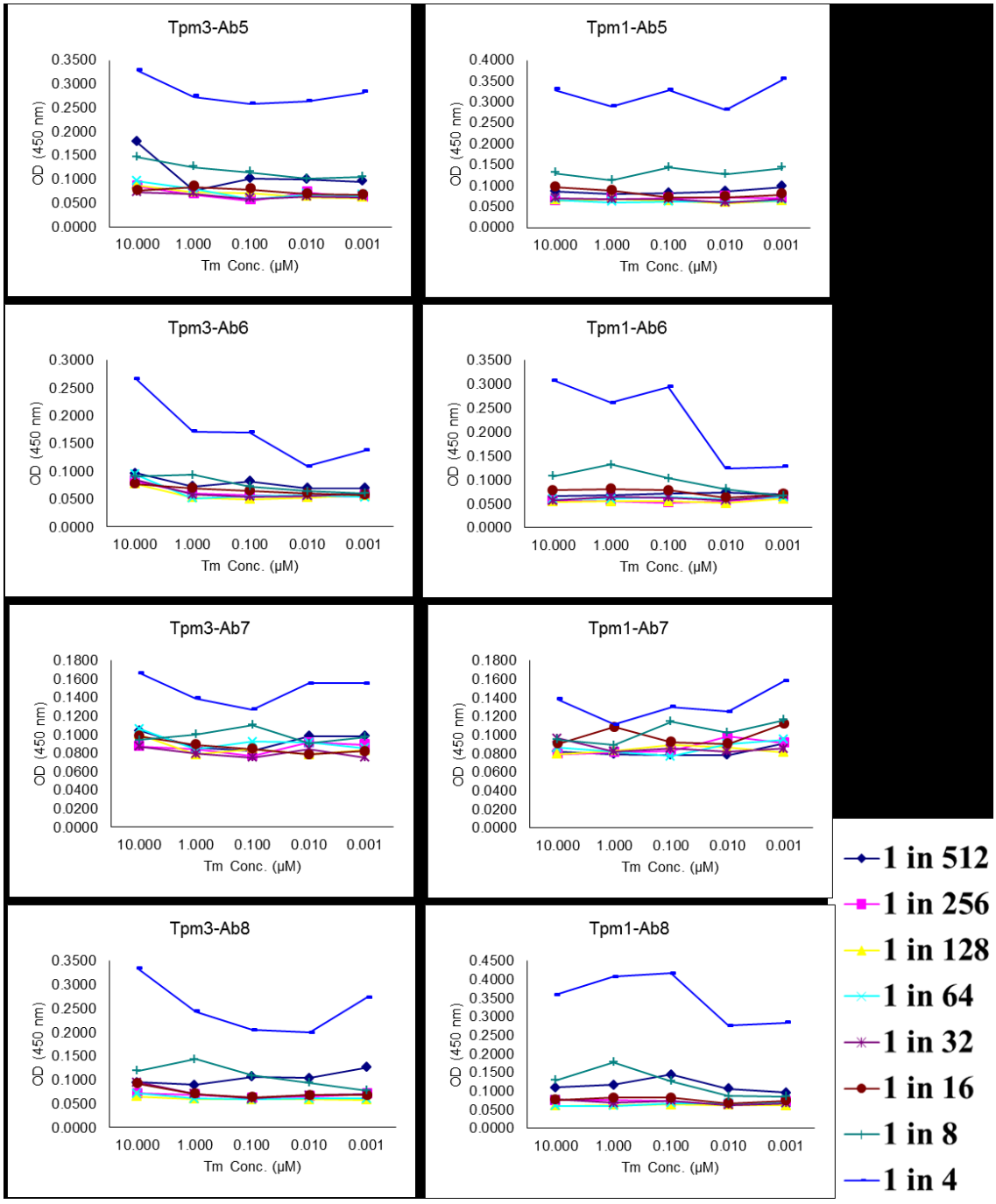

Figure 3.18: Preliminary ELISA assay with varying dilutions of Ab5, Ab6, Ab7 and Ab8 with different concentrations of Tpm3 and Tpm1. Varying dilutions of Abs were reacted to different concentrations of protein as explained in methodology. OD was measured at 450 nm and plots were generated by taking OD on Y-axis and the concentrations of Tm on X-axis. Series of the curves are shown on the side.

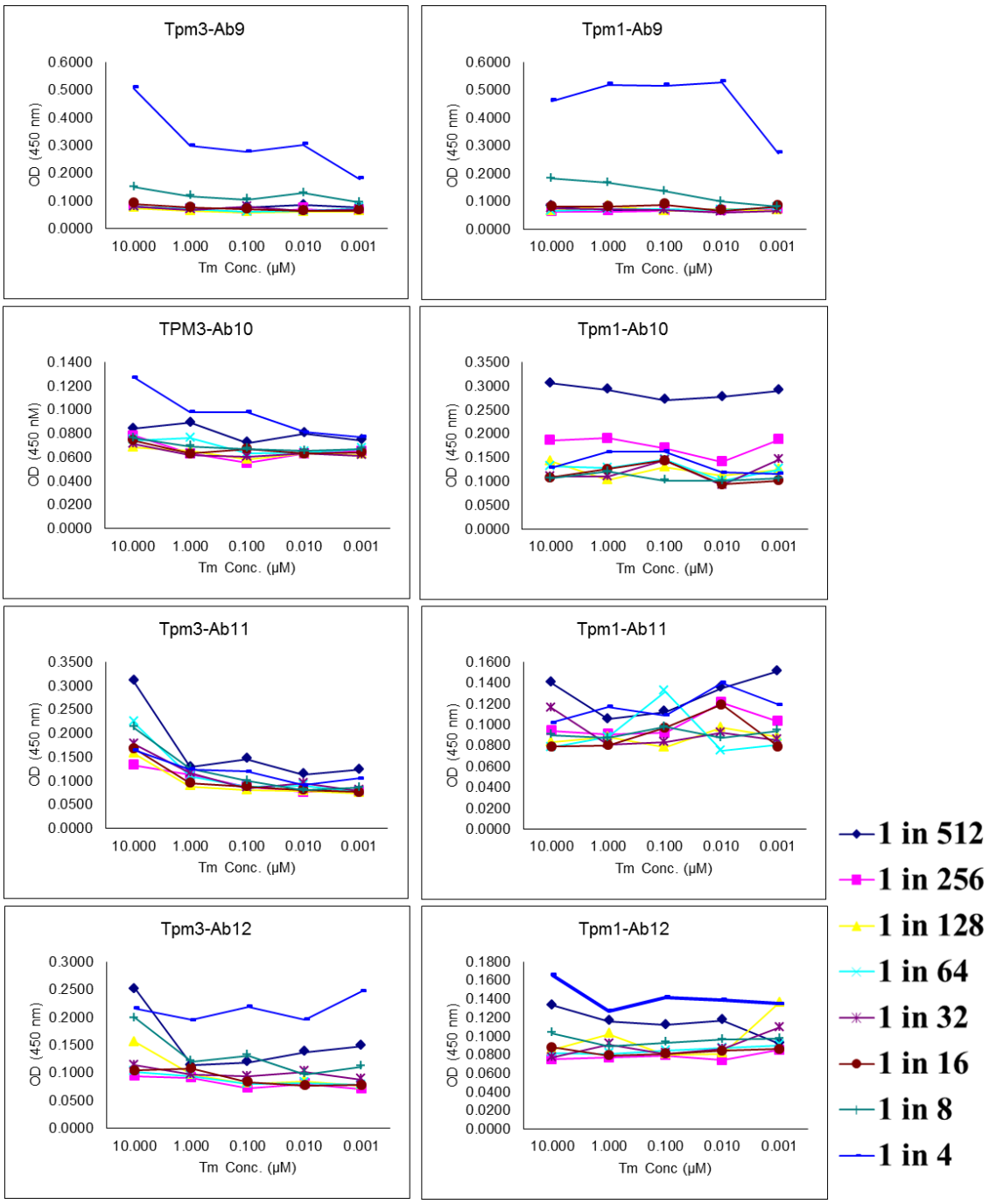

Figure 3.19: Preliminary ELISA assay with varying dilutions of Ab9, Ab10, Ab10 and Ab11 with different concentrations of Tpm3 and Tpm1. Varying dilutions of Abs were reacted to different concentrations of protein as explained in methodology. OD was measured at 450 nm and plots were generated by taking OD on Y-axis and the concentrations of Tm on X-axis. Series of the curves are shown on the side.

3.5.3.3 Quantification of Tpm1 and Tpm3 using monoclonal antibodies

The data obtained from the ELISA results were analysed using 4 parameter logistic model for interpretation of the sensitivity of the antiboides to Tpm3 as explained in section 3.4.6.

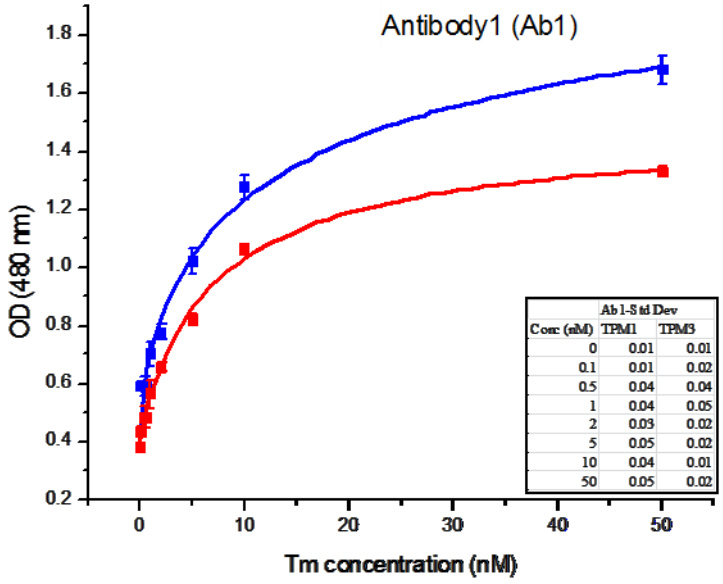

Figure 3.20: Elisa affinity curve of Ab1 with Tpm1 and Tpm3. The assay was developed to measure the specificity of monoclonal antibody affinity to Tpm3.12st by varying concentration of protein (0.1nM to 50nM) with constant concentration of antibody at 1/16000 dilution. The curves were generated using 4 parameter logistic nonlinear regression model as explained in the section 3.4.6. The intensity (OD) measured at 450 nm taken on Y-axis against the concentration of the protein on X-axis. The data is the mean of triplicate reactions. Blue - Tpm1 and Red - Tpm3. The table shows the standard deviation of the triplicate reactions.

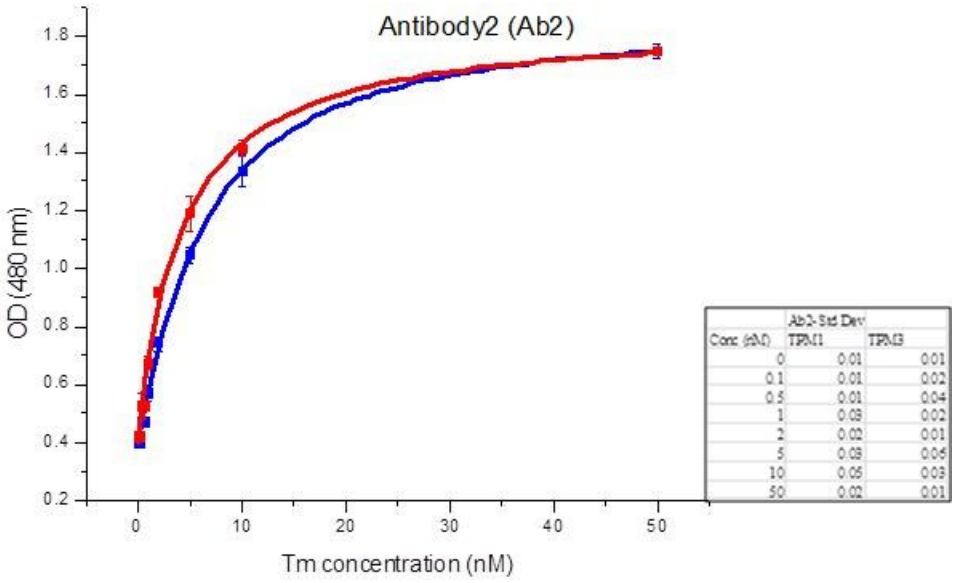

Figure 3.21: Elisa affinity curve of Ab2 with Tpm1 and Tpm3. The assay was developed to measure the specificity of monoclonal antibody affinity to Tpm3.12st by varying concentration of protein (0.1nM to 50nM) with constant concentration of antibody at 1/16000 dilution. The curves were generated using 4 parameter logistic nonlinear regression model as explained in the section 3.4.6. The intensity (OD) measured at 450 nm taken on Y-axis against the concentration of the protein on X-axis. The data is the mean of triplicate reactions. Blue - Tpm1 and Red - Tpm3. The table shows the standard deviation of the triplicate reactions.

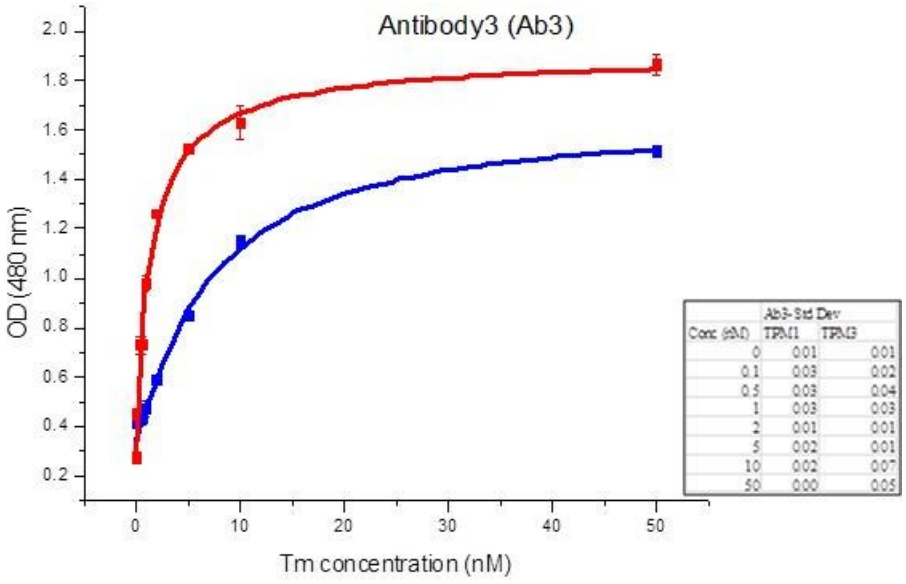

Figure 3.22: Elisa affinity curve of Ab3 with Tpm1 and Tpm3. The assay was developed to measure the specificity of monoclonal antibody affinity to Tpm3.12st by varying concentration of protein (0.1nM to 50nM) with constant concentration of antibody at 1/16000 dilution. The curves were generated using 4 parameter logistic nonlinear regression model as explained in the section 3.4.6. The intensity (OD) measured at 450 nm taken on Y-axis against the concentration of the protein on X-axis. The data is the mean of triplicate reactions. Blue - Tpm1 and Red - Tpm3. The table shows the standard deviation of the triplicate reactions.

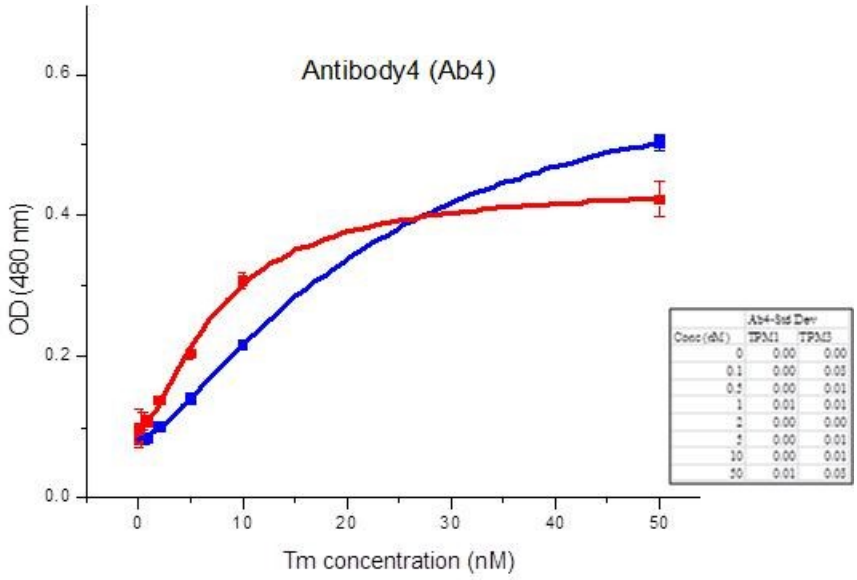

Figure 3.23: Elisa affinity curve of Ab4 with Tpm1 and Tpm3. The assay was developed to measure the specificity of monoclonal antibody affinity to Tpm3.12st by varying concentration of protein (0.1nM to 50nM) with constant concentration of antibody at 1/16000 dilution. The curves were generated using 4 parameter logistic nonlinear regression model as explained in the section 3.4.6. The intensity (OD) measured at 450 nm taken on Y-axis against the concentration of the protein on X-axis. The data is the mean of triplicate reactions. Blue - Tpm1 and Red - Tpm3. The table shows the standard deviation of the triplicate reactions.

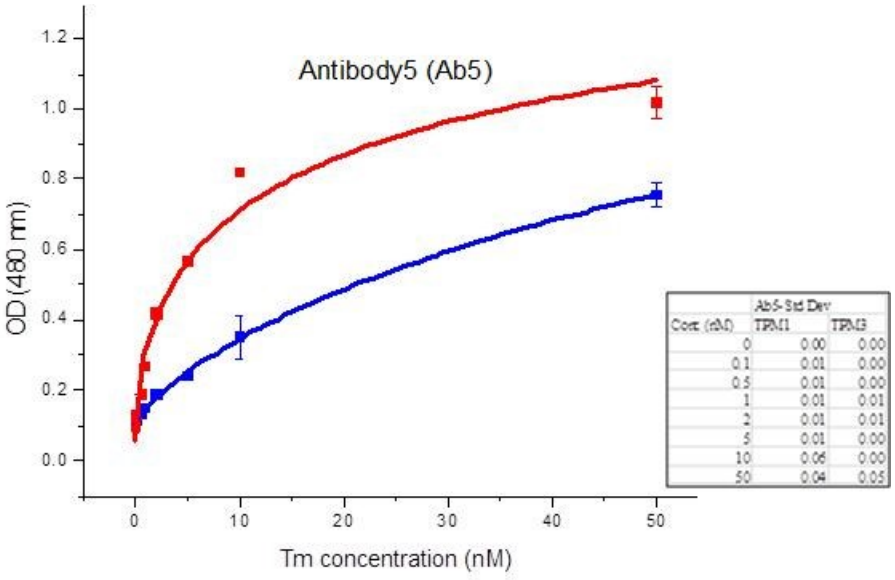

Figure 3.24: Elisa affinity curve of Ab5 with Tpm1 and Tpm3. The assay was developed to measure the specificity of monoclonal antibody affinity to Tpm3.12st by varying concentration of protein (0.1nM to 50nM) with constant concentration of antibody at 1/16000 dilution. The curves were generated using 4 parameter logistic nonlinear regression model as explained in the section 3.4.6. The intensity (OD) measured at 450 nm taken on Y-axis against the concentration of the protein on X-axis. The data is the mean of triplicate reactions. Blue - Tpm1 and Red - Tpm3. The table shows the standard deviation of the triplicate reactions.

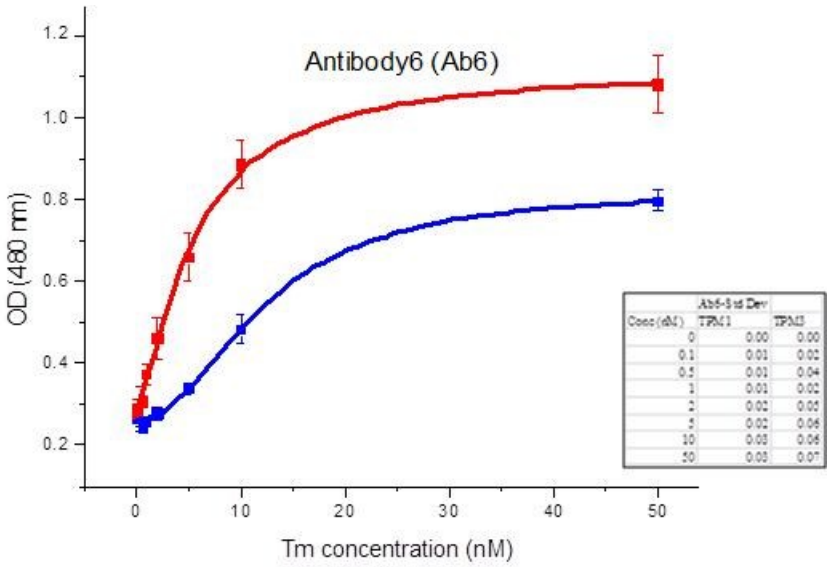

Figure 3.25: Elisa affinity curve of Ab6 with Tpm1 and Tpm3. The assay was developed to measure the specificity of monoclonal antibody affinity to Tpm3.12st by varying concentration of protein (0.1nM to 50nM) with constant concentration of antibody at 1/16000 dilution. The curves were generated using 4 parameter logistic nonlinear regression model as explained in the section 3.4.6. The intensity (OD) measured at 450 nm taken on Y-axis against the concentration of the protein on X-axis. The data is the mean of triplicate reactions. Blue - Tpm1 and Red - Tpm3. The table shows the standard deviation of the triplicate reactions.

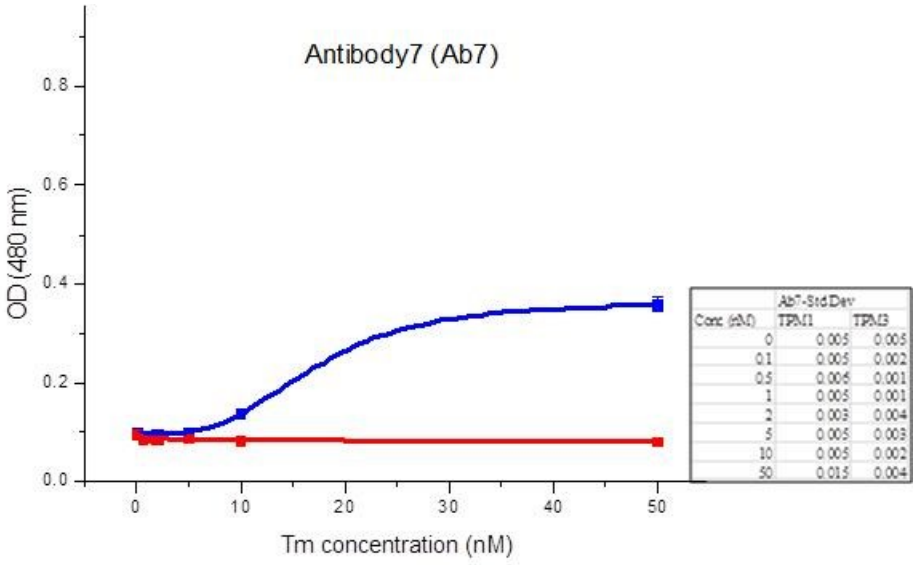

Figure 3.26: Elisa affinity curve of Ab7 with Tpm1 and Tpm3. The assay was developed to measure the specificity of monoclonal antibody affinity to Tpm3.12st by varying concentration of protein (0.1nM to 50nM) with constant concentration of antibody at 1/16000 dilution. The curves were generated using 4 parameter logistic nonlinear regression model as explained in the section 3.4.6. The intensity (OD) measured at 450 nm taken on Y-axis against the concentration of the protein on X-axis. The data is the mean of triplicate reactions. Blue - Tpm1 and Red - Tpm3. The table shows the standard deviation of the triplicate reactions.

Table 3.4: values obtained from fitting ELISA data to 4 parameter logistic model.

	Tpm1				Tpm3			
	A1	A2	X0	P	A1	A2	X0	P
Ab1	0.433	2.231	13.975	0.662	0.400	1.491	7.064	0.925
Ab2	0.404	1.874	6.124	1.133	0.399	1.851	4.084	1.003
Ab3	0.344	1.654	7.105	1.120	0.277	1.918	1.382	0.865
Ab4	0.081	0.636	22.222	1.425	0.094	0.443	7.769	1.510
Ab5	0.105	2.120	128.328	0.782	0.058	1.741	22.848	0.550
Ab6	0.260	0.827	12.332	2.046	0.282	1.125	5.433	1.355
Ab7	0.096	0.366	16.994	3.211	0.096	0.069	21.687	0.337

Note: A_1 – initial value, A_2 – final value, x_0 – slope, p – slope factor. Ab – antibody.

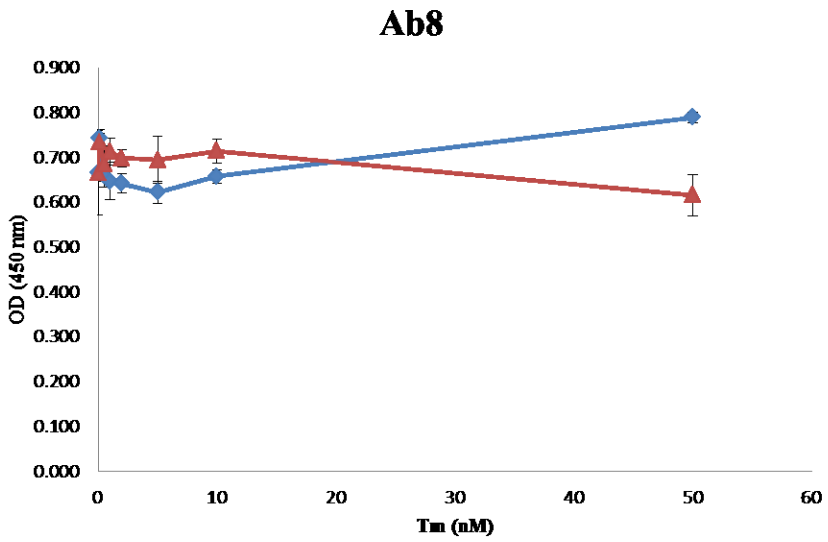

	Ab8-Std Dev	
Conc (nM)	TPM1	TPM3
0	0.09	0.09
0.1	0.01	0.03
0.5	0.03	0.04
1	0.04	0.03
2	0.02	0.02
5	0.02	0.05
10	0.02	0.03
50	0.01	0.05

Figure 3.27: Elisa affinity curve of Ab8 with Tpm1 and Tpm3. The assay was developed to measure the specificity of monoclonal antibody affinity to Tpm3.12st by varying concentration of protein (0.1nM to 50nM) with constant concentration of antibody at 1/16000 dilution. The curves were generated using 4 parameter logistic nonlinear regression model as explained in the section 3.4.6. The intensity (OD) measured at 450 nm taken on Y-axis against the concentration of the protein on X-axis. The data is the mean of triplicate reactions. Blue - Tpm1 and Red - Tpm3. The table shows the standard deviation of the triplicate reactions.

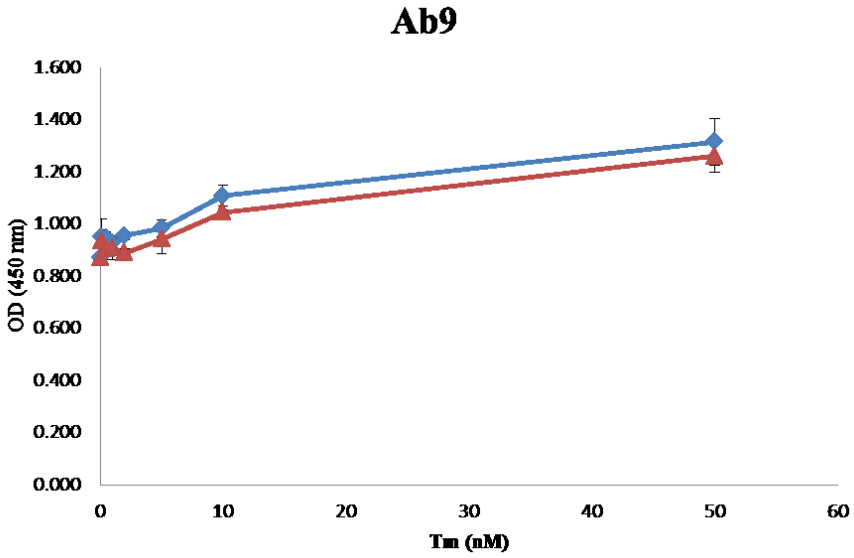

	Ab9-Std Dev	
Conc (nM)	TPM1	TPM3
0	0.01	0.01
0.1	0.07	0.04
0.5	0.02	0.02
1	0.02	0.05
2	0.02	0.02
5	0.03	0.06
10	0.04	0.01
50	0.09	0.06

Figure 3.28: Elisa affinity curve of Ab9 with Tpm1 and Tpm3. The assay was developed to measure the specificity of monoclonal antibody affinity to Tpm3.12st by

varying concentration of protein (0.1nM to 50nM) with constant concentration of antibody at 1/16000 dilution. The curves were generated using 4 parameter logistic nonlinear regression model as explained in the section 3.4.6. The intensity (OD) measured at 450 nm taken on Y-axis against the concentration of the protein on X-axis. The data is the mean of triplicate reactions. Blue - Tpm1 and Red - Tpm3. The table shows the standard deviation of the triplicate reactions.

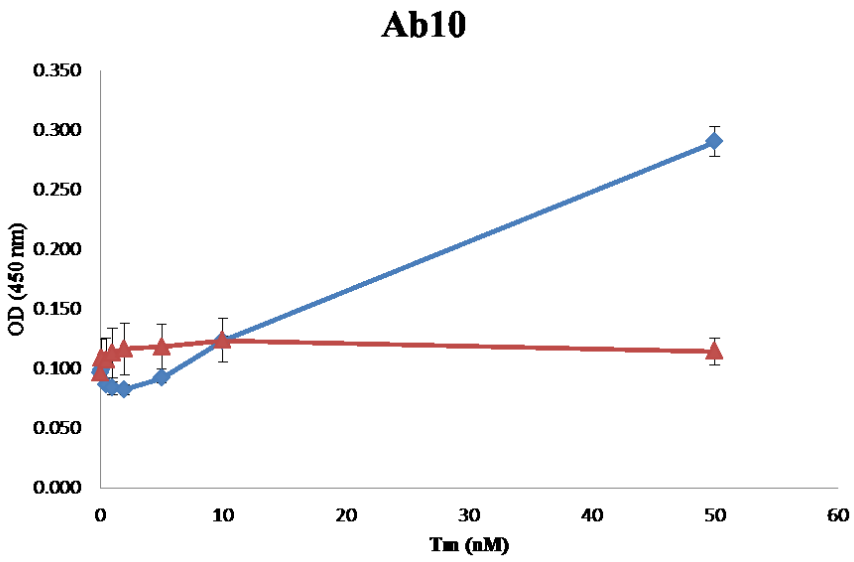

	Ab10-Std Dev	
Conc (nM)	TPM1	TPM3
0	0.006	0.006
0.1	0.003	0.016
0.5	0.002	0.018
1	0.006	0.021
2	0.004	0.022
5	0.004	0.019
10	0.004	0.018
50	0.013	0.011

Figure 3.29: Elisa affinity curve of Ab10 with Tpm1 and Tpm3. The assay was developed to measure the specificity of monoclonal antibody affinity to Tpm3.12st by varying concentration of protein (0.1nM to 50nM) with constant concentration of antibody at 1/16000 dilution. The curves were generated using 4 parameter logistic nonlinear regression model as explained in the section 3.4.6. The intensity (OD) measured at 450 nm taken on Y-axis against the concentration of the protein on X-axis. The data is the mean of triplicate reactions. Blue - Tpm1 and Red - Tpm3. The table shows the standard deviation of the triplicate reactions.

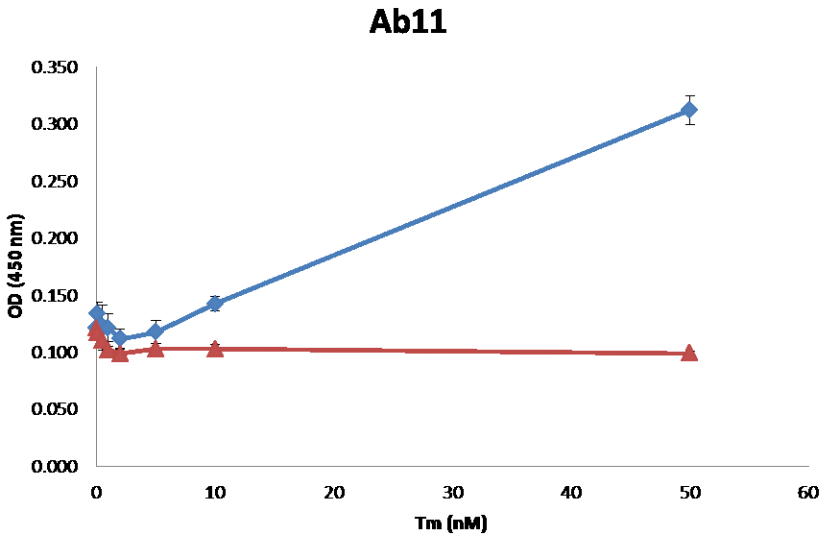

	Ab11-Std Dev	
Conc (nM)	TPM1	TPM3
0	0.001	0.001
0.1	0.010	0.005
0.5	0.019	0.008
1	0.012	0.004
2	0.009	0.004
5	0.010	0.005
10	0.007	0.004
50	0.013	0.002

Figure 3.30: Elisa affinity curve of Ab11 with Tpm1 and Tpm3. The assay was developed to measure the specificity of monoclonal antibody affinity to Tpm3.12st by varying concentration of protein (0.1nM to 50nM) with constant concentration of antibody at 1/16000 dilution. The curves were generated using 4 parameter logistic nonlinear regression model as explained in the section 3.4.6. The intensity (OD) measured at 450 nm taken on Y-axis against the concentration of the protein on X-axis. The data is the mean of triplicate reactions. Blue - Tpm1 and Red - Tpm3. The table shows the standard deviation of the triplicate reactions.

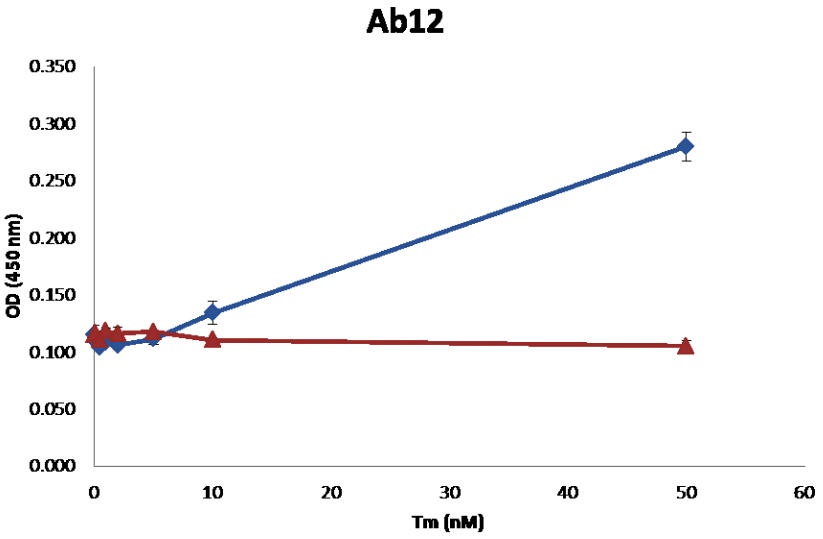

	Ab12-Std Dev	
Conc (nM)	TPM1	TPM3
0	0.008	0.008
0.1	0.003	0.002
0.5	0.001	0.001
1	0.001	0.003
2	0.003	0.006
5	0.005	0.000
10	0.010	0.002
50	0.013	0.005

Figure 3.31: Elisa affinity curve of Ab11 with Tpm1 and Tpm3. The assay was developed to measure the specificity of monoclonal antibody affinity to Tpm3.12st by varying concentration of protein (0.1nM to 50nM) with constant concentration of antibody at 1/16000 dilution. The curves were generated using 4 parameter logistic

nonlinear regression model as explained in the section 3.4.6. The intensity (OD) measured at 450 nm taken on Y-axis against the concentration of the protein on X-axis. The data is the mean of triplicate reactions. Blue - Tpm1 and Red - Tpm3. The table shows the standard deviation of the triplicate reactions.

Figure 3.20Figure 3.31 shows the plots of ELISA for individual antibodies and the table on the side of the plots gives the standard deviation of the results obtained for triplicate reactions. Ab8 to Ab12 (Figure 3.28 toFigure 3.31) did not have any reaction at lower concentration and were saturated at higher concentrations and does not show any sigmoidicity to use them in the 4PL model. Hence these antibodies were not shown with the 4PL model as they would not give any meaningful curves. Table 3.5 shows the overall results data obtained from western blotting and ELISA results and the reactivity of all the antibodies grouped according to the peptides they react with the relative ratio of sensitivity of Ab1 to Ab6 with Tpm1 and Tpm3. From the table it is observed that Ab3 (VIIEGDLERT – P4) and Ab5 (DELYAQKLKY-P5) shows higher sensitivity to Tpm3 than Tpm1 at the same concentration of protein. Ab1 has higher affinity to Tpm1 and Ab2, 4 and 6 does not show much difference in sensitivity between the two proteins. Table 3.4 gives the values obtained from the 4PL model where the sensitivity of the Abs could be seen from x_0 values.

Table 3.5: Table showing the peptides numbers where the antibody is binding, the experimental results and the relative ratio of the sensitivity of Ab to the specific peptide. Ratio was calculated from the slopes of Tpm1 and Tpm3. Ratios of Abs 7-12 was not calculated as there was no linearity exhibited from the reaction of these Abs with the Tm isoforms. P1, P2, P3, P4 and P5 are the peptide number reacting with the antibodies which are grouped together with similar colour.

Peptide Sequence/No.	Antibody number	Residue position	Experimental results western blot	Sensitivity Ratio ELISA	Isoform with high sensitivity ELISA
EQAEAEQKQA P1	5	24-33	Tpm1 --- Tpm3 Tpm4	2.91	Tpm3
EERSKQLEDE P2	7 (8,10,11,12)	34-43	--- --- --- ---	-	-
EERSKQLEDE P2	8	34-43	Tpm1 --- Tpm3 Tpm4	-	-
EERSKQLEDE P2	10	34-43	Tpm1 --- Tpm3 Tpm4	-	-
EERSKQLEDE P2	11	34-43	Tpm1 --- Tpm3 Tpm4	-	-
EERSKQLEDE P2	12	34-43	Tpm1 --- Tpm3 Tpm4	-	-
EAEKAADESE P3	4	116-125	Tpm1 Tpm2 Tpm3 Tpm4	0.40	Tpm3
VIIEGDLERT P4	3	171-180	Tpm1 --- Tpm3 Tpm4	5.81	Tpm3
DELYAQKLKY P5	1 (2,6,9)	259-268	Tpm1 --- Tpm3 Tpm4	0.83	Tpm1
DELYAQKLKY P5	2	259-268	Tpm1 --- Tpm3 Tpm4	1.21	Tpm3
DELYAQKLKY P5	6	259-268	Tpm1 --- Tpm3 Tpm4	0.36	Tpm3
DELYAQKLKY P5	9	259-268	Tpm1 Tpm2 Tpm3 Tpm4	-	-

3.6 Discussion

Tropomyosin isoform pattern in humans are extensively studied in recent years (Gunning et al., 2005; Hook et al., 2004; Marston et al., 2013; Maytum et al., 2011; Peng et al., 2013). For these studies many isoform specific antibodies have been generated to identify the diverse isoforms expressed by tropomyosin family (Schevzov et al., 2011). From the research so far, it is well extablished that human tropomyosin isoforms are highly conserved and have high sequence similarity having few residue variations at the N-terminal and C-terminal ends of the sequence (Gunning et al., 2008b).

The use of different promoters differentiates the N-termini of the isoforms. Exon 1a along with 2a or 2b gives to high molecular weight Tms and the alternative 1b exon at the N-termini gives low molecular weight Tms. At the same time the sequence selectivity of the exons at the C-terminal between 9a, 9b, 9c and 9d gives sequence divergence at the C-termini. The sequence similarity of the exons of different genes is found to be higher than the sequence similarity of alternative exons of the same gene (Lees-Miller and Helfman, 1991).

There are many antibodies available that are characterised for specific Tm isoform. Few are monoclonal and few are polyclonal antibodies that identify specific Tm isoform (Schevzov et al., 2011). Only one antibody is available for Tpm3 protein isoforms, which identifies all the protein isoforms that are generated by Tpm3 gene. Lin et al., (1985) produced monoclonal antibodies for chicken Tm isoforms. According to Lin et al., CG1 reacts with all the skeletal muscle isoforms Tpm1 and Tpm3 and CG3 reacts to all the isoforms of Tm. However recent studies show that CG1 reacts with all the Tm isoforms and the results from this study also show that it reacts to all Tpm1, Tpm2, Tpm3 and

Tpm4 (Tpm4 needs more confirmatory tests to assign as Tpm4 in this study) similar to the previous studies (Hook et al., 2011; Marston et al., 2013b; Schevzov et al., 2011). From western blotting analysis the CG3 antibody showed reaction with HMW Tpm3 and Tpm4. If the CG3 antibody epitope is designed for 1b exon of Tpm3 gene (Schevzov et al., 2005) which is responsible for encoding LMW Tms, and it is not supposed to react with HMW Tpm3. May be there is cross reactivity of the antibody or there must be some discrepancy regarding the epitope sequence of CG3. However according to Lin et al., (1985) who originally produced CG3 antibody mentioned that CG3 has cross reactivity with Tpm1 but has strong reactivity with Tpm3.

In this study the Tm isoform produced are all HMW isoforms with the exon sequence 1a,2b, 3, 4, 5, 6b, 7, 8, 9a (Figure 3.7). It can be clearly seen that Tpm4 has higher C-terminal sequence variance compared to other three isoforms. Tpm1, Tpm2 make up the skeletal muscle and Tpm3 is found in slow twitch skeletal muscle (also referred to as α_sTm) and Tpm4 is found in smooth muscles. As mentioned before in this chapter (section 3.2), the isoform variance of C-terminal may be due to the functional differences of smooth muscle from skeletal muscle (Gunning et al., 2008b; Lees-Miller and Helfman, 1991).

The 12 monoclonal antibodies designed were depended solely on HMW Tpm3. The preliminary checker board assay was used to establish the Ab sensitivity and protein concentration to be used for further quantification analysis. The data obtained from standard curves (Figure 3.14, Figure 3.15 Figure 3.16) Ab dilution of 1/8 and 1/ 16 showed lower back ground noise. This was compared with presence of both isoforms of protein Tpm1 and Tpm3 where the background noise was lower at 1/8 and 1/16 dilution

of Ab and also it reaches saturation limit of intensity. Hence for further assays 1/8 dilution of Ab was chosen for quantification analysis.

The experimental results of western blotting coincide with the quantification of ELISA in respect to the sensitivity of various peptides. Dot blot results were not comparable with the western blotting and ELISA results. The sensitivity of the antibodies was different for each peptide even though the epitope of sequence is similar to the same peptides. The Ab1, Ab2, Ab6 and Ab9 have affinity for same peptide (P5-DELYAQKLKY) located at the C-terminal of the sequence on Exon 9, however the reaction of each antibody to the same peptide is different. Ab1 showed higher sensitivity to Tpm1 than Tpm3 (with a slope value of x_0 13.975 for Tpm1 and 7.064 for Tpm3 from Table 3.4) even tought the sensitivity is higher the Tpm3 reaches saturation faster as seen by the values and the curves. On the other hand Ab2, Ab6 had higher sensitivity to Tpm3 than Tpm1 and Ab9 reacted to all Tm four isoforms Tpm1, Tpm2, Tpm3 and Tpm4 along with Ab4 which recognizes peptide 3 (P3-EAEKAADESE) located on exon 3. The Ab7 (P2-EERSKQLEDE) peptide 2, located in between exons 1 and 2 did not react to any of the isoforms from both western blotting data and ELISA data (Table 3.4 and Figure 3.26). From western blotting data Ab8, Ab10, Ab11 and Ab12 had very low reactivity to Tpm1, Tpm3 and from ELISA results the sensitivity of these antibodies was visible only at higher concentrations of protein with no reaction at lower concentrations. Hence the 4PL model was not applied to antibodies Ab8 – Ab12 as they do not agree with the sigmoidicity of the curves and no meaningful curves and values would be obtained to validate them. The only antibody that had substantial differentiation of sensitivity from Tpm1 was Ab3 (P4) which was five times higher than Tpm1. Even though Ab5 was

expected to bind only to Tpm3 due to the presence of more variable residues in the epitope (peptide 1 –P1) experimental results did not give the same predicted outcome. Unfortunately none of the antibodies could be used to identify specific HMW Tpm3 but Ab4 and Ab9 could be used for identifying all the Tm isoforms.

In general 5 out of 10-15 of each epitope influence strong binding and substitution at these binding sites contribute to reducing the binding constant to two-three folds. The binding of the antibody to the epitope also depends on the availability of the binding sites due to the structural arrangement of the protein (Dougan et al., 1998; Frank, 2002). Sometimes the antigen raised against a particular epitope may have higher binding capacity to the relevant epitope due to the antibody valence (number of interacting binding sites) to the target epitope (Regenmortel, 1998). Due to the few mentioned reasons, the antibodies raised against Tpm3 sequence and the high sequence similarity with the other Tm isoforms, different antibodies show variable sensitivities to Tpm3 and Tpm1.

From the data obtained from western blotting, low molecular weight bands between 20 kDa and 15 kDa were visible on the assay developed gels. Denaturation of the protein may be due to the heat when the protein was denatured with heat at 95 ^{0}C before running on SDS-PAGE. According to Pato et al., (1981) N-terminal of 1-13 base pairs and central region of 123-183 base pairs are susceptible to proteolytic denaturation. Antibodies that are used in this study are specific to certain peptide in the sequence. It is expected that the protein bands with different antibodies show different bands, but all the antibodies reacted with same denatured protein bands which indicated that the residues in those denatured bands must be having higher similarity with the antibody peptides.

In conclusion, due to the very high sequence similarity of tropomyosin isoforms, it is a challenging task to design an antibody that reacts with only one isoform of tropomyosin. CG3 which was confirmed by many studies to be specific to only Tpm3 does not seem to be accurate as it has shown some cross reactivity with Tpm4 as well. It was also confirmed by Lin et al (1985) that CG3 has high cross reactivity with other isoforms of tropomyosin. Form this study it is observed that designing an antibody by combining the sequence of peptides P1 and P2 (aa 24 -43) locating on Exon 1a and 2b may have an advantage of producing an antibody specific to Tpm3.12st.

Chapter IV: Method Development for Quantification of Thin Filament Protein Isoforms from Tissue Lysates

4 Introduction

Analytical techniques in biomedical research form a holistic approach in understanding human diseases to the protein level have the potential to identify novel therapeutic targets and biomarkers which act as prognostic indicators. Heart disease is one of the most common disorders of muscle. It is one of the most common causes of death in the United Kingdom, most of which are caused due to disorders in muscle. According to the British Heart foundation, nearly 41% of total deaths in the UK are due to heart failure (Lloyd-Jones et al., 2010) and nearly 1 in 9 deaths reported were because of heart failure in 2010 (Go et al., 2014). Other disease like nemaline myopathy, Congenital myopathy with fibre type disproportion (CFTD) (Nance et al., 2012), Alzheimer's disease (Reitz et al., 2011) and cancer tumours relating to cytoskeleton (Stehn et al., 2013) are related to muscle disorders caused due to genetic mutations and alternative splicing. Comprehensive analysis of the proteoforms (a unified term designated to define all the entities present in the proteome such as protein degradation products, RNA splice variants, isoforms and PTMs of a gene product) is necessary to identify, understand, diagnose and treatment of these disease.

A proteome is the cell and time specific protein compliment of a genome (Wilkins et al., 1996). Genome is largely a fixed entity and identical for all the cells in a single organism and is consistent among species, the proteome is constantly variable and extremely complex as it is continuously affected by external and internal factors of the cell such as temperature, nutrition, drugs and chemicals , signaling networks to name a few (Pandey and Mann, 2000). Decoding the proteome of a system is essential to understand the cellular and molecular interactions in relation to their functions in health and disease. However due to the dynamic nature of proteome with large plethora of complex post translational modifications, isoform expressions and sequence variants analysis of proteome of a system is very challenging (Neverova and Van Eyk, 2005).

Human gene consists of nearly 30,000 genes and the number of proteins expressed is 100 times greater due to the mRNA processing and post translational modification of proteins (O'Donovan et al., 2001). Due to the high complexity of proteome and the number of proteins expressed a single technique is not sufficient to analyse all the proteins present. A combination of techniques for separation and identification are required. Liquid chromatography and mass spectrometry are the most predominant techniques used for analysis of proteins and PTMs (Patterson and Aebersold, 2003).

Importance of proteomics analysis for studying thin filament proteome

Myofilament proteome analysis is found to be difficult in many studies with current methods using 2D gel electrophoresis with tandem mass spectroscopy or peptide mass fingering printing (PMF) to analyse complex protein mixtures in the proteome.

Separation of all the proteins is hampered by very wide range of pI of proteins and their varying molecular weights. The staining methods available are not suitable for all proteins and their associated protein abundance reflect the efficiency of the technique (Arrell et al., 2001b; Labugger et al., 2002). These techniques involving 2D gel is laborious and time consuming as not only do 2D gels typically require an overnight run, any data obtained usually require further processing such as isolating the protein spot and incomplete recovery of peptides after trypsin digestion result in loss of information obtained for the proteins of interest regarding the position of PTMs and sequence variations arising due to point mutations (Zhang and Ge, 2011b). However, several studies have shown myofilament proteome changes using these classic techniques (Erban, 2011; Scruggs et al., 2010).

Mass spectrometry by 'top down' proteome analysis is one of the emerging techniques which provides a 'birds eye' view of all the proteoforms. The top down method involves analysis of intact proteins. This method has an advantage of preventing any loss of information caused from sample preparation and handling process (Zhang and Ge, 2011) Some progress in this area has already been made with Ge et al., (2009b) used top-down high resolution mass spectrometry analysis to characterize cardiac myosin binding protein-c phosphorylation sites and tropomyosin isoforms (Peng et al., 2013) individually. The phosphorylation sites of rat cardiac troponin have been reported by Solis et al., (2008) by top-down MS using electron capture dissociation ionisation.

A variety of mutations occurring in thin filament have been reported that causes different types of cardiomyopathy. There is a lot of literature available in case of Troponins and especially TnI (Ge et al., 2009b; Seidman and Seidman, 2011; Tardiff, 2011b). Alpha Tm is found to cause FHC due to altered contractile function with Asp175Asn mutation and is reported to lead to severe dilated cardiomyopathy (DCM) (Prabhakar et al., 2001; Regitz-Zagrosek et al., 2000; Thierfelder et al., 1994). Protein kinase C (PKC) phosphorylation of both TnI and Tm (Sarko and Pollack, 2002; Vahebi et al., 2007) are considered important PTMs in the thin filament. Degradation products of TnI (Wu et al., 1998) are used as a biomarker for HCM, as they are released in the bloodstream following a myocardial damage. Table 4.1 gives the list of few PTMs occurring in sarcomere proteins with the mass in Daltons that is shown in mass spectrometry analysis.

Table 4.1: Few of the major post-translational modifications occurring in sarcomeric proteins and their functions.

PTM	Δ mass * (Da)	Process	Functions
Acetylation	+42	Introduction of acetyl functional group by acetyltransferases at N-treminal position of the protein sequence catalyzed by methionine aminopeptidase (MetAP)	Protein stability, protein regulation, prevent protein degradation at N-terminus (Gunning et al., 2008a).
Phosphorylation	+80 (Ser, Thr, Tyr)	Protein kinases play an important role in phosphorylation of proteins. Oxidative phosphorylation uses ATP to phosphorylate certain amino acids in the protein sequence.	Activation or inactivation of proteins and their regulation, molecular interactions and signalling. eg., PKC –Serine residues in TnI (Sarko and Pollack, 2002), Tm (Vahebi et al., 2007) PKA, PKC, Cam II – MyBP-C (Lim et al., 1985; Stelzer et al., 2007), MLCK - Myosin RLC (Yuan and Solaro, 2008)
Degradation	>1000	Ubiquitin/proteosome system (UPS) Ca^{2+} dependant or calpain-mediated protein degradation.	Degradation of TnI is vastly studied for cardiac disfunction, as it even considered to be biomarker for Hypertrophic cardiac myopathy (Wu et al., 1998)
Oxidation Nitrosylation	-27 (Arg) +15 (lys) +16(Met)	Reactive-oxygen species (ROS) and Reactive – Nitrogen species (RNS) play major role in cellular processes.	Protein regulation and signalling There is profound evidence showing excess production of ROS and RNS in acute and chronic heart failure conditions in animals and humans (Prasan et al., 2007; Seddon et al., 2007).

	+45 (NO_2)		

*The mass data is obtained from http://www.abrf.org/index.cfm/dm.home.
PKC-Protein kinase C, PKA -Protein kinase A, MyBP-C – Myosin binding protein C, MLCK – myosin light chain kinase, RLC- regulatory light chain.

The ‘top down’ proteomics approach presents the next level in understanding muscle diseases related to heart, skeletal muscle diseases, cancers and other neurodegenerative diseases and cardiac adaptations, where the physiological changes and genetic mutations are responsible for cardiac adaptations can be explained in terms of the changes occurring in sarcomere at the protein level. The post-translational modifications (PTMs) of sarcomere proteins affect the structure and function of proteins resulting in shifts in isoform populations, forming degradation products, addition or deletion of protein availability, altered protein expression, availability of Ca^{2+} ions and ATPase activity (Tardiff, 2011b; Zhang and Ge, 2011b). These changes are being identified using advanced techniques of mass spectrometry for protein isoform identification, PTMs and protein interactions (Arab et al., 2006b; Arrell et al., 2001b; Peng et al., 2010; White and Eyk, 2007).

Challenges in ‘top down’ MS approach

For top down mass spectrometry one of the main challenge is the protein solubility. For the ‘bottom up’ analysis proteins are digested by an enzyme where protein solubility does not pose any issue. However in top down approach, where intact protein is used for analysis having a soluble protein is the major factor as MS needs the proteins to be ionised (Gregorich and Ge, 2014) The reagents used for solubilising proteins like SDS and Triton X are not compatible for MS analysis.

Another major is the size of the protein affect the signal to noise ratio in MS analysis. Top down method allows protein analysis of the size no larger than 70 kDa (approximately of the m/z ratio < 4000 not more than 35 charge states). Proteins larger

than that are associated with difficulty in detection and fragmentation in MS (Compton et al., 2011).

Protein separation/fractionation is one the crucial step for mass spectrometry analysis. The proteome of thin filament is highly dynamic and due it complexity protein separation effective separation techniques are required for top-down MS. The most popular method for fractionation of intact proteins is reverse phase liquid chromatography (RPLC) which separates proteins based on their hydrophobicity. This method one of the most compatible techniques available due to the use of organic solvents acetonitrile and formic acid or trifluoroacetic acid (TFA) (Neverova and Eyk, 2002). Many advanced LC methods such as 2D LC or 4D LC are developed recently coupled with RPLC for proteome analysis. 2D LC is separation of protein by their pI and then coupled online or offline with RPLC and 4D is separation of protein by their pI in the first step followed by gel-eluted liquid entrapment electrophoresis, which separates proteins depending on their size and coupled with RPLC and MS for direct analysis (Neverova and Van Eyk, 2005). C5 or C8 columns are used for top-down MS are suitable for separation of proteins (Wagner et al., 2002). The most commonly used MS analysis is RPLC connected to ESI-MS/MS for intact protein analysis which maintains the gentle ionisation technique keeping the peptide bonds intact for MS analysis (Cole, 2000) There are many other techniques in LC coupled with MS which is beyond to discuss in this study (Gregorich and Ge, 2014; Gregorich et al., 2014).

Quantification and data analysis is also one of the major challenge to over come in top down MS. Changes in the protein expression using protein abundance of m/z value is not sufficient for quantifying proteins. Measuring the abundance by MS and consequently the

abundance of peptides generated by MS/MS is used for quantifying the protein modification and their expression levels (Bantscheff et al., 2012; Ong and Mann, 2005; Peng et al., 2010; Peng et al., 2013; Pesavento et al., 2006).

Major Sarcomeric Proteins

The sarcomere consists of alternating thick and thin filaments that form the major contractile apparatus in the muscle. The proteins in the thick filament constitute myosin heavy and light chains which interact with the thin filament protein actin regulated by tropomyosin and troponins. Table 4.2 gives an overview of major sarcomeric proteins that are responsible in regulating the normal functioning of the heart showing the difference in molecular weight of actin, tropomyosin and troponin complex protein in humans, rabbit, chicken and mouse.

The hypothesis on which this project is based is that the heart adapts in response to disease and physiological changes. A significant part of that adaptation is changes in the muscle protein isoforms expressed and the post translational modification of them. Quantification of the isoforms expressed and their PTMs will therefore give insight into heart adaptation and potentially act as a prognostic indicator.

In order to understand the changes taking place in sarcomere it is important to understand the role of sarcomeric proteins that regulate the cardiac function. There are studies defining individual protein phosphorylation of sarcomere, but currently there is no quantitative data available for protein levels and their post translational modification covering a range of thin filament proteins (actin, tropomyosin and troponin) in diseased and normal states of thin filament proteins.

This study is an attempt to establish a method to extract the muscle regulatory proteins from chicken and mouse skeletal muscle and chicken heart left ventricle muscle and mouse heart. The study provides optimisation of buffers used for thin filament proteins, storage limit of tissue lysates and preliminary optimisation method of reverse phase (RP) HPLC technique for isolation of these proteins which is suitable for top down mass spectrometry technique that will provide a “birds eye view” of thin filament proteome providing information of PTMs of all the proteins together with one single extraction, reducing the time for analysis and sample size.

Table 4.2: Major Sarcomeric proteins and their molecular weight.

Protein	Human	Chicken	Rabbit	Mouse	Function
Myosin Heavy Chain (MHC) (Da)	220 000				Both MHC and MLC binds to actin binding sites thorough the myosin heads to initiate motor muscle contraction and relaxation
Myosin Light Chain (MHC) (Da)	20 000				
α Actin	42051				Back bone of the thin filament and plays a major role in contraction-relaxation along with Tm and Tn complex to form actin binding complex that regulate muscle functioning.
αTropomyosin (Tpm1.1) (Da)	32708.5 (Lees-Miller and Helfman, 1991)	32960 (Gooding et al., 1987)	32680.5 (Stone and Smillie, 1978)	32680.5 (Gariboldi et al., 1995)	Binds to actin and regulate the interaction of actin-myosin filaments during contraction-relaxation process.
βTropomyosin (Tpm2.2) (Da)	32850.5 (Libri et al., 1990)	28671 (Helfman et al., 1983)	32836.7 (Stone and Smillie, 1978)	32957.7 (Strausberg et al., 2002)	
Troponin T (TnT) (Da)	28152 (Wu et al., 1994)	31141(Sk) (Pearlstone and Smillie, 1982) 35985.7 (C) (Druyan et al., 2007)	27809.7 (alpha) 29683.3 (beta) (Pan and Potter, 1992)	32299.9 (Sk) (Koch et al., 1997) 35498 (C) (Kobayashi et al., 2013)	Links the Tn complex and binds to tropomyosin.
Troponin I (TnI)	24007.1	21234.4 (Sk)	21,214 (Sk)	21357.5 (Sk)	Binds to actin and inhibits actomyosin

(Da)	(Hijazi et al., 2014)	(Blumenschein et al., 2006) 23628.0 (C) (Hastings et al., 1991)	(Vassylyev et al., 1998) 24122.6 (C) (Grand and Wilkinson, 1977)	(Koppe et al., 1989) 24258.7 (C) (Ausoni et al., 1994)	ATPase depending on the Ca^{2+} sensitivity.
Troponin I (TnC) (Da)	18387 (Zhang et al., 2013)	18430.5 (Dvoretsky et al., 2002)	18402.5 (Predicted NCBI)	18420.5 (Grote et al., 2013)	Ca^{2+} binding site

4.1 Material and Methods

4.1.1 Extraction of myofilament proteins

Thin filament proteins were extracted from chicken pectoral muscle and left ventricle of the heart and wild type mouse thigh muscle and whole heart. Chicken heart and muscle were obtained from freshly killed chicken that was between 16 weeks old and stored at -20^{0}C. Mouse heart and thigh muscle were obtained from 12 weeks old wild type mouse. The tissues and heart were kept on ice immediately after dissection and stored at -80 ^{0}C after couple of hours until use. Approximately 100mg of tissue was taken and homogenised with a motor and pestle and from that two sets of whole protein extracts were made with approximately 5mg and 2mg of tissue. The tissue was homogenized in 200µl of different buffers containing 1 mM of benzamidine hydrochloride (inhibitor for trypsin, thrombin, arginine specific serine proteases) and 1 mM of PMSF (trypsin, chymotrypsin, cysteine proteases and mammalian acetylcholinesterase) as protease inhibitors. Tissues were taken from frozen samples of left ventricle of chicken heart and pectoral muscle. In case of mouse samples, whole heart was homogenised and the amount required was taken from the tissue homogenate. The extraction was repeated three times for reproducibility. Table 4.3 below shows the different buffers used for extraction.

Table 4.3: Different buffer conditions used for extraction of thin filament proteins from muscle tissue. KCl – Potassium chloride, NaCl – Sodium chloride, SDS – sodium dodecyl sulphate.

Homogenization condition	Buffers
1	6M Urea
2	1M KCl
3	6M Urea + 1M KCl
4	6M Urea + 1M KCl+ 0.5% TritonX-100
5	1M NaCl
6	6M Urea + 1M NaCl+ 0.5% TritonX-100
7	6M Urea + 1M NaCl+ 0.5% TritonX-100
8	6M Urea + 1M NaCl+ 0.5% SDS

Approximately 5 mg and 2 mg of tissue simple was homogenized in 200 µl of buffer using an Eppendorf homogenizer for five minutes on ice and vortex for 5 min. Samples were centrifuged at 13000 rpm for 5 min at 4 ^{0}C. 20 µl of pre-dialysed sample extract was denatured in 20 µl 4X SDS buffer at 95 ^{0}C for 5 min and stored at 4 ^{0}C to run on the gel along with dialysed samples. The rest of the extract was subjected to micro dialysis overnight in low salt buffer containing 2 mM pH 8.8 Tris-HCl, 2 mM CaCl, and 0.2 mM Dithiothreitol (DTT) to precipitate myosin. The dialysed samples were spun at 13000 rpm for 5 min to remove any precipitate and 20 µl of sample is denatured with 4X SDS buffer. Proteins were separated on 13.5% SDS-acrylamide gel and visualised by staining with coomassie stain (0.1% Commassie blue G250, 25% Methanol and 5% Acetic acid) over night for saturation, quantified by scanning them with Biorad GS800 calibrated densitometer. Approximately 100 ng of sample was loaded on the gels. The gels were

scanned along with AFGA density strip tablet and Stouffer 21 transmission step wedge which acts as a standard for constructing a calibration curves. Protein quantification was performed using ImageJ software (Schneider et al., 2012). Total protein concentration of the tissue lysates was estimated using BCA assay.

Determining the storage time for the tissue lysates

From the results obtained from tissue extracts from 5 mg and 2 mg tissue lysates, 3 buffer conditions were chosen according to the amount of protein yield form each buffer to estimate the length of time the proteins could be stored for analysis. This experiment was performed with chicken skeletal muscle and left ventricle heart muscle tissues. For skeletal muscle tissue buffers KCl, NaCl and Urea-NaCl- SDS were chosen and for heart tissue Urea, Urea-KCl and Urea-NaCl were chosen as the amount of protein was higher in those buffers for that particular tissue. The tissue lysates were analysed using the same method as the whole tissue extracts stated about using SDS-PAGE and Image J software. Dialysed lysates were analysed on the same day of extraction, 1 day of freezing, 1 week of freezing and 4 weeks of freezing both at -20 ^{0}C and -80 ^{0}C.

Extraction of control proteins

Control proteins (CP) are the proteins that are left after actin extraction from the acetone powder. CP has high concentrations of tropomyosin and troponin complez proteins (TnT, TnI and TnC). The solid residue obtained after actin extraction (Chapter II, section 2.4.3.1) was suspended in buffer containing 10 mM Tris-HCl, 20 mM DTT and 1 mM sodium azide and stirrer at room temperature for five hours. The muscle suspension was filtered through a cheese cloth and the filtrate was stored at 4 ^{0}C overnight. To the

measured volume of the filtrate ammonium sulphate is added to 40% saturation slowly while stirring on ice. The filtrate is incubated on ice while stirring for 30 min and the precipitate was separated by spinning at 9K rpm for 30 min. The pellet is discarded and to the filtrate ammonium sulphate is added increasing the saturation to 60%. The filtrate was incubated on ice for 30 min and precipitate obtained was left in the ammonium sulphate and stored at 4 ^{0}C. For optimising the RP-HPLC CP were used as a standard for tropomyosin and troponin elution times for comparison with tissue lysates. The proteins were precipitated out form 60% ammonium sulphate solution by spinning the 200 µl of the filtrate at 9K rpm for 30 min. The palette is resuspended in 5 mM Tris with 0.5 mM DTT. The proteins were dialysed against 1 mM ammonium bromide buffer for HPLC analysis.

Reverse-phase HPLC technique

After optimising the amount of the tissue required for the proteins to analysed to be 2 mg, separate extractions were made to optimise method for separation and identification of thin filament proteins primarily actin, tropomyosin isoforms and troponin I, troponin T and troponin C. The lysates were dialysed overnight at 4 ^{0}C in 1 mM ammonium bromide ($(NH_4)Br$) buffer. The lysates were stored in an ice box at 4 ^{0}C to avoid denaturation from freeze-thaw cycles. Proteins were analysed within 2 days of extraction. Control proteins (CP) (mainly tropomyosin and troponin isoforms) extracted during the procedure of extraction of pure actin form muscle acetone powder both from rabbit and chicken muscle acetone powder were used as control to identify the protein peaks from the tissue extracts. Water CapLC was used with reverse phase SUPELCO analytical Discovery BIO wide pore C5 column (10cm x 1.0 mm, particle size 3 µM, pore size 300Å) with 40

µl/min flow rate and 25 µl of sample was injected containing approx., 200 ng of total protein. Protein elution profiles were monitored by extinction at 280 nm. Proteins were eluted by increase in hydrophobicity using far UV acetonitrile with 0.1% formic acid as buffer B and Milli Q ultrapure water with 0.1% formic as buffer A.

To optimise the method first a gradient from 1% B to 60% was developed to for elution profiles. After finding the prominent proteins were primarily eluting form 20% - 40% B, gradient was changed from 20% to 50% B for collection of fraction and analysing the fractions on the SDS-PAGE gel. The gradient method used is given in the Table 4.4 with a flow rate of 40 µl/min.

Table 4.4: Gradient method for separation of thin filament proteins.

Time (min)	B%
0.0	1.0
5.0	1.0
5.01	20
45.0	50
45.01	100
50.0	100.0
50.01	1.0
60.0	1.0

CP samples from chicken and rabbit were run 3 times to check the reproducibility of the column. As the protein extraction did not vary much with different buffers, single buffer extraction was selected for each skeletal and heart tissues. Proteins extracted from KCl for skeletal muscle and Urea-KCl for heart tissue were chosen for analysis of both mouse

and chicken lysates to maintain comparison. The reverse phase fraction for each prominent peak were collected, approximately 50-100 µl. Collected fractions were concentrated using SpeedVac (Savant Speec vac concentrator) until completely dry, 10 µl of 2x Lamellae buffer was added and heated at 95 ^{0}C for 5 min and analysed using 7 cm, 13.5% SDS-PAGE gels, stained by coomassie blue (G250 coomassie brilliant blue), de-stained with 25% methanol and 7% acetic acid and the gels equilibrated in water before scanning with Biorad GS800 calibrated densitometer. The gels were analysed using imageJ software.

4.2 Results

4.2.1 Myofilament Protein Extraction

4.2.1.1 Skeletal Muscle Tissue

To optimise the method for extraction of myofilaments proteins from skeletal and cardiac muscles eight different homogenization conditions were used with two different sample amounts. Figure 4.1 shows the gels with all the eight buffer conditions, dialysed and undialysed protein bands extracted from both 5 mg and 2 mg tissue. Known amount of BSA was loaded on the gel as an internal standard. The relative staining intensities of the protein bands were calculated by relative to the BSA band intensity of the same gel, dividing the value with a standard BSA band intensity.

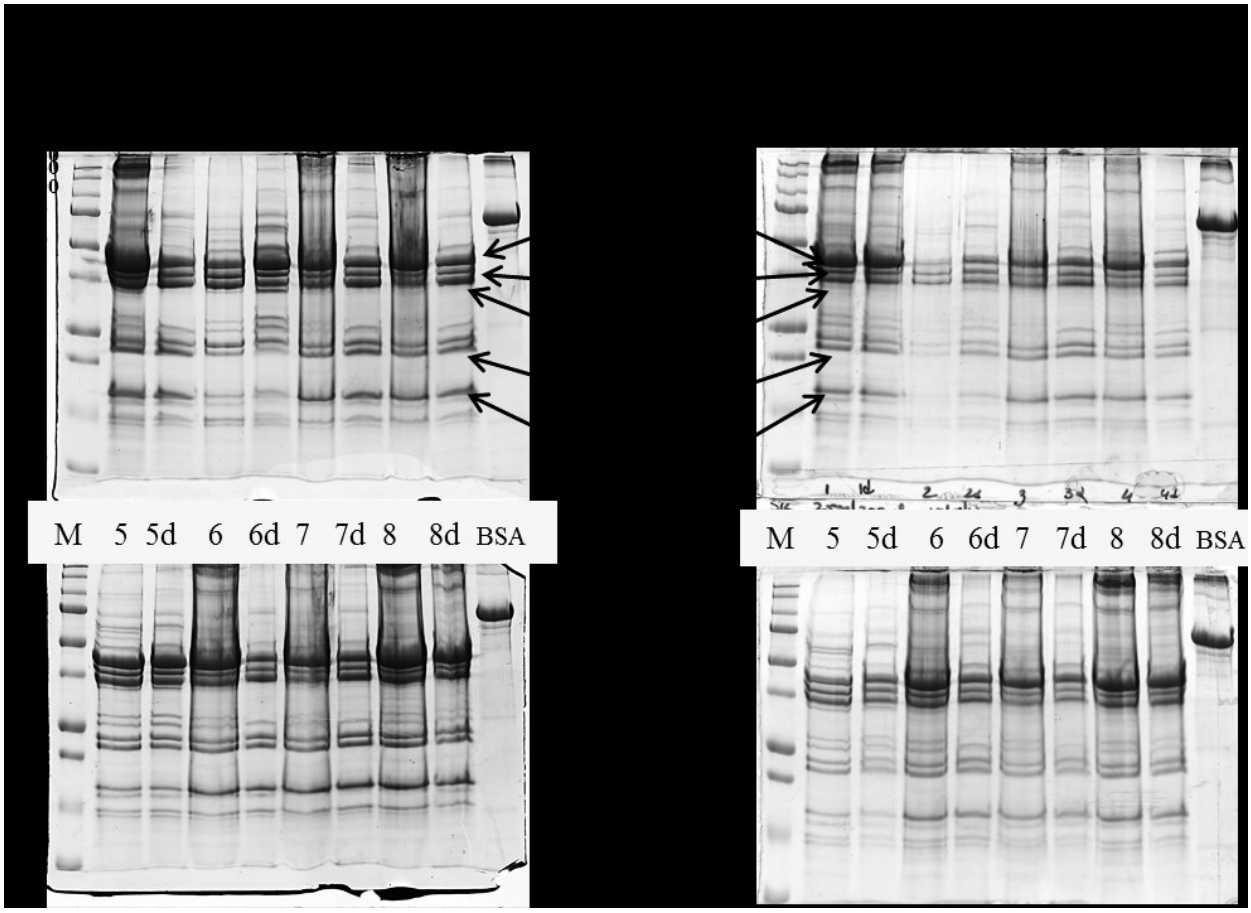

Figure 4.1: Chicken pectoral muscle proteins visualised in SDS-PAGE. Chicken pectoral muscle – 5 mg and 2mg in 200µl buffer. M-Marker, 1-Urea, 2-potassium chloride (KCl), 3-Urea+KCl (UK), 4-UK+TritonX-100, 5-NaCl, 6-Urea+NaCl (UN), 7-UN+TritonX-100 (UNT), 8-UN+sodium dodecylsulphate (UNS). d-dialysed, skTnT-skeletal troponin T, (I and C). Low molecular weight skTnC is yet to be confirmed and is labelled comparing with previously confirmed protein bands.

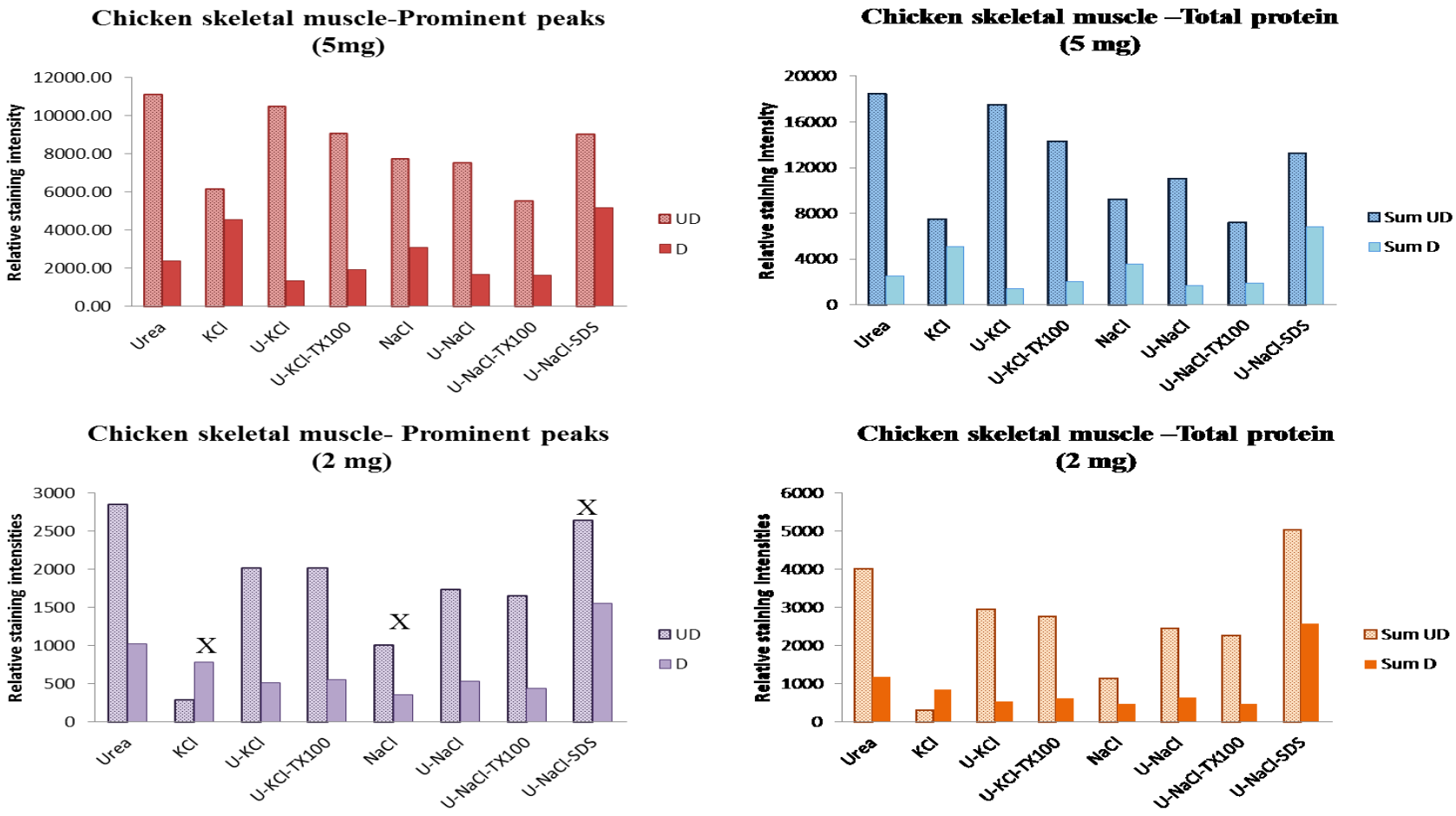

Figure 4.2:Chicken pectoral muscle tissue extraction quantification using Image J. 2 mg and 5 mg tissue lysates in 200µl buffer : U-Urea, KCl-potassium chloride, UK-Urea+KCl, NaCl-Sodium chloride, SDS-sodium dodecylsulphate, UD-Undialysed, D-Dialysed, X – buffers selected for further analysis.The prominent peaks are protein bands that are identified highlighted in Fig.5.3.

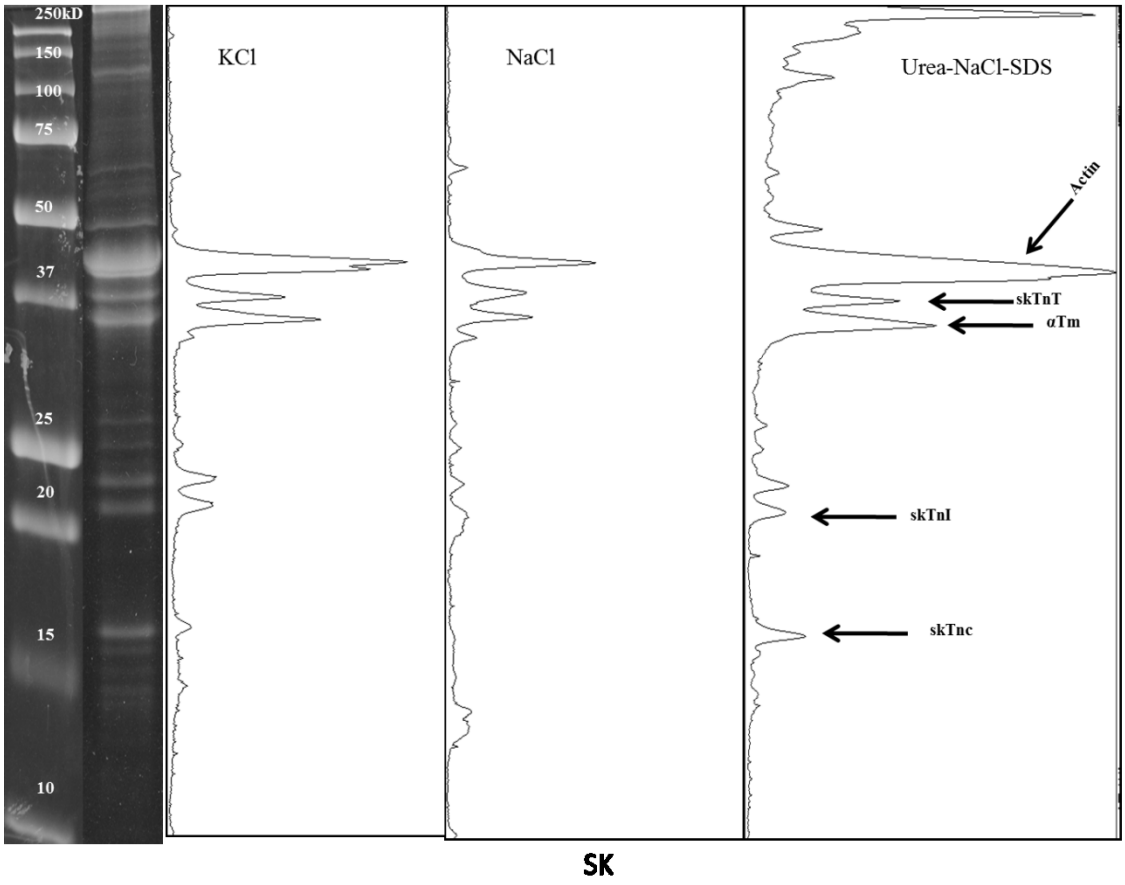

Figure 4.3: Extraction profile for chicken pectoral muscle with 2 mg tissue. Pectoral muscle protein bands from Image J quantification peaks of three short listed buffers KCl, NaCl and Urea-NaCl-SDS from the prominent peaks obtained from Coomassie stained SDS-PAGE gels.

The prominent proteins labelled (actin, tropomyosin and troponins) and the other visible protein bands on the gel were used for quantification of band intensities to obtain the total protein using Image J software. Figure 4.2 shows the sum of the protein band intensities obtained from Coomassie stained SDS-PAGE gels of skeletal muscle form 5 mg and 2 mg tissue extractions. Among the eight conditions three buffer conditions were short listed depending on the total protein and the amount of prominent proteins visible on the gel after dialysis. The proteins on SDS page were labelled according to Maytum et al.,

(2003). The protein bands can be observed as peaks from the spectrum obtained from Image J analysis of SDS-PAGE as shown in Figure 4.3 which is taken from 2 mg tissue extraction. Form the data obtained from 5 mg and 2 mg together, KCl, NaCl and Urea+NaCl+SDS (UNS) buffers were shortlisted with a relative staining intensity of 844.8, 482.9 and 2580.7 of total protein respectively for further analysis of skeletal muscle proteins. The above buffer were chosen as protein gels from these buffers show complete removal of myosin (220 kDa) after dialysis with low salt buffer (Figure 4.1) as myosin seems to precipitate out after dialysis. Removal of myosin is important as this is a very high molecular weight protein and being a relatively sticky and insoluble protein which will have high back ground effect during HPLC separation as well as mass spectrometry analysis.

4.2.1.2 Heart muscle tissue extraction

Figure 4.4 shows the Coomassie stained SDS-PAGE gels for the tissue lysates from the extraction of proteins from the left ventricle of heart tissue samples. However from both (2 mg and 5 mg) of the extraction profiles, buffers containing urea and detergents gave a higher amount of protein but from the Figure 4.4 it can be seen that the lower molecular proteins in the gel are not resolved completely. The same is observed in the reproduced gels as well. It is a well-known fact that detergents affect the mass spectrometric analysis by high back ground noise ratio in mass spectrum and hence to be removed before analysis by dialysing in low salt buffer. Hence for heart samples buffers without detergents were chosen to reduce the back ground noise in MS analysis. Buffers containing Urea, Urea-KCl and Urea-NaCl with band intensities of 3045.5, 2079.6 and

1836 respectively, were chosen as it is observed from Figure 4.6 that these buffers give good resolution of proteins from heart muscle and also there is higher amount of purified protein after dialysis compared to other buffers. Another reason for favouring these buffers is the removal of myosin after dialysis. This may be because some proteins after dialysis must have been precipitated out and proteins show higher resolution after dialysis.

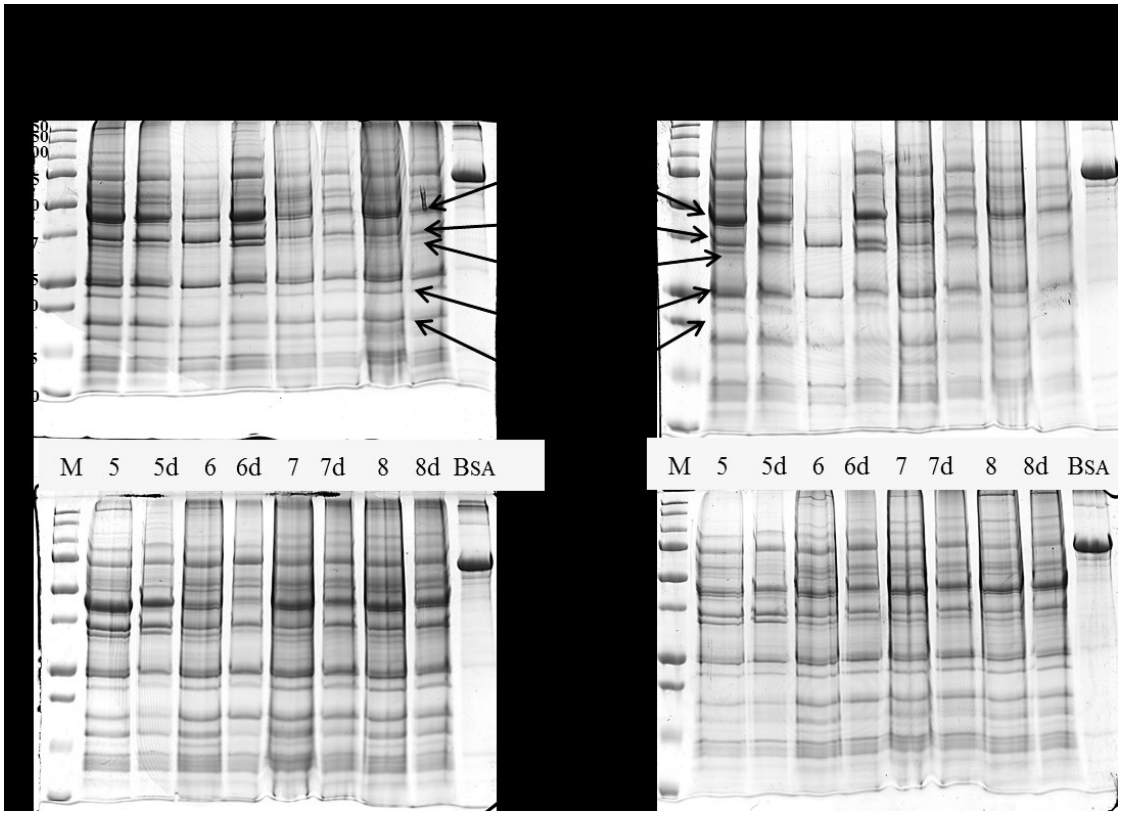

Figure 4.4: Proteins of left ventricle of the chicken heart visualized on SDS-PAGE gel. Heart left ventricle-5mg and 2mg in 200µl buffer. M-Marker, 1-Urea, 2-potassium chloride (KCl), 3-Urea+KCl (UK), 4-UK+TritonX-100, 5-NaCl, 6-Urea+NaCl (UN), 7-UN+TritonX-100 (UNT), 8-UN+sodium dodecylsulphate (UNS). d-dialysed, cTnT-skeletal troponin T, (I and C). Low molecular weight cTnC is yet to be confirmed and is labelled comparing with previously confirmed protein bands.

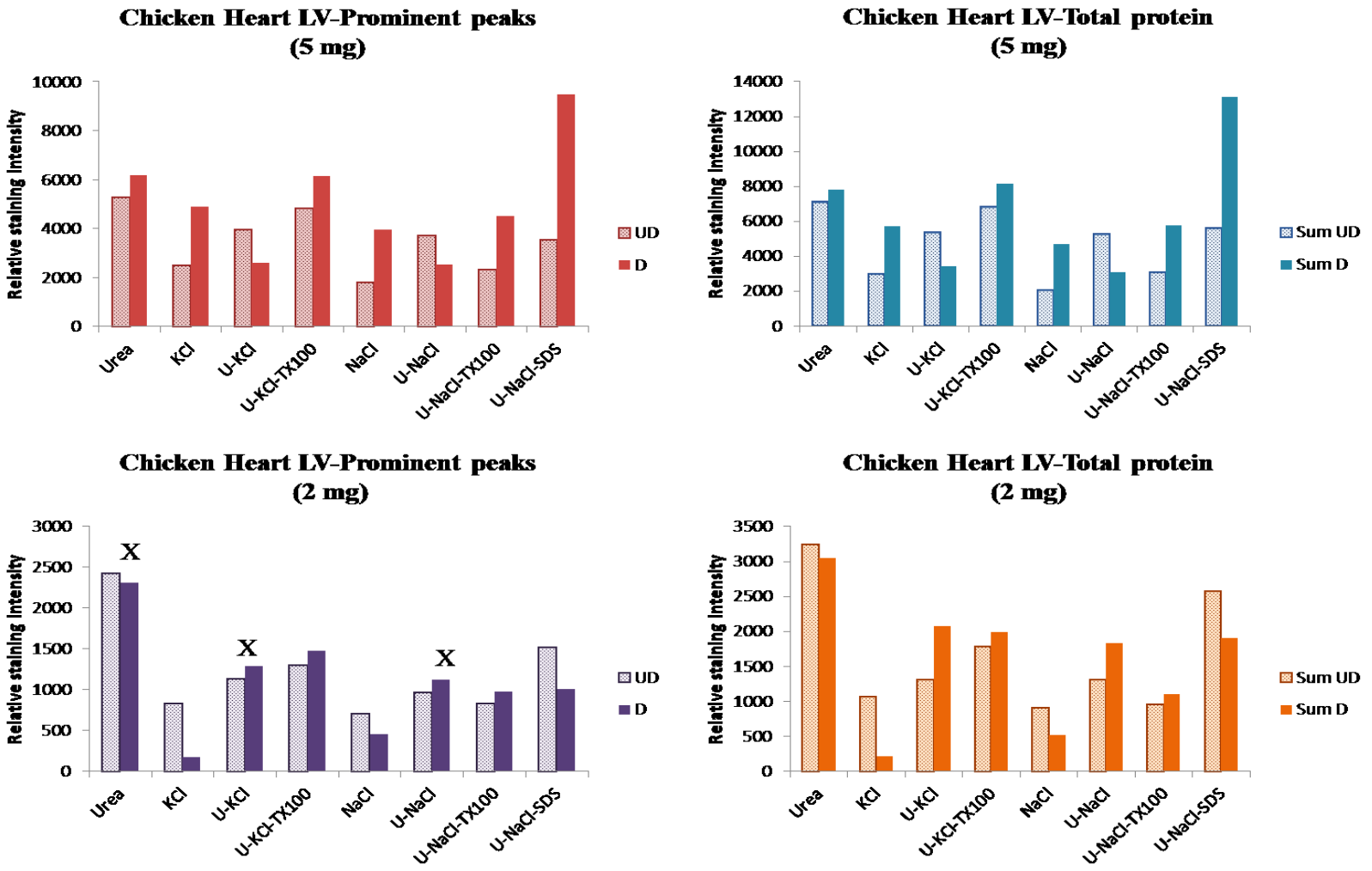

Figure 4.5: Chicken heart-left ventricle (LV) tissue extraction quantification using Image J. 2 mg and 5 mg tissue lysates in 200µl buffer : U-Urea, KCl-potassium chloride, UK-Urea+KCl, NaCl-Sodium chloride, SDS-sodium dodecylsulphate, UD-Undialysed, D-Dialysed, X – buffers selected for further analysis.

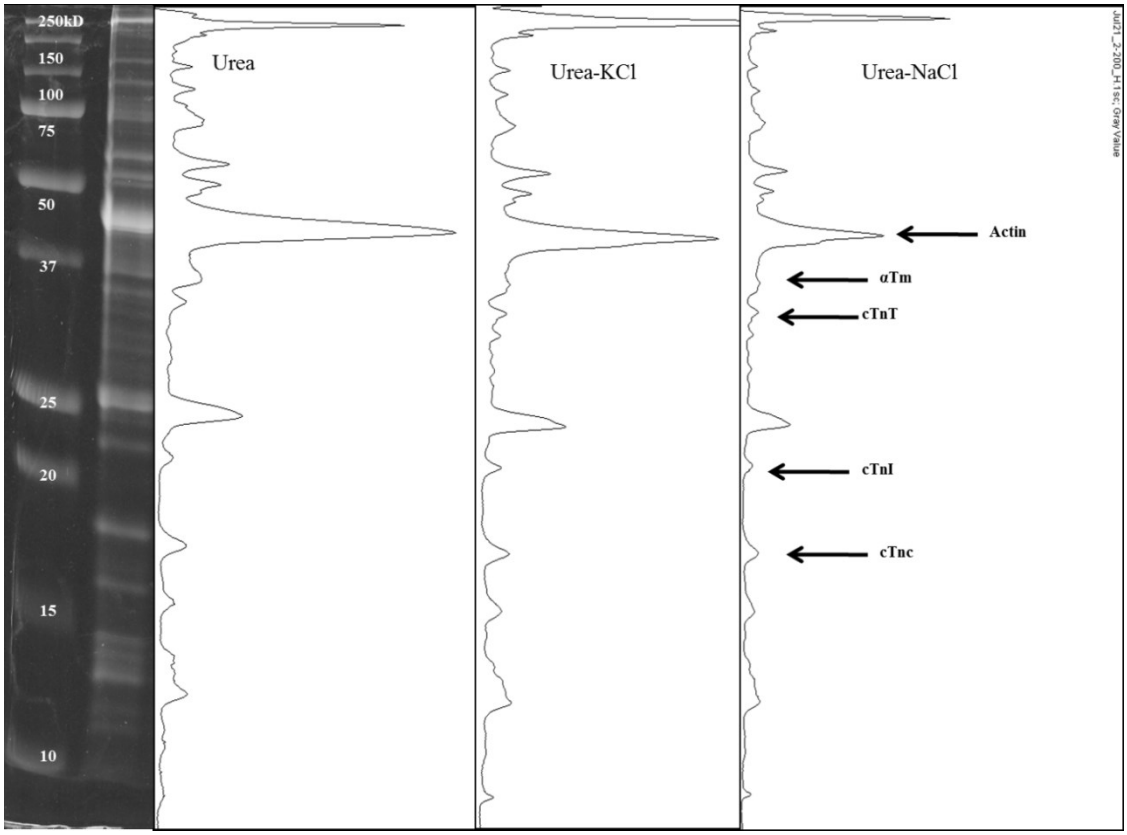

Figure 4.6: Heart muscle Left ventricle protein profile from Image J quantification peaks of three short listed buffers Urea, Urea- KCl, Urea-NaCl .

Figure 4.6 shows the spectrum obtained from the quantification of SDS gels by using image J analysis with the short listed buffers.

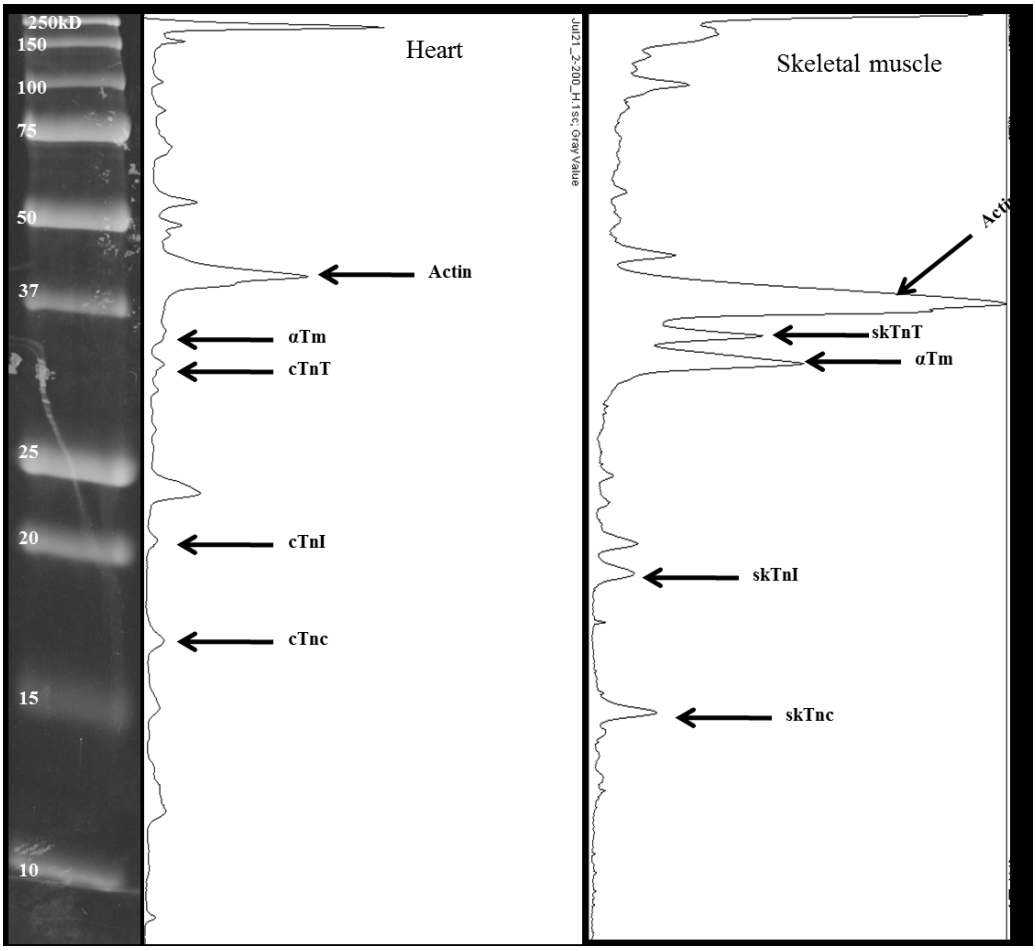

Figure 4.7: Difference in the protein profile of the heart and skeletal muscle.

Figure 4.7 shows the difference in the skeletal and heart muscle proteins separation on SDS page, the proteins are distributed and separated differently on SDS page may be due to the difference in the isoforms of skeletal and heart muscle proteins. With help of MS analysis it may be possible to see the difference in the skeletal and cardiac protein difference and their PTMs. The low molecular weight proteins (cTnC and skTnC) masses are yet to be confirmed. The labelling is based on assumption of theoretical mass and data obtained from previous research.

Both skeletal muscle and heart tissue extracts were performed in triplicates, however quantification for all the buffers was done only for one replicate. Triplicate quantification was performed for storage time experiments using short listed buffers for both types of tissues. Both tissues have been observed to prefer different salt and urea condition for solubilising the respective proteins.

4.2.1.3 Mouse Skeletal and heart extracts

Wild type mouse skeletal muscle from thigh area and heart were used for extraction of thin filament proteins using the same buffers as used for chicken heart LV. Triplicate extractions were made and used for HPLC analysis. The triplicates are shown in Figure 4.23, quantification was not performed for these extracts with densitometry, as the buffers were already selected using chicken samples, total protein form the extracts was quantified by BCA assay. It can be seen form Figure 4.8 and the gels from Figure 4.23 that the distribution of proteins on SDS-PAGE are different between chicken and mouse cardiac proteins may be due to difference in the isoform distribution in both species.

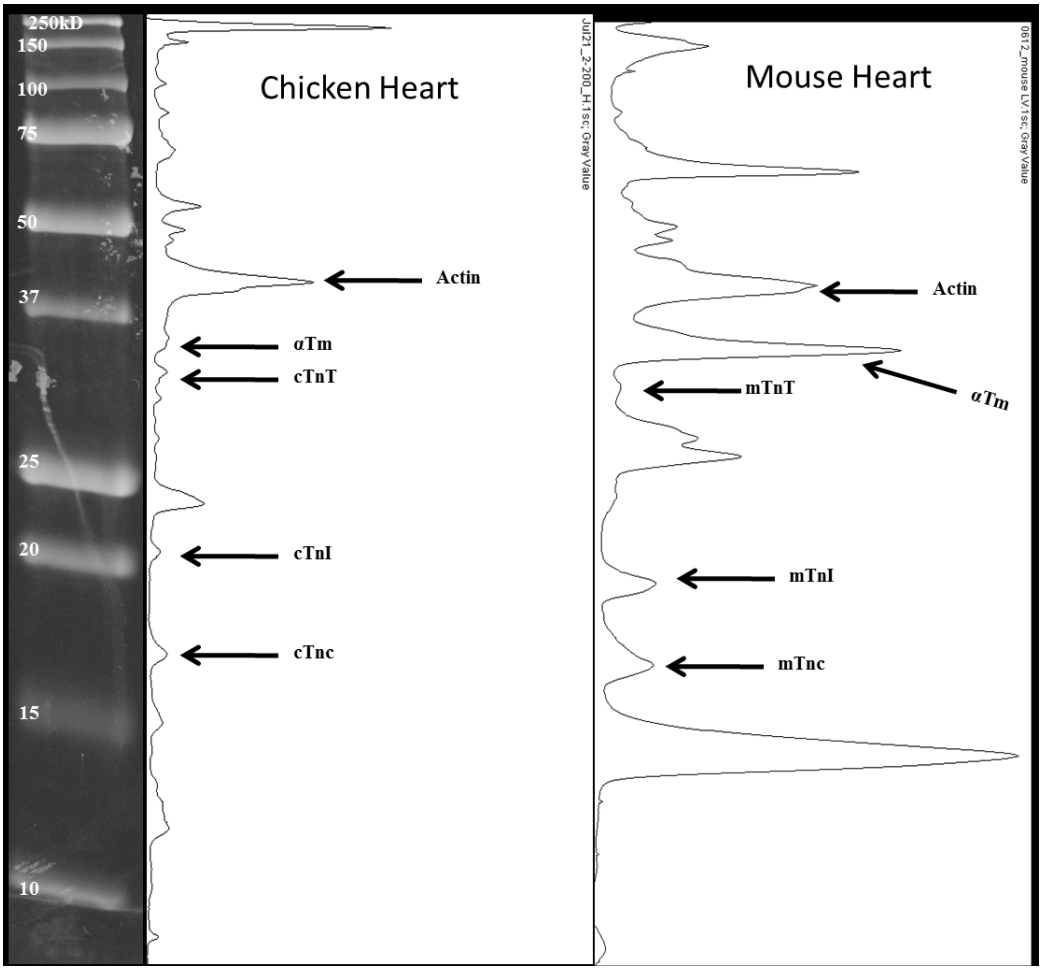

Figure 4.8: Difference in the protein distribution of chicken and mouse heart proteins on SDS-PAGE. Image spectrum generated by using Image J software.

4.2.2 Storage of tissue extracts

4.2.2.1 Skeletal muscle samples

Shortlisted buffers were used to extract proteins for checking the storage limitations of the tissue lysates after extractions. This is important when using human tissue samples as the sample would be limited for extraction and analysis. Three technical replicate extractions were prepared and analysed using densitometry of SDS-PAGE gel images. The gel images for skeletal muscle and heart muscle are shown in Figure 4.9 and Figure 4.12 respectively. The replicates were performed for reproducibility and hence error was not calculated as there would be a large difference with the gels being treated separately and the staining time and destaining time effects the density of the bands even though care was taken to keep the timing as close as possible, BSA as a standard. Analysis was done as described previously.

The quantification data of average relative staining densities of total proteins from all three replicates and the data obtained from single replicate are in given in Figure 4.12. As previously observed from Figure 4.1, buffer with detergent SDS, gave higher amount of total protein yield than the buffers with only salts.

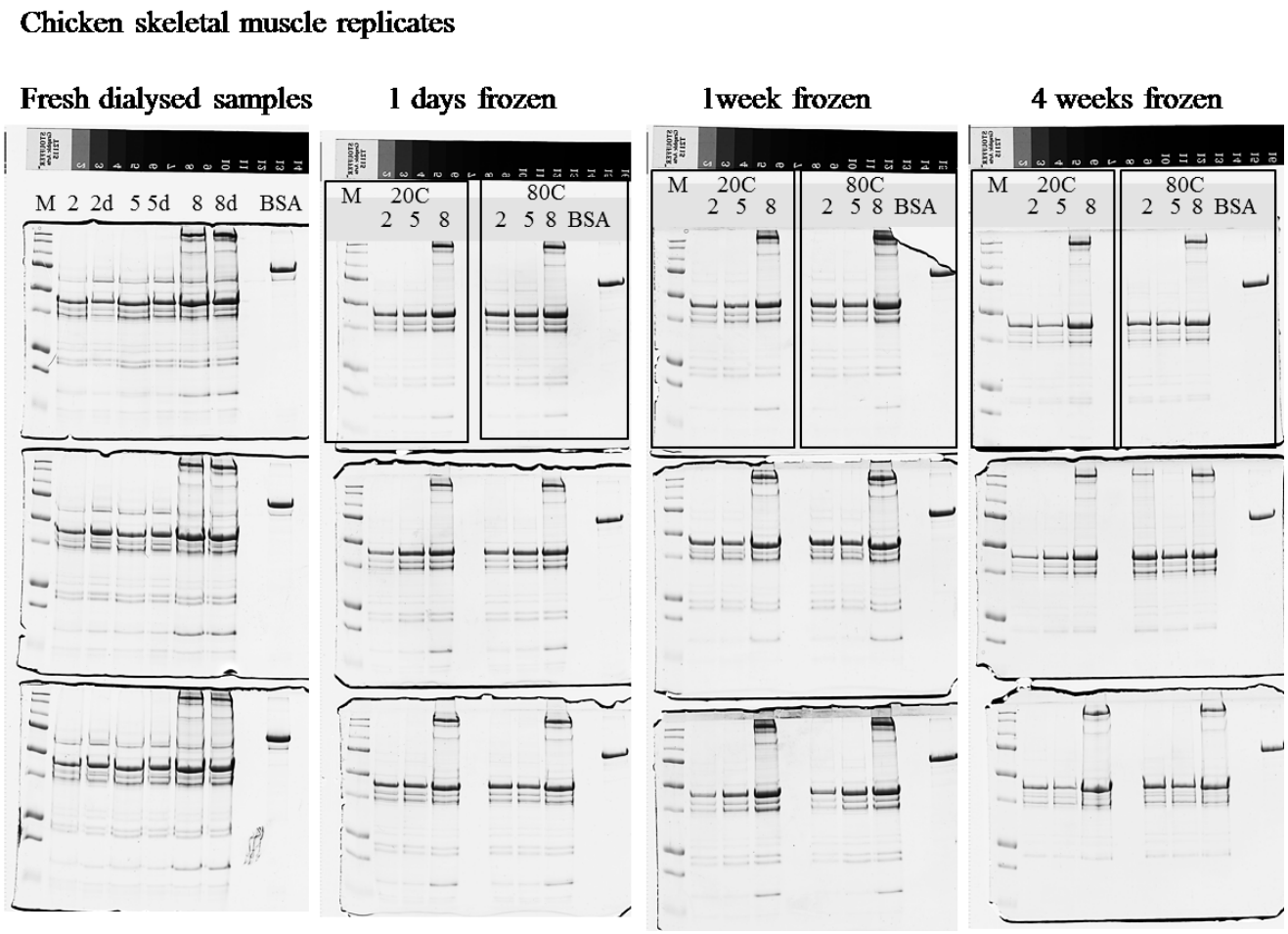

Figure 4.9: Chicken skeletal muscle tissue extracts triplicates. Experiment was performed as explained in methodology. 2- KCl, 5- Nacl, 8 – Urea-Nacl –SDS. Samples were thawed on ice for sample preparation for analyzing with SDS-PAGE.

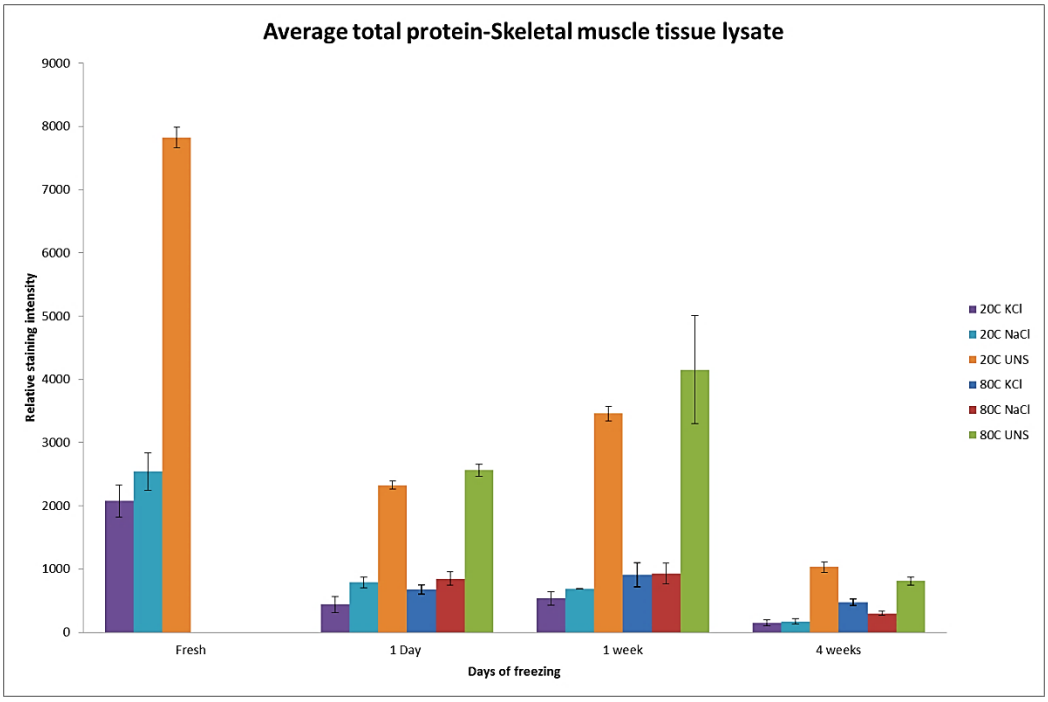

Figure 4.10: Average of relative staining ratios of skeletal proteins lysates stored at -20C and -80C.

UNS have higher extractions but myosin is left in the lysates after dialysis. KCl seems to have better storage capacity than NaCl, however at 20 ^{0}C NaCl have slightly higher protein than KCl in contract with 80 ^{0}C where KCl is left with higher protein. It also observed that in one day there is substantial loss of protein, however freezing for one day and one week does not have much difference, but 4 weeks freezing is not preferable (Figure 4.9 and Figure 4.10). However, as long as protein bands are visible on an SDS-PAGE, it would be enough protein for analysis using mass spectrometry. It has to be added that, unless mass spectrometry analysis is performed it is not known how much the proteins are proteolysed. It can be observed that for some reason samples frozen for one day and one week does not show much difference in protein loss, however protein stored

at -80 ^{0}C have more protein left in the lysates than the lysates stored at -20 ^{0}C. In both cases, there is substantial loss of protein by storing the samples for four week.

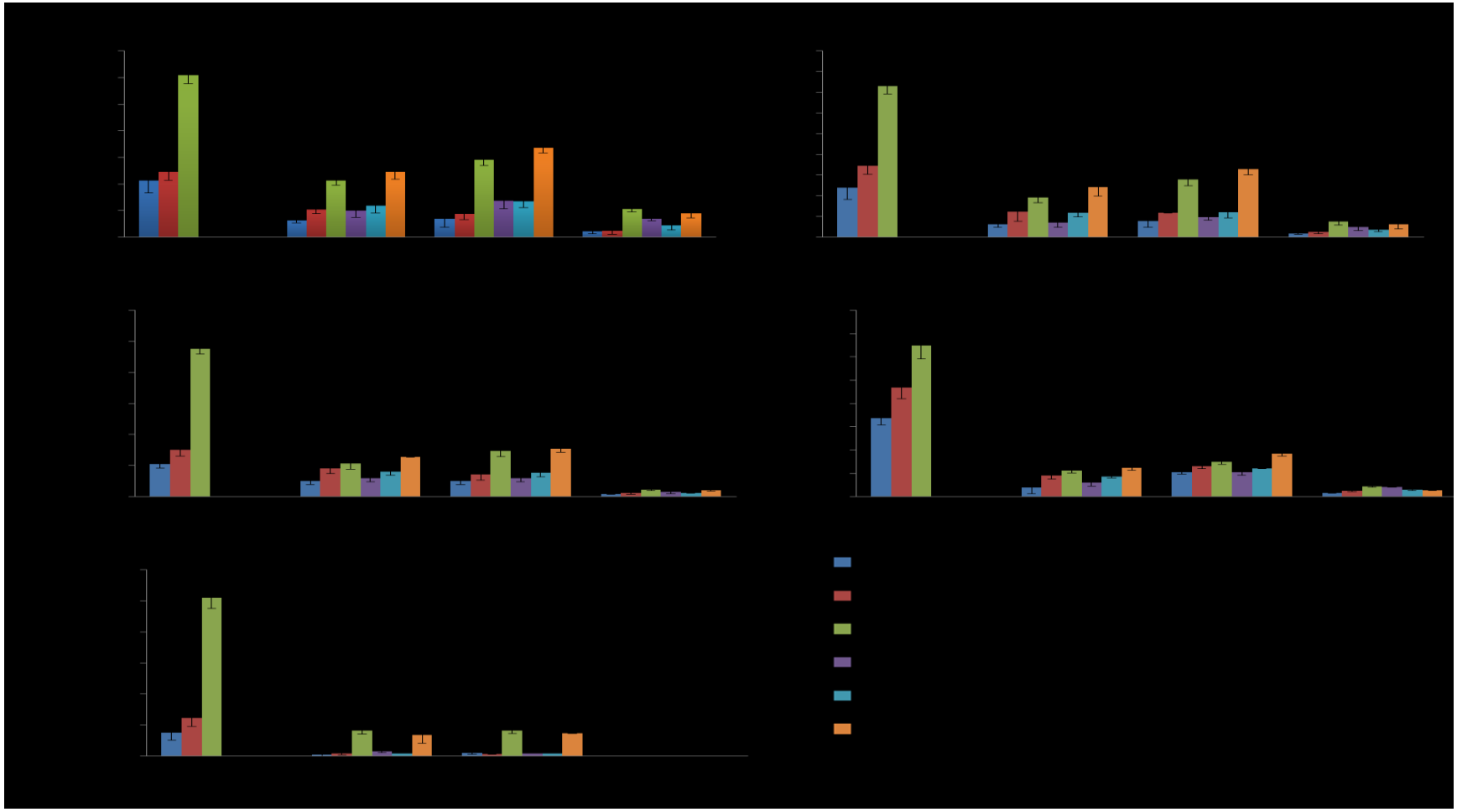

Figure 4.11: Relative staining intensities of individual prominent protein bands of skeletal muscle and the difference in freezing times. Averages are taken from triplicate data.

The data obtained from quantification of stored samples was also used to check the variation of individual prominent proteins actin, tropomyosin and troponins (TnT, TnI and TnC) and their affect due to storage shown in Figure 4.11. For some reason proteolysis is different at -20 ^{0}C and -80 ^{0}C with NaCl and KCl with all the individual proteins, actin, Tm, and Tn's. Actin and Troponin I seems to favor KCl and Tm and TnT, TnC seems to store well in NaCl. Both KCl and NaCl could be used for mass spectrometry analysis, however NaCl forms protein adducts and effect mass spectrometry analysis by reducing the overall molecular ion abundance and signal distribution for any given charged state (Flick et al., 2012). It is also observed that after four week TnC is completely lost or may be its not left enough to be visible on a gel. The concentration of salts could be reduced by buffer substitution with ammonium bicarbonate or ammonium bromide which are volatile and are evaporated during mass spectrometry analysis. The relative loss in intensities has been observed relatively similar with other replicates, the figures shows the average of the data taken from all the replicates.

4.2.2.2 Heart LV samples

The heart samples treated similar to skeletal muscle samples other than that the buffers used were different. Urea, Urea-KCl and U-NaCl were used for extraction of heart muscle proteins. Figure 4.12 shows the triplicate SDS gels of all the freezing conditions. The relative staining intensities were calculated same as skeletal muscle proteins.

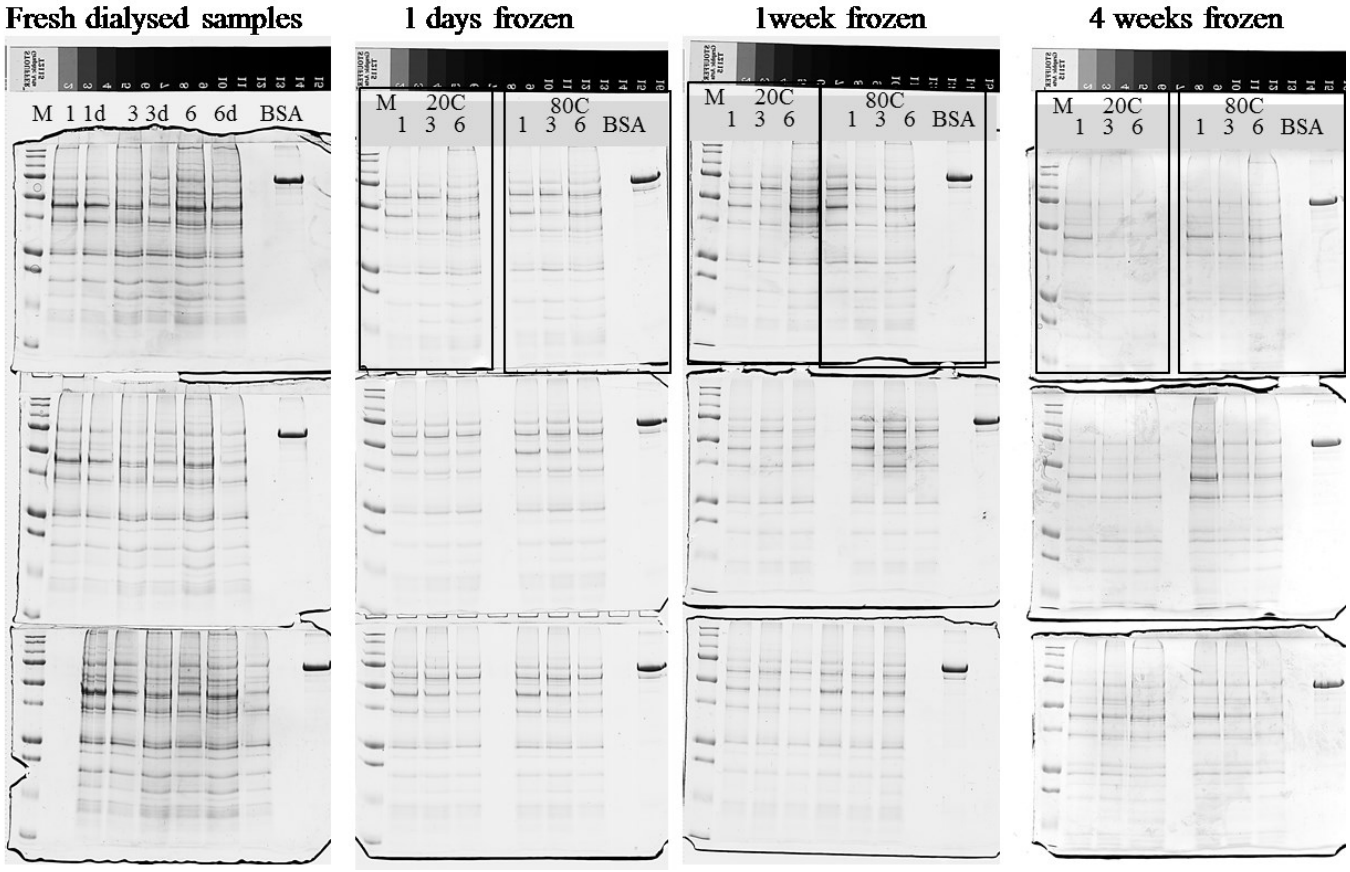

Figure 4.12: Chicken heart LV tissue extracts triplicates. Experiment was performed as explained in methodology. 1Urea, 3-Urea-KCl, 6– Urea-NaCl. Samples were thawed on ice for sample preparation for analyzing with SDS-PAGE.

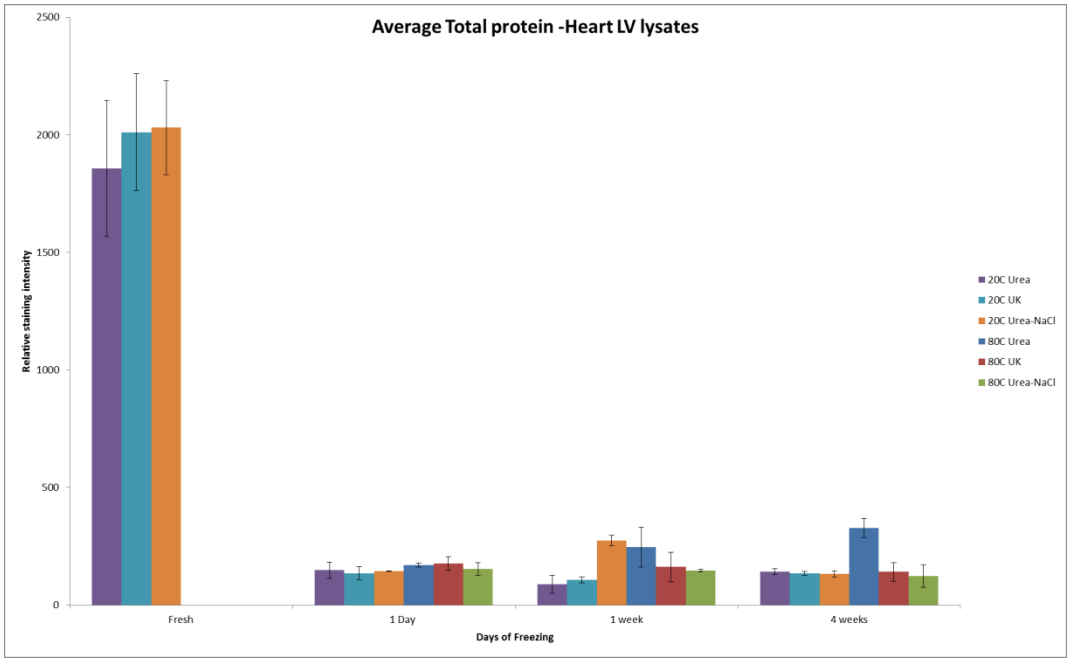

Figure 4.13: Average of the relative staining ratios of heart protein lysates stored at -20C and -80C.

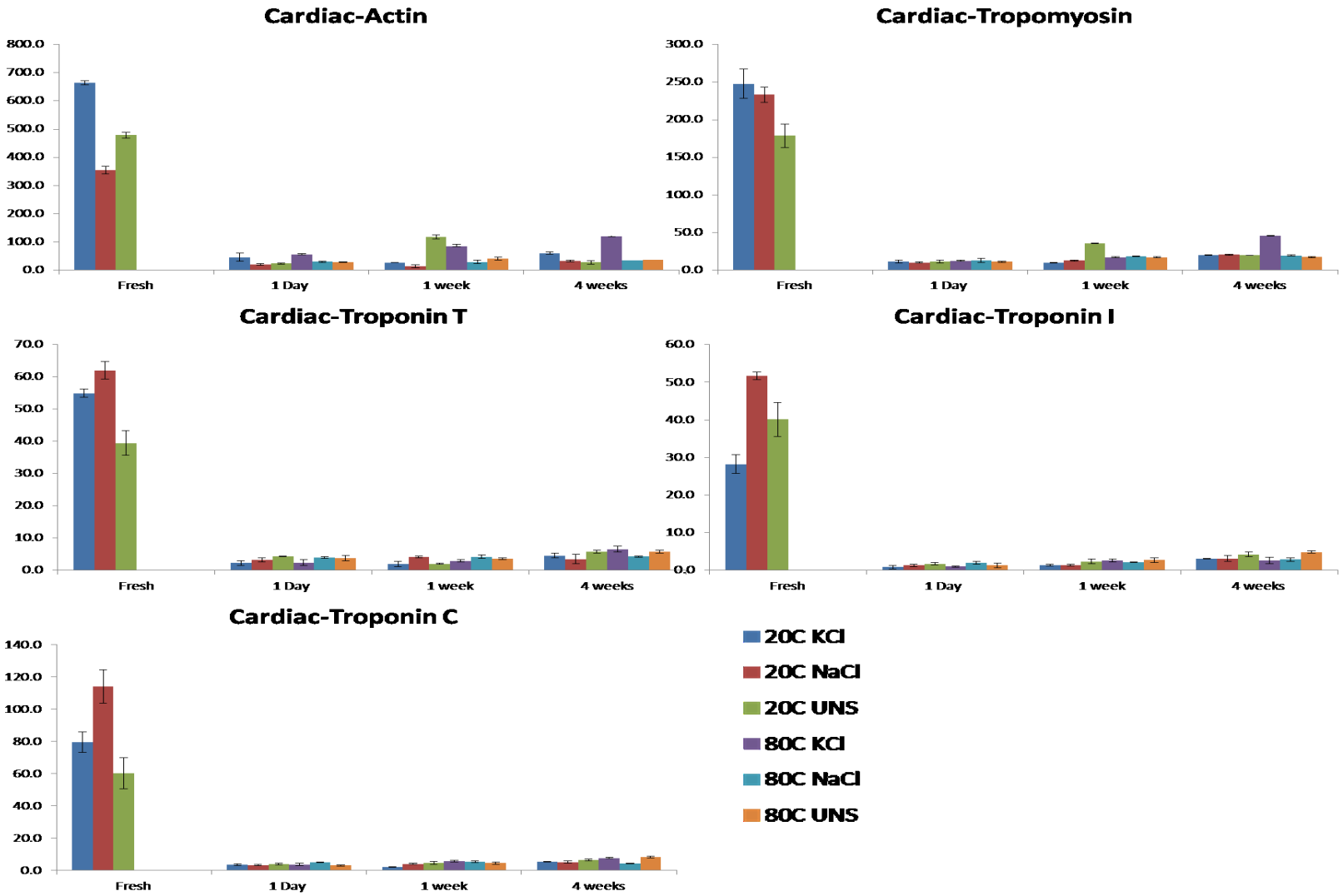

Figure 4.14: Relative staining intensities of individual prominent protein bands of heart LV muscle and the difference in freezing times taken from triplicate data.

The cardiac muscle proteins also had substantial loss similar to skeletal muscle proteins. Form Figure 4.13 it is seen that there is an increase in intensity for -20 ^{0}C UK and -80 ^{0}C Urea for one week freezing samples, which is due the back ground staining of the gel as seen from Figure 4.12. Otherwise the loss seems to be similar without effect of how long the sample is stored.

Form the data presented in Figure 4.14, actin, tropomyosin and troponins of cardiac muscle are found to last longer from degradation in Urea-KCl buffer both at -20 ^{0}C and -80 ^{0}C, however they seem to be less stable than the skeletal muscle proteins.

Form both muscle tissues, it is observed that one week storage is better than one day storage, if it needs to be stored for one day, it is better to store the sample at 4 ^{0}C rather than freezing.

4.2.3 BCA quantification

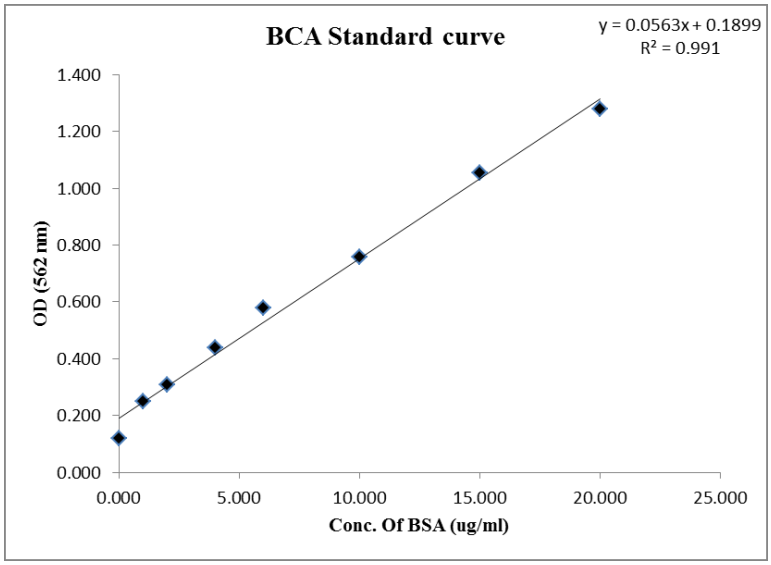

Figure 4.15: BCA quantification standard curve - skeletal and cardiac muscle proteins.

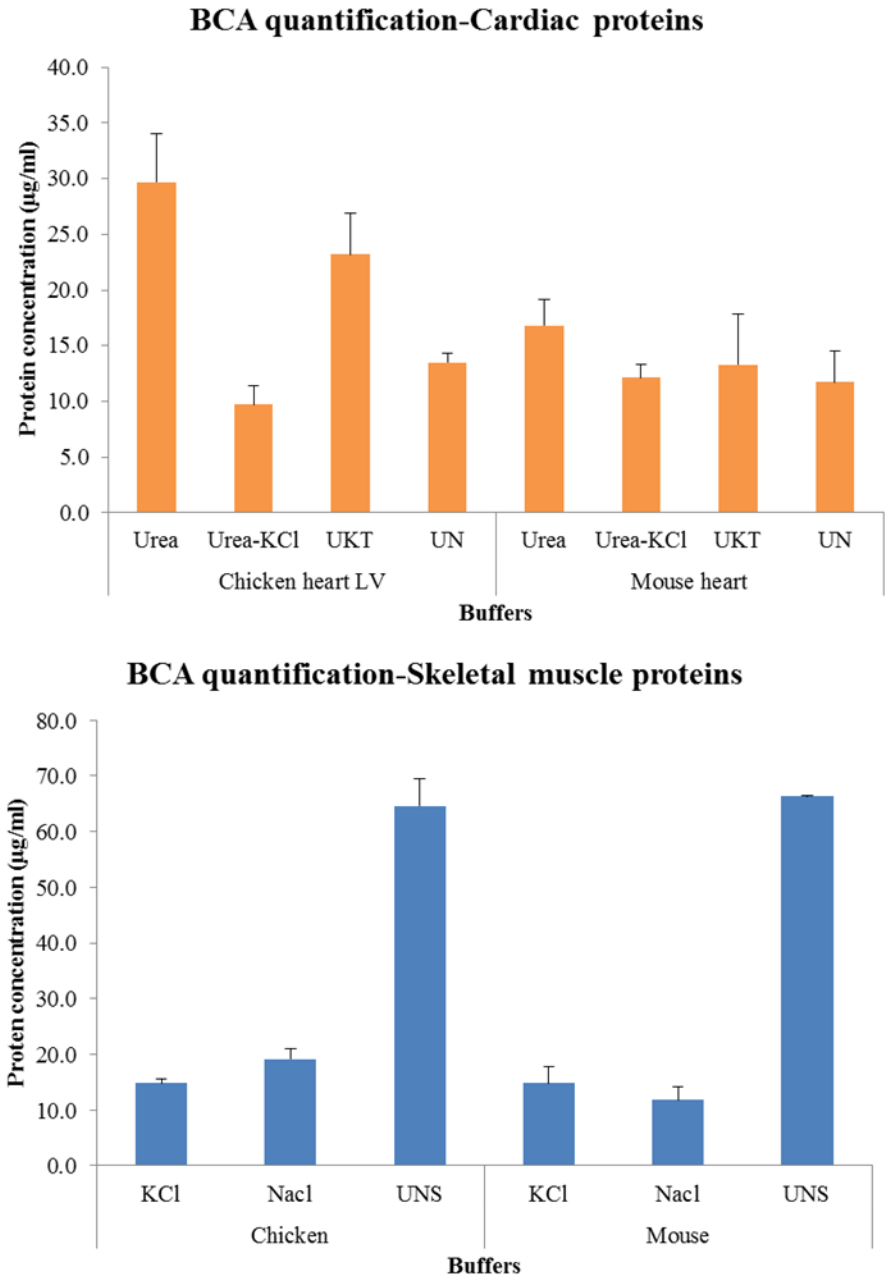

Figure 4.16: Protein concentration of dialysed samples of skeletal muscle and cardiac muscle protein extracts by BCA assay.

Figure 4.15 shows the standard curve of the BCA quantification used for quantifying total protein from tissue lysates shown in Figure 4.16.

4.2.4 Reverse Phase HPLC analysis

Control proteins of rabbit muscle extracted during the preparation of actin from acetone muscle powder. The protein lysate consist mainly of Tropomyosin and Troponin complex. As seen in the Figure 4.17a, the lane labelled T is the dialysed protein lysate containing troponin complex (Tnc, TnT, and TnI)and tropomyosin with traces of actin, as actin has already been extracted for actin polymerisation studies. The tropomyosin band separation clearly shows αTm (32680 Da) and βTm (32836.5 Da) (Table 4.2). The proteins lysate was dialysed in 1 mM ammonium bromide and this seems to keep proteins stable for analysis. The elution profile (Figure 4.17b) shows the separation of all the proteins present in the lysate.

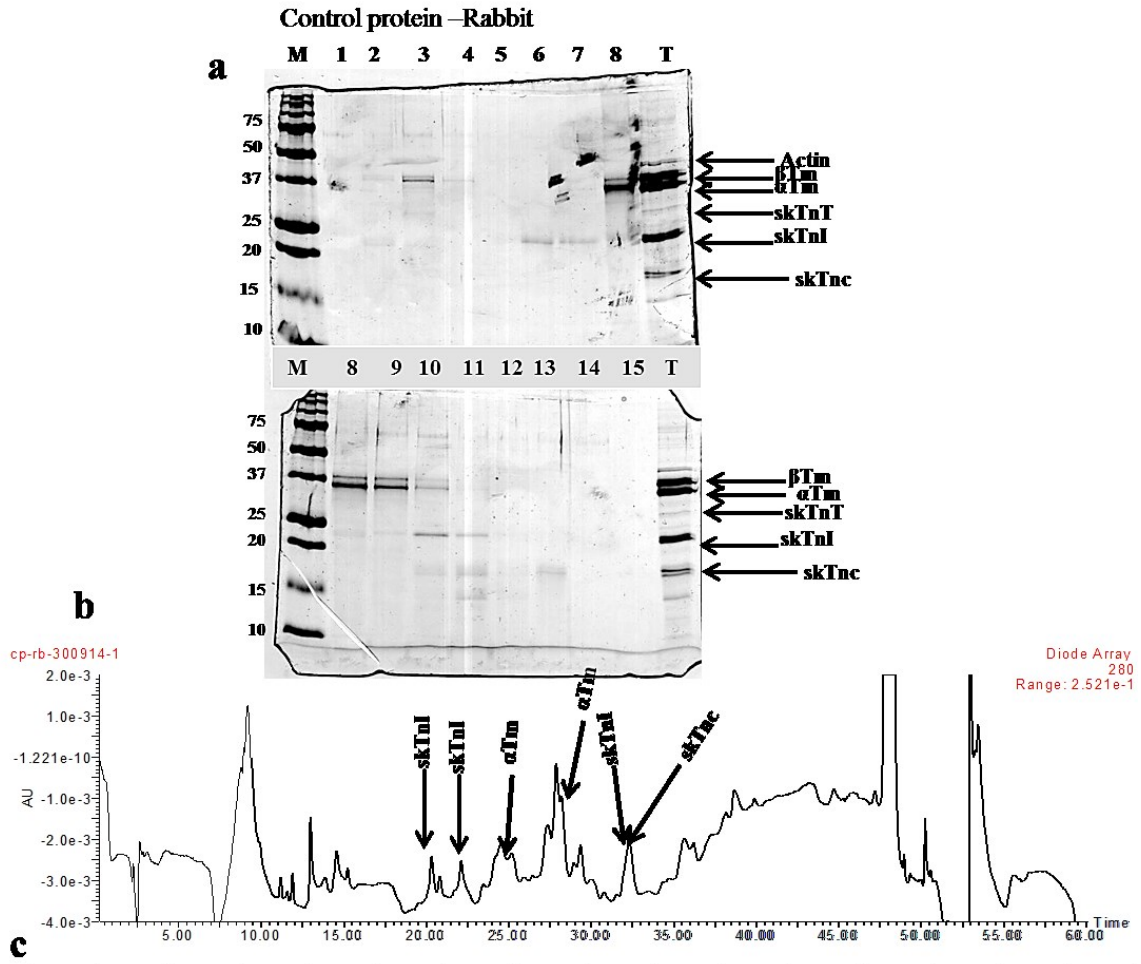

c

Peak no	1	2	3	4	5	6	7	8	9	10	11	12	13	14	15
Time (min)	7-11	12	15	17	19	21	23	23-26	27-28	29	31-32	33	35	39	48
%B	20-24	26	27-28	29	30	31-32	33	34-36	36-37	38	39	41	43	46	100

Figure 4.17: RP liquid chromatography (LC) elution profile of Rabbit skeletal muscle proteins. a. SDS gel showing the proteins of control proteins (CP) of rabbit skeletal muscle extracted form acetone muscle powder (mainly containing tropomyosin and troponin with traces of actin) and the eluents collected form the LC profile. b. elution profile of HPLC run. c. table showing the peak number, retention time and the % B relating to the elution profile. The peak number resembles the number of the peak in the elution profile and on the gel for comparison. T- the dialysed CP proteins loaded for comparison.

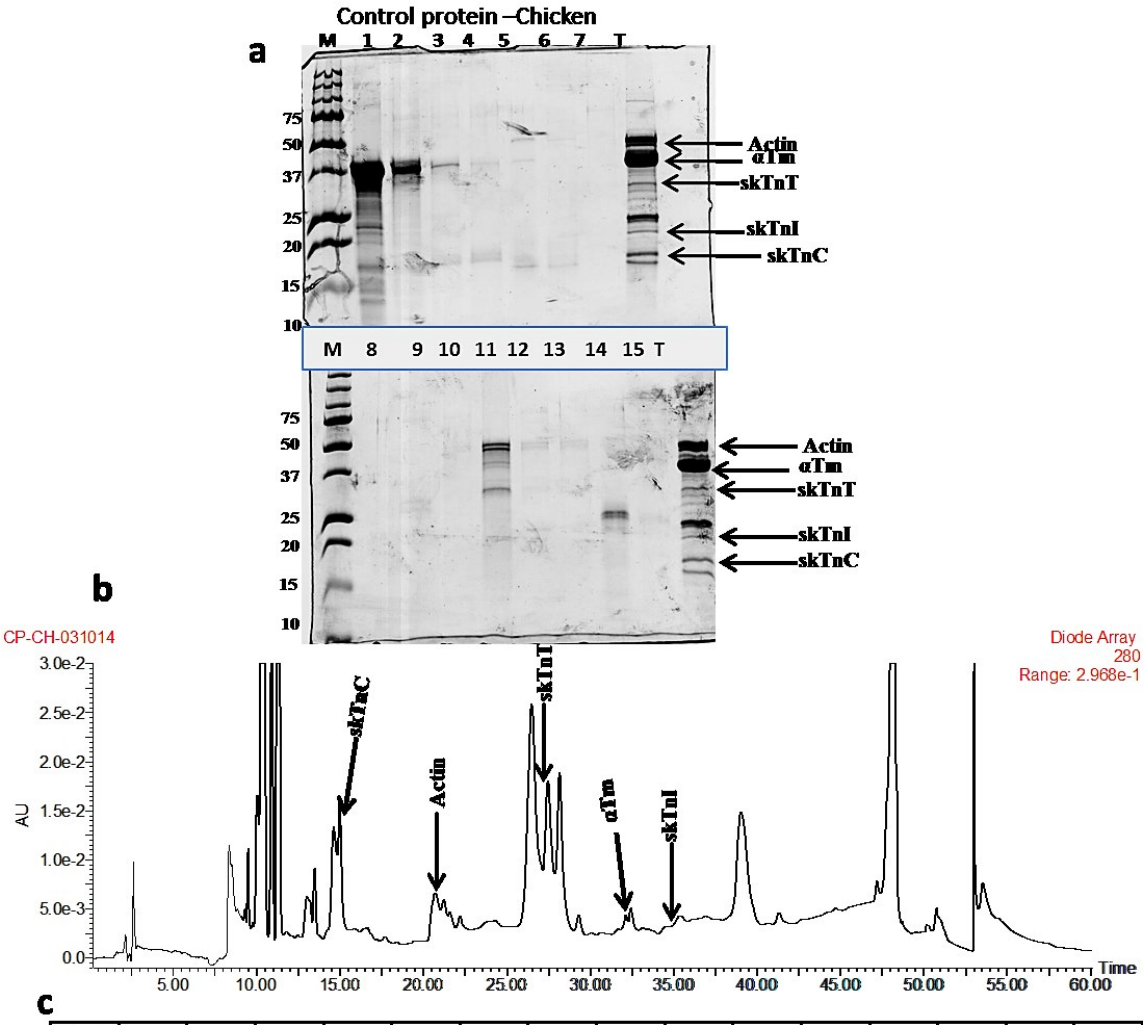

c

Peak no	1	2	3	4	5	6	7	8	9	10	11	12	13	14	15
Time (min)	8	10-12	13	14-15	16	16.5	20-22	24	26-28	29	32	35	39	41	48
%B	20	23-20	27	28	29	30	32	34	35-37	38.5	40	42	45	47	100

Figure 4.18: RP liquid chromatography elution profile of chicken control proteins. a. SDS gel showing the proteins of control proteins (CP) of chicken skeletal muscle extracted form acetone muscle powder (mainly containing tropomyosin and troponin with traces of actin) and the eluents collected form the LC profile. b. elution profile of HPLC run. c. table showing the peak number, retention time and the % B relating to the elution profile. The peak number resembles the number of the peak in the elution profile and on the gel for comparison. T- the dialysed CP proteins loaded for comparison.

Studying Figure 4.18, the CP of chicken skeletal muscle, from the tissue lysate it is clearly seen that actin is not completely removed from the lysate after actin preparation.

The protein lysate have high concentration of proteins and it seems the elution profile seen on the gels have all the protein separated frequently and not only in one single elution time. However at 30-32% B (100 % acetonitrile), TnT seems to elute and also low molecular weight protein band around 15 kDa is also eluted along with TnT. However chicken TnI did not seem to elute at the same time as of rabbit TnI. Chicken TnC is in comparison with rabbit TnC elution percentage.

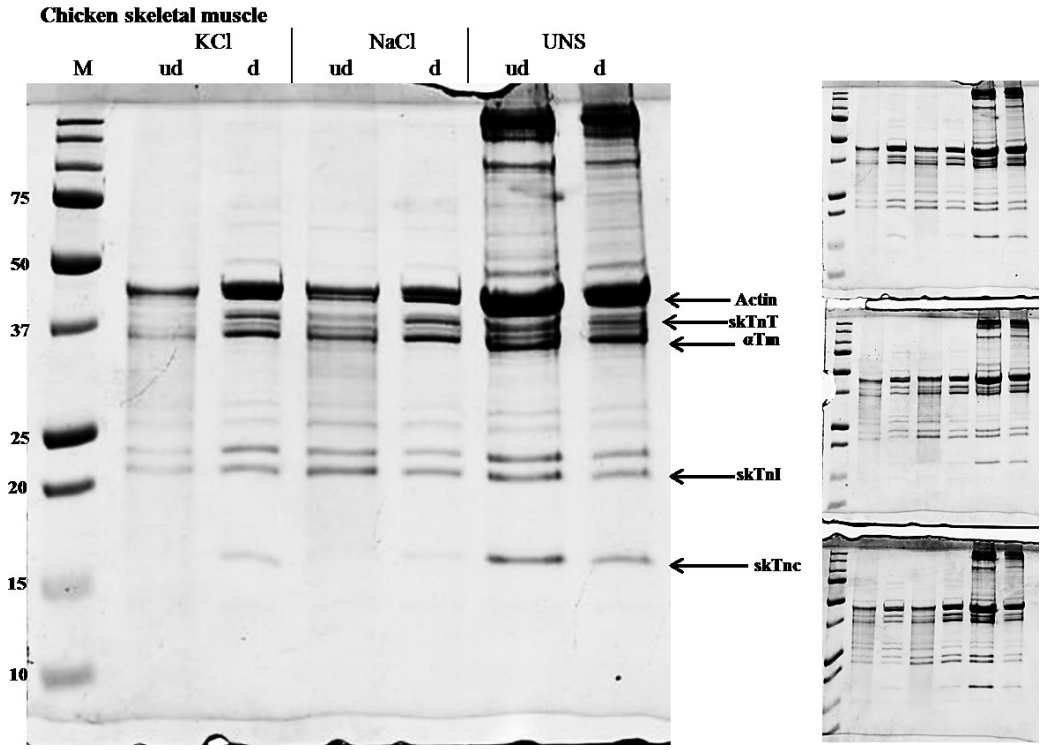

Figure 4.19: Chicken skeletal muscle protein extraction in triplicates for LC separation of proteins. Skeletal muscle proteins were freshly prepared for optimizing the LC method.

Figure 4.19 shows the freshly prepared chicken skeletal muscle lysates undialysed and dialysed (dialysed in low salt buffer as explained in methodology section 4.1.1) samples. After dialysis proteins seem to get more concentrated and resolved completely. The proteins extracted from KCl was used for using to separate protein by LC, as KCl shows higher concentration of proteins and UNS have still lot of soluble myosin left in the lysate, which is a notorious sticky protein and is not suitable for running through LC column. From the elution profile (Figure 4.20) TnC eluted very much later in comparison with Tm and other Tn complex, may be because in presence of actin in tissue

lysates and the tropomyosin, TnT complex is still bound tightly in contrast to CP proteins where actin is removed from the lysate.

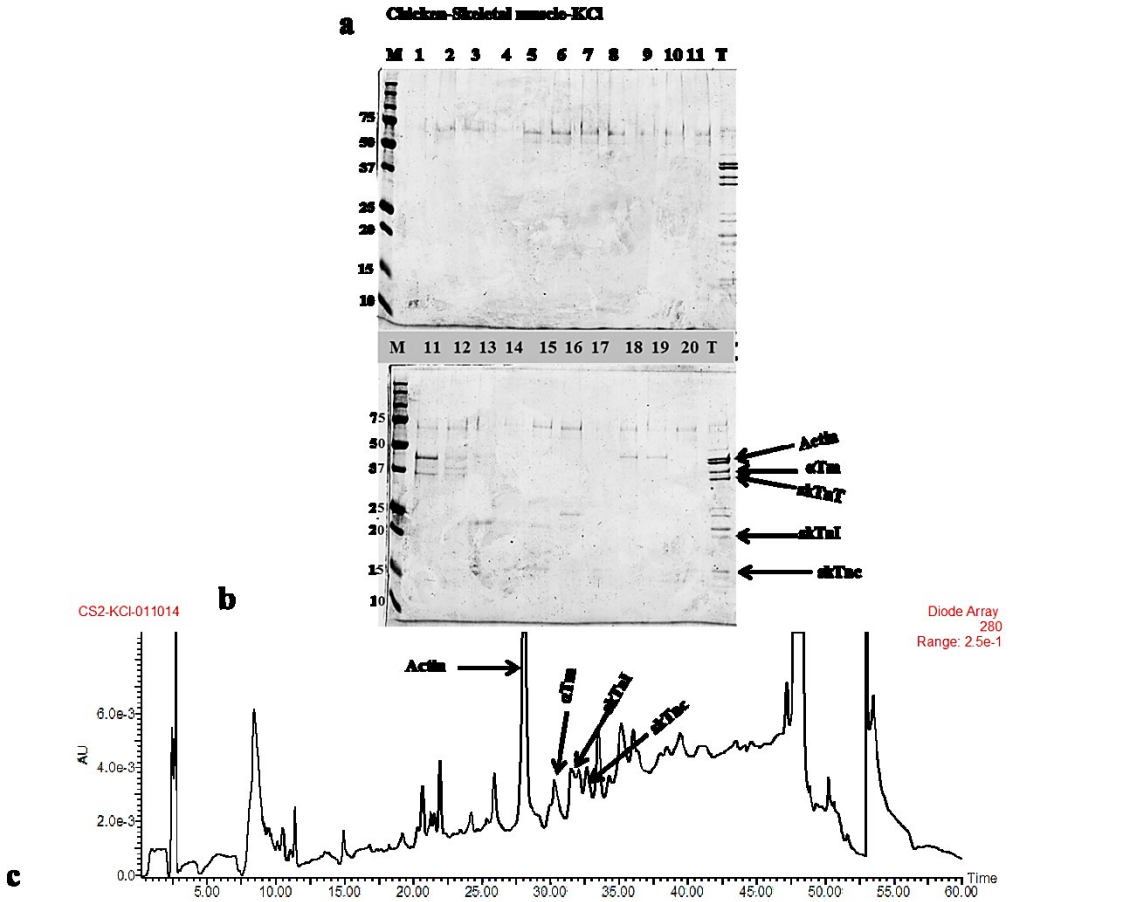

c

Peak no	1	2	3	4	5	6	7	8	9	10	11	12	13	14	15	16	17	18	19	20
Time (min)	9	11	12.5	14.5	16	18.5	20	21.5	23	25.5	27.5	30	31	32	32.5	34.5	35.5	39	40	46
%B	24	25	26	27	28	30	31	32	34.5	35.5	37	38	39	40	41	42	44	45	46-47	100

Figure 4.20: RP LC elution profile of chicken skeletal muscle. a. SDS gel showing the proteins of chicken skeletal muscle extracted form tissue in KCl and the eluents collected form the LC profile. b. elution profile of HPLC run. c. table showing the peak number, retention time and the % B relating to the elution profile. The peak number resembles the number of the peak in the elution profile and on the gel for comparison. T- the dialysed CP proteins loaded for comparison. Maximum effort was taken to emphasise the eluent protein bands on the gel during scanning, however they are not visible in the pictures as the band staining intensities were very low.

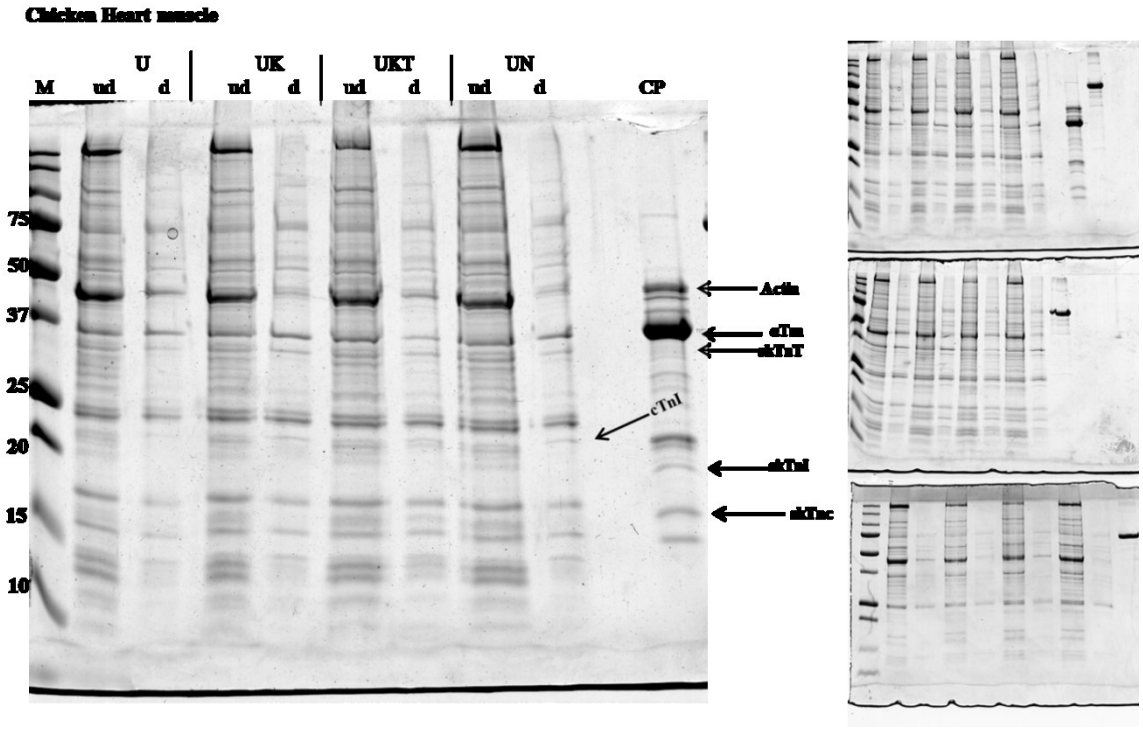

Figure 4.21: Chicken heart LV tissue lysates and triplicates. Freshly prepared for use in optimizing the LC method.

From the Figure 4.21, it is seen that buffer containing Urea-KCl with Triton X-100 gave good protein extraction and better resolution of proteins on the gel after dialysis, and from the solution profile, separation of protein from both UKT and UK were performed, but UKT did not give any recognizable bands on the gel from the eluents. Figure 4.22 shows the solution profile of protein form UK and the gel from UKT and it seems only Troponin complex is being eluted at the same %B as of skeletal proteins from both the solution profiles. UKT seem to keep the troponin complex intact in the buffer system and may TnT from the UKT has been eluted along with other Tn complex proteins. Actin and tropomyosin are not seen on the gel, may be because the lysates were stored on ice at -

4^0C for 3 days before analysis avoiding freezing the samples. The results from the storage experiments showed (Figure 4.14) cardiac proteins does not show stability during storage, hence may be the other proteins must have been degraded.

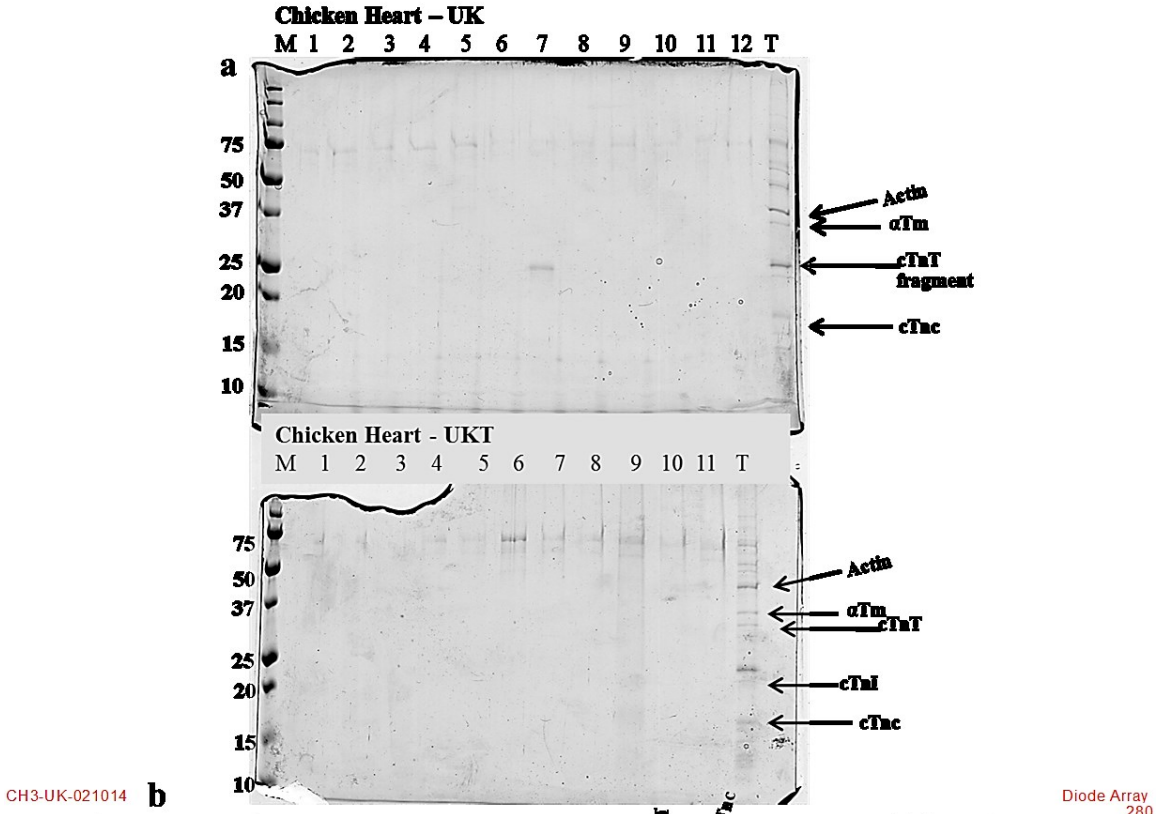

c

Peak no	1	2	3	4	5	6	7	8	9	10	11	12
Time (min)	8-10	12	15-17	19-21	24	25-26	27	32	35	36-37	43-45	49-50
%B	20-24	25	27-29	31	34	35.5	37	40	42-43	44-45	48-49	100

Figure 4.22: Chicken heart RP –HPLC elution profile. a. SDS gel showing the proteins of chicken heart muscle and the eluents collected form the LC profile. b. elution profile of HPLC run. c. table showing the peak number, retention time and the % B relating to the elution profile. The peak number resembles the number of the peak in the

elution profile and on the gel for comparison. T- the dialysed CP proteins loaded for comparison. Maximum effort was taken to emphasise the eluent protein bands on the gel during scanning, however they are not visible in the pictures as the band staining intensities were very low.

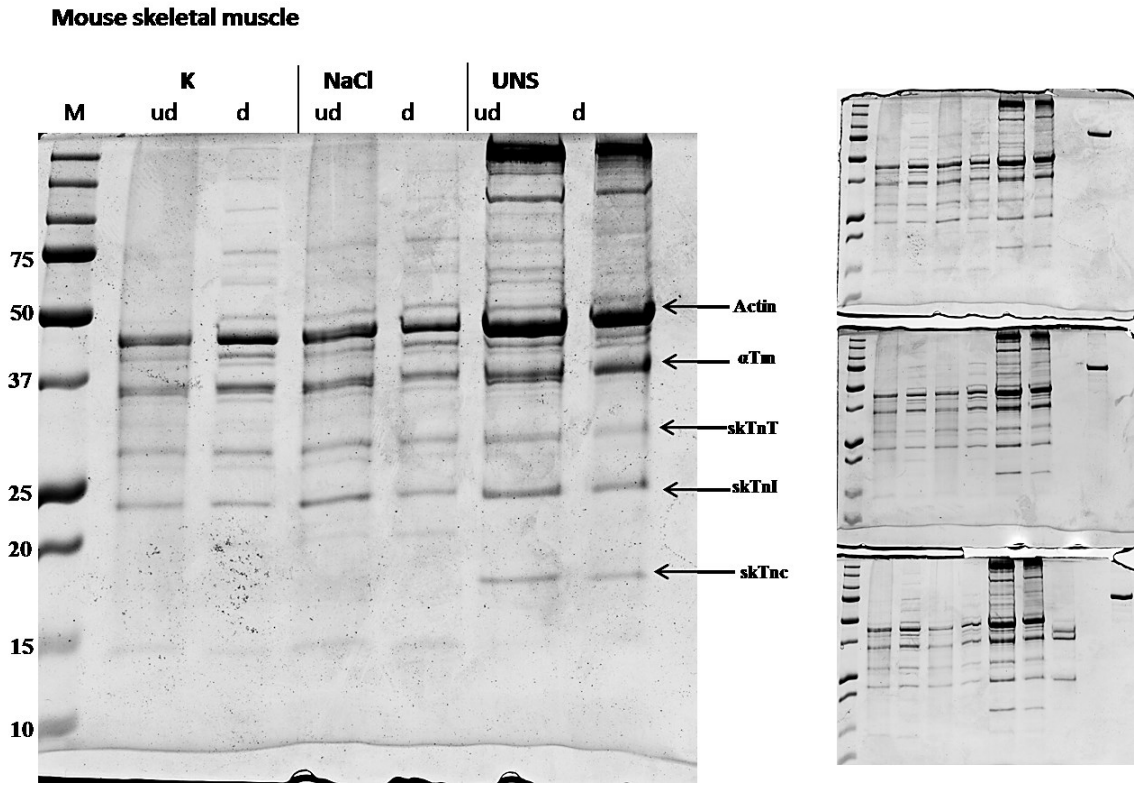

Figure 4.23: Mouse skeletal muscle extracts and triplicates. Ud-undialysed, d-dialysed, M- marker, K-KCl, Na – NaCl, UNS- Urea-NaCl-SDS.

Mouse skeletal extraction (Figure 4.23) shows urea with salt and detergent keeps myosin solubilize in the lysate without precipitating out in the even after dialysis. KCl and NaCl have similar extraction profiles, but KCl seems to have better resolution of TnT complex. The elution profile of mouse skeletal proteins (Figure 4.24) from buffer KCl show the separation of actin and tropomyosin at 36% and 37 % of B respectively in similar to chicken skeletal protein elution profile. Troponin complex proteins were not visible, however a band of approximately 13 kDa is observed on the gel which may be a fragment

of TnT (Ohtsuki, 1979) on SDS page. At around 42% all the proteins are eluted. Elution of protein with UNS were also however no identifiable bands on the SDS-gel were observed and hence the data is not given.

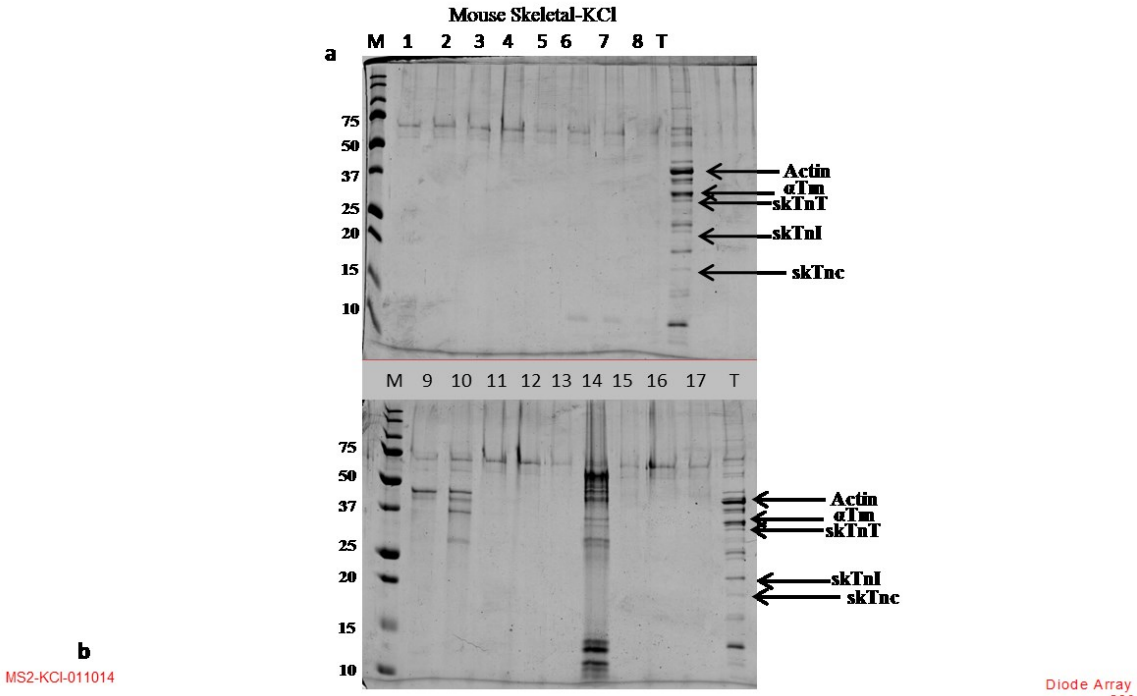

c

Peak no	1	2	3	4	5	6	7	8	9	10	11	12	13	14	15	16	17
Time (min)	4	8	12	16.5	21	22	23	25.5	26	27.5	30.5	32-33	34.5	36	37.5	40.5	47
%B	20-21	22	26	28	32	30	34	35	36	37	39	40	41.5	42	43	44	100

Figure 4.24: Reverse phase LC separation of mouse skeletal proteins. a. SDS gel showing the proteins of mouse skeletal muscle and the eluents collected form the LC profile. b. elution profile of HPLC run. c. table showing the peak number, retention time and the % B relating to the elution profile. The peak number resembles the number of the peak in the elution profile and on the gel for comparison. T- the dialysed CP proteins loaded for comparison.

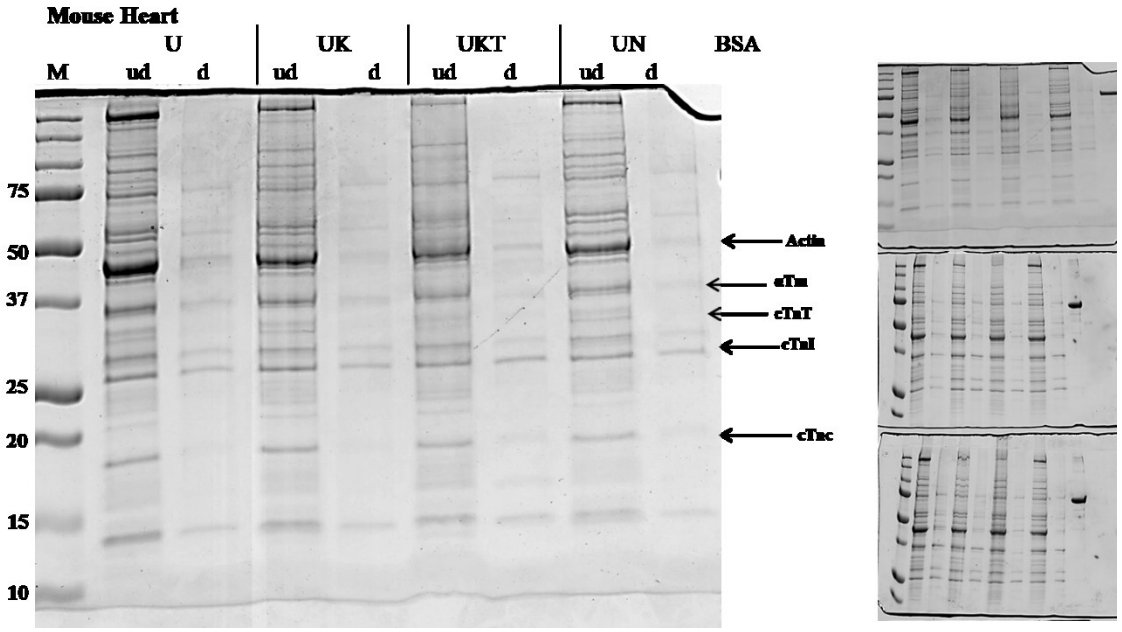

Figure 4.25: Mouse heart tissue extracts and triplicates. U-Urea, UK-Urea-KCl, UKT-Urea-KCl-Triton X100, UN-Urea-NaCl. Ud-undialysed, d- dialysed, M-marker.

Four buffers were used to check the extraction of mouse heart tissues (Figure 4.25) All the four buffer used, urea, UK, UKT and UN have shown to precipitate out myosin, and on the gel all buffers seem to show similar resolution of proteins, however a substantial loss of protein is observed after dialysis. Two buffer UK and UKT were selected for separation of protein by LC column, only UK profile is shown, as UKT gels did not show any identifiable bands hence the data is not shown. The elution profile shows (Figure 4.26) separation of Tropomyosin and Troponin T, at 36% and 38% B respectively. The bands are not clearly visible due to the gel background.

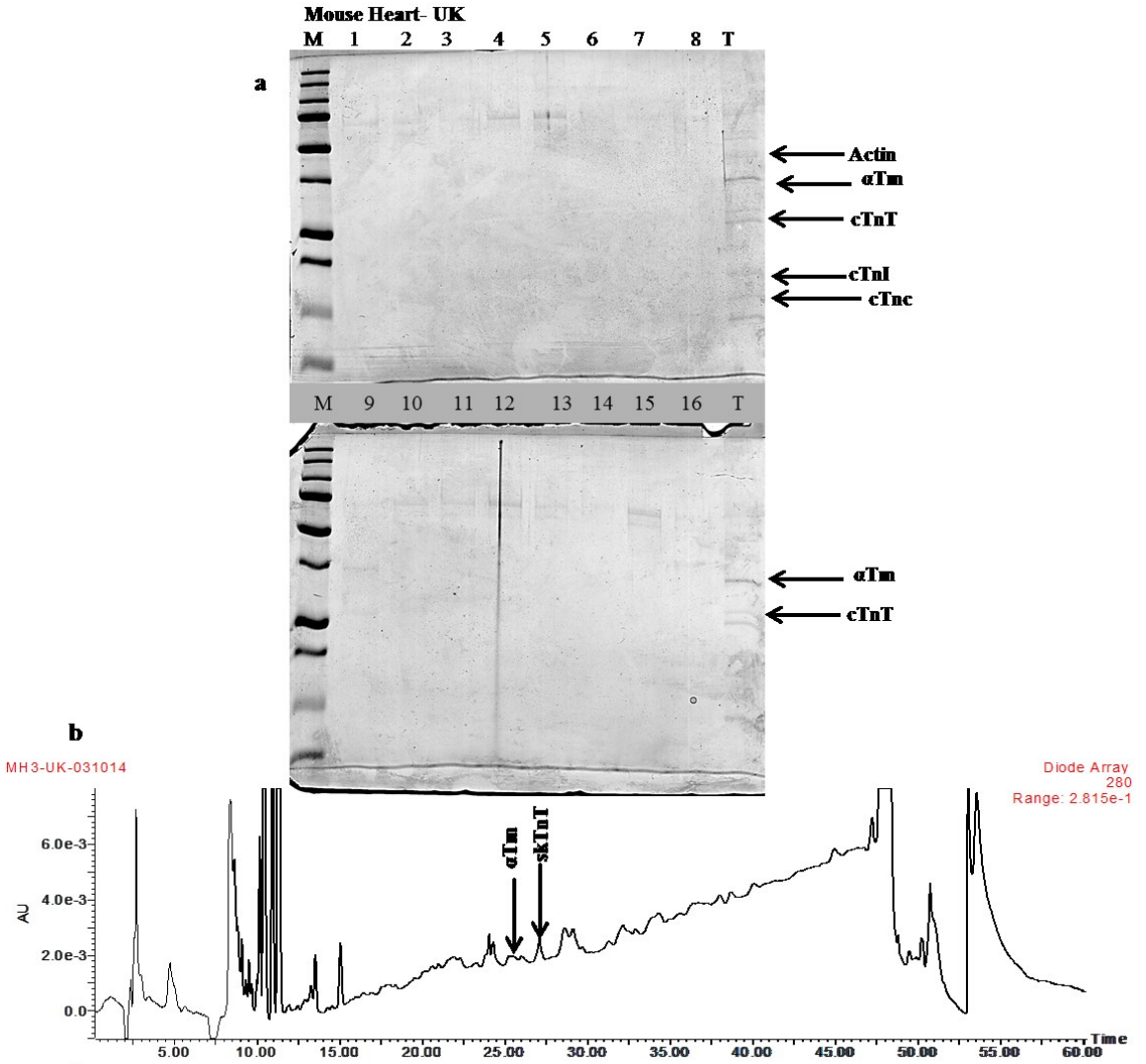

c

Peak no	1	2	3	4	5	6	7	8	9	10	11	12	13	14	15	16
Time (min)	4	8	10	12.5	14	16-18	20	24	26	27.5	32	33	34	37	43-46	48
%B		20	-	-	27	29-31	32	34	36	38	39	40	42	44	46-48	100

Figure 4.26: Elution profile of RP-LC for mouse heart proteins. a. SDS gel showing the proteins of mouse heart muscle and the eluents collected form the LC profile. b. elution profile of HPLC run. c. table showing the peak number, retention time and the % B relating to the elution profile. The peak number resembles the number of the peak in the elution profile and on the gel for comparison. T- the dialysed CP proteins loaded for comparison. Maximum effort was taken to emphasise the eluent protein bands on the gel during scanning, however they are not visible in the pictures as the band staining intensities were very low.

4.3 Discussion

Extraction of thin filament proteins

The thin filament proteins including actin, tropomyosin and troponin are the key mediators for contraction of cardiac muscle and skeletal muscle for performing the basic physiological functions of movement. Analysis of these proteins with a holistic approach will help to understand of human diseases relating to muscle disorders such as heart diseases.

In this study, an efficient extraction method is being developed for extraction of thin filament proteins using different buffer conditions with minimum amount of 2 mg tissue and also estimated the storage limitations of proteins in each buffer. This extraction procedure dramatically reduces the complexity of extraction method for thin filament proteins to study whole myofilament proteome relevant to heart left ventricle and skeletal muscle proteins. The analysis of thin filament of heart and skeletal muscle proteins by proteomic techniques has always been challenging due to the availability of biopsy samples especially heart samples and is limited by its small sample size. The amount of tissue chosen (2 mg) in this method is to reflect the amount of tissue available when human tissue is used which is very minimum from the methods available so far for thin filament tissue extraction methods. This method is modified from Labugger et al., (2002) who used 100 mg of tissue in four times volume of buffer. Here the amount of sample used and the volume of buffer is significantly reduced to 2 mg in 200 µl of buffer. The amount of tissue used in this method is the minimum amount of tissue used for a extraction of thin filament proteins for proteome analysis so far. Recently Peng et al., (2014b) developed method for analysis of cardiac myofilament proteome of swine heart

using 5 mg of protein in HEPES buffer for loading of 500 µg of sample per analysis and others . Anderson et al., (1991) used ~1 g of tissue from human heart for extraction of TnT isoforms and Erban (2011) also used 100 mg of tissue from mite bodies for purification for analysis of tropomyosin , actin and troponin using 2D gels. This method is an attempt to skip 2D gel analysis and also protein digestion step for analysis of protein by top-down mass spectrometry of the whole thin filament proteome. The amount of protein loaded on the SDS gel was ~200 ng and which was successful in visualizing the protein bands of actin, tropomyosin, TnT, TnI and TnC and myosin light chains identified using previous research results (Maytum et al., 2003). The main challenges to overcome for tissue extractions for mass spectrometry analysis is that the proteins extracted in the lysates should be pure for identification of proteins and their post-translational modifications. Secondly, it is important how long a tissue lysates could be stored for analysis.

Form the extraction profiles of chicken pectoral muscle (Figure 4.1), chicken heart (Figure 4.4), mouse skeletal (Figure 4.23) and mouse heart (Figure 4.25) shows the SDS page gels of the samples mentioned extraction. The major thin filament proteins were successfully identified from all the tissue samples with the small amount of protein lysate loaded (200 ng).

Storage of tissue and tissue lysates

The storage differences in time and differences in buffer conditions, it is clearly seen that there is substantial loss of protein even after one day of storage after dialysis (Figure 4.10 and Figure **4.11**) for chicken skeletal samples and Figure 4.13 and Figure 4.14 for heart samples. Freezing the extracted samples for one week or 4 weeks at -20 ^{0}C or -80 ^{0}C

does not vary much in losing the proteins. However this cannot be decided only by SDS page analysis, it would be beneficial to analyse the samples by mass spectrometry. As our mass spectrometer was broken and there was not enough time and funding to outsource the analysis, MS analysis was not performed.

It is important to consider the storage of tissues as well along with tissue lysates. The chicken skeletal muscle used in this study was frozen for 3 years. Comparing the Figure 4.1, Figure 4.9 and Figure 4.18, the number of protein bands visible are reduced from as the samples was stored at -20 ^{0}C and the difference in time of extraction and storage is in the order of 6 months to 1 year. After first extraction, the muscle was completely thawed in the fridge overnight due to power failure in the laboratory. The extraction from Figure 4.9 and Figure 4.18 were prepared after this incident with a time difference of few months, it can be clearly seen that the proteins are being degraded even in the tissue after thawing and freezing back. In the same manner heart samples extracted from frozen chicken hearts for couple of years from Figure 4.4 and Figure **4.11** and the tissue extracts from Figure 4.20 were prepared with in couple of months of freshly frozen chicken heart. From this it can be stated that out most care needs to be taken during proteomic analysis of tissues as freeze-thaw cycles may degrade the proteins which may result in loss of information while studying diseases.

Though there are many studies for tissue extraction and analysis (referenced in the above discussion) so far, there are no studies that reported regarding the storage of tissue and protein lysates. This gives an insight into the innate importance of storage of tissues for analysis of disease states.

Reverse phase liquid Chromatography

The RP- liquid chromatography elution profiles show that it is possible to elute thin filament proteins all at the same time to study the thin filament proteome with single extraction using a simple C5 column with a minimum sample amount loaded onto the column as less as ~100 ng. The preliminary method developed showed the separation of major thin filament actin, tropomyosin, troponin complex protein in rabbit, chicken and mouse samples. If this method is suitable for the tissue samples of these animals, it is possible to analyse human tissue samples with this minimum amount of sample size. Other methods available so far for proteome analysis shows either single protein isoforms by top-down mass spectrometry (Peng et al., 2013) using state-of-art advance MS systems like FTIR-MS or by peptide mass finger printing by tryptic digested peptides suing ESI-Tandem MS (Arrell et al., 2001b; Erban, 2011; Labugger et al., 2002). As the proteins fractions collected and run on the gel are visible on the gel with such a small amount of sample using Coomassie staining, more sensitive staining method like silver stain will enable to visualize the protein bands more clearly. There are many other proteins that are visible on the gel which may be the fragments of troponin, that can be seen around 20 kDa and 13 kDa (Ohtsuki, 1979) myosin light chain seen around 20 kDa and other isoforms and smaller additional proteins. If mass spectrometry analysis is applied there is high possibility of identifying these proteins. In the non-availability of MS system, monoclonal antibodies specific to all the known proteins could be used to identify the protein bands.

Acetonitrile used in this method is one of the most compatible solvents for MS analysis (Neverova and Van Eyk, 2005), is another advantage for this method for analysis of thin

filament proteome for top down MS as use of methanol for prolonged use in RPLC may result in methylation of few proteins during analysis (Gregorich and Ge, 2014).

In conclusion, this study shows an efficient method for extraction of tissue samples with minimum amount of sample size and the RP-HPLC method developed gives efficient myofilament protein separation suitable for mass spectrometry analysis. When the proteins are visible on an SDS-PAGE, it can be noted that the sample lysate used has enough proteins required for identification by MS analysis. This method surpass the use of time consuming 2D gel analysis and may prove useful for identification and quantification of proteins and their changes in various forms of cardiac and skeletal muscle diseases with a single extraction reducing the time for analysis and sample size.

Chapter V

5 Conclusion

Expression of tropomyosin 3.12st in E.coli

Tropomyosin 3.iso12st protein encoded by *TPM3* gene found in slow twitch muscle fibers. It is found to be responsible for many muscle disorders caused by genetic mutations such as described in sections 1.6, 1.7 and 1.8. In the present study Tpm3.12st was successfully expressed in *E.coli* and its actin binding affinity was characterised in comparison with three other protein isoforms encoded with the alternative genes of tropomyosin (Tpm1.1st, Tpm2.2st and Tpm4.1cy). Tpm1.1st is the most extensively studied tropomyosin isoform from the time tropomyosin was discovered (Gunning et al., 2008a; Hitchcock-DeGregori et al., 1985; Lehman et al., 2000a; Schevzov et al., 2005; Spudich and Watt, 1971; Wegner, 1979). Tpm2.2 has also been characterised. Tpm3.12st and nonmuscle Tpm4.1cy are not characterised so far for its actin binding affinity. Marston et al., (2013) expressed Tpm3.12st in baculovirus expression system to study the isoform variations in comparison with tissue extracts of tropomyosin however it was not characterised for its actin binding properties. Tropomyosin is one the thin filament proteins which plays a major role in regulating actin filaments in muscle and nonmuscle cells. Hence understand how this isoform is affecting in comparison with other major striated muscle isoforms (Tpm1 and Tpm2) and non-muscle isoform (Tpm4) is very important to decipher its role in health and disease states.

Tpm3 was successfully expressed in *E. coli* with three variants of N-terminal extension. Tpm3-Met, Tpm3-MM and Tpm3-(M)ASM were purified and checked for its actin

binding affinity along with Tpm1 (with N-terminal AS), Tpm2 (Without N-terminal AS) and Tpm4 (with N-terminal AS). The N-terminal extension with AS mimics the post-translational modification process of N-terminal acetylation (Monteiro et al., 1994) and is required to maintain its 'local' structure for head-to-tail polymerisation and for actin binding (Urbancikova and Hitchcock-DeGregori, 1994) as discussed in section 2.4.2.3 Proteins expressed were found to be pure and the molecular weight is confirmed by mass spectrometry showed the protein to be Tpm3 with a molecular weight of 32823.6, 32950.8 and 32821.1 for Tpm3-Met, MM and MASM variants respectively. From the mass it is confirmed that MASM variant lost its N-terminal Met and the other two variants had intact Met (Table 2.3). Tpm4 isoform produced had a mass difference of ~57 Da, the possibility of losing the C-terminal lysine was higher but could be confirmed at with the available data. Further investigation is need to confirm the sequence.

Actin binding affinity

These variants were studied for their actin binding affinity along with Tpm1 and Tpm2 as the later were characterised for their binding affinity (Heald and Hitchcock-DeGregori, 1988; Maytum et al., 2001). Cosedimentation assays were performed for their actin binding affinity using ultra centrifugation. The tropomyosin affinity to actin is important for its regulatory function in physiological conditions. Tpm3-MASM was found to have similar binding affinity as Tpm1 with 0.2 μM tropomyosin (half saturation). However Met and MM bound to actin weekly with half saturation of ~6 μM and 8 μM respectively (Figure 2.24Figure 2.25Figure 2.26). Even though Met was expected not to bind actin efficiently, however MM was expected to bind to actin in similar way to Tpm1 as this resembles the original sequence of human Tpm3 isoform and also the presence of two

small MM should be retaining the actin binding property. However this was not the case, as MM affinity to actin was very low. From this it can be stated that the original N-terminal sequence of Tpm3 (Figure 2.1) should be having a single methionine residue rather than two methionine. Further investigation in this area is need to confirm the sequence and it would be advantage to study the stability of the tropomyosin polymers using circular dichroism to differentiate the stability with in the three variants of tropomyosin.

Effect of tropomyosin isoforms on actin polymerisation

Characterising the role of tropomyosin isoform function in non-muscle actin polymerisation produced very interesting results and has high potential for future work in understanding the dynamics of actin polymerisation in presence of different isoforms of tropomyosin (section 2.2) Different muscle and non-muscle isoforms affect rate of actin polymerisation differently by effecting either initiation or elongation or affecting both of the mechanisms (Keiser and Wegner, 1985; Wegner, 1982b). Since 1990's there have been very few studies that carried out effect of tropomyosin isoforms on actin polymerisation. Although there are many studies on the structural analysis of interaction of actin-tropomyosin (Ecken et al., 2014; Lehman et al., 2000b), the information available on isoform specificity on actin polymerisation is limited. This work provides the preliminary information on the isoform specificity on actin polymerisation dynamics.

The present study shows contradictory results obtained from previous studies which states that tropomyosin inhibits actin polymerisation (Hitchcock-DeGregori et al., 1988; Kouyama and Mihashi, 1981; Lal and Korn, 1986). The present study shows the data that tropomyosin accelerates the initiation stage of actin polymerisation, however inhibits the

elongation process, but the amount of filament formation seems to be higher in presence of tropomyosin for some isoforms (section 2.5.8, Table 2.5). It is also observed that it's the concentration of tropomyosin that is affecting the actin polymerisation kinetics and varying the actin concentration does not have any effect on individual polymerisation stages of actin such as initiation or elongation. As the concentration of actin increases the polymerisation is faster without affecting the critical concentration. However, from the data available critical concentration of actin is affected in presence of tropomyosin as there seem to be higher amount of filament formation in presence of tropomyosin observed from the increase in fluorescence intensity after the polymerisation reaches a steady state (which is an indicator of critical concentration of monomer actin). Further investigation is needed to understand the role of tropomyosin and isoform specificity on actin polymerisation. From the data available a kinetic model needs to develop to accurately justify the data.

Identification of Tpm3.12st using monoclonal antibodies

An attempt was made to design an monoclonal antibody to react specifically to Tpm3.12st (Chapter III). None of the 12 antibodies produced did not have specificity to only Tpm3.12st, however one of the antibody (Ab3) reacting to P4 have higher sensitivity to Tpm3.12st than Tpm1.1st (Table 3.5) Due to very high sequence similarity of tropomyosin isoforms, it is a difficult task to design an antibody specific to only one isoform. Gajbhiye et al., (2012) identified Tpm3 isoforms from laparoscope samples of women reproductive organs having cystic fibrosis. However the peptides when matched with the high molecular weight Tpm3 sequence were having sequence similarity with Tpm1 and Tpm4. From the observation of this study and previous studies (Schevzov et

al., 2011a), an antibody designed with Tpm3.12st sequence form amino acids 24 to 43 may have high chances of producing an antibody specific to Tpm3.12st. The ELISA screening method developed is very useful to check the sensitivity of antibodies and to quantify the Tm-antibody reactivity. Accurate quantification of tropomyosin isoforms is key to understanding their function and the effects of modulation of isoform composition in health and disease.

Resolution of thin filament proteome using RPLC

A successful preliminary optimization of an effective method for extraction of thin filament proteins mainly actin, tropomyosin and troponin and other small soluble proteins was established using a minimum amount of 2 mg of tissue sample with different buffer conditions. This method surpass the use of 2D gels and has the potential of identifying proteins and their isoforms and post-translational modifications found in the skeletal and cardiac muscle proteins using top down mass spectrometry. The RPLC method developed was successful in identification of actin, tropomyosin and troponin subunits. The amount of sample loaded on the column was ~100 ng and it is the first time anyone used such a small amount to identify thin filament proteins although there have been few research groups that developed method for analysis of cardio proteome (Peng et al., 2014b) and Matthijs Jan Faber (PhD research work 2012 from Erasmus university of Rotterdam). As with this amount of sample a protein band is visible on a SDS-gel page there is possibility of using much lower amount of sample using the buffer conditions.

The method once optimized has a great potential to use as a diagnostic indicator to identify the protein modifications in diseased heart in a very short amount of time with minimum amount of sample. This will enable to understand the cause of muscle

adaptation due to age, exercise or diseases in humans. This method is also useful for quantification of identified protein isoforms and the ratio of the of the isoform composition by top-down mass spectrometry as it established to be in compatible with MS analysis. The method also has an advantage in its ability to prediction of functional and structural changes occurring in thin filament.

The work in this thesis, establishes various methods to quantify tropomyosin isoforms identify the function and composition of tropomyosin isoforms and to quantify the changes in the dynamics of actin polymerisation in presence of various tropomyosin isoforms and provides some research questions for future work in understanding the role of tropomyosin in muscle and nonmuscle cells in health and disease.

5.1 Future Work

The work presented in this thesis although have produced some successful results, the work could be extended in characterizing the tropomyosin isoforms because of significance of these isoforms in maintaining the muscle's health. It is important to understand the role of specific tropomyosin isoforms, in this case Tpm3.12st, in order to recognize the modifications occurring during the diseased states and how it is affecting in comparison with other major striated muscle isoforms (Tpm1 and Tpm2) and non-muscle isoform (Tpm4).

Characterisation of Tpm3.12st

Studying the stability of different variants of Tpm3.12st isoforms using circular dichroism to further characterize the protein would be useful to compare this protein with other striated tropomyosin isoforms as well as for confirmation of the N-terminal

sequence. Studies involving the comparison of difference in the binding affinity of recombinant protein with tissue extracted from pure tropomyosin.

Further extending the characteristion of tropomyosin isofroms in their role in actin polymerization as it is well established fact that tropomyosin isoforms in non-muscle cells are in different concentrations depending on the function of the region of the cell. The importance of studying the effect of tropomyosin on actin polymerisation is it gives the ability to quantitatively measure the incorporation of monomer to polymer and how presence of tropomyosin molecule affects this polymer association.

A specific answer to whether tropomyosin plays a role in actin polymerisation is not available so far and there is no data available for explaining the reasons even thought it is well established that tropomyosin plays a significant role in regulating actin filaments as explain in section 2.2.4. The present study provides qualitative data showing that tropomyosin effect the inititation rate of actin polymerisation and the effect is different with various tropomyosin isoforms. Inorder to achieve a better understanding of diverse functions of tropomyosin isofroms in actin polymerisation it is important to study and establish a experimental protocol to obtain more data to decipher the significant role played by tropomyosins in actin polymer formation.

From the data obtained in this study more data relating to nucleation – elongation rate constants need to be collected. Measuring the filament length of F-actin after polymerisation by tagging it by phallodin and obtaining data using fluorescence microscopy would give information of the filament length of actin in presence and absence of tropomyosin and also whether tropomyosin initiaties fragmentation of actin filaments in specific conditions. Secondly, the initial G-actin and final G-actin and F-

actin concentration needs to be measured to check the critical concentration of monomeric actin in presence and absence of tropomyosin, which may give approximate values in comparison to biological systems.

Some of the methods mentioned below can be applied for studying actin polymerisation:

- Polymerisation can be studied under fluorescent microscopy by labelling tropomyosin with fluorescent dye such as N-(1- anilinonaphth-4-y1) maleimide (Morris and Lehrer, 1984) or (dimethylamino)naphthalene (Weigt et al., 1991) label covalently linked to tropomyosin can be used along with pyrene labelled G-actin to see how tropomyosin is effecting the nucleation / initiation stage of actin polymerisation. The effect of tropomyosin on actin can be studied with i. various concentration of tropomyosin, ii. Various concentration of actin iii. different concentration of Mg^{2+} and K^{+} ions
- By collecting the above data mentioned, developing a kinetic model to accurately present the data and to explain polymerisation kinetics of actin in presence of tropomyosin.
- Single molecule fluorescent imaging (Desai et al., 2014; Kad and Van Houten, 2014) by using single tropomyosin molecule in a pool of G-actin may help to investigate the initiation step by polymerizing G-actin in presence of tropomyosin alone.

Identification of tropomyosin isofroms

In this study twelve antibodies with five peptides were generated in order to differentiate Tpm3.12st isofrom from other muscle and non-muscle isofroms. From the results obtained as explained in section 3.5.3.3, designing an antibody for Tpm3.12st isoform

from amino acids residues of 24-43 (Figure 3.7) may produces a monoclonal antibody which may be only specific to Tpm3.12st.

On the other hand a method was developed for extraction of thin filament proteins and separation of the proteins using reverse phase liquid chromatography. The method developed has potential in using for identification and quantification of tropomyosin isofroms, actin and troponin isofroms from one single extraction with minimum amount of tissue sample (2 mg). Proteins were successfully separated and identified on an SDS PAGE gel comparing from previous research. However, using specific antibodies for identification of α-actin, TnC, TnI and TnT, myosin light chains, and tropomyosin will confirm the proteins eluted from the separation of proteins form the tissue lysate. Optimizing the method for analysis of the proteins by mass spectrometry would be highly advantages to identify isoforms and post translational modification of thin filament proteins. This method could be beneficial to extend it to analysis of human biopsy samples to investigate the differential expression of proteins and PTMs where the amount of tissue available is critical for analysis.

6 Appendix

6.1 List of chemicals and reagents

Table 6.1: List of Chemicals

Chemicals / Reagents / Reagent kits	Suppliers
Acrylamide-Bisacrylamide	30% Protogel
Adenosine triphosphate (ATP)	Sigma Aldrich
Agar	Fisher Scientific
Agar for electrophoresis	Bioline
Ammonium bicarbonate	Acros Organics
Ammonium bromide	Fisher scientific
Ampicillin	Sigma Aldrich
Ammonium persulfate (APS)	Fisher scientific
Amersham Hybond ECL Nitrocellulose membrane	GE Healthcare
Bacteriological peptone	Oxoid
Benzamidine hydrochloride	Sigma Aldrich
Bromophoenol Blue	Fisher Biotech
Clones	Thermo scientific
Calcium chloride	BDH
Citric acid	Fisher Scientific
Coomassie brilliant blue G250	Fisher Scientific
DNA plasmid extraction Kit	Eppendorf
Deoxynucleotide Triphosphates (dNTPs)	Thermo Scientific
Dextran	BDH
Dimethyl sulfoxide (DMSO)	Sigma Aldrich
Dimethylformamide (DMF)	Sigma Aldrich
Dithiothreitol (DTT)	Sigma Aldrich
Ethanol (absolute)	Fisher Scientific
Ethidium bromide	Sigma Aldrich
Ethylenediaminetetraacetic acid (EDTA)	BDH
Ethylene glycol-bis(2-aminoethylether)tetraacetic acid	BDH

(EGTA)	
Formic acid	Fisher Scientific
Gel purification kit	Eppendorf
Glacial acetic acid	Fisher Scientific
Glucose	AnalaR
Glycerol	Fisher Scientific
Glycine	Fisher Scientific
Hydrochloric acid	Fisher Scientific
Iso Propanol	Fisher Scientific
Isopropyl-β-D-thiogalactopyranoside (IPTG)	Melford
3-(N-Morpholino)propanesulfonic acid (MOPS)	BDH
N-(1-Pyrenyl)iodoacetamide	Sigma Aldrich
β-Mercaptoethanol	Sigma Aldrich
Magnesium chloride	Fisher Scientific
Magnesium sulfate	Fisher Scientific
Methanol	Fisher Scientific
Milk powder	Marvel original dried skimmed milk powder
Nunc-immuno maxisorp , flat bottom 96well plates	Sigma-Aldrich
Primers	Thermo Scientific
PCR buffer	Thermo Scientific
Protein marker	Biorad Precision plus
Phenylmethylsulfonyl fluoride (PMSF)	Sigma Aldrich
Polyethylene glycol	Fisher Scientific
Potassium chloride	Fisher Scientific
Potassium monophosphate	BDH
Pyrene iodoacetamide	Sigma Aldrich
Restriction enzymes	New England Biolabs (NEB)
Sodium azide	BDH
Sodium chloride	Fisher Scientific
Sodium dodecyl sulfate (SDS)	Fisher Scientific
Sodium hydroxide	BDH
Sodium phosphate	Fisher Scientific
Sodium monophosphate	BDH

Sodium ortho pohophate	BDH
Sucrose	BDH
Sulphuric acid	Sigma Aldrich
3,3',5,5'- Tetramethylbenzidine (TMB)	Sigma Aldrich
N,N,N',N'-Tertamethylethylenediamine (TEMED)	Sigma Aldrich
Taq Polymerase	Thermo Scientific
Tris Base	Fisher Scientific
Triton X	Sigma Aldrich
Tween 20	Sigma Aldrich
Urea	Fisher Scientific
Yeast Extract	Oxoid

6.2 BUFFERS

Resolving Gel (13.5%)

Chemical	30% Protogel Acrylamide (2gels)
Acrylamide-Bisacrylamide	3.6ml
Resolving buffer (4x – 1.5M, pH8.8))	2.0 ml
dH_2O	2.33 ml
Ammonium Persulfate (APS)	50ul
TEMED	15ul

Stacking Gel

Chemical	30% Protogel Acrylamide (2gels)
Acrylamide –Bisacrylamide	1.07 ml
Stacking buffer (0.5M, pH 6.8)	1.0 ml
dH_2O	1.9 ml
APS	30ul
TEMED	10ul

Resolving buffer

Chemical	250ml
1.5M Tris base (MW 121.14)	45.42 g
0.4% SDS	10g
dH_2O	250ml

Dissolve Tris in 150ml water and adjust the pH to 8.8 using HCl and add SDS and make up the volume to 250ml.

Stacking Buffer

Chemical	250ml
0.5mM Tris(1.5M Stock , pH 8.8)	83.3 ml
0.4% SDS	10g

To 83.3 ml of 1.5 M Tris Stock, add 100ml dH_2O, adjust the pH to 6.8 and add SDS and make up to 250ml with water.

Extraction buffers for muscle tissue

Chemical (mol weight)	50ML
6M Urea (60.06)	18.018g
1M KCl (74.56)	3.728g
1M NaCl (58.44)	2.92g
0.5% Triton X	0.25ml
0.5% SDS	0.25g

Low salt buffer for dialysis

Chemical	1L
2mM Tris	1ml from 1.0M Tris-HCl stock, pH 8.
2mM $CaCl_2$	1ml from 1M $CaCl_2$ stock
0.2mM DTT	0.015g (15µg)

4X SDS loading buffer

Chemical	10ml
0.5M Tris-HCl pH 6.8	2.5ml (can use stacking buffer)
Gylcerol	4.0ml
10% SDS	0.25g (250mg)(Use solid)
0.1% Bromophenol blue	50mg
β mercaptoethanol	1ml

Coomassie Stain – Brilliant blue G (or commassie blue G250)

Chemical	500ml
0.1%Coomassie blue G250	500mg
25% Methanol	125ml
5% Acetic acid	25ml

10X SDS Running buffer

Chemical	500ml	1000ml
Tris base (solid)	15.15g	30.3g
Glycine	72.0g	144.0g
SDS	5.0g	10.0g

Protease Inhibitors

0.1M PMSF stock – 0.01744g in 1ml ethanol

0.1M Benzamidine - 0.01566g in 1ml ethanol

10ul of stock give 1mM in 1ml buffer

LB medium

Chemical	1L	500ml	250ml	100ml
Bactopeptone	10g	5g	2.5g	1.0g
Yeast extract	5g	2.5g	1.25g	0.5g
NaCl	5g	2.5g	1.25g	0.5g
Agar (1.5%)	15g	7.5g	3.75g	1.5g

pH 7.5 with NaOH

Ampicillin stock 100mg/ml: Working concentration (100µg/ml) : 1µl to 1ml give 100µg/ml

1L medium – 100mg solid

IPTG stock 100mg/ml: Working concentration (100ug/ml) : 1µl to 1ml give 100µg/ml

1L medium – 100mg of solid

Competent cell preparation media

Medium A

10mM $MgSO_4$	0.5ml from 1M stock
0.2% Glucose	1ml from 10% stock

*1ml is saved for storage process at the end

Stocks for medium A

$MgSO_4$ – 1M	12.324g in 50ml
Glucose 10%	5g in 50ml

*Filter sterilize then before storing

Storage solution B

Glycerine	36%
PEG	12%
$MgSO_4$	12mM

*Added to LB medium and filter sterilized

Lysis buffer

Chemical	100ml
20mM Tris pH 7.5	0.242g
150mM NaCL	0.8766g
5mM EDTA	0.2081g

From stocks

Stock	Conc.	100ml	250ml
1M Tris-HCl pH 7.5	20mM	2ml	5ml
NaCl (Use solid)	150mM	0.8766g	2.193g
500mM EDTA	5mM	1ml	2.5ml

Phosphate buffer

1M NaH_2PO_4 + 1M Na_2HPO_4 – 100ml

1M NaH_2PO_4	1M Na_2HPO_4
12g	14.2g

*Mix both the solutions to pH 7.0. For 500ml-5mM working solution – 2.5ml of 1M

TIP* - take di-basic first and add the acidic mono-basic to it.

PBS buffer

Chemical	1L	500ml
NaCl	80g	40g
KCl	2.0g	1.0g
Sodium monophosphate (dihydrate) $Na_2HPO_4.2H_2O$	14.4	7.2
Potassium monophosphate (KH_2PO_4)	2.5g	1.2g

10X TAE buffer

Chemical	500ml
40mM Tris base	24.2g
20mM Glacial acetic acid	5.7ml
1mM EDTA (dibasic)	0.186g

Western blotting transfer buffer

Chemical	250ml	500ml
48mM Tris base	1.45g	2.91g
39mM Glycine	1.465g	0.733g
SDS	0.187g	0.095g
20% Methanol	100ml	50ml

Note: Make it fresh when ever needed.

Citric-EDTA-Dextrane sulfate buffer

Chemical	100ml
Citric acid	0.21g
1% Dextran sulfate	1g
EDTA	0.37g

6.3 ProtParam – Tpm3 Sequence information

Protein sequence information extracted from ExPASy-ProtParam tool.

ProtParam-TPM3-Met

```
MEAIKKKMQM LKLDKENALD RAEQAEAEQK QAEERSKQLE DELAAMQKKL KGTEDELDKY
70         80         90         100        110        120
SEALKDAQEK LELAEKKAAD AEAEVASLNR RIQLVEEELD RAQERLATAL QKLEEAEKAA
130        140        150        160        170        180
DESERGMKVI ENRALKDEEK MELQEIQLKE AKHIAEEADR KYEEVARKLV IIEGDLERTE
 190        200        210        220        230        240
ERAELAESKC SELEEELKNV TNNLKSLEAQ AEKYSQKEDK YEEEIKILTD KLKEAETRAE
250        260        270        280
FAERSVAKLE KTIDDLEDEL YAQKLKYKAI SEELDHALND MTSI
```

Number of amino acids: 284

Molecular weight: 32818.7

Theoretical pI: 4.68

Top of Form

Extinction coefficients:

This protein does not contain any Trp residues. Experience shows that this could result in more than 10% error in the computed extinction coefficient.

Extinction coefficients are in units of M^{-1} cm^{-1}, at 280 nm measured in water.

Ext. coefficient 8940

Abs 0.1% (=1 g/l) 0.272, assuming all pairs of Cys residues form cystines

Ext. coefficient 8940

Abs 0.1% (=1 g/l) 0.272, assuming all Cys residues are reduced

Estimated half-life:

The N-terminal of the sequence considered is M (Met).

The estimated half-life is: 30 hours (mammalian reticulocytes, in vitro).

>20 hours (yeast, in vivo).

>10 hours (Escherichia coli, in vivo).

Instability index

The instability index (II) is computed to be 43.92

This classifies the protein as unstable.

Aliphatic index: 83.70

ProtParam – Tpm3 -MM
User-provided sequence:

```
        10         20         30         40         50         60
MMEAIKKKMQ MLKLDKENAL DRAEQAEAEQ KQAEERSKQL EDELAAMQKK LKGTEDELDK

        70         80         90        100        110        120
YSEALKDAQE KLELAEKKAA DAEAEVASLN RRIQLVEEEL DRAQERLATA LQKLEEAEKA

       130        140        150        160        170        180
ADESERGMKV IENRALKDEE KMELQEIQLK EAKHIAEEAD RKYEEVARKL VIIEGDLERT

       190        200        210        220        230        240
EERAELAESK CSELEEELKN VTNNLKSLEA QAEKYSQKED KYEEEIKILT DKLKEAETRA

       250        260        270        280
EFAERSVAKL EKTIDDLEDE LYAQKLKYKA ISEELDHALN DMTSI
```

Number of amino acids: 285
Molecular weight: 32949.9
Theoretical pI: 4.68
Total number of negatively charged residues (Asp + Glu): 80
Total number of positively charged residues (Arg + Lys): 52
Atomic composition:

Carbon	C	1410
Hydrogen	H	2343
Nitrogen	N	391
Oxygen	O	493
Sulfur	S	9

Formula: $C_{1410}H_{2343}N_{391}O_{493}S_9$
Total number of atoms: 4646
Extinction coefficients:
This protein does not contain any Trp residues. Experience shows that this could result in more than 10% error in the computed extinction coefficient.
Extinction coefficients are in units of M^{-1} cm^{-1}, at 280 nm measured in water.
Ext. coefficient 8940
Abs 0.1% (=1 g/l) 0.271, assuming all pairs of Cys residues form cystines
Ext. coefficient 8940
Abs 0.1% (=1 g/l) 0.271, assuming all Cys residues are reduced
Estimated half-life:
The N-terminal of the sequence considered is M (Met).
The estimated half-life is: 30 hours (mammalian reticulocytes, in vitro).
>20 hours (yeast, in vivo).
>10 hours (Escherichia coli, in vivo).
Instability index:
The instability index (II) is computed to be 43.70
This classifies the protein as unstable.
Aliphatic index: 83.40
Grand average of hydropathicity (GRAVY): -1.040

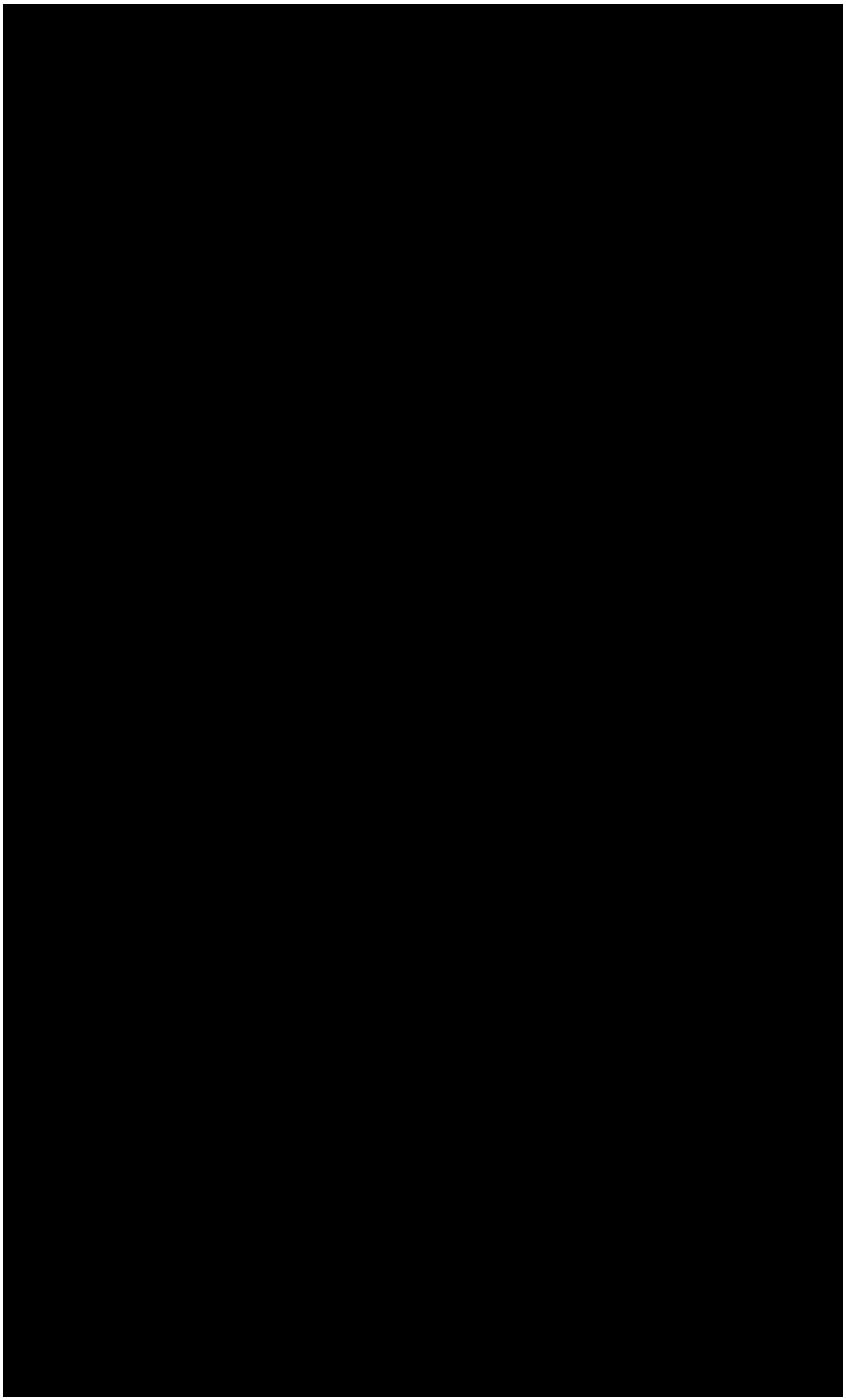

6.4 Duplicates of Elisa Preliminary checker board optimization.

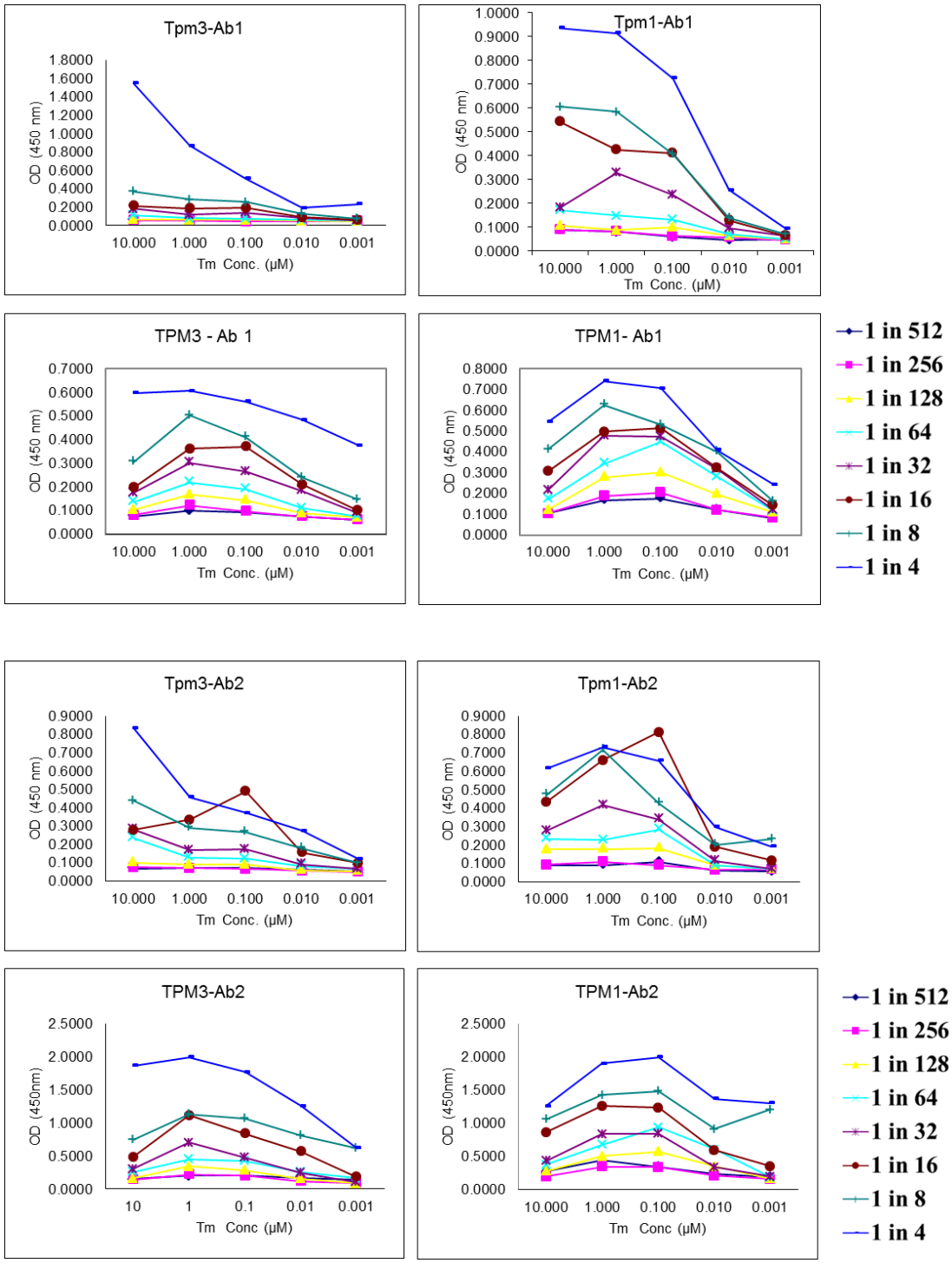

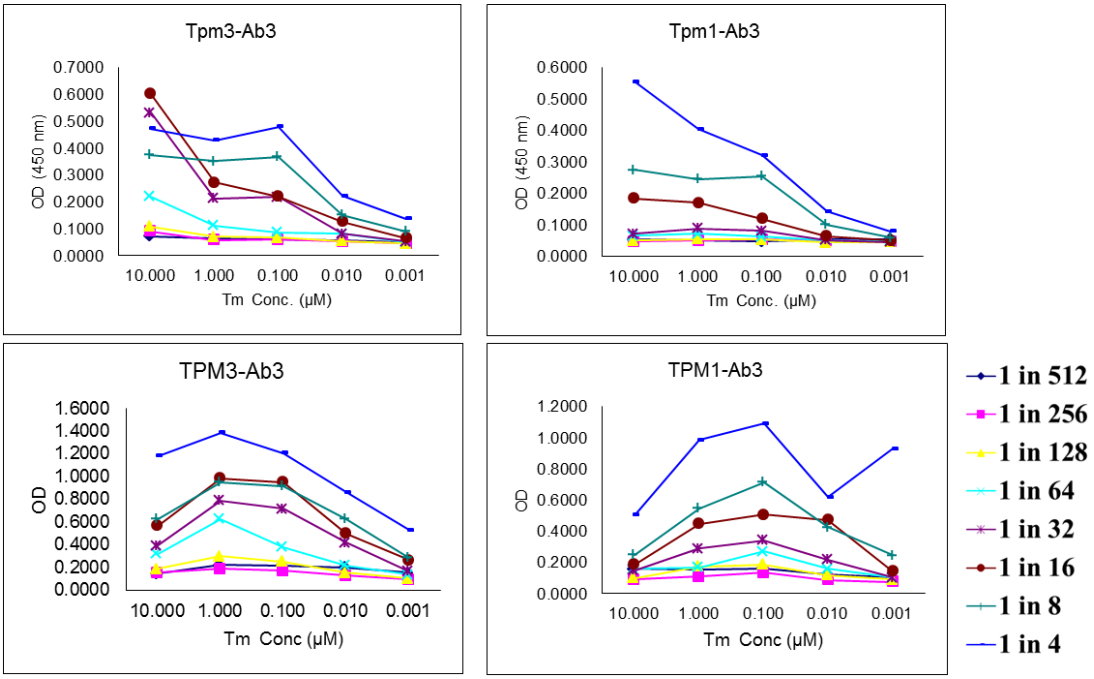
Tpm3-Ab3
OD (450 nm)
0.7000
0.6000
0.5000
0.4000
0.3000
0.2000
0.1000
0.0000
10.000 1.000 0.100 0.010 0.001
Tm Conc. (µM)
Tpm1-Ab3
OD (450 nm)
0.6000
0.5000
0.4000
0.3000
0.2000
0.1000
0.0000
10.000 1.000 0.100 0.010 0.001
Tm Conc. (µM)
TPM3-Ab3
OD
1.6000
1.4000
1.2000
1.0000
0.8000
0.6000
0.4000
0.2000
0.0000
10.000 1.000 0.100 0.010 0.001
Tm Conc (µM)
TPM1-Ab3
OD
1.2000
1.0000
0.8000
0.6000
0.4000
0.2000
0.0000
10.000 1.000 0.100 0.010 0.001
Tm Conc (µM)
1 in 512
1 in 256
1 in 128
1 in 64
1 in 32
1 in 16
1 in 8
1 in 4

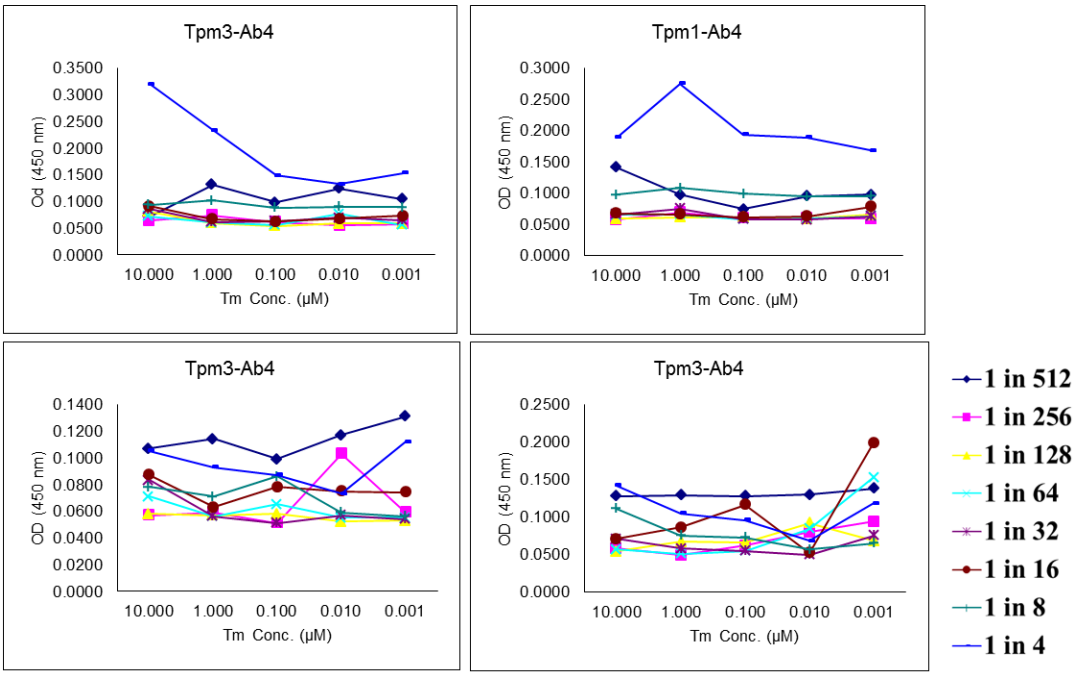
Tpm3-Ab4
Od (450 nm)
0.3500
0.3000
0.2500
0.2000
0.1500
0.1000
0.0500
0.0000
10.000 1.000 0.100 0.010 0.001
Tm Conc. (µM)
Tpm1-Ab4
OD (450 nm)
0.3000
0.2500
0.2000
0.1500
0.1000
0.0500
0.0000
10.000 1.000 0.100 0.010 0.001
Tm Conc. (µM)
Tpm3-Ab4
OD (450 nm)
0.1400
0.1200
0.1000
0.0800
0.0600
0.0400
0.0200
0.0000
10.000 1.000 0.100 0.010 0.001
Tm Conc. (µM)
Tpm3-Ab4
OD (450 nm)
0.2500
0.2000
0.1500
0.1000
0.0500
0.0000
10.000 1.000 0.100 0.010 0.001
Tm Conc. (µM)
1 in 512
1 in 256
1 in 128
1 in 64
1 in 32
1 in 16
1 in 8
1 in 4

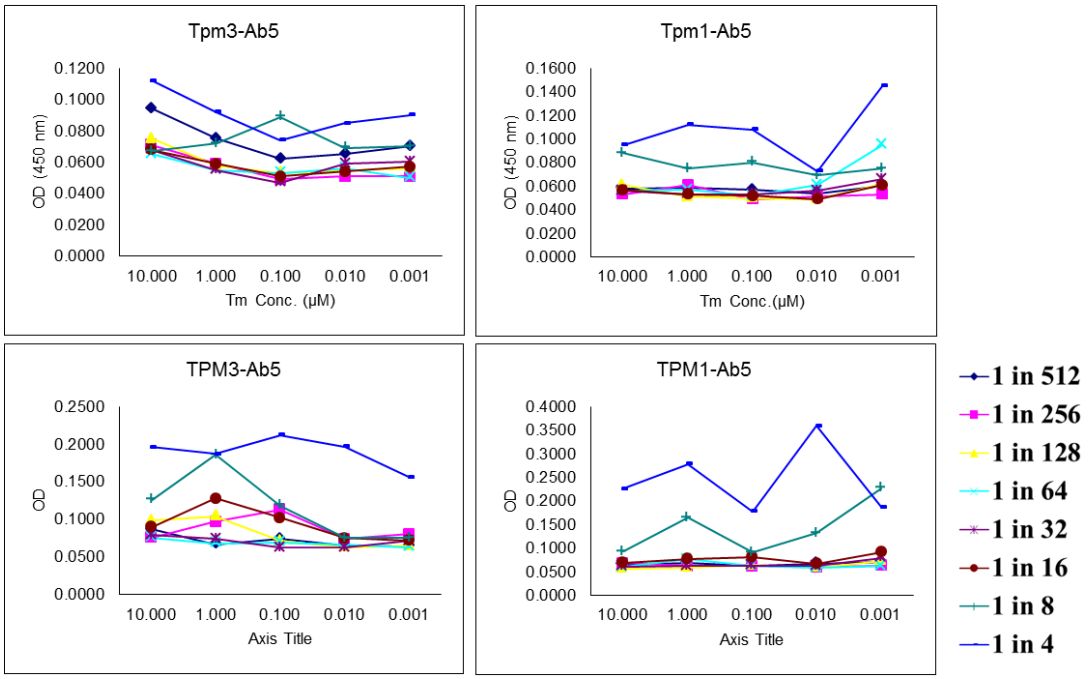
Tpm3-Ab5
OD (450 nm)
0.1200
0.1000
0.0800
0.0600
0.0400
0.0200
0.0000
10.000 1.000 0.100 0.010 0.001
Tm Conc. (μM)
Tpm1-Ab5
OD (450 nm)
0.1600
0.1400
0.1200
0.1000
0.0800
0.0600
0.0400
0.0200
0.0000
10.000 1.000 0.100 0.010 0.001
Tm Conc.(μM)
TPM3-Ab5
OD
0.2500
0.2000
0.1500
0.1000
0.0500
0.0000
10.000 1.000 0.100 0.010 0.001
Axis Title
TPM1-Ab5
OD
0.4000
0.3500
0.3000
0.2500
0.2000
0.1500
0.1000
0.0500
0.0000
10.000 1.000 0.100 0.010 0.001
Axis Title
1 in 512
1 in 256
1 in 128
1 in 64
1 in 32
1 in 16
1 in 8
1 in 4

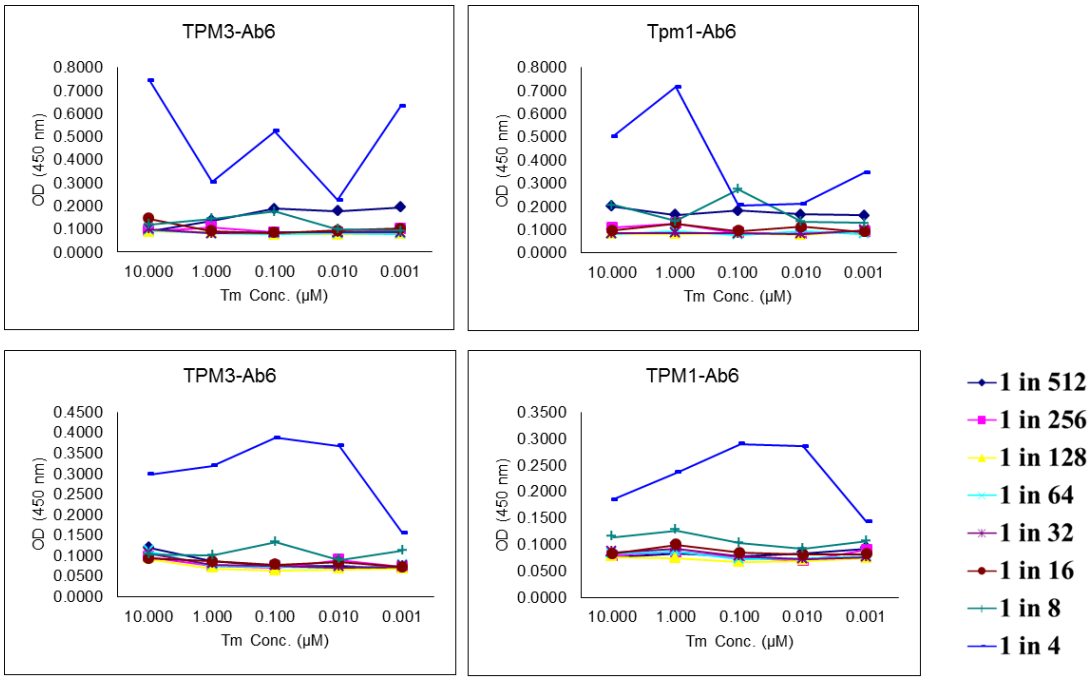
TPM3-Ab6
OD (450 nm)
0.8000
0.7000
0.6000
0.5000
0.4000
0.3000
0.2000
0.1000
0.0000
10.000 1.000 0.100 0.010 0.001
Tm Conc. (μM)
Tpm1-Ab6
OD (450 nm)
0.8000
0.7000
0.6000
0.5000
0.4000
0.3000
0.2000
0.1000
0.0000
10.000 1.000 0.100 0.010 0.001
Tm Conc. (μM)
TPM3-Ab6
OD (450 nm)
0.4500
0.4000
0.3500
0.3000
0.2500
0.2000
0.1500
0.1000
0.0500
0.0000
10.000 1.000 0.100 0.010 0.001
Tm Conc. (μM)
TPM1-Ab6
OD (450 nm)
0.3500
0.3000
0.2500
0.2000
0.1500
0.1000
0.0500
0.0000
10.000 1.000 0.100 0.010 0.001
Tm Conc. (μM)
1 in 512
1 in 256
1 in 128
1 in 64
1 in 32
1 in 16
1 in 8
1 in 4

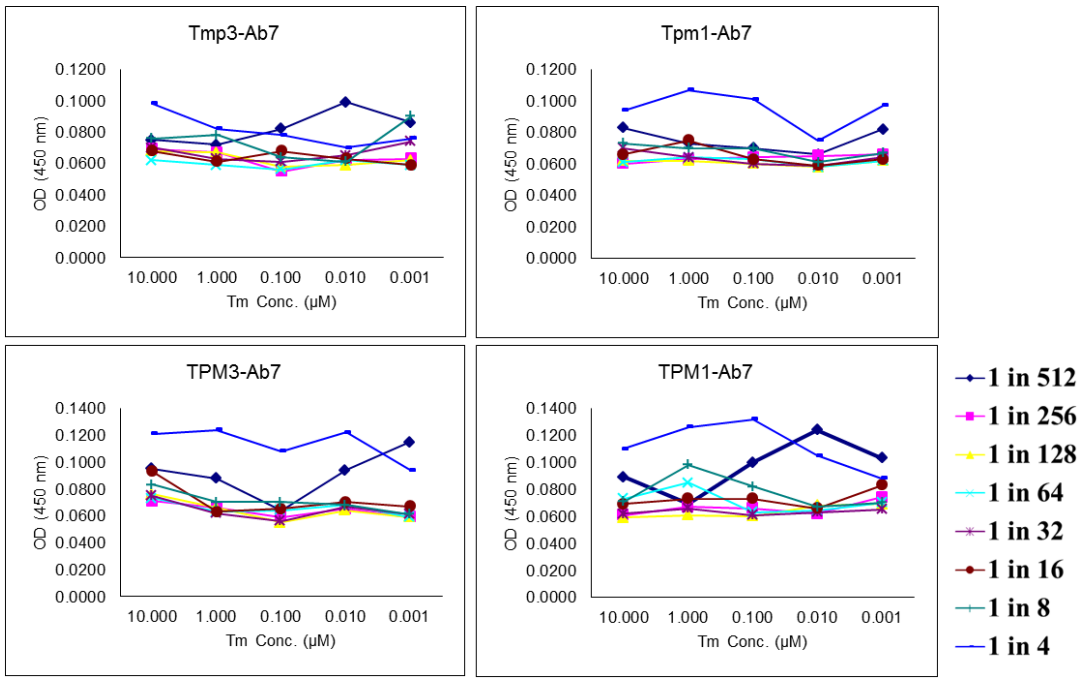
Tmp3-Ab7
Tpm1-Ab7
TPM3-Ab7
TPM1-Ab7
OD (450 nm)
Tm Conc. (μM)
10.000 1.000 0.100 0.010 0.001
1 in 512
1 in 256
1 in 128
1 in 64
1 in 32
1 in 16
1 in 8
1 in 4

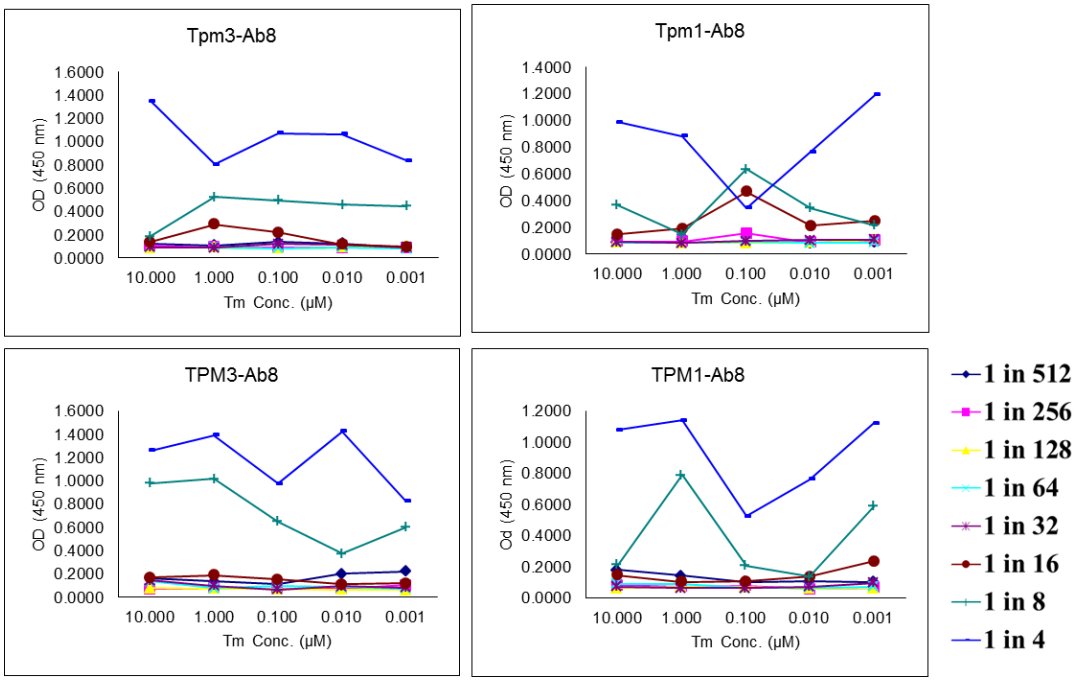
Tpm3-Ab8
Tpm1-Ab8
TPM3-Ab8
TPM1-Ab8
OD (450 nm)
Od (450 nm)
Tm Conc. (μM)
10.000 1.000 0.100 0.010 0.001
1 in 512
1 in 256
1 in 128
1 in 64
1 in 32
1 in 16
1 in 8
1 in 4

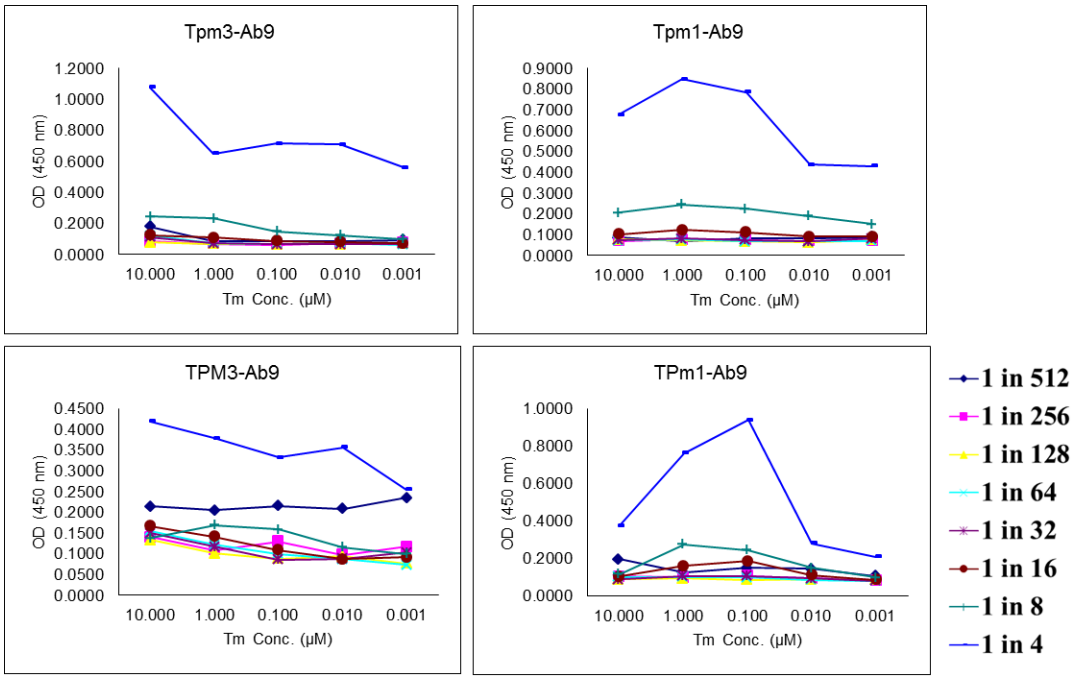
Tpm3-Ab9
OD (450 nm)
Tm Conc. (μM)
10.000 1.000 0.100 0.010 0.001
Tpm1-Ab9
TPM3-Ab9
TPm1-Ab9
1 in 512
1 in 256
1 in 128
1 in 64
1 in 32
1 in 16
1 in 8
1 in 4

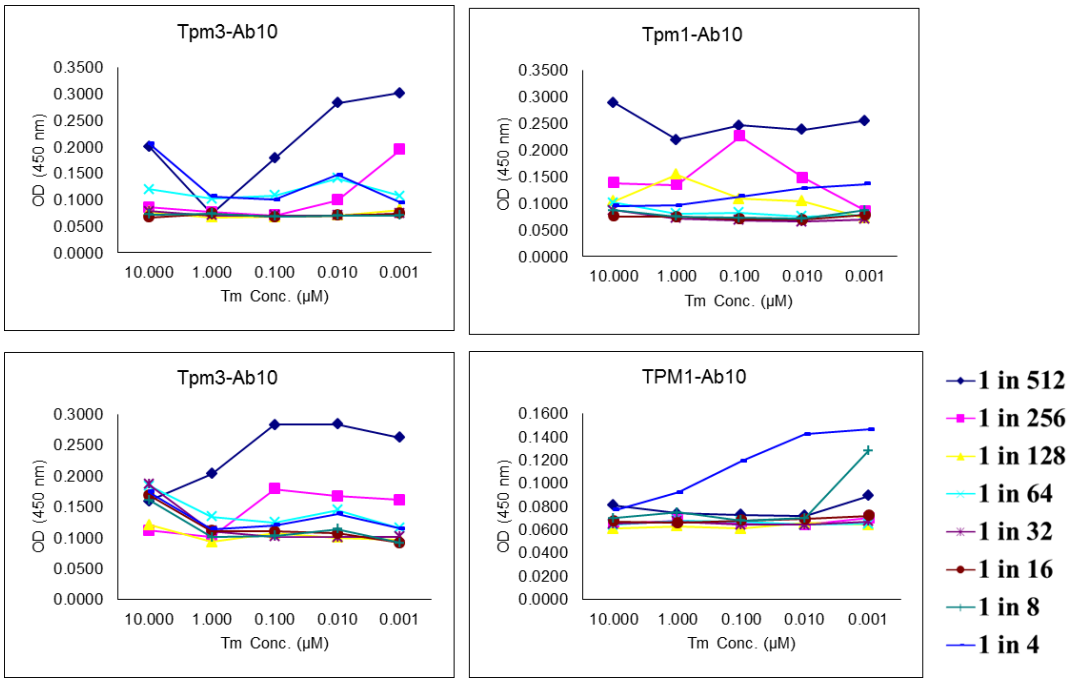
Tpm3-Ab10
OD (450 nm)
Tm Conc. (μM)
10.000 1.000 0.100 0.010 0.001
Tpm1-Ab10
TPM1-Ab10
1 in 512
1 in 256
1 in 128
1 in 64
1 in 32
1 in 16
1 in 8
1 in 4

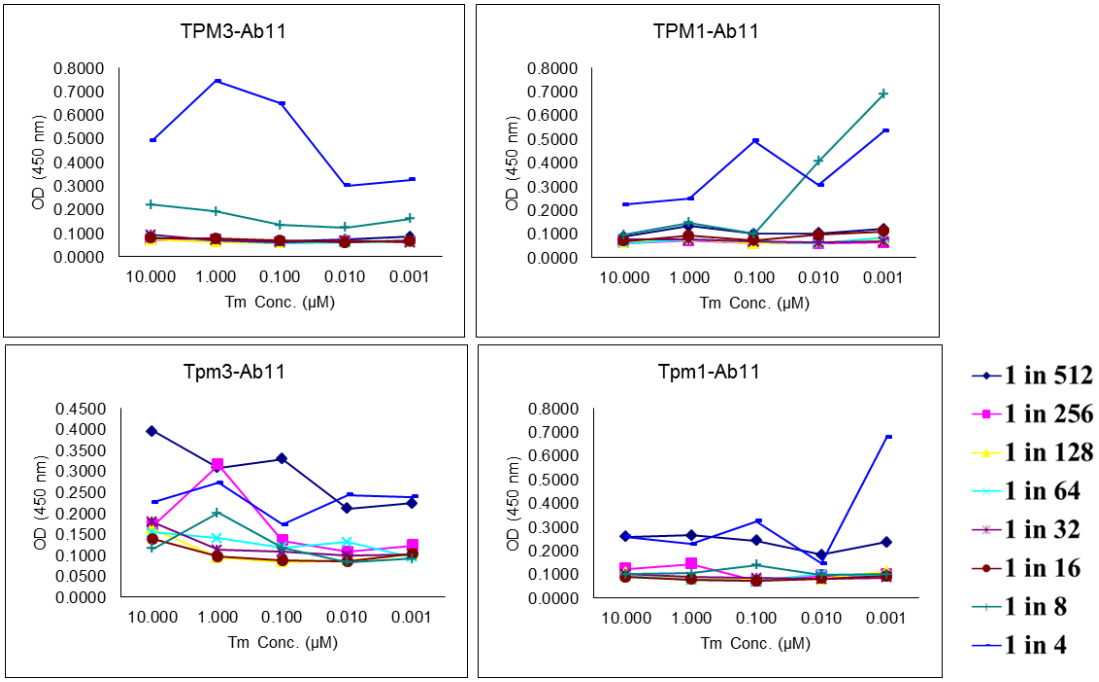
TPM3-Ab11
TPM1-Ab11
Tpm3-Ab11
Tpm1-Ab11
OD (450 nm)
Tm Conc. (μM)
10.000
1.000
0.100
0.010
0.001
1 in 512
1 in 256
1 in 128
1 in 64
1 in 32
1 in 16
1 in 8
1 in 4

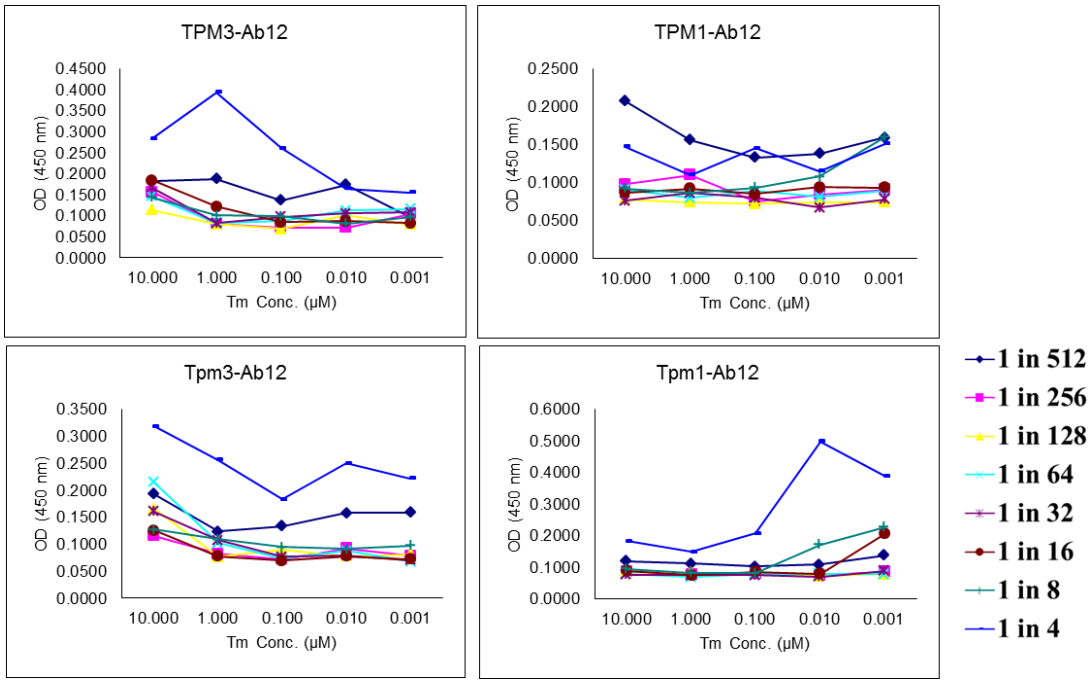
TPM3-Ab12
TPM1-Ab12
Tpm3-Ab12
Tpm1-Ab12
OD (450 nm)
Tm Conc. (μM)
10.000
1.000
0.100
0.010
0.001
1 in 512
1 in 256
1 in 128
1 in 64
1 in 32
1 in 16
1 in 8
1 in 4

References

Anderson, P. A., Malouf, N. N., Oakeley, A. E., Pagani, E. D. and Allen, P. D. (1991). Troponin T isoform expression in humans. A comparison among normal and failing adult heart, fetal heart, and adult and fetal skeletal muscle. *Circ. Res.* **69**, 1226–33.

Arab, S., Gramolini, A. O., Ping, P., Kislinger, T., Stanley, B., van Eyk, J., Ouzounian, M., MacLennan, D. H., Emili, A. and Liu, P. P. (2006a). Cardiovascular proteomics: tools to develop novel biomarkers and potential applications. *J. Am. Coll. Cardiol.* j. jacc. 2006.06. 063v1.

Arab, S., Gramolini, A. O., Ping, P., Kislinger, T., Stanley, B., van Eyk, J., Ouzounian, M., MacLennan, D. H., Emili, A. and Liu, P. P. (2006b). Cardiovascular proteomics: tools to develop novel biomarkers and potential applications. *J. Am. Coll. Cardiol.* **48**, 1733–41.

Arrell, D. K., Neverova, I. and Eyk, J. E. Van (2001a). Cardiovascular proteomics: evolution and potential. *Circ. Res.* **88**, 763–773.

Arrell, D. K., Neverova, I., Fraser, H., Marban, E. and Eyk, J. E. Van (2001b). Proteomic Analysis of Pharmacologically Preconditioned Cardiomyocytes Reveals Novel Phosphorylation of Myosin Light Chain 1. *Circ. Res.* **89**, 480–487.

Ausoni, S., Campione, M., Picard, A., Moretti, P., Vitadello, M., De Nardi, C. and Schiaffino, S. (1994). Structure and regulation of the mouse cardiac troponin I gene. *J. Biol. Chem.* **269**, 339–46.

Bailey, K. (1948). Tropomyosin: a new asymmetric protein component of the muscle fibril. *Biochem. J.* **43**, 271–279.

Baneyx, F. and Mujacic, M. (2004). Recombinant protein folding and misfolding in Escherichia coli. *Nat. Biotechnol.* **22**, 1399–408.

Bantscheff, M., Lemeer, S., Savitski, M. M. and Kuster, B. (2012). Quantitative mass spectrometry in proteomics: critical review update from 2007 to the present. *Anal. Bioanal. Chem.* **404**, 939–65.

Blumenschein, T. M. A., Stone, D. B., Fletterick, R. J., Mendelson, R. A. and Sykes, B. D. (2006). Dynamics of the C-terminal region of TnI in the troponin complex in solution. *Biophys. J.* **90**, 2436–44.

Bradshaw, R. a, Brickey, W. W. and Walker, K. W. (1998). N-terminal processing: the methionine aminopeptidase and N alpha-acetyl transferase families. *Trends Biochem. Sci.* **23**, 263–7.

Brown, J. H., Kim, K. H., Jun, G., Greenfield, N. J., Dominguez, R., Volkmann, N., Hitchcock-DeGregori, S. E. and Cohen, C. (2001). Deciphering the design of the tropomyosin molecule. *Proc. Natl. Acad. Sci. U. S. A.* **98**, 8496–501.

Bryce NS1, Schevzov G, Ferguson V, Percival JM, Lin JJ, Matsumura F, Bamburg JR, Jeffrey PL, Hardeman EC, Gunning P, Weinberger RP. (2003). Specification of actin filament function and molecular composition by tropomyosin isoforms. *Mol. Biol.cell.* **14**, 1002-16.

Buzan, J. M. and Frieden, C. (1996). Yeast actin: polymerization kinetic studies of wild type and a poorly polymerizing mutant. *Proc. Natl. Acad. Sci. U. S. A.* **93**, 91–5.

Canepari, M., Pellegrino, M. A., D'antona, G. and Bottinelli, R. (2010). Skeletal muscle fibre diversity and the underlying mechanisms. *Acta Physiol.* **199**, 465–476.

Cardelli, L., Caron, E., Gardner, P., Kahramanoğulları, O. and Phillips, A. (2009). A Process Model of Actin Polymerisation. *Electron. Notes Theor. Comput. Sci.* **229**, 127–144.

Cho, Y. J., Liu, J. and Hitchcock-DeGregori, S. E. (1990). The amino terminus of muscle tropomyosin is a major determinant for function. *J. Biol. Chem.* **265**, 538–545.

Clos, J. and Brandau, S. (1994). pJC20 and pJC40-two high-copy-number vectors for T7 RNA polymerase-dependent expression of recombinant genes in Escherichia coli. *Protein Expr. Purif.* **5**, 133–137.

Cole, R. B. (2000). Some tenets pertaining to electrospray ionization mass spectrometry. **772**, 763–772.

Compton, P. D., Zamdborg, L., Thomas, P. M. and Kelleher, N. L. (2011). On the scalability and requirements of whole protein mass spectrometry. *Anal. Chem.* **83**, 6868–74.

Cooke, R. (1975). The role of the bound nucleotide in the polymerization of actin. *Biochemistry* **14**, 3250–6.

Cooper, G. M. (2000). Actin, Myosin, and Cell Movement. Sunderland (MA): Sinauer Associates.

Cooper, J. A., Buhle, E. L., Walker, S. B., Tsong, T. Y. and Pollard, T. D. (1983a). Kinetic evidence for a monomer activation step in actin polymerization. *Biochemistry* **22**, 2193–2202.

Cooper, J. a, Walker, S. B. and Pollard, T. D. (1983b). Pyrene actin: documentation of the validity of a sensitive assay for actin polymerization. *J. Muscle Res. Cell Motil.* **4**, 253–62.

Coulton, A., Lehrer, S. and Geeves, M. (2006). Functional homodimers and heterodimers of recombinant smooth muscle tropomyosin. *Biochemistry*. **45**, 12853–12858.

Coulton, A. T., East, D. a, Galinska-Rakoczy, A., Lehman, W. and Mulvihill, D. P. (2010). The recruitment of acetylated and unacetylated tropomyosin to distinct actin polymers permits the discrete regulation of specific myosins in fission yeast. *J. Cell Sci.* **123**, 3235–43.

Creed, S. J., Desouza, M., Bamburg, J. R., Gunning, P. and Stehn, J. (2011). Tropomyosin isoform 3 promotes the formation of filopodia by regulating the recruitment of actin-binding proteins to actin filaments. *Exp. Cell Res.* **317**, 249–261.

Crick, F. H. (1952). Is alpha-keratin a coiled coil? *Nature* **170**, 882–3.

Criddle, a H., Geeves, M. a and Jeffries, T. (1985b). The use of actin labelled with N-(1-pyrenyl)iodoacetamide to study the interaction of actin with myosin subfragments and troponin/tropomyosin. *Biochem. J.* **232**, 343–9.

Cummins, P. and Perry, S. V (1973). The subunits and biological activity of polymorphic forms of tropomyosin. *Biochem. J.* **133**, 765–77.

Desai, R. a, Geeves, M. a and Kad, N. M. (2014). Using Fluorescent Myosin to Directly Visualize Cooperative Activation of Thin Filaments. *J. Biol. Chem.* **290**, 1915–1925.

Dougan, D., Malby, R. and Gruen, L. (1998). Effects of substitutions in the binding surface of an antibody on antigen affinity. *Protein Eng.* **11**, 65-74.

Drabikowski, W. and Nowak, E. (1968). Studies on the Interaction of F-Actin with. **5**, 376–384.

Druyan, S., Cahaner, A. and Ashwell, C. M. (2007). The expression patterns of hypoxia-inducing factor subunit alpha-1, heme oxygenase, hypoxia upregulated protein 1, and cardiac troponin T during development of the chicken heart. *Poult. Sci.* **86**, 2384–9.

Dvoretsky, A., Abusamhadneh, E. M., Howarth, J. W. and Rosevear, P. R. (2002). Solution structure of calcium-saturated cardiac troponin C bound to cardiac troponin I. *J. Biol. Chem.* **277**, 38565–70.

Ecken, J. Von der, Müller, M. and Lehman, W Manstein DJ, Penczek PA, Raunser S. (2014). Structure of the F-actin--tropomyosin complex. *Nature*. **519**, 114-117.

Engvall, E. and Perlmann, P. (1971). Enzyme-linked immunosorbent assay (ELISA) quantitative assay of immunoglobulin G. *Immunochemistry* **8**, 871–874.

Erban, T. (2011). Purification of tropomyosin, paramyosin, actin, tubulin, troponin and kinases for chemiproteomics and its application to different scientific fields. *PLoS One* **6**, e22860.

Erickson, H. P. (2007). Evolution of the cytoskeleton. *Bioessays* **29**, 668–77.

Farah, C. S., Miyamoto, C. A., Ramos, C. H., da Silva, A. C., Quaggio, R. B., Fujimori, K., Smillie, L. B. and Reinach, F. C. (1994). Structural and regulatory functions of the NH2- and COOH-terminal regions of skeletal muscle troponin I. *J. Biol. Chem.* **269**, 5230–40.

Findlay, J. W. A. and Dillard, R. F. (2007). Appropriate Calibration Curve Fitting in Ligand Binding Assays. **9**, 260–267.

Flashman, E. (2004). Cardiac Myosin Binding Protein C: Its Role in Physiology and Disease. *Circ. Res.* **94**, 1279–1289.

Flick, T. G., Cassou, C. A., Chang, T. M. and Williams, E. R. (2012). Solution additives that desalt protein ions in native mass spectrometry. *Anal. Chem.* **84**, 7511–7.

Flicker, P. F., Phillips, G. N. and Cohen, C. (1982). Troponin and its interactions with tropomyosin. An electron microscope study. *J. Mol. Biol.* **162**, 495–501.

Frank, S. (2002). *Immunology and evolution of infectious disease.* Princeton (NJ): Princeton University Press.

Frieden, C. (1983). Polymerization of actin: mechanism of the Mg2+-induced process at pH 8 and 20 degrees C. *Proc. Natl. Acad. Sci.* **80**, 6513–6517.

Frieden, C. and Goddette, D. W. (1983). Polymerization of actin and actin-like systems: evaluation of the time course of polymerization in relation to the mechanism. *Biochemistry* **22**, 5836–5843.

Gajbhiye, R., Sonawani, a, Khan, S., Suryawanshi, a, Kadam, S., Warty, N., Raut, V. and Khole, V. (2012). Identification and validation of novel serum markers for early diagnosis of endometriosis. *Hum. Reprod.* **27**, 408–17.

Gariboldi, M., Manenti, G., Dragani, T. A. and Pierotti, M. A. (1995). Chromosome mapping of nine tropomyosin-related sequences in mice. *Mamm. Genome* **6**, 273–7.

Ge, Y., Rybakova, I. N., Xu, Q. and Moss, R. L. (2009). Top-down high-resolution mass spectrometry of cardiac myosin binding protein C revealed that truncation alters protein phosphorylation state. *Proc. Natl. Acad. Sci. U. S. A.* **106**, 12658–63.

Geeves, M. A., Fedorov, R. and Manstein, D. J. (2005). Molecular mechanism of actomyosin-based motility. *Cell. Mol. Life Sci.* **62**, 1462–77.

Geeves, M. A, Hitchcock-DeGregori, S. E. and Gunning, P. W. (2014). A systematic nomenclature for mammalian tropomyosin isoforms. *J. Muscle Res. Cell Motil.* **36,** 147-53.

Gimona, M., Watakabe, a and Helfman, D. M. (1995). Specificity of dimer formation in tropomyosins: influence of alternatively spliced exons on homodimer and heterodimer assembly. *Proc. Natl. Acad. Sci. U. S. A.* **92**, 9776–80.

Go, A. S., Mozaffarian, D., Roger, V. L., Benjamin, E. J., Berry, J. D., Blaha, M. J., Dai, S., Ford, E. S., Fox, C. S., Franco, S., et al. (2014). *Heart disease and stroke statistics--2014 update: a report from the American Heart Association.*

Gomes, A. V, Guzman, G., Zhao, J. and Potter, J. D. (2002). Cardiac troponin T isoforms affect the Ca2+ sensitivity and inhibition of force development. Insights into the role of troponin T isoforms in the heart. *J. Biol. Chem.* **277**, 35341–9.

Gooding, C., Reinach, F. C. and Macleod, A. R. (1987). Complete nucleotide sequence of the fast-twitch isoform of chicken skeletal muscle alpha-tropomyosin. *Nucleic Acids Res.* **15**, 8105.

Goodman, D. B., Church, G. M. and Kosuri, S. (2013). Causes and effects of N-terminal codon bias in bacterial genes. *Science* **342**, 475–9.

Gordon, A. M., LaMadrid, M. A., Chen, Y., Luo, Z. and Chase, P. B. (1997). Calcium regulation of skeletal muscle thin filament motility in vitro. *Biophys. J.* **72**, 1295–1307.

Gordon, A. M., Homsher, E. and Regnier, M. (2000). Regulation of contraction in striated muscle. *Physiol. Rev.* **80**, 853–924.

Grand, R. J. and Wilkinson, J. M. (1977). The amino acid sequence of rabbit slow-muscle troponin I. *Biochem. J.* **167**, 183–92.

Gregorich, Z. R. and Ge, Y. (2014). Top-down proteomics in health and disease: challenges and opportunities. *Proteomics* **14**, 1195–210.

Gregorich, Z. R., Chang, Y.-H. and Ge, Y. (2014). Proteomics in heart failure: top-down or bottom-up? *Pflugers Arch.* **466**, 1199–209.

Gregorio, C. C. and Antin, P. B. (2000). To the heart of myofibril assembly. *Trends Cell Biol.* **10**, 355–62.

Greenfield, N. J., Hitchcock-Degregori, S. E. (1993). Conformational intermediates in the folding of a coiled-coil model peptide of the N-terminus of tropomyosin and aa-tropomyosin. *Protein Sci.* **8,** 1263-73.

Grote, P., Wittler, L., Hendrix, D., Koch, F., Währisch, S., Beisaw, A., Macura, K., Bläss, G., Kellis, M., Werber, M., et al. (2013). The tissue-specific lncRNA Fendrr is an essential regulator of heart and body wall development in the mouse. *Dev. Cell* **24**, 206–14.

Gunning, P. W., Schevzov, G., Kee, A. J. and Hardeman, E. C. (2005). Tropomyosin isoforms: divining rods for actin cytoskeleton function. *Trends Cell Biol.* **15**, 333–341.

Gunning, P., O'neill, G. and Hardeman, E. (2008). Tropomyosin-based regulation of the actin cytoskeleton in time and space. *Physiol. Rev.* **88**, 1–35.

Harris, D. E. and Warshaw, D. M. (1993). Smooth and skeletal muscle actin are mechanically indistinguishable in the in vitro motility assay. *Circ. Res.* **72**, 219–224.

Hastings, K. E., Koppe, R. I., Marmor, E., Bader, D., Shimada, Y. and Toyota, N. (1991). Structure and developmental expression of troponin I isoforms. cDNA clone analysis of avian cardiac troponin I mRNA. *J. Biol. Chem.* **266**, 19659–65.

Heald, R. W. and Hitchcock-DeGregori, S. E. (1988). The structure of the amino terminus of tropomyosin is critical for binding to actin in the absence and presence of troponin. *J. Biol. Chem.* **263**, 5254–5259.

Helfman, D. M., Feramisco, J. R., Fiddes, J. C., Thomas, G. P. and Hughes, S. H. (1983). Identification of clones that encode chicken tropomyosin by direct immunological screening of a cDNA expression library. *Proc. Natl. Acad. Sci. U. S. A.* **80**, 31–5.

Helfman, D. M., Berthier, C., Grossman, J., Leu, M., Ehler, E., Perriard, E. and Perriard, J. C. (1999). Nonmuscle tropomyosin-4 requires coexpression with other low molecular weight isoforms for binding to thin filaments in cardiomyocytes. *J. Cell Sci.* **112**, 371–80.

Hijazi, Z., Siegbahn, A., Andersson, U., Granger, C. B., Alexander, J. H., Atar, D., Gersh, B. J., Mohan, P., Harjola, V.-P., Horowitz, J., et al. (2014). High-sensitivity troponin I for risk assessment in patients with atrial fibrillation: insights from the Apixaban for Reduction in Stroke and other Thromboembolic Events in Atrial Fibrillation (ARISTOTLE) trial. *Circulation* **129**, 625–34.

Hitchcock-DeGregori, S. E. and Heald, R. W. (1987). Altered actin and troponin binding of amino-terminal variants of chicken striated muscle alpha-tropomyosin expressed in Escherichia coli. *J. Biol. Chem.* **262**, 9730–9735.

Hitchcock-DeGregori, S. E., Lewis, S. F. and Chou, T. M. T. (1985). Tropomyosin lysine reactivities and relationship to coiled-coil structure. *Biochemistry* **24**, 3305–3314.

Hitchcock-DeGregori, S., Sampath, P. and Pollard, T. (1988). Tropomyosin inhibits the rate of actin polymerization by stabilizing actin filaments. *Biochemistry.* **27**, 9182–9185.

Holmes, K. and Lehman, W. (2008). Gestalt-binding of tropomyosin to actin filaments. *J. Muscle Res. Cell Motil.* **29**, 213-9.

Höög, J. O., Weis, M., Zeppezauer, M., Jörnvall, H. and von Bahr-Lindström, H. (1987). Expression in Escherichia coli of active human alcohol dehydrogenase lacking N-terminal acetylation. *Biosci. Rep.* **7**, 969–74.

Hook, J., Lemckert, F. and Qin, H. (2004). Gamma tropomyosin gene products are required for embryonic development. *Mol. Cell Biol.* **24**, 2318–2323.

Hook, J., Lemckert, F., Schevzov, G., Fath, T. and Gunning, P. (2011). Functional identity of the gamma tropomyosin gene: Implications for embryonic development, reproduction and cell viability. *Bioarchitecture* **1**, 49–59.

Houdusse, A, Love, M. L., Dominguez, R., Grabarek, Z. and Cohen, C. (1997). Structures of four Ca2+-bound troponin C at 2.0 A resolution: further insights into the Ca2+-switch in the calmodulin superfamily. *Structure* **5**, 1695–1711.

Hwang, C. S., Shemorry, A. and Varshavsky, A. (2010). N-terminal acetylation of cellular proteins creates specific degradation signals. *Science,* **327**, 973-977.

Johnson, M., Coulton, A. T., Geeves, M. A. and Mulvihill, D. P. (2010). Targeted amino-terminal acetylation of recombinant proteins in E. coli. *PLoS One* .**5**, e15801.

Josephygg, P. D., Elingg, T. and Mason, P. (1982). The Horseradish Peroxidase-catalyzed Oxidation of 3,5,3',5'- Tetramethylbenzidine. *J Biol. Chem.* **257**, 3669-75.

Kabsch, W., Mannherz, H. G., Suck, D., Pai, E. F. and Holmes, K. C. (1990). Atomic structure of the actin:DNase I complex. *Nature* **347**, 37–44.

Kad, N. M. and Van Houten, B. (2014). Single molecule approaches: watching DNA repair one molecule at a time. Preface. *DNA Repair (Amst).* **20**, 1.

Keiser, T. and Wegner, A. (1985). Isolation from bovine brain of tropomyosins that bind to actin filaments with different affinities. *FEBS Lett.* **187**, 76–80.

Kim, H. K., Kim, R.-R., Oh, J.-H., Cho, H., Varshavsky, A. and Hwang, C.-S. (2013). The N-Terminal Methionine of Cellular Proteins as a Degradation Signal. *Cell* **156**, 158–169.

Kirwan, J. P. and Hodges, R. S. (2010). Critical interactions in the stability control region of tropomyosin. *J. Struct. Biol.* **170**, 294–306.

Kobayashi, T. and Solaro, R. J. (2005). Calcium, thin filaments, and the integrative biology of cardiac contractility. *Annu. Rev. Physiol.* **67**, 39–67.

Kobayashi, M., Debold, E. P., Turner, M. A. and Kobayashi, T. (2013). Cardiac muscle activation blunted by a mutation to the regulatory component, troponin T. *J. Biol. Chem.* **288**, 26335–49.

Koch, A., Juan, T. S., Jenkins, N. A., Gilbert, D. J., Copeland, N. G., McNiece, I. K. and Fletcher, F. A. (1997). cDNA cloning and chromosomal mapping of mouse fast skeletal muscle troponin T. *Mamm. Genome* **8**, 346–8.

Koppe, R. I., Hallauer, P. L., Karpati, G. and Hastings, K. E. (1989). cDNA clone and expression analysis of rodent fast and slow skeletal muscle troponin I mRNAs. *J. Biol. Chem.* **264**, 14327–33.

Kouyama, T. and Mihashi, K. (1981). Fluorimetry Study of N-(1-Pyrenyl) iodoacetamide-Labelled F-Actin. *Eur. J. Biochem.* **114,** 33-8.

Kovacs, J. M., Mant, C. T. and Hodges, R. S. (2006). Determination of intrinsic hydrophilicity/hydrophobicity of amino acid side chains in peptides in the absence of nearest-neighbor or conformational effects. *Biopolymers* **84**, 283–97.

Kudla, G., Murray, A. W., Tollervey, D. and Plotkin, J. B. (2009). Coding-sequence determinants of gene expression in Escherichia coli. *Science* **324**, 255–8.

Kwok, S. C. and Hodges, R. S. (2004). Stabilizing and destabilizing clusters in the hydrophobic core of long two-stranded alpha-helical coiled-coils. *J. Biol. Chem.* **279**, 21576–88.

Labugger, R., McDonough, J. L., Neverova, I. and Eyk, J. E. Van (2002). Solubilization, two-dimensional separation and detection of the cardiac myofilament protein troponin T. *Proteomics* **2**, 673–678.

Laemmli, U. K. (1970). Cleavage of structural proteins during the assembly of the head of bacteriophage T4. *Nature* **227**, 680–5.

Lal, A. and Korn, E. (1986). Effect of muscle tropomyosin on the kinetics of polymerization of muscle actin. *Biochemistry.* **25,** 1154-8.

Lamkin, M., Tao, T. and Lehrer, S. S. (1983). Tropomyosin-troponin and tropomyosin-actin interactions: a fluorescence quenching study. *Biochemistry* **22**, 3053–3058.

Lees-Miller, J. (1990). Three novel brain tropomyosin isoforms are expressed from the rat alpha-tropomyosin gene through the use of alternative promoters and alternative RNA processing. *Mol. Cell.Biol.* **10,** 1729-42.

Lees-Miller, J. P. and Helfman, D. M. (1991). The molecular basis for tropomyosin isoform diversity. *Bioessays* **13**, 429–437.

Leger, J., Bouveret, P., Schwartz, K. and Swynghedauw, B. (1976). A comparative study of skeletal and cardiac tropomyosins. *Pflügers Arch. Eur. J. Physiol.* **362**, 271–277.

Lehman, W., Hatch, V., Korman, V., Rosol, M., Thomas, L., Maytum, R., Geeves, M. A., Eyk, J. E. Van, Tobacman, L. S. and Craig, R. (2000a). Tropomyosin and actin isoforms modulate the localization of tropomyosin strands on actin filaments1. *J. Mol. Biol.* **302**, 593–606.

Lehman, W., Hatch, V., Korman, V., Rosol, M., Thomas, L., Maytum, R., Geeves, M. a, Van Eyk, J. E., Tobacman, L. S. and Craig, R. (2000b). Tropomyosin and actin isoforms modulate the localization of tropomyosin strands on actin filaments. *J. Mol. Biol.* **302**, 593–606.

Lehman, W., Orzechowski, M., Li, X. E., Fischer, S. and Raunser, S. (2013). Gestalt-binding of tropomyosin on actin during thin filament activation. *J. Muscle Res. Cell Motil.* **34**, 155–63.

Lehninger, A., Nelson, D. and Cox, M. (2008). Lehninger Principles of Biochemistry. New York : W.H. Freeman.

Leszyk, J., Dumaswala, R., Potter, J. D., Gusev, N. B., Verin, A. D., Tobacman, L. S. and Collins, J. H. (1987). Bovine cardiac troponin T: amino acid sequences of the two isoforms. *Biochemistry* **26**, 7035–42.

Li, X. E., Holmes, K. C., Lehman, W., Jung, H. and Fischer, S. (2010). The shape and flexibility of tropomyosin coiled coils: implications for actin filament assembly and regulation. *J. Mol. Biol.* **395**, 327–39.

Li, Z., Yang, R., Zhao, J., Yuan, R., Lu, Q., Li, Q. and Tse, W. (2011a). Molecular diagnosis and targeted therapy of a pediatric chronic eosinophilic leukemia patient carrying TPM3-PDGFRB Fusion. *Pediatr. Blood Cancer* **56**, 463–466.

Li, X. E., Tobacman, L. S., Mun, J. Y., Craig, R., Fischer, S. and Lehman, W. (2011b). Tropomyosin position on F-actin revealed by EM reconstruction and computational chemistry. *Biophys. J.* **100**, 1005–13.

Libri, D., Mouly, V., Lemonnier, M. and Fiszman, M. Y. (1990). A nonmuscle tropomyosin is encoded by the smooth/skeletal beta-tropomyosin gene and its RNA is transcribed from an internal promoter. *J. Biol. Chem.* **265**, 3471–3.

Lim, M. S., Sutherland, C. and Walsh, M. P. (1985). Phosphorylation of bovine cardiac C-protein by protein kinase C. *Biochem. Biophys. Res. Commun.* **132**, 1187–1195.

Lin, J. J., Chou, C. S. and Lin, J. L. (1985). Monoclonal antibodies against chicken tropomyosin isoforms: production, characterization, and application. *Hybridoma* **4**, 223–42.

Lin, J. J., Hegmann, T. E. and Lin, J. L. (1988). Differential localization of tropomyosin isoforms in cultured nonmuscle cells. *J. Cell Biol.* **107**, 563–72.

Lloyd-Jones, D., Adams, R. J., Brown, T. M., Carnethon, M., Dai, S., Simone, G. De, Ferguson, T. B., Ford, E., Furie, K. and Gillespie, C. (2010). Heart disease and stroke statistics—2010 update. *Circulation* **121**, e46–e215.

Lowther, W. T. and Matthews, B. W. (2000). Structure and function of the methionine aminopeptidases. *Biochim. Biophys. Acta* **1477**, 157–67.

Lymn, R. W. and Taylor, E. W. (1971). Mechanism of adenosine triphosphate hydrolysis by actomyosin. *Biochemistry* **10**, 4617–24.

Manning, E., Tardiff, J. and Schwartz, S. (2011). A model of calcium activation of the cardiac thin filament. *Biochemistry.* **50,** 7405-13.

Marston, S. B., Copeland, O., Messer, A. E., Macnamara, E., Nowak, K., Zampronio, C. G. and Ward, D. G. (2013b). Tropomyosin isoform expression and phosphorylation in the human heart in health and disease. *J. Muscle Res. Cell Motil.* **34**, 189–97.

Martini, F. (2001). *Fundamentals of anatomy and physiology*. Prentice Hall.

Martini, F., Nath, J. L. and Gollahon, L. (2008). Fundamentals of anatomy & physiology (8th Int Ed.) with CD-ROM. *Recherche* **67**, 2.

Maytum, R. and Konrad, M. (2006). N-terminally acetylated tropomyosin generated in E. coli by coexpression of the S. cerevisiae NatB acetylation complex shows functional properties in vitro. *Microbial Cell Factories*. **5, 7**6.

Maytum, R., Lehrer, S. S. and Geeves, M. a (1999). Cooperativity and switching within the three-state model of muscle regulation. *Biochemistry* **38**, 1102–10.

Maytum, R., Geeves, M. A. and Konrad, M. (2000). Actomyosin regulatory properties of yeast tropomyosin are dependent upon N-terminal modification. *Biochemistry* **39**, 11913–11920.

Maytum, R., Konrad, M., Lehrer, S. S. and Geeves, M. A. (2001). Regulatory properties of tropomyosin effects of length, isoform, and N-terminal sequence. *Biochemistry* **40**, 7334–7341.

Maytum, R., Westerdorf, B., Jaquet, K. and Geeves, M. a (2003). Differential regulation of the actomyosin interaction by skeletal and cardiac troponin isoforms. *J. Biol. Chem.* **278**, 6696–701.

Maytum, R., Gunning, P., Lin, J., Copeland, O., Bayliss, C. and Marston, S. (2011). Analysis of Tropomyosin (Tm) Isoforms in Heart Muscle by LC/MS and Western Blotting Demonstrates Previously Uncharacterised High-Level Expression of γ Tm. *Biophys. J.* **100**, 371a.

McKillop, D. F. and Geeves, M. A. (1993). Regulation of the interaction between actin and myosin subfragment 1: evidence for three states of the thin filament. *Biophys. J.* **65**, 693–701.

Meerson, F. and Breger, A. (1977). The common mechanism of the heart's adaptation and deadaptation: hypertrophy and atrophy of the heart muscle. *Basic Res. Cardiol.* **72,** 228-34.

Monteiro, P. B., Lataros, R. C. and Ferro, J. A. (1994). Functional a-Tropomyosin Produced in Escherichia coli. **269**, 10461–10466.

Moraczewska, J., Nicholson-Flynn, K. and Hitchcock-DeGregori, S. E. (1999). The ends of tropomyosin are major determinants of actin affinity and myosin subfragment 1-induced binding to F-actin in the open state. *Biochemistry* **38**, 15885–15892.

Morris, E. P. and Lehrer, S. S. (1984). Troponin-tropomyosin interactions. Fluorescence studies of the binding of troponin, troponin T, and chymotryptic troponin T fragments to specifically labeled tropomyosin. *Biochemistry* **23**, 2214–2220.

Murakami, K., Stewart, M., Nozawa, K., Tomii, K., Kudou, N., Igarashi, N., Shirakihara, Y., Wakatsuki, S., Yasunaga, T. and Wakabayashi, T. (2008). Structural basis for tropomyosin overlap in thin (actin) filaments and the generation of a molecular swivel by troponin-T. *Proc. Natl. Acad. Sci. U. S. A.* **105**, 7200–7205.

Murphy, R. A., Herlihy, J. T. and Megerman, J. (1974). Force-generating capacity and contractile protein content of arterial smooth muscle. *J. Gen. Physiol.* **64**, 691–705.

Muthuchamy, M., Pajak, L., Howles, P., Doetschman, T. and Wieczorek, D. F. (1993). Developmental analysis of tropomyosin gene expression in embryonic stem cells and mouse embryos. *Mol. Cell. Biol.* **13**, 3311–3323.

Nance, J. R., Dowling, J. J., Gibbs, E. M. and Bönnemann, C. G. (2012). Congenital Myopathies: An Update. *Curr. Neurol. Neurosci. Rep.* 1–10.

Nefsky, B. and Bretscher, A. (1992). Yeast actin is relatively well behaved. *Eur. J. Biochem.* **206**, 949–55.

Neverova, I. and Eyk, J. E. Van (2002). Application of reversed phase high performance liquid chromatography for subproteomic analysis of cardiac muscle. *Proteomics* **2**, 22–31.

Neverova, I. and Van Eyk, J. E. (2005). Role of chromatographic techniques in proteomic analysis. *J. Chromatogr. B Anal. Technol. Biomed. Life Sci.* **815**, 51–63.

Nishimura, A., Moritai, M., Nishimura, Y. and Sugino, Y. (1990). A rapid and highly efficient method for preparation of competent Escherichia coli cells. **18**, 6169.

O'Donovan, C., Apweiler, R. and Bairoch, A. (2001). The human proteomics initiative (HPI). *Trends Biotechnol.* **19**, 178–81.

Ohtsuki, I. (1979). Molecular arrangement of troponin-T in the thin filament. *J. Biochem.* **86**, 491–7.

Ong, S.-E. and Mann, M. (2005). Mass spectrometry-based proteomics turns quantitative. *Nat. Chem. Biol.* **1**, 252–62.

Ono, S. and Ono, K. (2002). Tropomyosin inhibits ADF/cofilin-dependent actin filament dynamics. *J. Cell Biol.* **156**, 1065–1076.

Oosawa, F. and Asakura, S. (1975). *Thermodynamics of the Polymerization of Protein*. Academic Press.

Pak, C. W., Flynn, K. C. and Bamburg, J. R. (2008). Actin-binding proteins take the reins in growth cones. *Nat. Rev. Neurosci.* **9**, 136–147.

Palm, T., Greenfield, N. J. and Hitchcock-DeGregori, S. E. (2003). Tropomyosin ends determine the stability and functionality of overlap and troponin T complexes. *Biophys. J.* **84**, 3181–9.

Pan, B. S. and Potter, J. D. (1992). Two genetically expressed troponin T fragments representing alpha and beta isoforms exhibit functional differences. *J. Biol. Chem.* **267**, 23052–6.

Pandey, A. and Mann, M. (2000). Proteomics to study genes and genomes. *Nature* **405**, 837–846.

Parry, D. a D., Fraser, R. D. B. and Squire, J. M. (2008). Fifty years of coiled-coils and alpha-helical bundles: a close relationship between sequence and structure. *J. Struct. Biol.* **163**, 258–69.

Pato, M., Mak, A. and Smillie, L. (1981). Fragments of rabbit striated muscle alpha-tropomyosin. I. Preparation and characterization. *J. Biol. Chem.* **256**, 593-601.

Patterson, S. D. and Aebersold, R. H. (2003). Proteomics: the first decade and beyond. *Nat. Genet.* **33 Suppl**, 311–23.

Pearlstone, J. and Smillie, L. (1982). Binding of troponin-T fragments to several types of tropomyosin. Sensitivity to Ca2+ in the presence of troponin-C. *J. Biol. Chem.* **257**, 10587-92.

Peng, Y., Chen, X., Sato, T., Rankin, S. A., Tsuji, R. F. and Ge, Y. (2010). Rapid Purification and High-Resolution Top-down Mass Spectrometric Characterization of Human Salivary α-Amylase. *Anal. Chem.* **84**, 3339-46.

Peng, Y., Yu, D., Gregorich, Z., Chen, X., Beyer, A. M., Gutterman, D. D. and Ge, Y. (2013). In-depth proteomic analysis of human tropomyosin by top-down mass spectrometry. *J. Muscle Res. Cell Motil.* **34**, 199–210.

Peng, Y., Ayaz-Guner, S., Yu, D. and Ge, Y. (2014a). Top-down mass spectrometry of cardiac myofilament proteins in health and disease. *Proteomics. Clin. Appl.* **8**, 554–68.

Peng, Y., Gregorich, Z. R., Valeja, S. G., Zhang, H., Cai, W., Chen, Y.-C., Guner, H., Chen, A. J., Schwahn, D. J., Hacker, T. a, et al. (2014b). Top-down proteomics reveals concerted reductions in myofilament and Z-disc protein phosphorylation after acute myocardial infarction. *Mol. Cell. Proteomics* **13**, 2752–64.

Perry, S. V (2001). Vertebrate tropomyosin: distribution, properties and function. *J. Muscle Res. Cell Motil.* **22**, 5–49.

Pesavento, J. J., Mizzen, C. A. and Kelleher, N. L. (2006). Quantitative analysis of modified proteins and their positional isomers by tandem mass spectrometry: human histone H4. *Anal. Chem.* **78**, 4271–80.

Pette, D. and Staron, R. S. (2000a). Myosin isoforms, muscle fiber types, and transitions. *Microsc. Res. Tech.* **50**, 500–509.

Pette, D. and Staron, R. S. (2000b). Myosin isoforms, muscle fiber types, and transitions. *Microsc. Res. Tech.* **50**, 500–9.

Phillips, D. M. (1963). The presence of acetyl groups of histones. *Biochem. J.* **87**, 258–63.

Pittenger, M. F., Kazzaz, J. a and Helfman, D. M. (1994). Functional properties of non-muscle tropomyosin isoforms. *Curr. Opin. Cell Biol.* **6**, 96–104.

Pittenger, M., Kistler, A. and Helfman, D. (1995). Alternatively spliced exons of the beta tropomyosin gene exhibit different affinities for F-actin and effects with nonmuscle caldesmon. *J. Cell Sci.* **108**, 3253-65.

Pollard, T. D. (2007). Regulation of actin filament assembly by Arp2/3 complex and formins. *Annu. Rev. Biophys. Biomol. Struct.* **36**, 451–477.

Pollard, T. and Borisy, G. (2003). Cellular motility driven by assembly and disassembly of actin filaments. *Cell.* **112**, 453-65.

Pollard, T. D. and Cooper, J. A. (2009). Actin, a central player in cell shape and movement. *Science* **326**, 1208–12.

Porstmann, T. and Kiessig, S. T. (1992). Enzyme immunoassay techniques an overview. *J. Immunol. Methods* **150**, 5–21.

Prabhakar, R., Boivin, G. P., Grupp, I. L., Hoit, B., Arteaga, G., Solaro, J. R. and Wieczorek, D. F. (2001). A Familial Hypertrophic Cardiomyopathy [alpha]-Tropomyosin Mutation Causes Severe Cardiac Hypertrophy and Death in Mice. *J. Mol. Cell. Cardiol.* **33**, 1815–1828.

Pragay, D. A. and Gergely, J. (1968). Effect of tropomyosin on the polymerization of ATP--G-actin and ADP--G-actin. *Arch. Biochem. Biophys.* **125**, 727–33.

Prasan, A. M., McCarron, H. C. K., Zhang, Y. and Jeremy, R. W. (2007). Myocardial release of nitric oxide during ischaemia and reperfusion: effects of L-arginine and hypercholesterolaemia. *Hear. Lung Circ.* **16**, 274–281.

Purcell, I., Bing, W. and Marston, S. (1999). Functional analysis of human cardiac troponin by the in vitro motility assay: comparison of adult, foetal and failing hearts. *Cardiovasc Res.* **43,** 884-91.

Rajan, S., Jagatheesan, G., Karam, C. N., Alves, M. L., Bodi, I., Schwartz, A., Bulcao, C. F., D'Souza, K. M., Akhter, S. A. and Boivin, G. P. (2010a). Molecular and functional characterization of a novel cardiac-specific human tropomyosin isoform. *Circulation* **121**, 410–418.

Rajan, S., Jagatheesan, G., Karam, C. N., Alves, M. L., Bodi, I., Schwartz, A., Bulcao, C. F., D'Souza, K. M., Akhter, S. a, Boivin, G. P., et al. (2010b). Molecular and functional characterization of a novel cardiac-specific human tropomyosin isoform. *Circulation* **121**, 410–8.

Regenmortel, M. Van (1998). Measurement of antigen-antibody interactions with biosensors. *J. Mol Recognit.* **11**, 163-7.

Regitz-Zagrosek, V., Erdmann, J., Wellnhofer, E., Raible, J. and Fleck, E. (2000). Novel mutation in the α-tropomyosin gene and transition from hypertrophic to hypocontractile dilated cardiomyopathy. *Circulation* **102**, e112–e116.

Reitz, C., Brayne, C. and Mayeux, R. (2011). Epidemiology of Alzheimer disease. *Nat. Rev. Neurol.* **7**, 137–52.

Rethinasamy, P. and Muthuchamy, M. (1998). Molecular and physiological effects of α-tropomyosin ablation in the mouse. *Circ Res.* **82**, 116-23.

Richards, T. A. and Cavalier-Smith, T. (2005). Myosin domain evolution and the primary divergence of eukaryotes. *Nature* **436**, 1113–8.

Rubenstein, P. A. (1990). The functional importance of multiple actin isoforms. *Bioessays* **12**, 309–15.

Sarko, J. and Pollack, C. V (2002). Cardiac troponins1. *J. Emerg. Med.* **23**, 57–65.

Schaertl, S., Lehrer, S. S. and Geeves, M. A. (1995). Separation and characterization of the two functional regions of troponin involved in muscle thin filament regulation. *Biochemistry* **34**, 15890–15894.

Schevzov, G., Vrhovski, B., Bryce, N. S., Elmir, S., Qiu, M. R., O'neill, G. M., Yang, N., Verrills, N. M., Kavallaris, M. and Gunning, P. W. (2005). Tissue-specific tropomyosin isoform composition. *J. Histochem. Cytochem.* **53**, 557–70.

Schevzov, G., Fath, T. and Vrhovski, B. (2008). Divergent regulation of the sarcomere and the cytoskeleton. *J. Biol Chem.* **283**, 275-83.

Schevzov, G., Whittaker, S. P., Fath, T., Lin, J. J. and Gunning, P. W. (2011). Tropomyosin isoforms and reagents. *Bioarchitecture* **1**, 135–164.

Schiaffino, S. and Reggiani, C. (2011). Fiber types in mammalian skeletal muscles. *Physiol. Rev.* **91**, 1447–531.

Schmidt, W., Wang, A. and Leavis, P. (2014). Direct Visualization of Tropomyosin Isoform Binding to F-Actin. *Biophys. J.* **106**, 165a.

Schneider, C. A., Rasband, W. S. and Eliceiri, K. W. (2012). NIH Image to ImageJ: 25 years of image analysis. *Nat. Methods* **9**, 671–675.

Scruggs, S. B., Reisdorph, R., Armstrong, M. L., Warren, C. M., Reisdorph, N., Solaro, R. J. and Buttrick, P. M. (2010). A novel, in-solution separation of endogenous cardiac sarcomeric proteins and identification of distinct charged variants of regulatory light chain. *Mol. Cell. Proteomics* **9**, 1804–1818.

Seddon, M., Looi, Y. H. and Shah, A. M. (2007). Oxidative stress and redox signalling in cardiac hypertrophy and heart failure. *Heart* **93**, 903.

Seidman, J. G. and Seidman, C. (2001). The Genetic Basis for Cardiomyopathy: Review from Mutation Identification to Mechanistic Paradigms. *Cell* **104**, 557–567.

Seidman, C. E. and Seidman, J. G. (2011). Identifying sarcomere gene mutations in hypertrophic cardiomyopathy: a personal history. *Circ. Res.* **108**, 743–50.

Sept, D. and McCammon, J. a (2001). Thermodynamics and kinetics of actin filament nucleation. *Biophys. J.* **81**, 667–74.

Smith, D. A., Maytum, R. and Geeves, M. A. (2003). Cooperative regulation of myosin-actin interactions by a continuous flexible chain I: actin-tropomyosin systems. *Biophys. J.* **84**, 3155–3167.

Solaro, R. J. and Van Eyk, J. (1996). Altered interactions among thin filament proteins modulate cardiac function. *J. Mol. Cell. Cardiol.* **28**, 217–30.

Solis, R. S., Ge, Y. and Walker, J. W. (2008). Single amino acid sequence polymorphisms in rat cardiac troponin revealed by top–down tandem mass spectrometry. *J. Muscle Res. Cell Motil.* **29**, 203–212.

Spudich, J. A. and Watt, S. (1971). CONTROL MECHANISMS AND BIOCHEMICAL GENETICS : The Regulation of Rabbit Skeletal Muscle Contraction : I . BIOCHEMICAL STUDIES OF THE INTERACTION OF THE TROPOMYOSIN-TROPONIN COMPLEX WITH ACTIN AND THE PROTEOLYTIC FRAGMENTS OF The Regulation of Rabbit Skelet. *J Biol Chem.* **246**, 4866-4871.

Stark, B. and Sladewski, T. (2010). Tropomyosin and myosin-II cellular levels promote actomyosin ring assembly in fission yeast. *Mol. Biol Cell.* **21**, 989-1000.

Stehn, J. R., Haass, N. K., Bonello, T., Desouza, M., Kottyan, G., Treutlein, H., Zeng, J., Nascimento, P. R. B. B., Sequeira, V. B., Butler, T. L., et al. (2013). A novel class of anticancer compounds targets the actin cytoskeleton in tumor cells. *Cancer Res.* **73**, 5169–82.

Stelzer, J. E., Patel, J. R., Walker, J. W. and Moss, R. L. (2007). Differential roles of cardiac myosin-binding protein C and cardiac troponin I in the myofibrillar force responses to protein kinase A phosphorylation. *Circ. Res.* **101**, 503–511.

Stone, D. and Smillie, L. B. (1978). The amino acid sequence of rabbit skeletal alpha-tropomyosin. The NH2-terminal half and complete sequence. *J. Biol. Chem.* **253**, 1137–48.

Straub, F. B. and Feuer, G. (1950). Adenosinetriphosphate the functional group of actin. *Biochim. Biophys. Acta* **4**, 455–470.

Strausberg, R. L., Feingold, E. A., Grouse, L. H., Derge, J. G., Klausner, R. D., Collins, F. S., Wagner, L., Shenmen, C. M., Schuler, G. D., Altschul, S. F., et al. (2002). Generation and initial analysis of more than 15,000 full-length human and mouse cDNA sequences. *Proc. Natl. Acad. Sci. U. S. A.* **99**, 16899–903.

Tardiff, J. C. (2011a). Thin Filament Mutations. *Circ. Res.* **108**, 765–782.

Tardiff, J. C. (2011b). Thin filament mutations: developing an integrative approach to a complex disorder. *Circ. Res.* **108**, 765–82.

Thierfelder, L., Watkins, H., MacRae, C., Lamas, R., McKenna, W., Vosberg, H. P., Seldman, J. G. and Seidman, C. E. (1994). [alpha]-tropomyosin and cardiac troponin T mutations cause familial hypertrophic cardiomyopathy: A disease of the sarcomere. *Cell* **77**, 701–712.

Tobacman, L. S. and Korn, E. D. (1983). The kinetics of actin nucleation and polymerization. *J. Biol. Chem.* **258**, 3207–14.

Tobacman L.S (1996). Thin filament-mediated regulation of cardiac contraction. *Annu Rev Physiol.* **58**, 447-81.

Urbancikova, M. and Hitchcock-DeGregori, S. E. (1994). Requirement of amino-terminal modification for striated muscle alpha-tropomyosin function. *J. Biol. Chem.* **269**, 24310–5.

Vahebi, S., Ota, A., Li, M., Warren, C. M., de Tombe, P. P., Wang, Y. and Solaro, R. J. (2007). p38-MAPK induced dephosphorylation of α-tropomyosin is associated with depression of myocardial sarcomeric tension and ATPase activity. *Circ. Res.* **100**, 408–415.

Van den Ent, F., Amos, L. A. and Löwe, J. (2001). Prokaryotic origin of the actin cytoskeleton. *Nature* **413**, 39–44.

Vassylyev, D. G., Takeda, S., Wakatsuki, S., Maeda, K. and Maéda, Y. (1998). Crystal structure of troponin C in complex with troponin I fragment at 2.3-A resolution. *Proc. Natl. Acad. Sci. U. S. A.* **95**, 4847–52.

Veitch, N. C. (2004). Horseradish peroxidase: a modern view of a classic enzyme. *Phytochemistry* **65**, 249–259.

Wagner, K., Miliotis, T., Marko-Varga, G., Bischoff, R. and Unger, K. K. (2002). An automated on-line multidimensional HPLC system for protein and peptide mapping with integrated sample preparation. *Anal. Chem.* **74**, 809–20.

Wallar, B. J. and Alberts, A. S. (2003). The formins: active scaffolds that remodel the cytoskeleton. *Trends Cell Biol.* **13**, 435–46.

Weber, A., Pennise, C., Babcock, G. G., Fowler, V.M. (1994). Tropomodulin caps the pointed ends of actin filaments. *J Cell Biol.* **127**, 1627-35.

Wegner, a (1976). Head to tail polymerization of actin. *J. Mol. Biol.* **108**, 139–150.

Wegner, A. (1979). Equilibrium of the actin-tropomyosin interaction. *J. Mol. Biol.* **131**, 839–53.

Wegner, A. (1980). The interaction of alpha, alpha- and alpha , beta-tropomyosin with actin filaments. *FEBS Lett.* **119**, 245–8.

Wegner, A. (1982). Spontaneous fragmentation of actin filaments in physiological conditions. *Nature.* **296**, 266-267.

Wegner, A. (1982). Kinetic analysis of actin assembly suggests that tropomyosin inhibits spontaneous fragmentation of actin filaments. *J. Mol. Biol.* **161**, 217–227.

Wegner, A. and Engel, J. (1975). Kinetics of the cooperative association of actin to actin filaments. *Biophys. Chem.* **3**, 215–25.

Wegner, A. and Ruhnau, K. (1988). Rate of binding of tropomyosin to actin filaments. *Biochemistry* **27**, 6994–7000.

Wegner, A. and Savko, P. (1982). Fragmentation of actin filaments. *Biochemistry* **21**, 1909–13.

Wei, B. and Jin, J.-P. (2011). Troponin T isoforms and posttranscriptional modifications: Evolution, regulation and function. *Arch. Biochem. Biophys.* **505**, 144–54.

Weigt, C., Wegner, A. and Koch, M. H. (1991). Rate and mechanism of the assembly of tropomyosin with actin filaments. *Biochemistry* **30**, 10700–7.

White, M. Y. and Eyk, J. E. Van (2007). Cardiovascular proteomics: past, present, and future. *Mol. Diagnosis Ther.* **11**, 83–95.

Wilkins, M. R., Sanchez, J. C., Gooley, A. A., Appel, R. D., Humphery-Smith, I., Hochstrasser, D. F. and Williams, K. L. (1996). Progress with proteome projects: why all proteins expressed by a genome should be identified and how to do it. *Biotechnol. Genet. Eng. Rev.* **13**, 19–50.

Wu, Q. L., Jha, P. K., Raychowdhury, M. K., Du, Y., Leavis, P. C. and Sarkar, S. (1994). Isolation and characterization of human fast skeletal beta troponin T cDNA: comparative sequence analysis of isoforms and insight into the evolution of members of a multigene family. *DNA Cell Biol.* **13**, 217–33.

Wu, A. H. B., Feng, Y. J., Moore, R., Apple, F. S., McPherson, P. H., Buechler, K. F. and Bodor, G. (1998). Characterization of cardiac troponin subunit release into serum after acute myocardial infarction and comparison of assays for troponin T and I. *Clin. Chem.* **44**, 1198–1208.

Xiao, Q., Zhang, F., Nacev, B. A., Liu, J. O. and Pei, D. (2010). Protein N-terminal processing: substrate specificity of Escherichia coli and human methionine aminopeptidases. *Biochemistry* **49**, 5588–99.

Yuan, C. and Solaro, R. J. (2008). Myofilament proteins: From cardiac disorders to proteomic changes. *PROTEOMICS–Clinical Appl.* **2**, 788–799.

Zhang, H. and Ge, Y. (2011). Comprehensive Analysis of Protein Modifications by Top-Down Mass Spectrometry. *Circ. Cardiovasc. Genet.* **4**, 711.

Zhang, X. L., Tibbits, G. F. and Paetzel, M. (2013). The structure of cardiac troponin C regulatory domain with bound Cd2+ reveals a closed conformation and unique ion coordination. *Acta Crystallogr. D. Biol. Crystallogr.* **69**, 722–34.

Zhao, L., Zhao, X., Tian, T., Lu, Q., Skrbo-Larssen, N., Wu, D., Kuang, Z., Zheng, X., Han, Y., Yang, S., et al. (2008). Heart-specific isoform of tropomyosin4 is essential for heartbeat in zebrafish embryos. *Cardiovasc. Res.* **80**, 200–8.

Zhou, N. E., Kay, C. M. and Hodges, R. S. (1992). Synthetic model proteins: the relative contribution of leucine residues at the nonequivalent positions of the 3-4 hydrophobic repeat to the stability of the two-stranded alpha-helical coiled-coil. *Biochemistry* **31**, 5739–46.

Zhu, B., Zhou, N. E., Kay, C. M. and Hodges, R. S. (1993). Packing and hydrophobicity effects on protein folding and stability : Effects of @ -branched amino acids , valine and isoleucine , on the formation and stability of two-stranded a-helical coiled coils / leucine zippers. 383–394.